UNIVERSITY OF CALIFORNIA, SAN DIEGO

Aging and Longevity after Photoperiod Induced Variations in Life History

A dissertation submitted in partial satisfaction of the requirements for the degree of

Doctor of Philosophy

in

Psychology

by

Evan Eric Raiewski

Committee in charge:

Professor Michael Gorman, Chair
Professor Stephan Anagnostaras
Professor Stuart Brody
Professor Karen Dobkins
Professor David Welsh

2013

The Dissertation of Evan Eric Raiewski is approved, and it is acceptable in quality and form for publication on microfilm and electronically:

_____

_____

_____

_____

_____

Chair

University of California, San Diego

2013

DEDICATION

This dissertation is dedicated to my loving and supportive family, the Raiewskis, and also the Nascas, who together define everything important to me.

Especially to Nichole, my wife, my best friend, my strongest supporter. I cherish our life together and would be lost without you.

And to my parents, Eric and Rebecca, who were always there for me. My mother instilled in me the belief I could accomplish anything I set my mind to. My dad was there to remind me there was nothing of value I would ever accomplish without hard work.

Last but not least, to my daughter Violet. Your arrival has motivated me more than anything else to advance from my comfortable career as a graduate student. You are a bright and shining star. For you I strive to become a better teacher, parent, and person.

EPIGRAPH

The true nature of the world is veiled, and if you shine a bright light on it, you can't expose that truth; it melts away with the shadows in which it is cloaked. The truth is too awesome for us to stare directly at it, and we are meant to glimpse it only with the periphery of our vision. If the landscape of your mind is too dark with fear or doubt or anger, you are blind to all truth. But if your mental landscape is too bright with certitude and arrogance, you are snow-blind and likewise unable to see what lies before you. Only the moonlit mind allows wonder, and it is in the thrall of wonder that you can see the intricate weave of the world of which you are but one thread.

- *Dean Ray Koontz*

TABLE OF CONTENTS

LIST OF FIGURES

LIST OF TABLES

ACKNOWLEDGEMENTS

I must first acknowledge the patience, mentorship, and professionalism of my advisor, Michael Gorman. I could not and would not have gotten this opportunity without his support and encouragement. It was Michael's biological psychology class in 2004 which spurred my interest in Chronobiology, when he urged me to enroll in the circadian rhythms class taught by himself, Stuart Brody and Jeff Elliott. Little did I know that I was in the company of Chronobiology's finest.

A hearty thank you to all of the Gorman Lab members for their unforgettable camaraderie: Jenn Evans, Jenny Trujillo, Gena Glickman, Liz Harrison, Carina Block, Qays Poonawala, Mandy Sinning, Hazim Khan, Genevieve McConnell, Jeremy Johnson, and Jon Sun. I have also especially enjoyed the knowledge, wisdom, and friendship of Jeff Elliott, although I will never use Graphpad Prism despite your full and hearty endorsement. I must also acknowledge Antonio Mora and Bob Sundberg for top notch animal care throughout all of my studies. Finally, without the tremendous help of Tanya Wolfson with this unwieldy dataset, I would not be done.

I thank all of my committee members, Stuart Brody, David Welsh, Karen Dobkins, Stephan Anagnostaras, and Michael Gorman for their time and efforts in providing critical feedback during the shaping of my dissertation thesis.

Last but not least, a special tribute to my fallen camarades: Kawika Deleon, Ricardo Barraza, Josh Kynoch, and Jay Blessing. I can never repay your sacrifice, so instead I continue to live life to the fullest, take nothing for granted, and never forget.

VITA

Education

University of California, San Diego- La Jolla, California
Doctor of Philosophy in Experimental Psychology, June 2013
Master of Arts in Experimental Psychology, June 2006
Bachelor of Science in Experimental Psychology, June 2005

Publications

Peer-Reviewed Articles

Raiewski, E. E., Elliott, J. A., Evans, J. A., Glickman, G. L., & Gorman, M. R. (2012). Twice daily melatonin peaks in Siberian but not Syrian hamsters under 24 hour Light:Dark:Light:Dark Cycles. *Chronobiology International, 29*(9), 1206-1215.

ABSTRACT OF THE DISSERTATION

Aging and Longevity after Photoperiod Induced Variations in Life History

by

Evan Eric Raiewski

Doctor of Philosophy in Psychology

University of California, San Diego, 2013

Professor Michael Gorman, Chair

In many organisms sexual maturity occurs at an age approximately equal to one third of their maximal lifespan. This relationship has been shown to be at least partially genetically determined, as fruit flies specifically selected for delayed sexual maturity also tend to have an increase in lifespan (Luckinbill & Clare, 1985). However, it was previously unknown whether delaying sexual maturity via

environmental manipulations would increase longevity compared to genetically similar animals undergoing puberty at an earlier age. An ideal species with which to test this hypothesis is the Siberian hamster (*Phodopus sungorus*), whose breeding season occurs during spring and summer: Pups born early in breeding season begin puberty at 25 days of age, whereas pups born late in the season instead transition to a winter phenotype and delay puberty until the following spring. Prior work with this species suggests physiological ramifications of the winter state (i.e., reduced caloric intake, daily torpor, enhanced immune function, sexual quiescence, increased melatonin biosynthesis) might potentially promote a "slow-aging" effect that could extend lifespan. The present study is the first to directly test these hypotheses by comparing lifespan among hamsters with drastically different life histories through exposure to one of six different photoperiod histories, accompanied by longitudinal collection of body weight, pelage, 24 h body temperature, and wheel running behavior, concluded with post-mortem organ weight analysis. Results reveal the juvenile life stage was increased from 3.2% to 20.2% of total lifespan duration, without consequence to longevity or rates of aging. In addition, induction into one or multiple winter states did not increase lifespan or slow aging. The degree of kidney hypertrophy was most predicted by the timing of puberty onset in male hamsters, suggesting the onset of reproductive hormones as a risk factor. A multivariate cox regression survival analysis accounted for 29% of lifespan variability among all hamsters, identifying body weight parameters to be the single most influential variable in predicting lifespan. While this study firmly demonstrates that the manipulation of photoperiod life history does not directly influence longevity, an explanation involving

the potential degree of chronodisruption between photoperiod groups might account for observed differences in lifespan.

CHAPTER 1. INTRODUCTION

Overview

Life history refers to the timing and duration of key events in an organism's lifetime, establishing a framework for categorizing developmental milestones into discrete and serial stages. Life history theory, which draws from principles of evolutionary biology, asserts the timing of these events are shaped by natural selection in order to produce the largest possible number of surviving offspring (Hill, 1993; Charnov & Berrigan, 1990). Across species, there is a correlation between the age of sexual maturity and lifespan; it has been reported that a majority of organisms typically achieve sexual maturity at roughly one-third of their maximal lifespan (Prothero 1993; Wootton 1987; Baer & Gaitz, 1971). This relationship is at least partially genetically determined: Specifically selecting for late versus early sexual maturity in *Drosophila melanogaster* results in an extension of lifespan (Luckinbill & Clare, 1985). However, among genetically equivalent subjects, it is unknown if manipulating the duration of one early life stage (i.e., adolescence) simply reduces the proportion of life spent in other life stages, without altering maximal lifespan, or altogether displaces the timeline of transitioning toward other life stages, which would extend lifespan, (see Figure 1.1). If manipulating the age of puberty could extend or reduce lifespan, or potentially alter rates of aging, it could have beneficial consequences to human health and quality of life in later years.

The developmental timetables of some organisms strictly adhere to an

inflexible, genetically determined program as a function of chronological age; other species are sensitive to environmental factors that can initiate or retard development. An ideal animal model with which to investigate how differences in life history affect aging and lifespan would involve a species known to heavily rely on environmental conditions for the initiation of developmental transitions. One primary environmental factor vital to many creatures is the time of year: a number of physiological and behavioral changes are dependent upon seasonal timing, resulting in differences to fur and pelage, hibernation, body weight, sexual behavior, and immune function.

In mammals, a circadian timing system is responsible for aligning biological processes to cyclic daily (circadian) and annual (circannual) environmental variation through the integration of photic information. In this chapter I will identify and describe the circadian timing system as the critical biological link facilitating alignment of cellular processes to circadian and circannual environmental rhythms. Circadian control of pineal melatonin, its importance to photoperiodism, and possible cellular health mechanisms will be discussed. Third, I will review somatic differences and differentiation of developmental timing in the Siberian hamster which arise as a function of photoperiodic history, and present literature indicating that these changes in turn influence rates of aging. Conventions for assessing circadian and non-circadian aging will be included. An account of the limited mammalian studies measuring aging and lifespan as affected by light history will also be discussed. Maladaptive health consequences resulting from continual rhythm disturbance are reviewed, in addition to discussing a bifurcated rhythm protocol being tested as a means to alleviating these

harmful repercussions. Last, the specific aims investigated in this dissertation are presented.

The Mammalian Circadian System

Three components constitute a fully functional master pacemaker. The first is an endogenous, self-sustained 24 h timer. The second component is a mechanism facilitating alignment between the internal state of the master pacemaker and the environment. The third requirement is the ability to disseminate daily temporal information in order to facilitate coordination among organ systems and tissues (Moore, 1995). In mammals, the master pacemaker is the Suprachiasmatic Nucleus (SCN) of the anterior hypothalamus (Moore & Leak, 2001). While SCN tissue maintains overt rhythm generation at the aggregate level, it is composed of self-sustaining oscillators located within individual neurons (Herzog et al., 2004; Yamazaki et al., 2000) producing stable but unequal period lengths between 20-28h (Welsh et al., 1995). Autonomous rhythms of individual oscillators are maintained through specialized core clock genes driving transcription-translation feedback loops, a process approximating 24 hours (Albrecht, 2002; Ko & Takahashi, 2006; Reppert & Weaver, 2002). This temporal cycling gives rise to a partitioning of the organism's daily processes into their respective circadian phases of subjective day and subjective night. In rodents subjective day is associated with lower body temperature, long bouts of behavioral inactivity, as well as peak electrical activity and c-fos expression within the SCN (Shearman et al., 1997). Hallmark indicators of subjective night (in nocturnal

rodents) include elevated body temperature (Refinetti & Menaker, 1992a, 1992b), increased behavioral activity (Pittendrigh & Daan, 1976), the biosynthesis of melatonin (Arendt, 2000), and attenuation of electrical activity within the SCN (Welsh et al., 1995).

Circadian Entrainment by Sunlight

A population of retinal ganglion cells found to be intrinsically photosensitive (ipRGCs) utilize the photopigment melanopsin to integrate and transmit light information to the SCN (Sollars et al., 2003; Morin et al., 2003; Beaulé et al., 2003). Using reliable daily time stimuli or Zeitgeber Times (ZTs), namely light at dusk and dawn, the master pacemaker adopts a specific temporal alignment to the environmental cycle (Roenneberg & Foster, 1997), or phase angle of entrainment, by appropriately delaying or advancing the timing of the clock each day (Meijer & Schwartz, 2003). Resetting circadian rhythms by changing the timing of a ZT is called a phase shift. It is the new timing of the core clock genes that define the direction and magnitude of the resulting phase shift. Light early in subjective night (hours after dusk) delays the circadian system while light during late subjective night (hours before dawn) advances the clock (Daan & Pittendrigh, 1976).

Circadian Output

It has recently been determined this 24 h genetic oscillation is not limited to cells in the SCN, but found in liver, lung, and bone tissues, but when isolated, these

rhythms dampen out over time, requiring a daily synchronizing mechanism, ultimately orchestrated through SCN controlled output. Synaptic and humoral outputs from the SCN likely organize oscillators in other mammalian tissues to one another and the environment (Mohawk et al., 2012).

One mechanism for disseminating temporal information of the SCN is the rhythmic control of melatonin secretion, a hormone produced in the pineal gland. Aside from neurons containing melatonin receptors such as the medial basal hypothalamus and pars tuberalis, the SCN contains receptors with a high affinity for melatonin (Liu et al., 1997), though the role of melatonin action here is not completely known. Melatonin production continues throughout subjective night, until early subjective day when SCN neurons resume firing, inhibiting the pineal pathway until the following subjective night. Light during subjective night induces immediate early gene c-fos (Illnerová et al., 2000) and promotes the process of a phase shift, as well as initiating SCN electrical activity and rapidly suppressing melatonin biosynthesis (Nelson & Takahashi, 1991). Because melatonin synthesis is strictly confined to hours of subjective night, it is an important mechanism whereby daylength timing and duration information is disseminated. Melatonin waveform is consequently also a gold standard for measuring onset and offset of subjective night in the hands of circadian researchers (Illnerová & Sumová, 1997). Together, the gears of the clock (utilizing photic information from the light-dark environment) and the hands of the clock provide a mechanistic means to biological synchrony and comprise necessary elements of an adaptive and functional circadian system.

Photoperiodism

Another primary function of the SCN is to prepare the organism for annual variations in the environment as the earth travels around the sun. Photoperiodism refers to animals undertaking dramatic transformations in physiology and behavior as a function of the time of year. Many mammals demonstrate profound seasonal variations in sexual function, body weight, fur pelage, food intake, immune function, and locomotor activity (Hazlerigg & Wagner, 2006; Hazlerigg, 2012). These changes are presumably due to increases in evolutionary pressure to avoid pregnancy and the dangers associated with failed reproduction during winter months, when caloric intake would conflict with available resources in the environment. The SCN controls the transitions between biological profiles, or phenotypes, (i.e., winter state and summer state) through regulation of the nightly duration of melatonin biosynthesis in the pineal gland (Elliott 1976; Gorman et al., 2001a, 2001b). In ecosystems sufficiently far from the equator, for example at a latitude of 60 degrees, nights are long (19 h) in the winter and short (5 h) during summer; this is reflected in the waveform of various day and night activities within the SCN. For instance in Long-Day (LD) photoperiods, daily electrical activity and cfos in the SCN are elevated throughout a higher proportion of the 24 h photoperiod, while nightly activities such as locomotor activity (in nocturnal animals), melatonin synthesis, and core clock gene expression are condensed (Refinetti, 2006; de la Iglesia et al., 2004; Messager et al., 2000; Mrugala et al., 2000; Sumová et al., 2007; Sumová et al., 2003). Importantly, the nightly duration of melatonin synthesis is proportional to scotophase duration, conveying information

representative of the environmental photoperiod (Elliott & Tamarkin, 1994; Illnerová, 1991, Illnerová et al., 2000).

Hamster Life History

During fall and winter, or in lab conditions maintaining Short-Day (SD) lighting conditions, Siberian hamsters undergo somatic regression and transition to the winter phenotype, exhibiting complete sexual quiescence, severely regressed gonad volume, reduced behavioral activity, 10-20% reduction in body mass, fattening, white pelage fur, and lethargy (Butler et al., 2010; Gorman 1995; Gorman & Zucker, 1995a; Goldman 1991; Goldman & Darrow, 1983). Unlike the reproductively active summer state, this winter phenotype is not permanent under SD exposure. Hamsters become photorefractory where the summer state spontaneously reemerges (i.e., recrudescence), typically after 20-25 weeks in SD (Gorman & Zucker, 1995b). The exact mechanism driving this refractory timekeeping is not fully understood but is heuristically described as an interval timer of functional value (Gorman, 2001), as the transition between winter and summer phenotypes accrues slowly over 2-3 months, at a time that coincides with the onset of breeding season which lasts roughly one month before summer solstice to three months after. As a consequence, the age and timing of pubertal development in the Siberian hamster is determined by early photoperiodic history, dependent upon the timing of birth within the breeding season, or most directly, the timing of birth relative to summer solstice. The breeding season spans from late spring (May) until the end of summer (September). Pups born in May are

exposed to long and increasing daylengths, immediately undergo puberty by five weeks, and typically produce their own offspring during the same summer they were born. Pups born in late summer or early fall are exposed to shorter, and decreasing daylengths, which results in the initial emergence of the winter state, thereby delaying transition to summer phenotype, and consequently delaying puberty, until the following spring (Gorman, 2001; Butler et al., 2007a). Of primary interest for the purposes of this paper, are the long-term consequences of immediate or delayed puberty with regard to aging and longevity. Considering the lifespan of the Siberian hamster is typically only two to three years in a controlled, predator-free laboratory environment (estimated mean 30 months), the difference in timing between life stage transitions (juvenile to adult) would predict 97% (29/30 months) of life in adulthood when immediately going through puberty compared to 73% (22/30 months) of lifetime in adulthood for those pups born late in the fall.

Naturalistic lighting is typically not employed in laboratory settings, but instead animals are housed under fixed artificial photoperiods providing enough daily light (i.e., photophase) to maintain the reproductively capable summer state. Explicitly, Long Days (LDs) are photoperiod conditions providing a photophase long enough to drive the stimulatory summer state; Short Days (SD) refer to a short duration of daily light sufficient to induce the inhibitory winter state. The minimum photophase duration necessary to drive the LD summer phenotype is called the critical daylength (CD), and is roughly 13 hours in the Siberian hamster (Hoffmann 1982); however, this varies between species but also as a function of prior photoperiod

history. Transferring 15 day old Siberian pups reared in 12 hours of light and 12 hours of dark (e.g., LD12:12) to LD16:8 more than doubles the mean testis weight by six weeks old compared to pups instead transferred to LD14:10, and even results in testis size significantly larger than pups of the same age raised from birth under LD16:8 (Gorman 1995). It is evident that a simplistic and proportional relationship between photophase and developmental rates cannot account for these results. Simulated Natural Photoperiods (SNPs) employed in the laboratory make incremental daily adjustments to the photophase duration by minutes each day by changing the timing of lights on and lights off to reflect annual daylight variations representative of a specified latitude. Hamsters housed under more rapidly changing photoperiods display significantly faster weight gain than those in slowly changing photoperiods. In addition, hamsters exposed to SNPs for two weeks are significantly heavier than hamsters in LD16:8, despite the fact hamsters in the latter condition received more absolute daylight (Gorman, 1995). While the CD of 13 h light is reliably replicated in fixed photoperiods, photoperiodic recrudescence has been facilitated in gradually increasing daylengths approaching 12.3 h, and photo-refractoriness has been induced with SNPs by gradually decreasing daylengths as long as 15.3 h (Gorman & Zucker, 1995a). The maximally stimulatory photoperiodic stimulus appears not to be the longest photophase of fixed length, but rather increasing photophase duration rapidly each day, demonstrating differences in somatic and reproductive growth rates between naturalistic and artificial photoperiod exposure. However, there has never been a study

that has determined whether these early life photoperiod driven differences in weight gain have any effect on lifespan.

Photoperiodic effects upon Aging and Lifespan

To my knowledge, only a single mammalian study has investigated how yearly patterns of photoperiod specifically influence lifespan: Experimental evidence identifies parameters of the annual photoperiodic waveform to influence mortality rates in the primate mouse lemur (*Microcebus murinus*; Perret, 1997). Male and female mean survival is proportionally reduced when housed in an artificially accelerated 8 month periodic cycle, alternating between 5 months in LD14:10 and 3 months in LD8:16, compared to lemurs exposed to natural sunlight which ranged LD8:16 to LD16:8 at latitude 48° N over 12 mo. Independent of gender and photoperiodic condition, when expressing lifespan as mean number of seasonal cycles, the average lifespan in each condition was 5 seasonal cycles, indicating the life expectancy of these lemurs is putatively related to the number of seasonal cycles. Unfortunately, the experimental design cannot pinpoint the manipulation responsible for driving the reduction in absolute lifespan in the accelerated season condition, as there were several unequal factors among treatments, such as natural vs. discretely abrupt seasonal transitions, proportion of life in photo-stimulatory and photo-inhibitory photoperiods, minimum and maximum hours of light, and exposure to vast differences in light spectrum wavelengths and intensity. Critical examination aside, these results, in conjunction with the variable timetable of sexual maturity observed in

the Siberian hamster, generate testable hypotheses as to whether differences in timing of puberty can cause differences in lifespan through photoperiodic control.

Although it has not been determined whether early life history differentiation (of puberty timing or weight gain) affects lifespan, there is reason to believe it can alter rates of aging. Age-related measures of reproductive fertility in females appeared different in post-pubertal females who delayed puberty from exposure to short days and those who immediately attained puberty through exposure to long days (Place et al., 2004). At 36 weeks of age, delayed maturity female hamsters exhibited a higher percentage of successfully birthed litters, had a greater litter size, and were estimated to have twice as many primordial follicles remaining in comparison to cohorts undergoing immediate sexual maturity. Manipulations resulting in delayed aging naturally support the hypothesis that these effects might also extend lifespan. Explicitly, if one photoperiod condition is found to slow aging compared to another photoperiod condition found to hasten aging, it follows that one would predict the group where the aging process is slowed would live longer. Determining this outcome is the primary focus of this dissertation.

It has been demonstrated that individual rates of aging, determined through a battery of biological and behavioral assessments, can account for up to 50% of the variation in lifespan among a cohort of old mice (Ingram et al., 1982; Ingram, 1983; Ingram & Reynolds, 1986). For example, if two older, age-matched subjects are assessed on some measure assumed to index aging (i.e., kidney function, physical fitness, thermoregulation etc.), the subject whose scores are more consistent with those

of younger subjects would be predicted to live longer than the subject whose scores more closely reflect those of much older subjects. In this dissertation, I will refer to biological aging as the consideration of individual rates of aging and the utility it bears toward accounting for individual differences in life expectancy, completely independent of chronological age. It is unknown how the manipulation of life history might subsequently alter rates of aging and ultimately lifespan, but there are several reasons to surmise that it might. First, as described above for mouse lemurs and hamsters, empirical evidence demonstrates the pattern of seasonal photoperiod putatively affects lifespan (Perret, 1997), and delayed aging of the reproductive system accompanies an extended juvenile life stage (Place et al., 2004). In addition, photoperiod manipulation post-puberty exerts age-delaying effects to the female reproductive axis in the Siberian hamster (Place and Cruickshank, 2010). Second, evolutionary theory asserts a proportional relationship between age of sexual maturity and lifespan, and therefore in this context the manipulation of sexual maturity suggests a proportional effect in lifespan. Third, there are a host of variables affected by photoperiod proposed to have repercussions on rates of aging or life expectancy: Reduced caloric intake, altered immune function, curtailed testosterone, and increased melatonin synthesis all accompany the short-day (SD) induced winter phenotype. It may also be the case that the summer to winter transition is predominantly harmful, or the winter to summer transition may prove extremely challenging to some facet of an animals' health, or possibly both transitions result in accelerated aging compared to a fixed and stable photoperiod. .

Life History Among Photo-stimulatory vs. Photo-inhibitory Photoperiods

It may not be transitions between phenotypes which prove harmful, but one of the many different parameters in physiology differentially associated with summer and winter phenotypes which may be responsible for the hastened demise of mouse lemurs housed in accelerated annual cycles. For example, melatonin is considered to be an oncostatic agent, a powerful anti-oxidant, protecting nuclear DNA from degradation by free radicals and decreasing likelihood of cancerous cell formation (Erren et al., 2003). Even a lack of melatonin has been implicated as a human carcinogen (Portier, 2000). It has also been postulated that the diminished pineal melatonin signal accompanying old age is an evolutionarily driven mechanism which programs a hastened demise in older mammals: Mice receiving melatonin supplements are reported to outlive controls 3-5 mo (Pierpaoli & Regelson 1994), and mice receiving fetal pineal grafts, implanted into the thymus, also outlive controls. Therefore it is likely that LD environments are subject to receive less of the protective health benefits of melatonin compared to SD, though it is unclear what the critical physiological dose might be required to functionally decrease the risk of cancer formation (Wu et al., 2013).

Another possibility is that the somatic condition associated with sexually functional phenotypes presents more of a health insult than sexually regressed states. Evidence for this has been observed in castrated males: Castration removes the source of male sex hormones and has been found to prolong lifespan in numerous species

including human eunuchs, who are reported to live an average of 17.5 years longer (Min et al., 2012).

Body Weight and Lifespan

Body weight is a product of multiple biological processes, including metabolic rate, digestive function, genetic factors, hunger drive, age, and relatively speaking, the health of an organism. Birth weight alone is predictive of longevity in mice and humans (Miller et al., 2002; Ong, 2006). Transgenic mouse αMUPA, a mutant strain exhibiting spontaneous reduced caloric intake, demonstrate enhanced longevity, in addition to strong circadian rhythms at old age (Froy & Miskin, 2010; Froy & Miskin, 2007; Froy et al., 2006). Forced reduction of body weight through caloric restriction results in increased lifespan in mice (Nelson and Halberg, 1986a; 1986b), primates Weindruch, 1996) and may even predict longevity in humans (Roth et al., 2002); however, exact mechanisms explaining how restricted feeding facilitates preventing or delaying onset of age related diseases remain unknown. It is therefore of interest to discover whether the spontaneous reduction in caloric intake associated with the SD induced winter phenotype is sufficient to also increase longevity in Siberian hamsters subject to several short day seasons.

The Aging Circadian System

As this dissertation tests whether photoperiod history affects rates of aging and lifespan, it is appropriate to describe age related changes of the circadian system as

well as age related changes to biological functions governed by the circadian system. An age-related decline of a functional circadian system has been well established in older animals and is thought to contribute to physiological deterioration that compromises lifespan in later life stages (Pittendrigh and Daan, 1974). Nearly all physiological functions show diminished circadian amplitude with age, including locomotor activity, temperature, and melatonin secretion (Dijk et al., 1999; Mahlberg et al., 2006), but many of these changes may be more appropriately accounted for by the age-related decline in the functionality of biological systems directly governing these processes. Nonetheless, quantification of a deteriorating master pacemaker has been documented in older rodents exhibiting not simply diminished amplitude of circadian parameters but significant alterations to functional waveform: hypothalamic corticotrophin-releasing hormone mRNA and anterior pituitary proopiomelanocortin mRNA transcription are under rhythmic control, with middle aged rats exhibiting diurnal waveform in the dorsomedial paraventricular nuclei, but no discernible mRNA rhythm in older rats (Cai et al., 1997). In addition, fetal SCN transplants in older rats rescues mRNA rhythmicity but does not restore the previously robust amplitude, suggesting not only a functional deterioration of the SCN but also a breakdown in the signaling pathway from the SCN to hypothalamus in older animals.

Aging and Locomotor Activity

Perhaps the most basic and hallmark circadian function known even among non-chronobiologists is the regulation of rest and activity. In humans, aging is

associated with changes in sleep-wake patterns such as fragmented sleep, altered free running period, and waking up earlier (Czeisler et al., 1992; Bliwise, 1992; Dijk et al., 2000). Similarly, changes to parameters of locomotor activity in rodents are a reliable indicator of aging; a marked reduction in circadian structured locomotor activity is a prominent observation in most species at advancing age (Nakamura et al., 2011). The duration of nightly locomotor activity (alpha) also becomes shorter and highly fragmented, alongside more inactive periods dispersed throughout the active phase of the circadian rhythm (Penev et al., 1997; Farajnia et al., 2012). An increase in the number of bouts during the inactive phase is also correlated to advanced aged (McAuley et al., 2002), and when death is imminent, locomotor rhythms of mice (three days prior to death) essentially reveal complete inactivity and can be used to identify moribund status (Tankersley et al., 2003). Various changes to phase shifting in response to light are observed in older rodents (Valentinuzzi et al., 1997; Rosenberg et al., 1991), as well as non-photic responses to light (Turek et al., 1995). Temporal patterns of alpha expansion in response to short day transitions are attenuated in older animals (Scarbrough et al., 1997) in addition to advanced phase angles of entrainment (Zee et al., 1992). Finally, observations of either shortening (Rosenberg et al., 1991; Witting et al., 1994; Morin 1988; Pittendrigh & Daan, 1974) or lengthening (Gutman et al., 2011; Valentinuzzi et al., 1997; Farajnia et al., 2012; McAuley et al., 2002) of the free running period in older animals are abundant; however, the direction and magnitude of this observation is inconsistent across species and between studies.

Aging and Body Temperature

In addition to locomotor activity, body temperature is another biological function under circadian control known to deteriorate with age. Deficits to thermoregulation are documented in aged humans (Van Someren et al., 2002; Pandolf, 1997; Duffy et al., 1998; Kenney & Munce, 2003) and smaller mammals (Florez-Doquet & McDonald, 1998). Decreases in circadian mesor and amplitude of temperature in aged humans (Kelly 2006; Kelly 2007; Weitzman et al., 1982; Touitou et al., 1986; Vitiello et al., 1986; Monk, 1991), primates (Perret & Aujard, 2006), and rodents (Halberg, et al., 1981; Refinetti et al., 1990; Satinoff 1998; Yunis et al., 1974) are consistently reported; this is likely a consequence of a less efficient thermoregulatory system in advanced age, where the maximum peak daily temperature is reduced. Aged mouse lemurs have lower overall body temperature while free running in complete darkness compared to younger lemurs (Gomez et al., 2012), as well as lower body temperature during the scotophase and photophase in LD14:10 compared to young adults (Terrien et al., 2009). Furthermore, circadian waveform of body temperature has been used to predict mortality in aged mice, incorporating parameters of hypothermia and circadian periodicity weeks prior to death (Tankersley et al., 2003; Weinert et al., 2002; Weinert & Weinert, 1998), followed by the complete loss of circadian fluctuation and severe hypothermia presaging imminent death. The deterioration of body temperature rhythms thus provides favorable means toward studying age related changes in a circadian controlled function over a lifetime.

Accelerated Aging through Light History

Mammalian longevity studies are costly, time consuming, and therefore scarce; however, a modest amount of literature on the effects of chronodisruption reports increased rates of aging. When exposed to a light cycle with a period drastically different from its own, an organism will respond either by a) entraining to the light cycle, undergoing large phase shifts each day, b) abandon all attempt to align its endogenous rhythm with the environment and free run independent of the photoperiod, or in some cases c) become completely arrhythmic. Curiously these three adaptive strategies result in differing degrees of health insult. For example, after confirming no statistical difference in lifespan (Oklejewicz & Daan, 2002), tau/+ hamsters and wild type Syrian hamsters were raised in LD14:10, and parameters of kidney and heart function were assessed at 4 mo and 17 mo (Martino et al., 2008). Unlike 17 mo wild type, tau/+ mutants show abundant manifestation of heart disease indicators, exhibiting interstitial fibrosis, myocardial collagen deposits, and increased heart-to-body weight ratios. Active fibrosis and collagen deposition was found in the renal cortex of the tau/+ hamsters, indicative of the development of primary renal disease. A separate control group of tau/+ hamsters were maintained in LD12:10, a period which most closely resembles their internal period, and at 17 mo, kidney and heart pathology was no different from wild type hamsters in LD14:10, eliminating the notion these diseases are explained by pleiotropic gene effects of the tau mutation. A separate cohort of tau/+ hamsters in LD14:10 were subject to SCN ablation at 4 mo and pathology was studied at 17 mo, where heart-to-body weight ratios were found to

be no different than wild type hamsters, identifying some parameter of a chronically resetting SCN contributes to accelerated aging as a consequence of circadian desynchrony.

LDLD Entrainment

Health hazards associated with chronic misalignment to the external environment are not confined to laboratory experiments in mutant hamsters but are also prevalent in the human work force: Compared to day workers, an elevated risk of health insults are identified in permanent or rotating night shift workers, including increased rates of cardiovascular disease (Ha & Park, 2005), obesity (Suwazono et al., 2008), and cancer (Schernhammer et al., 2006). A novel approach to ameliorating health complications is under investigation through the employment of an entrainment protocol known as LDLD bifurcation: Animals exposed to twice daily scotophases readily bifurcate wheel running activity into both of the two shorter dark phases (Gorman, 2001) and steady state bifurcated entrainment is achieved. While far-reaching implications of bifurcated entrainment are currently being explored for human application, it is completely unknown what other possible long-term insults to health may accrue under this alternative entrainment protocol. For this reason the LDLD photoperiod is included in this dissertation.

Dissertation Objectives

The main objective of this dissertation is to assess effects of various photoperiod histories on mammalian longevity. Utilizing the Siberian hamster, *Phodopus sungorus*, I will examine how lifespan is affected through manipulation of life history in both naturalistic and artificial contexts, examining survival rates between hamsters (1) undergoing immediate or delayed sexual maturation, (2) living in naturalistic or artificial photoperiods, (3) varying in the proportion of life spent in the winter phenotype, and (4) subject to a bifurcated light regimen of interest to the Gorman laboratory as a possible strategy for addressing human shift-work. The remaining chapters describe and assess a battery of circadian and non-circadian measures obtained from hamsters longitudinally throughout the survival study. Multivariate regression analysis will generate a predictive model of mortality, allowing a fuller mechanistic account of biological processes underlying changes in lifespan as affected by SCN-mediated light exposure.

Specific Aims

A) I will test whether lifespan is influenced by chronological age of sexual maturity.

B) The influence of seasonal versus fixed photoperiod history on lifespan will be assessed, measured through life history differences between summer and winter phenotypes, (i.e., proportion of time in winter vs. summer state, amplitude of physiological variation, number of phenotype transitions).

C) Rates of aging will be longitudinally assessed in parameters of wheel running activity in a novel protocol.

D) Rates of aging will be longitudinally assessed among parameters of body temperature in a novel protocol.

E) I will analyze (post-mortem) vital organ weights as a function of age and photoperiod history in healthy controls compared to hamsters succumbing to natural death.

F) The utility of a multivariate cox regression survival model is assessed, incorporating timing of life history events and age-related changes to parameters in body weight, wheel running activity, and locomotor activity.

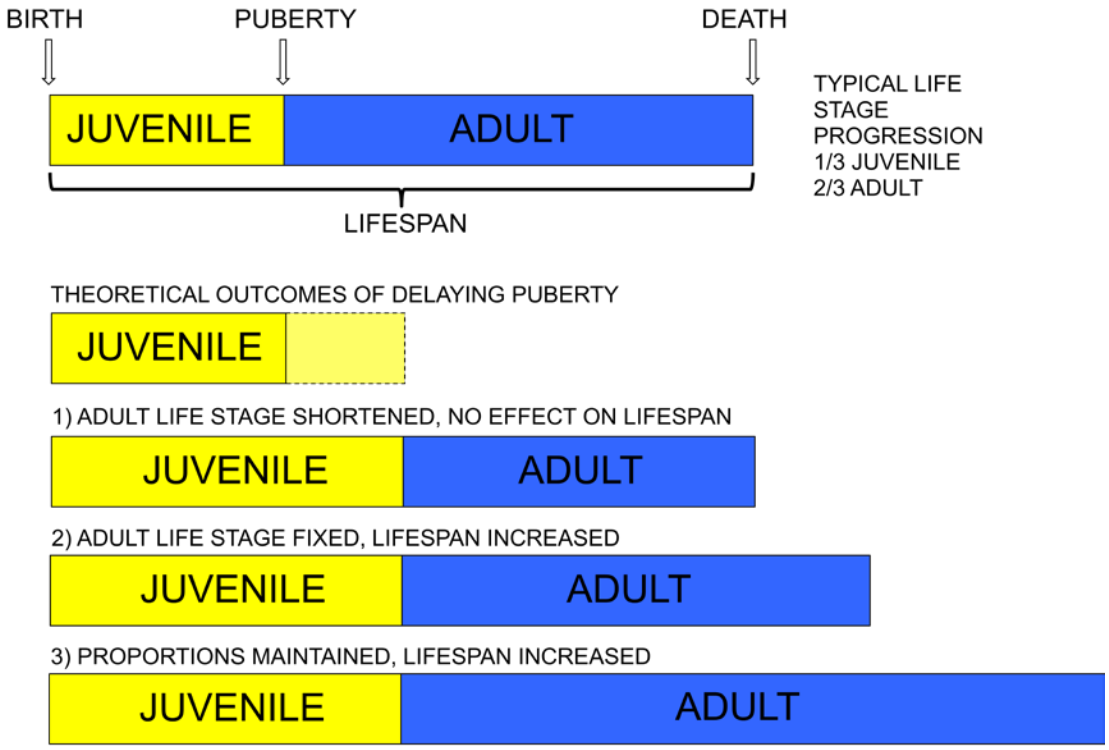

Figure 1.1. Three possible longevity outcomes resulting from extension of the juvenile life stage. Typical life stage progression (top) depicts evolutionary history theory stating most mammals undergo sexual maturity (e.g., puberty) at an age approximately equal to one-third of total lifespan. Three hypothetical outcomes may result from the prolongation of the juvenile life stage. First, delaying puberty results in no change to lifespan, and as a result, is accompanied by a shortened adult life stage. Second, the duration of adult life is maintained, and lifespan is increased by the number of days puberty was delayed. Third, the adult life stage maintains the fixed two-thirds proportion of time relative to the juvenile life stage duration and maximally increases lifespan.

CHAPTER 2. PHOTOPERIOD DRIVEN LIFE HISTORY DIFFERENCES DETERMINED THROUGH BODY WEIGHT AND PELAGE VARIATION

INTRODUCTION

Body Weight (BW) is a non-invasive physiological assessment remarkably useful for indirectly indexing parameters of substantial interest to this study, in three different components of life history. As reviewed in Chapter 1, literature cites BW as a relative measure of health, both early in life, and later as diminishing body weight correlates with advanced aging and in the end, predicts imminent death. Second, body weight correlates closely to testosterone output in male hamsters, and therefore allows estimation of the timing of puberty without needing to repeatedly chemically render hamsters unconscious in order to directly measure testes size. Finally, timing and strength of the photoperiodic response can be reliably assessed with changes in BW, especially when complemented with pelage scores. The purpose of this chapter is to determine whether these underlying parameters- overall BW, puberty timing, and photoperiodic response- can be manipulated through photoperiod history to influence longevity in a highly photoperiodic species, the Siberian hamster (*Phodopus sungorus*). The conclusions drawn with respect to survival analysis between photoperiod conditions in Chapter 4 will depend strongly on whether the desired manipulations (i.e., delaying puberty, photoperiod response to light timing) are confirmed through weekly BW analysis.

Experimental Design

Figure 2.1 depicts the photoperiod schematic of all six experimental conditions. 246 male and 80 female Siberian hamsters were weaned from the Gorman Lab Colony maintaining LD14:10 (Lights on 0600-1800 PST) at 18 days of age, born between the dates of December 18, 2007 and January 15, 2008. Hamsters were randomly assigned to live out the full duration of their natural life in one of six photoperiod conditions, the sole experimental manipulation of this dissertation. Two groups were maintained under Simulated Naturalistic Photoperiods (SNP) by weaning pups into one of two light tight photoperiod chambers, each equipped with SNP light timers (Paragon® EC71ST Electronic Sun Tracker Figures). The SNP timer was calibrated to a latitude of 50° N, yielding gradual changes in the daily photophase duration to reflect naturalistic annual fluctuations between a winter solstice of LD8:16 and summer solstice of LD16:8. For the first group, the SNP light cycle was set for a time of year coinciding with mid breeding season to facilitate early sexual maturity (SNP Early, or "SNP E") on SNP date, May 10, 18 days after the SNP timer increased past 14 hours of daily light, in order to also ensure a smooth photoperiod transition from the LD14:10 colony. The other SNP photoperiod condition was timed to reflect the end of the summer breeding season (SNP date September 5, 18 d after decreasing below 14 hour photophase), post-summer solstice, where pups were assumed to transition to the winter phenotype and delay puberty (SNP Delay condition or "SNP D") until the following photoperiod simulated spring season. The third photoperiod condition was constant exposure to Short Days "SD" consisting of LD8:16, where

hamsters would also enter the winter state and delay puberty until becoming photorefractory (i.e., spontaneously undergo sexual maturity despite the constant photo-inhibitory lighting), estimated to occur between 4-6 months of age. The fourth photoperiod condition was constant exposure to Long Day "LD" photoperiod of LD16:8, a photo-stimulatory light schedule that would rapidly induce sexual maturity. LD and SD photoperiod schedules were specifically chosen to match summer and winter solstices of the SNP groups. The fifth photoperiod condition consisted of square wave or Discrete Season "DS" photoperiod, where hamsters selected for this group lived under LD8:16, in the same chamber as SD hamsters, until 6 months of age, when they were transferred to the LD chamber exposed to LD16:8 until one year of age. These DS hamsters were shuttled between SD and LD photoperiod chambers every 6 months to create a discrete, artificially generated seasonal schedule roughly timed relative to the SNP D. Finally, hamsters in the last photoperiod group of this study were subjected to a schedule of 24 h light-dark-light-dark in LDLD8:4:8:4 "LDLD." The two photophases in the LDLD group occurred between 0900-1700 PST and 2100-0500 PST. Aside from LDLD, the middle of the other five photophase conditions occurred at 1300 PST, similar to the colony from which they were born. As a result, when hamsters in DS groups were transferred from LD8:16 to LD16:8, the photophase duration in the new condition doubled from 8 hours to 16 hours within a single day by initiating lights 4 h earlier and remaining on 4 h longer than the previous day. Hamsters were housed 4 per cage and siblings were divided up among photoperiod conditions; when more than six sibling pups were used they never

occupied the same cage. Dim scotophase illumination was provided via green LEDs. Hamsters incurring fight wounds were removed from the group cage and singly housed. At 3 months of age transponders were inserted subcutaneously into the upper back, allowing a scanning wand to identify hamsters quickly and also convey subcutaneous Body Temperature (BT) later described in Chapter 3.

The incorporation of these six specifically selected photoperiod groups serves to directly test how lifespan or rates of aging might be affected through the manipulation of photoperiod driven variations to life history. Explicitly, this design will test lifespan differences among early and delayed puberty through comparison of survival of SNP E, LDLD, and LD (early puberty) to SNP D, SD, and DS photoperiod groups. The influence of exposure to fixed vs. seasonally based photoperiod schedules on lifespan will be tested through the comparison between fixed (SD, LD, LDLD) and yearly (SNP E, SNP D, DS) conditions. Additionally, the number of winter phenotype transitions among these six groups also vary substantially ranging between 0 winter states (LD and LDLD), 1 winter state (SD), and multiple winter states in the seasonal schedules (SNP E, SNP D, DS), which will test the hypothesis that the "slow aging" effects associated with the winter state indeed attenuate measures of aging and ultimately, extend lifespan. The following analyses assess the timing and magnitude of life history variation as determined through Body Weight (BW) and pelage.

Delayed Puberty Timing- Methods

Procedure. Each week during cage change, hamsters were scanned, weighed, and pelage was subjectively scored. Hamsters were picked up individually out of the old cage, scanned for ID confirmation and weighed by an Ohaus© Scoutpro SPE401 digital scale coupled to the Bio Medic Data Systems, Inc.© DAS-6003 portable scanning device. Pelage was scored, and the hamster was placed into a fresh cage. All data were recorded digitally to a .txt file through the scanning device organized relative to the last scanned hamster, significantly limiting the number of errors accrued from the tens of thousands of measurements throughout the study. All statistical analyses throughout this dissertation include the use of SPSS©, Microsoft Excel©, and R©.

The subjective rating of pelage was visually scored on a seven point ordinal scale, ranging 1.0 (full summer) - 4.0 (full winter) at half increment intervals (e.g., 1.0, 1.5, 2.0, 2.5, 3.0, 3.5, 4.0), adopted from a method previously described (Duncan & Goldman, 1984a, 1984b).

Data Analysis. In this chapter life history differences in body weight (BW) patterns are characterized among six photoperiodic conditions. Utilizing weekly BW data (complemented by pelage) timing of puberty onset is determined and subsequent seasonal transitions in SNP E, SNP D, SD, and DS conditions. The influence of age at puberty onset towards the timing of age-related trends in older hamsters such as reduced photoperiodic BW response and overall BW decline in aged hamsters is tested. The attenuation of the photoperiodic response among seasonal groups (SNP E,

SNP D, DS) as measured by BW and pelage amplitude, and differences in timing of seasonal transitions as hamsters age are evaluated. SNP E and SNP D group comparison will determine whether age-related decline in seasonal amplitude is more closely associated with chronological days old, or rather the number of (either) summer or winter phenotype transitions. Group differences in maximum BW and age upon reaching maximum BW are assessed. Effects of living under LDLD on BW are investigated. Last, trends in body weight and pelage during the final year of life are analyzed for predictive value at the individual and group level, and whether age related changes are more reflective of absolute age or imminent death.

Early Photoperiod Effects. Random selection among pups into the six photoperiodic conditions was confirmed by assessing initial BW after weaning into groups to ensure equal BW means among conditions. Mean body weights among groups were equivalent at 18 day old weaning ($F_{(5,240)} = 1.5$, $p < .189$), grand mean wean weight = 18.2 g, standard deviation = 1.69 g. For the first five weeks of the experiment, pups were individually weighed at exactly 18, 25, 32, 39 and 46 days old (Table 2.1). After this period, hamsters were all weighed together on the same day on a weekly basis for logistical and practical reasons.

During the 8th day of the experiment (25 days old), a significant BW difference among groups emerged ($F_{(5,240)} = 23.8$, $p < .001$). Scheffe's post-hoc test confirmed homogenous subsets consisting of SNP E, LDLD, and LD in one subset, and SNP D, SD, and DS in the other. As expected, pups in the long day or increasing daylength photoperiods (SNP E, LDLD, LD) significantly outweighed pups in puberty

inhibitory photoperiods (SNP D, SD, DS; $t_{(244)} = 8.62$, $p < .001$), a trend that continued robustly throughout the last individually timed BW measurement at day 46. Post-hoc tests reveal homogenous subsets between these two growth patterns to persist during this time, with no significant differences among groups within their respective subsets at any week. This earliest differentiation implies both puberty onset in the immediate groups and physiological inhibition at 25 days of age in the delayed groups. Therefore, 25 days of age was used to define the timing of puberty onset among all male hamsters in SNP-E, LDLD, and LD, collectively referred to as Early Puberty groups. SNP D, SD, and DS will be collectively referred to as the Delayed Puberty groups.

Puberty onset in the Delayed Puberty groups was calculated using an algorithm fitting a moving 11-week cubic regression estimating weekly 1st and 2nd order derivatives in order to index growth rates of each hamster. The 1st order derivative values identified the initial local maximum following the initial local minimum associated with the non-permissive puberty growth inhibitions described above, at 25 d. If no other local maximums in the first year exceeded 80% of this growth rate, the age at this value defined the age of puberty onset. However if any additional local maximums in the first year reached slopes > 80% relative to this first local maximum, the local maximum whose timing was closest to 71 days prior to fur pelage dropping to 1.5 or 1.0 for three out of four consecutive weeks was selected. This parameter was incorporated because 71 days was the median latency found between puberty onset of SD hamsters demonstrating a single, unambiguous growth spurt and pelage scores as measured in the above fashion. Figure 2.2 illustrates BW and pelage of a

representative delayed puberty hamster and the derived algorithm estimating the onset of sexual maturity. The relationship between first order derivative of BW and latency of decreasing pelage scores are not significantly correlated, ($r_{(36)}$= -.027, p < .872). This evidence of a rather fixed latency among the two measures provides further validity as a structured constraint when choosing between more than one local maximum in calculating the growth spurt used to define puberty onset.

Delayed Puberty Timing- Results

Timing of puberty among Delayed Puberty groups was estimated using the algorithm described above and the results are illustrated in Figure 2.3. Table 2.2 summarizes additional parameter values obtained at the time of puberty (data in Table 2.2 represent actual BW values, not BW values predicted by cubic regression). One-way ANOVA reveals significant differences in puberty timing among Delayed Puberty groups ($F_{(2,116)}$ = 3.1, p < .040), where post-hoc comparisons depict SNP D to be older than SD at time of puberty (167 d and 146 d, respectively; DS = 158 d).

Delayed Puberty Timing- Discussion

Despite the younger age, SD had the lowest mean BW and smallest growth rates among Delayed Puberty groups during puberty onset. The earlier onset of SD may initially appear paradoxical in that the DS group was raised in the exact same chamber bearing LD8:16 for the first 6 months of life. However, both SD and DS group means estimate puberty well before 180 d of age, and it is important to note

these group differences at age of puberty are not remotely significant ($p < .414$). Significant differences in mean BW and mean growth rate between these two groups at time of puberty might be accounted for by the effect the photoperiod transfer of the DS group from LD8:16 to LD16:8 at 180 days had, since the algorithm incorporates a moving 11-week regression. It is possible the additional growth spurt associated with this transfer may have been a factor in one of two ways. The first way would be that the DS growth spurt which occurred in response to the short day to long day photoperiod slightly elevated the average BW in every hamster. This is rejected as a possibility because the real BW values were used at time of puberty and not the estimated values. Second, distributions of puberty timing appear non-normally distributed in DS: Elevated growth rates from the short to long day transfer could have possibly influenced the estimate of puberty timing in the DS group in a small subset of DS hamsters, specifically the later maturing animals. However, similar to the Early Puberty groups, where the initial non-puberty related growth spurt of the young pups could not be differentiated from the immediate additional puberty driven growth spurt, parsing out growth rates attributed to the unique DS transfer at 6 months would result in applying a unique algorithm specifically for this group, an undesirable option as it bordered on violating the integrity of group-wise estimates regarding delayed puberty timing. The additional parameter in the puberty estimate algorithm regarding the latency to summer pelage onset was designed to reduce noisy BW estimates alone as pelage would presumably change with the summer transformation according to the same rather inflexible timeline as the other groups.

An interesting trend with respect to delayed puberty timing is that the groups exposed to constant short day LD8:16 photoperiods through the first 180 days (SD and DS) reached puberty onset faster than the SNP D group. Combining SD and DS data and comparing to SNP D demonstrate a significantly earlier age of puberty ($t_{(118)}$ = 2.37, $p < .038$). This finding suggests a fundamental change in the putative interval timer regulating puberty inhibition: Accounting for the evidence of the interval timer at work in Delayed Photoperiod groups by 25 d of age, not at birth, the interval timer displayed 10.5% shorter latency in concluding the inhibitory process in fixed short day photoperiods [100 x {1-(152-25)/(167-25)}].

Lifetime BW trends, seasonal photoperiods-Methods

BW timing and amplitude were assessed in seasonal photoperiod groups (SNP E, SNP D, and DS) with the following algorithm: Utilizing the smoothed weekly BW data generated by the cubic regression employed to determine puberty timing, five week moving averages were calculated across the lifetime for individual BWs to find local peaks and troughs driven by summer and winter phenotype transitions, respectively, relative to positive and negative inflections of BW first derivative. Local maximums and minimums were identified in serial fashion until individual BWs exhibited a photoperiod-independent slow, gradual decline in BW associated with end of life (discussed below in "BW trends in last year of life"), identified when the last peak and trough were not statistically significant from one another. Within each local maximum the largest real weekly BW was chosen, where chronological age, SNP

date, and corresponding daily photophase duration (for SNP E and SNP D groups) were also determined. Similarly, time points highlighting local minimums were assessed and the lowest real BW within this interval was designated as the minimum time point. The only value obtained for all six groups was the initial maximum BW. For seasonal groups, the annual BW amplitudes were assessed by comparing group means from each photoperiod condition by order of 1st Summer transition (top panel, Table 2.3) in the DS group, the LD8:16-LD16:8 transition was arbitrarily regarded as Summer Solstice (June 21), and the LD16:8-LD8:16 transition was defined as Winter Solstice (Dec 21). BW trends were also assessed in similar fashion with respect to alignment of 1st Winter (bottom panel Table 2.3). It is acknowledged that in the arbitrary assignment of summer solstice to DS, the middle of the 6 months of LD16:8 photoperiod could have been selected but it was deemed more beneficial for it to be relative to SNP groups timing of maximum daylength exposure and have the solstice dates represent a qualitative change to the photoperiod environment. 1st Derivative growth rates calculated from the 11 week moving cubic regression algorithm were also plotted.

Lifetime BW trends, seasonal photoperiods- Results

Overall weekly means of male BW and pelage throughout the duration of the study are shown in Figure 2.4 and Figure 2.5, respectively. BW and pelage combined by photoperiod group are illustrated in Figure 2.6. Descriptively, the non-seasonal groups (SD, LD, LDLD) lifetime BW trends appear composed of three distinct phases:

Initial BW growth is strong throughout the first 4-6 months (accounting for variation between Early and Delayed groups), then tapers off, reaching maximum BW near 290 d (independent of puberty timing), and then begins a steady and systematic decline for the remaining life history. In the seasonal groups (SNP E, SNP D, DS), there is a clear and robust cyclic component to BW growth for 2-3 annual cycles, with maximum BW peaks declining each successive summer, after which a stable decline in BW is also observed.

Growth rates (e.g., 1st order derivatives) calculated by the moving 11-week cubic regression equation are paneled in Figure 2.7. As SNP E was the only seasonal photoperiod group to undergo Early Puberty, this group's rhythmic dampening pattern observed in annual BW trends was compared to SNP D and DS. To test BW histories across groups they were aligned with respect to the first summer, in which the first life stage (adolescence) ends and adulthood begins (e.g., undergoing puberty). Figure 2.8A and Figure 2.9A illustrate BW and pelage among these three groups aligned by the first summer solstice and their characteristics summarized in Table 2.4. Among this 1st summer based BW alignment, the maximum correlation coefficient obtained within any 100 week interval was $r_{(98)} = .778$ between SNP E and SNP D; $r_{(98)} = .580$ between SNP E and DS, and $r_{(98)} = .762$ between SNP D and DS (all $p < .05$).

Qualitatively, aligning the 3 seasonal groups by 1st winter (omitting SNP E's early 1st summer) and assessing mean BW history can be described as the uppercase letter "M," where BWs increase from the winter state, attain a peak value (the first arch), lower BW again in response to the SD inhibitory winter state, and then rise up

the following summer to reach the second and final distinct BW gain (the second arch, but not robust as the first summer response). BW responses to photoperiod after this second arch decisively "peter out" and are further described in the section below regarding "BW trends 1 year prior to death." The BW amplitude during the first year (summer to winter difference) was 15.68-16.14 g for all groups, where %BW loss to the winter transition was 29%, 29%, and 28% in SNP E, SNP D, and DS groups, respectively. The following summer to winter amplitude was more variable among groups, with mean amplitudes of 9.60 g, 12.75 g, and 21.10 g, producing %BW losses of 20%, 26%, and 39%. This results in amplitude attenuation of 59%, 81%, and 133% from year 1 to year 2 in SNP E, SNP D, and DS groups, respectively. Notably, the gain in amplitude from year 1 to year 2 in DS groups was mostly due to lower trough BWs in the second winter, as the sample size at this age among all three groups began to dwindle (SNP E = 6, SNP D = 9, DS = 5).

Upon closer inspection of SNP E and SNP D BW histories, a tighter relationship might be revealed if ignoring the 1st summer experienced by SNP E and aligning SNP E's second summer (see Figure 2.8B) with the 1st summers for SNP D and DS. Considering this relationship creates a difference of one year between timing of puberty among SNP E and the other two groups, there was no reason to believe a stronger relationship among BWs would underlie this arrangement. However, if the first winter phenotype transition is a bigger influence, or synchronizer upon biological aging (based on BW amplitude and waveform decline, rather than strict timing of sexual maturation) then this might be expected. Alternatively, SNP E was only

exposed to increasing daylengths long enough to achieve puberty but not to reach maximum BW, as summer solstice occurred around 9 weeks of age, when BW gain abruptly ceased. It is a possibility SNP E hamsters were not big enough for long enough, to fully "count" the puberty summer in the same way the other groups exposed to their first summer where they also reach maximum BW. Maximally aligned BW and pelage trends among the three seasonal groups are represented in Figures 2.8C. Ultimately, SNP E and SNP D groups attain a new BW correlation of $r_{(98)} = .977$ under this alignment (relative to 1st winter); this was also the maximal 100 week correlation coefficient among all possible alignments created at various offsetting weeks, (e.g., "sliding" the 100 week interval along one of the SNP BWs while the other remained fixed until the strongest correlation was found). Here SNP D had a median age of 113 days younger than SNP E hamsters. This "optimized" BW alignment resulted in correlation coefficients of $r = .859$ between SNP E and DS groups and $r = .908$ between SNP D and DS groups, where their real ages were only different by a week as DS had a median age of 122 days younger than SNP E. These BW trends among seasonal groups with respect to aligning the first winter (aka omitting SNP E's 1st summer) are consolidated in Table 2.5 and illustrated in Figure 2.10. When comparing trough and peak BW aligned by puberty summer (1st Summer), SNP E and SNP D groups are statistically significant through all comparisons made where each group has a sample size larger than n = 6, whereas in the Winter alignment arrangement these two groups do not differ statistically at any point.

Lifetime Pelage trends, seasonal photoperiods- Methods

To determine whether pelage scores followed this same alignment trend as BW, median values associated with the 3 groups were assessed, determining a 26 week period would contain the pelage waveform associated with the short day winter phenotype. These data were obtained for the first winter's pelage waveform (19-45 weeks following summer solstice in SNP groups), and exactly one year later the pelage waveform associated with the second winter phenotype. Due to pelage scoring data being both subjective and ordinal, Chi-square analysis were carried out separately for each winter. Pelage score categories with expected values less than 5 (i.e., 1.0, or 4.0) were omitted from the analysis in order to maintain integrity of the test.

Lifetime Pelage Trends, seasonal photoperiods- Results

Pelage timing relative to a) summer of puberty and b) 1st winter are illustrated in Figure 2.9. The initial winter pelage profile among the seasonal groups were equivalent, $X^2_{(6)} = 8.74$, $p < .25$, with median pelage scores of 1.5 or 2.0 making up for 90% of scores across all three groups. Conversely, pelage during the second winter was substantially different among groups, $X^2_{(4)}=27.40$, $p < .001$. Looking at median values among groups explains why, as 69% of SNP E counts = 2.0, 85% of SNP D counts = 1.5, and 58% of DS counts = 1.5 during the second pelage profile. This trend is evident upon visual inspection upon referring back to Figure 2.9, where SNP E

mean pelage appears to have a longer peak with consistently higher values across the 26 week interval.

Lifetime BW and Pelage, seasonal photoperiods- Discussion

While the main hypothesis driving this study was to determine if lifespan might be influenced by the manipulation of life history events, it was surmised the largest driving biological event that may emerge as a factor was the timing of puberty as mediated by photoperiod. Hamsters in the SNP E photoperiod were equivalent in BW gain as the other 2 Early Puberty groups, differentiating from the Delayed Puberty groups early on in the study and, in addition, complement a broad range of previous literature on the topic of seasonally driven puberty timing in the Siberian hamster. Therefore, although testis data were not measured, it can be confidently asserted that they indeed became sexually competent (as BW in this context closely tracks testicular function) at the same time as the other two Early Puberty groups differentiating via significant weight gain over Delayed Puberty groups after just 7 days in the puberty-permissive photoperiods. SNP E BW departed from this common Early Puberty trend of steady, gradual achievement of lifetime maximum BW, at mean age = 97 d, SNP Date = July 30, when the naturalistic photoperiod was decreasing the photophase duration to approximately 15.02 h (summer solstice = June 19, 16 h light).

In contrast to the early similarity in BW projections among all Early Puberty groups, BW and pelage trends of the SNP E hamsters are nearly identical to SNP D and DS groups when aligning initial SNP D and DS summers with the SNP E's second

summer (e.g., "1st Winter"), suggesting almost a putative "free" summer of initial puberty immune to biological consequence with respect to declining BW and pelage amplitude observed in each successive season. This is consistent not only with respect to mean peak and trough BW patterns, but also the timing with respect to the actual SNP date where these peaks and troughs occur (refer to Table 2.4 versus Table 2.5). Finally, the number of surviving hamsters exhibiting (BW based) photoperiodic responses is notably equivalent across groups if the second summer of SNP E is aligned with the first summer of SNP D and DS (see sample sizes below X-axis on Figures 2.10A versus 2.10B). Conversely, these similarities between SNP E and SNP D are not observed on any of these variables when assessed with regard to puberty as the synchronizing life history event. Therefore one of three conclusions can be made. First, perhaps the initial winter is a more influential life stage or life history synchronizing event with regard to BW and pelage trends compared to age at puberty. Second, perhaps species capable of being born early in a breeding season may have adapted the capacity to expedite immediate puberty without any permanent consequences to the organism's life stage timetable or rate of aging. The third possibility is that the fundamental changes in an organism's biology between adolescence and adulthood have no impact on life history events, although survival data must be recovered in order to support or validate implications of this interpretation of our data.

Of additional interest is that while SNP D and DS seasonal groups were exposed to similar histories, experiencing delayed puberty and some form of seasonal

photoperiod, that SNP E still bears a tighter correlation in BW history (SNP E-SNP D r = .977; SNP D-DS r = .908). These close similarities, despite the difference in timing also argues against confounding "lab room factors" or ambient effects, as SNP E and SNP D match equivalently, despite being in different physical photoperiod chambers, and these similar patterns are taking place at different actual physical times of the year. On closer inspection of mean BW patterns among these seasonal groups, it is evident that the waveforms among SNP groups and the square wave-based DS group are qualitatively distinct (Figure 2.4). The SNP group BW patterns tend to reflect the smooth, cosine-wave nature of the naturalistic photoperiod to which they were exposed, whereas the DS pattern of weight gain and loss can only be described as jagged and almost in discrete intervals of growths and losses, which interestingly, is also descriptive of the photoperiod schedule defining the group.

Although 1st winter BW data would be valuable to collect among SNP D and DS conditions, it was impossible to properly obtain, as rapid initial juvenile growth rates at this time (independent of sexual maturity) complicate the analysis. However, the collection of pelage scores among this first SNP D winter phenotype (as well as DS and SD groups) was obtained specifically to supplement seasonal trends represented by BW, as the primary measure; BW is continuous and objective, whereas the subjectivity of pelage scoring is less than ideal as a primary dependent variable in diagnosing phenotype state. Indeed, SNP D pelage scores during the first winter appear equivalent in intensity and duration as both SNP E first winter and DS and SD's pre-puberty winter. It is worth noting explicitly again that for all intents and

purposes that SD and DS physically shared the same chamber and were randomly distributed throughout the LD8:16 chamber during the first 6 months of life and in addition to bearing equivalent BWs and puberty timing, display identical pelage profiles (SD and DS groups; see Figure 2.5) as would be expected from a pseudo-"matched-pairs" control during the 1st 6 months of life.

Timing of Maximum BW

All 3 fixed photoperiod males arrived at equivalent lifetime maximum BWs (LDLD = 52.67, SD = 49.94, LD = 49.63, $F_{(2,122)} = 1.8$, $p < .057$) at statistically equivalent mean ages (LDLD = 285, SD = 297, LD = 279, $F_{(2,122)} = .51$, $p < .602$). Additionally, including SNP D's BW values and timing data into the analysis did not produce statistically significant differences, surprisingly revealing that puberty timing and the age which maximal BW is reached are not interactive factors. Data also show the photoperiods governing SNP E and DS had the most profound and opposite impacts on BW life history. The LD8:16-LD16:8 transition at 6 months in DS provoked a heavier maximum BW at a significantly earlier age (mean weight 56.49 g at 235 d). As for SNP E, this was the only group to have a qualitatively distinct BW history, in two respects: First, the initial immediate puberty growth was attenuated upon reaching summer solstice, at a significantly lower BW (45.38 g). Because of this lower initial BW maximum, this was the only seasonal group to display an increased mean BW during the second summer phenotype transition, making SNP E the oldest group at time of their absolute maximum BW. However, the mean BWs during the

SNP E second summer was no different than SNP Ds maximum BW during the first summer when puberty occurred, as discussed above. What follows is a distinct 3-tier stratification among BW histories between the earlier BW maximum in DS, the status quo for this study's BW maximum trends (SNP D, LDLD, SD, and LD), and a much later BW maximum in SNP E (405 d). Chapter 5 will assess these differences in BW parameters to determine if either timing or absolute mass are predictive of survival.

Finally, it is concluded that the qualitatively distinct photoperiod of LDLD, as assessed by BW patterns, did not significantly differ with respect to growth rate, maximal BW, or age at maximum BW when compared to the most closely matched photoperiod of our study, LD, with both groups experiencing early puberty, and a fixed absolute duration of 16 h of light per 24 h cycle.

Body Weight and Pelage Trends One Year Prior to Death

The final 52 weekly BW and pelage scores from each male hamster among all experimental groups were assessed. 17 hamsters did not live long enough to provide a full year of BW and pelage data and were excluded. A Mixed Model ANOVA (6 Groups x 52 Weeks) was used in both analyses.

Consistent with aging literature, overall, BW decreased as hamsters approached their demise ($F_{(51,\ 11373)} = 111.9$, $p < .001$), exhibiting a steady decline throughout the last year, and losing mass at a faster rate 4-8 weeks prior to death. A significant difference in the final year BW was found between groups, ($F_{(5,\ 223)} = 3.2$, $p < .008$) as well as significant Photoperiod x Week interaction ($F_{(255,\ 11373)} = 1.5$, $p <$

.001). Post-hoc Scheffe's tests reveal DS, the group with the heaviest weekly mean BW, to differ from the SD and LD, the two groups with the lowest weekly mean BW (MS_e= 2078.8, df = 223, $p < .009$ and $p < .026$ compared to DS, respectively). Weekly BW data are represented in two ways: a) as raw values, which are the actual weight measurements (Figure 2.11A), and b) as adjusted values, calculated by subtracting each hamster's final body weight measurement from each weekly raw weight (Figure 2.11B), to highlight the difference in body weight each week relative to final "death weight". In the adjusted BW values, for example, data during the final week for all hamsters = 0.0. Pelage trends in the final year of life are illustrated in Figure 2.11C.

Interestingly, DS hamsters also displayed a unique trend of gaining BW until 36-39 weeks prior to death, at which time they would also begin the decreasing trend, albeit at a lesser rate. It will be further examined in the survival chapter if the unique weight gain and loss trend in DS might be explained by a common temporal alignment of demise to the long day and short day transitions inherent to this photoperiod. While the remaining five photoperiod groups appeared equivalent with respect to decreasing BW patterns in the final year, it will be of interest to determine (in Chapter 4) whether the frequency of death appears to be influenced by SNP year among SNP E and SNP D groups.

To determine whether weekly body weight had any true predictive value of mortality, the trend of p values in the final year of life were investigated by assessing independent samples t tests and dependent samples t tests, comparing an array of current-to-previous BW means by averaging the last 1-4 weeks of life (current) to the

previous 2-12 weeks preceding death. Figure 2.12A illustrates the trend of p values among all groups' independent samples t-tests at every week of the final year of life, testing this week vs. last week; mean BW of the last 2 weeks vs. mean BW of the past 3-6 weeks; mean BW of the last 3 weeks vs. mean BW of the past 4-6 weeks, and finally, mean BW of the last 4 weeks vs. mean BW of the past 5-8 weeks. These data are novel in characterizing BW significance in population-wise mortality rate, but do not provide predictive or useful parameters toward identifying when a single individual may enter moribund status, where the actual current week prior to demise is an unknown variable.

Despite these data characterizing BW history only after knowing the date of death, comparing group body weight of one week to one week prior does not yield any mortality predictive value. In contrast, comparing the mean BW of the last 4 weeks of life to the mean BW of the last 5-8 weeks of life, at the population level, only reaches significance in the final 31 weeks of life, an early reliable indicator. In other words, statistically significant weight loss is consistently found week after week only once the hamsters have 31 weeks to live. At this point, p values associated with comparing either the mean of last 2 weeks vs. last 3-6 weeks, or the mean of the last 3 weeks vs. mean BW of last 4-6 weeks, only reaches $p < .01$ around 5 weeks prior to death. This may be a useful tool in indicating death not imminently, but rather > 30 weeks prior to death, and strikingly, the predictive nature of this assessment does not require knowledge of the age of the hamster.

As the more powerful and informative predictive value arguably only lies in predicting mortality at the individual level, dependent measures t tests were assessed at every week of the final year of life in all experimental males. At every week, t test measured a) mean BW of the most recent weeks (1-4 weeks from present) compared to b) mean BW of the previous weeks (3-12 weeks from present). Figure 2.12B shows the trends appear similar when comparing mean BW of the most recent 2-4 weeks against mean BW of anywhere from 3-12 weeks prior. Interestingly, individual hamsters reach and maintain until death a significant weight loss ($p < .05$, 2 tail) at 35 weeks prior to death, when comparing some recent interval of mean BW compared to a previous mean BW.

There was also an overall change in pelage across the final year of life, ($F_{(51,11322)}= 9.0$, $p < .001$) where mean and median pelage score during the final week of life = 1.5 (Figure 2.11C). Hamsters in non-seasonal photoperiods (LDLD, SD, and LD) gradually increased from a pelage = 1.0 common to their constant summer phenotype, whereas those housed in SNP-E, SNP-D, and DS appeared to diminish the amplitude of their winter phenotype response, creating significant photoperiod ($F_{(5,222)}= 17.1$, $p < .001$) and Photoperiod x Week interactions ($F_{(255,11322)}= 3.0$, $p < .001$). Interestingly, mean pelage in the DS group appears to decline from 1.75 at 52 weeks prior to death and flattens out at 1.4 around 36 weeks prior to death, where it remains until slightly increasing again around 8 weeks prior to death when it gradually increases again. These data, in conjunction with BW trend in this group, might suggest a stronger influence of photoperiod on timing of death than the other groups, as the

peak of weight gain loosely coincided with the darkening of pelage, suggesting a final transition to summer phenotype occurred 36-39 weeks prior to death, as well as a final winter transition 10-13 weeks prior to the average death.

CONCLUSION

This study was conducted where the only true independent variable was photoperiod schedule, in order to measure influence over dependent variables such as puberty timing, photoperiodic responses, rates of aging, and most important, survival. Weekly measurements of body weight, complemented by pelage, were an ideal measure to non-invasively determine whether our photoperiod manipulations indeed had the desired differentiation of life history events: Puberty timing, phenotype transitions, and trends in the final months of life are all reliably observed through changes in body weight.

The three early puberty groups began to demonstrate accelerated growth by 25 days old, where in contrast, the three delayed puberty groups transitioned into the winter phenotype, maintaining lower body weight and developing white pelage and ultimately delaying puberty onset until mean 156 days of age. In addition, weekly BWs provided the ability to measure whether the three groups exposed to seasonal photoperiods were in fact generating seasonal rhythms, as the Siberian hamster is a robustly photoperiodic species. First, non-seasonal conditions all generated lifetime BW history of similar patterns and reaching maximum BWs (49.63-52.67 g) at

equivalent ages (279-297 days), despite one of these groups being in a short day delayed puberty photoperiod schedule (SD). The three seasonal photoperiod groups all exhibited rhythmic BW variation, with highest mean BWs during long days and lowest BWs during short days; this pattern was strongly apparent despite the differential alignment of the annual photoperiod occurring at different ages in different groups, and also with respect to the physical real time of the year. This seasonal amplitude also attenuated each successive season, evident in both declining BW fluctuation and less robust winter pelage each consecutive short day season.

The trend in declining seasonal BW response was found most tightly correlated between groups when aligning the three seasonal photoperiods by first winter, and not by summer of puberty onset, revealing that when matching groups to biological age as measured by declining photoperiod responses, SNP E hamsters are chronologically 113 d older than SNP D and DS groups. Very few experiments have previously documented rates of aging in this particular species with respect to photoperiodic manipulation. One study demonstrates advanced reproductive aging in female hamsters born in early summer who undergo early puberty compared to females born late in summer who overwinter and prolong the juvenile state until the following spring (Place et al., 2004). These data appear in complete contrast to our results, where the SNP E born males rapidly underwent puberty, only to have their second summer season align most closely to the first summer of SNP D and DS hamsters. This difference might either be explained by gender differences, or from the fact that

measures of aging between studies were completely different (reproductive decline as measured by primordial follicle count and fertility versus assessing changes in BW).

The overall decline in photoperiodic responsiveness associated with advancing age may be a result of functional decline in one or more biological systems. First, the mechanism inducing the winter phenotype in the Siberian hamster is the long duration of pineal melatonin accompanying short days (or more directly, long nights). Pineal melatonin output has been reported compromised in older organisms, and a number of possible explanations are proposed. First, this could be a result of weakened SCN rhythm generation or diminishing output. Second, decreased pineal output or changes to melatonin waveform may be affected with age; calcification or hardening of the pineal gland has been implicated in the impairment of melatonin output (Hardeland, 2012). Third, regulation of hypothalamic thyroid hormone (T_3) has been identified as a key peptide in the metabolic phenotype of the Siberian hamster, where T_3 implants in SD hamsters induce summer type metabolic responses and testicular recrudescence.

Finally, analysis of BW in each hamster's final year of life reveals a trend in BW loss, which picks up significantly around 26-31 weeks until death. Finally, hamsters in the DS tended to gain weight roughly 48-52 weeks prior to death after which they conformed to the same rates of BW loss as the remaining groups, albeit from a higher mean weight. This trend in DS could be explained if there was a season-specific factor causing increased deaths during a specific timing of their discrete seasons as pelage for this group also decreases from 38-52 weeks prior to death, which coupled with the increasing BW at this time would be consistent with a winter to

summer phenotype transition at the time of death. Chapter 4 further investigates whether an increased instance of death among SNP E, SNP D, and DS photoperiods is associated with seasonal timing.

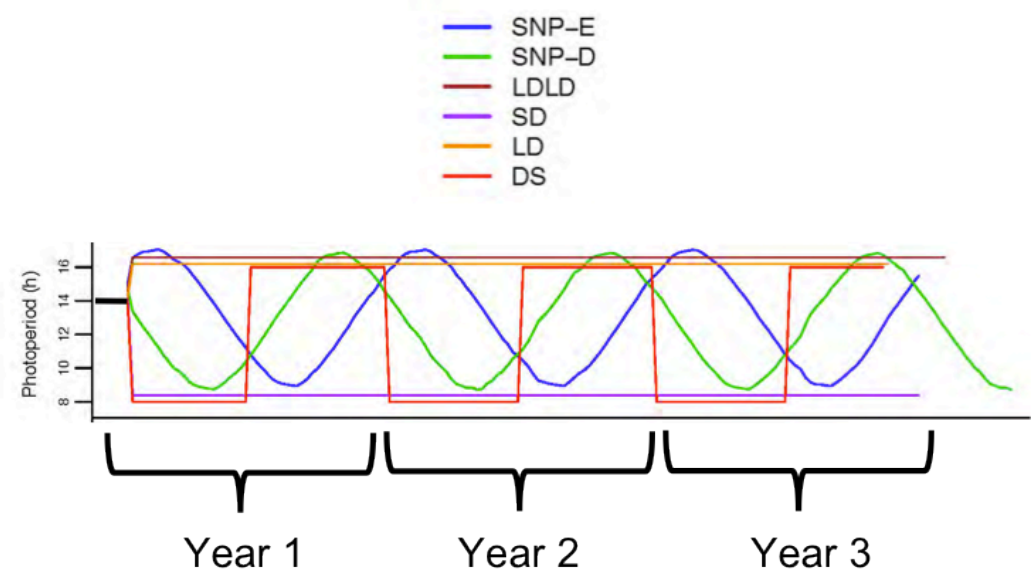

Figure 2.1. Schematic of the six photoperiod conditions employed in the study. Simulated Natural Photoperiod, Early Puberty = "SNP E" (Blue); Simulated Natural Photoperiod, Delayed Puberty = "SNP D" (Green); LDLD8:4:8:4 = "LDLD" (Tan); Short-Day, photo-inhibitory LD8:16 "SD" (Purple); Long-Day, photo-stimulatory LD16:8 = "LD" (Orange); Discrete Season = "DS" (Red). These photoperiod colors and abbreviations will persist throughout this dissertation. Three photoperiods vary seasonally- SNP E, SNP D, and DS, illustrated through changes to annual photoperiod duration (y-axis), ranging LD8:16 to LD16:8. SD is constant LD8:16; LD is constant LD16:8; LDLD receives two 8 h light pulses and is depicted as 16 h photophase. Drawing attention to the first six months, 3 photoperiod groups are visibly exposed to short or decreasing photophases (SNP D, SD, DS) that resultantly delay puberty. The other three groups are exposed to photo-stimulatory lighting (SNP E, LD, LDLD) and will facilitate immediate sexual maturity. Black solid line through the first 18 d depicts all animals were housed in LD14:10 colony prior to weaning at 18 d.

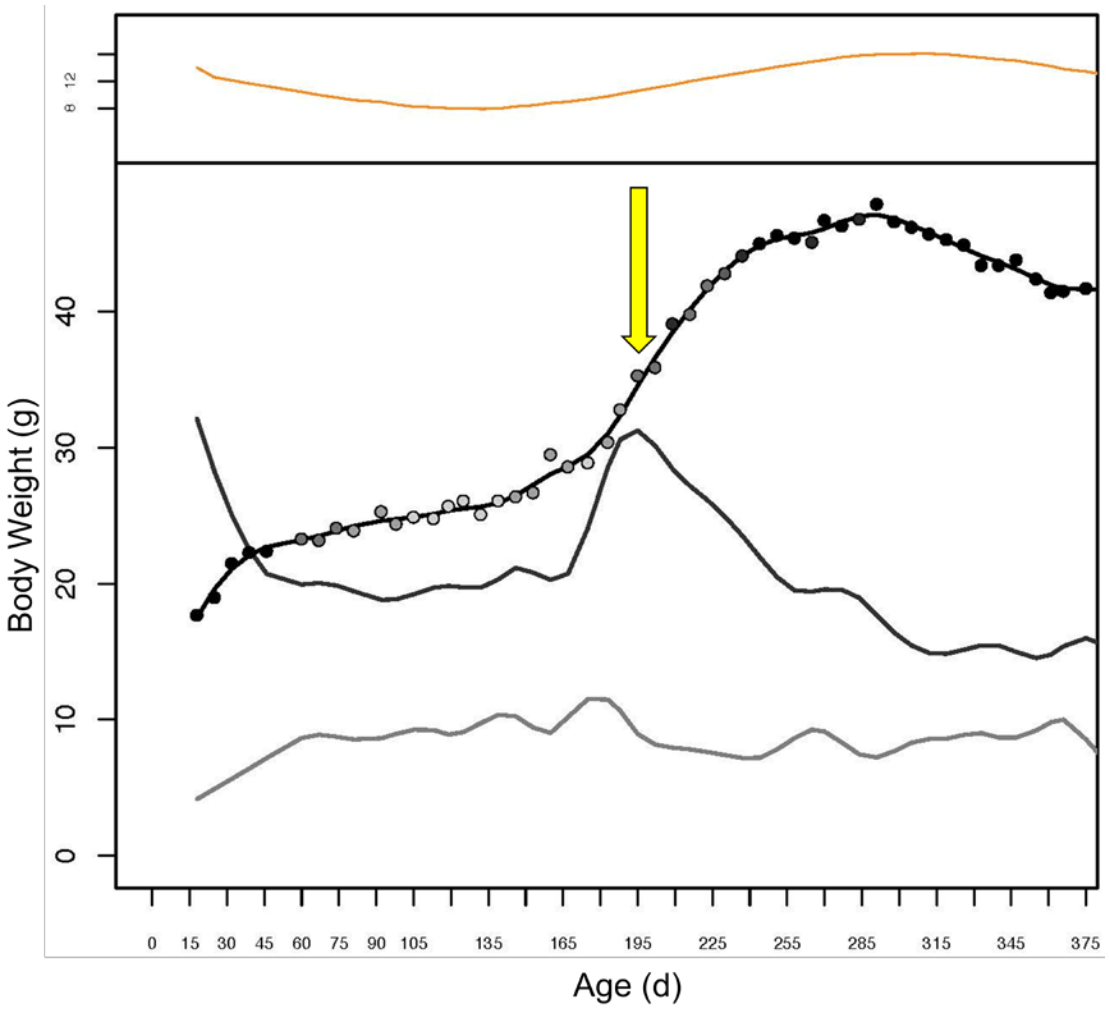

Figure 2.2. Representative weekly BW and Pelage history of a delayed puberty hamster through the first year of life. X-axis = Age (days), Y-axis = BW (g). Coloring of weekly data points represent pelage scores as follows: Black (summer) = 1.0, Dark Gray = 2.0, Light Gray = 3.0, White (winter) = 4.0. BW curve (top) was fitted using moving 11-week cubic regression. Darker gray line (middle) depicts 1st order derivative of the fitted BW curve; light grey line (bottom) represents 2nd order derivative. Arrow indicates calculated date of puberty onset. Chart on top of figure represents timing of SNP D photoperiod throughout the first year.

A

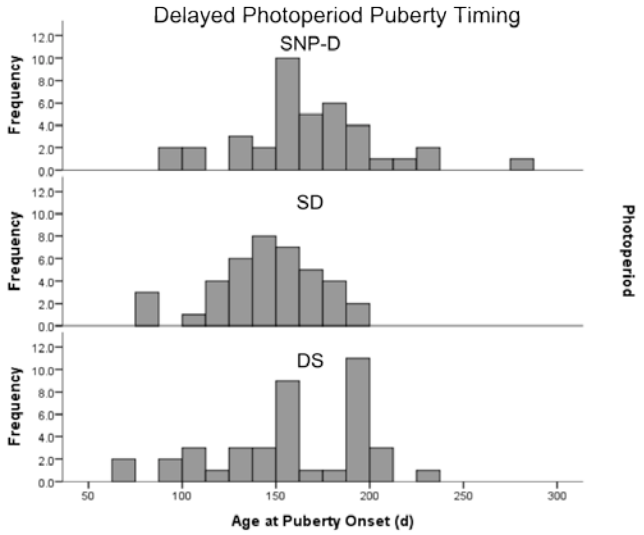

B

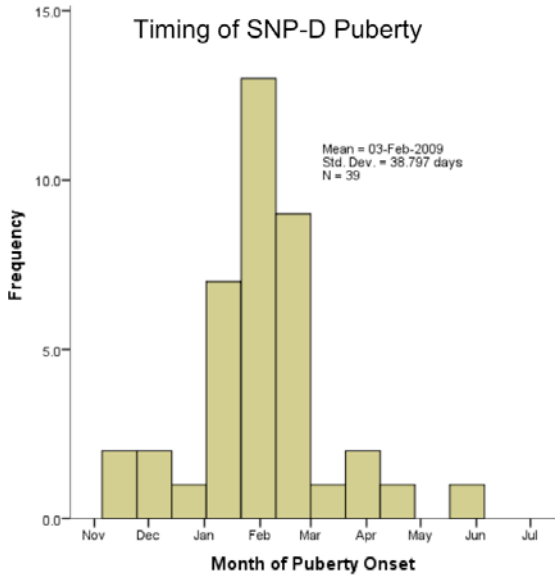

Figure 2.3. Timing of puberty onset (A) among individual hamsters in delayed puberty photoperiod groups. x-axis = Age (days), y-axis = Frequency. Top = SNP D (n = 39), middle = SD (n = 40), bottom = DS (n = 40). (B) Timing of SNP D puberty onset relative to SNP month (x-axis). Mean date of puberty onset = Feb 3.

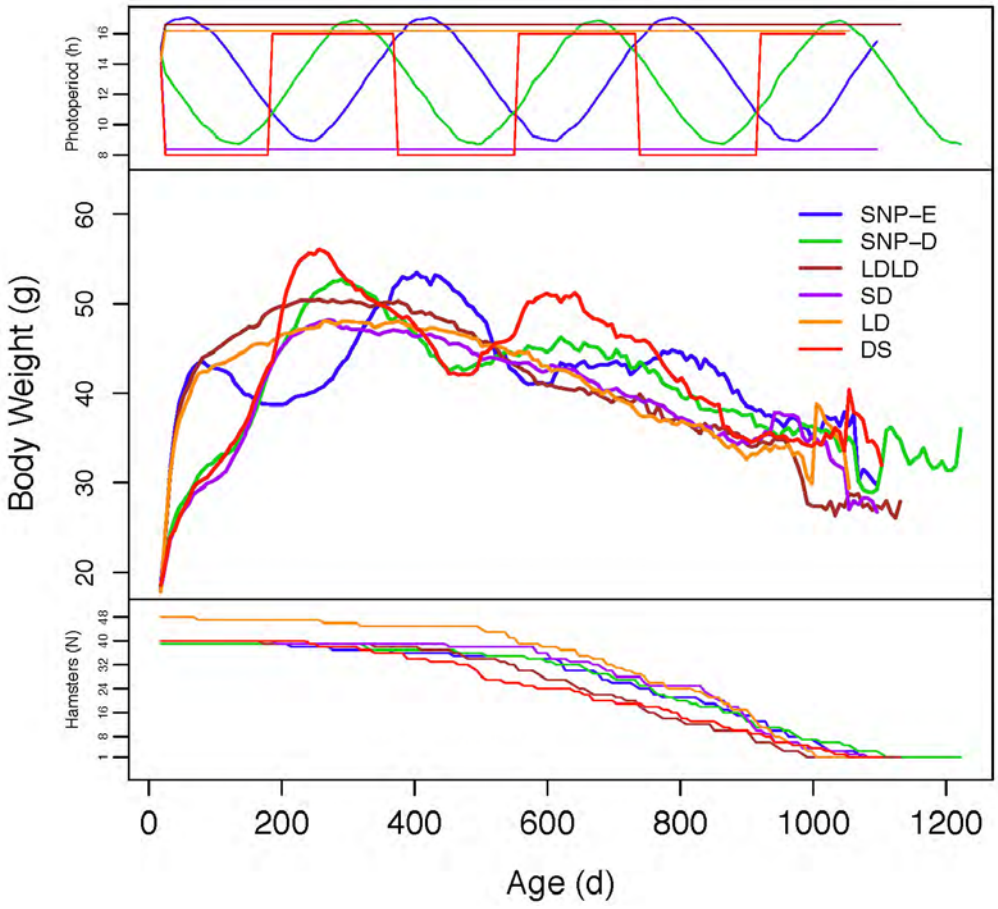

Figure 2.4. Overall lifetime hamster BW history. Mean BW among all male hamsters (N = 246) by photoperiod throughout the duration of the study. x-axis = Age (days), y axis = mean BW (g). Top panel depicts photoperiod timing of each photoperiod condition. Bottom panel represents number of hamsters living in each group over time.

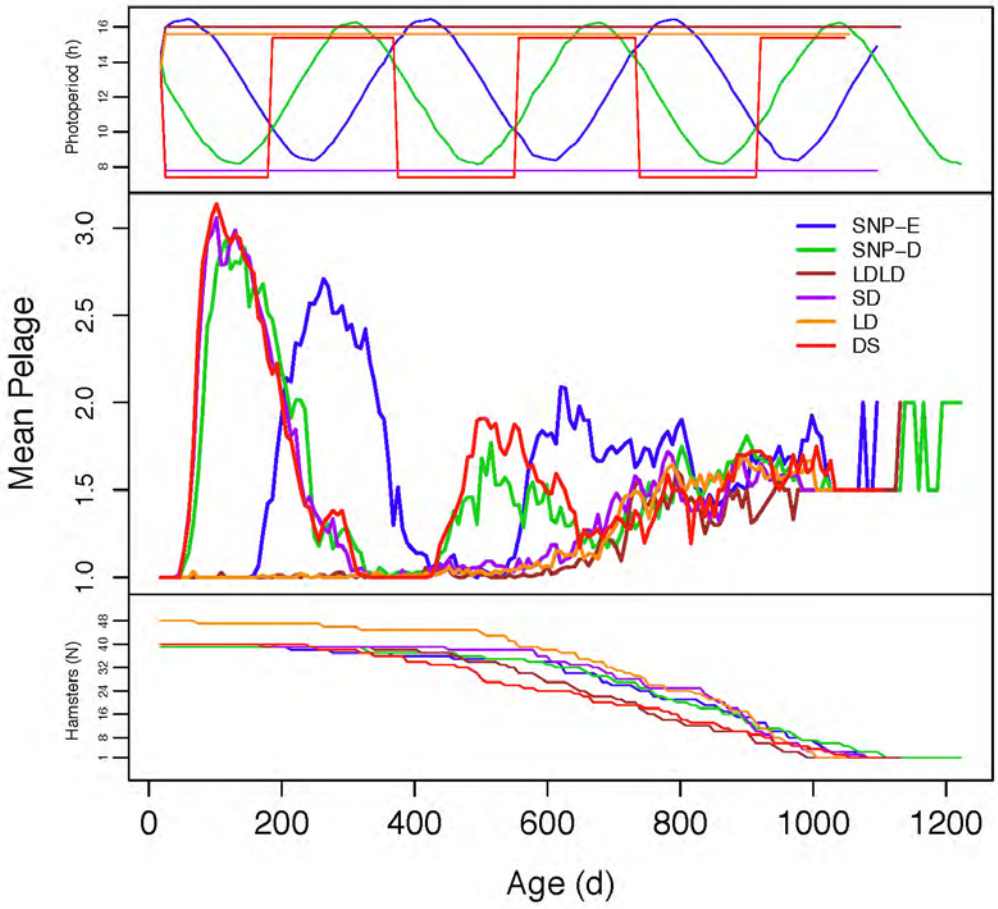

Figure 2.5. Overall lifetime hamster pelage history. Mean pelage scores (1.0 = complete summer pelage; 4.0 = complete winter pelage) among all male hamsters (N = 246) throughout the duration of the study. x-axis = age (days), y-axis = mean pelage score. Top panel depicts photoperiod timing of each photoperiod condition. Bottom panel represents number of hamsters living in each group over time.

A. SNP E Body Weight and Pelage History

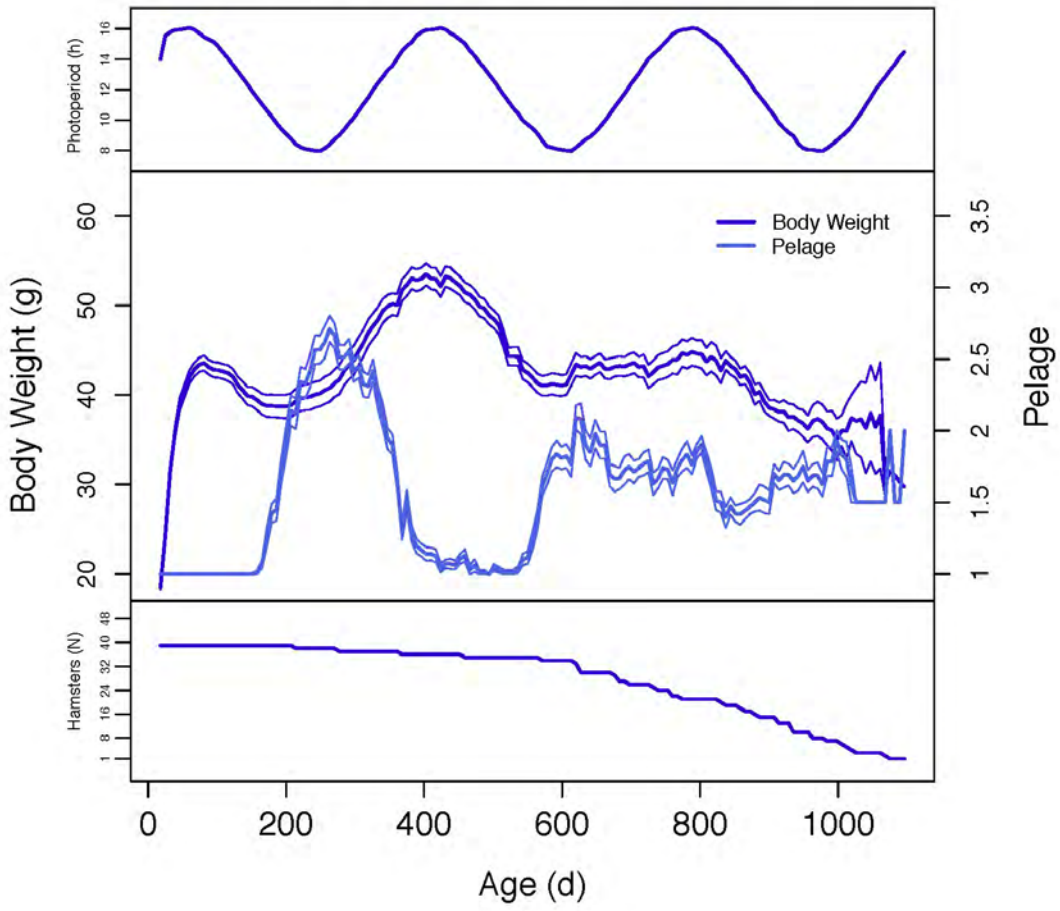

Figure 2.6. Lifetime weekly male body weight and pelage history. (A) SNP E mean ± SE hamster pelage and BW paneled by photoperiodic condition (top) and number surviving (bottom). X-axis = Age (d), y-axis (left) = Mean BW (g); Y-axis (right) = Mean pelage score. (B) SNP D, (C) LDLD, (D) SD, (E) LD, (F) DS. Conventions as in (A).

B. SNP D Body Weight and Pelage History

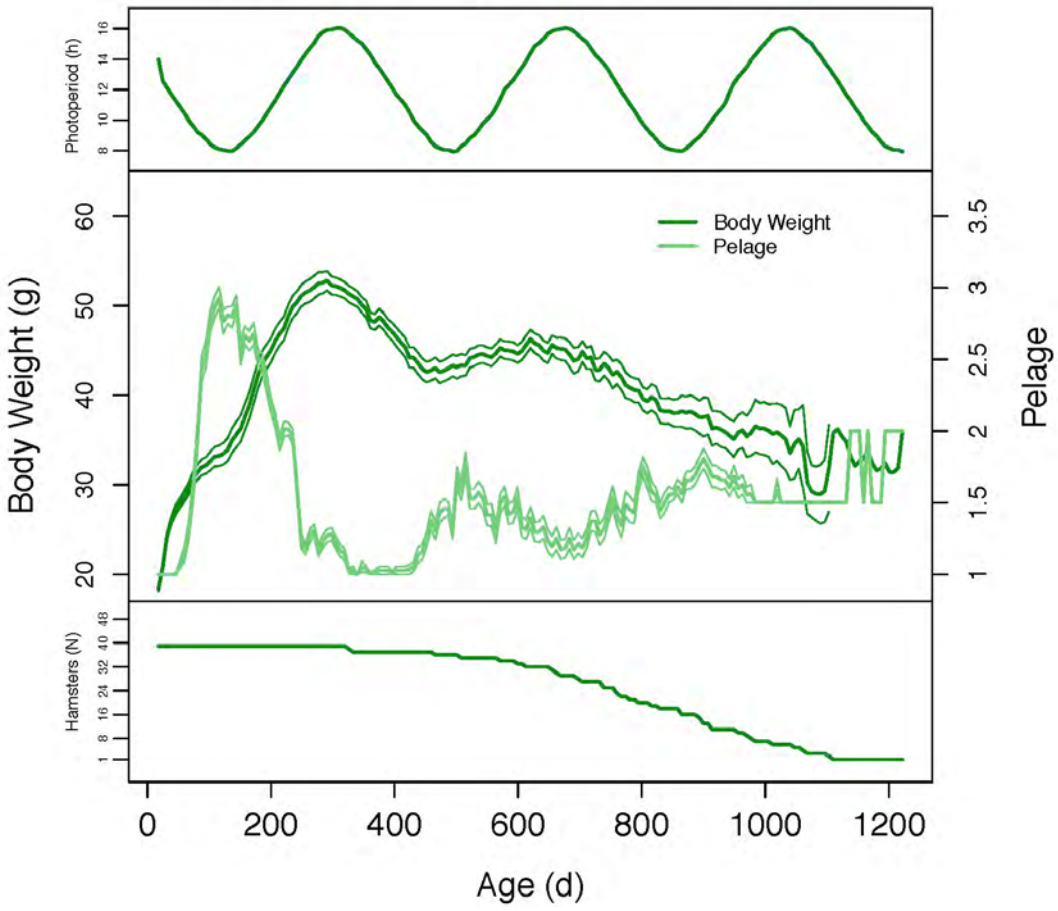

Figure 2.6. Continued.

C. LDLD Body Weight and Pelage History

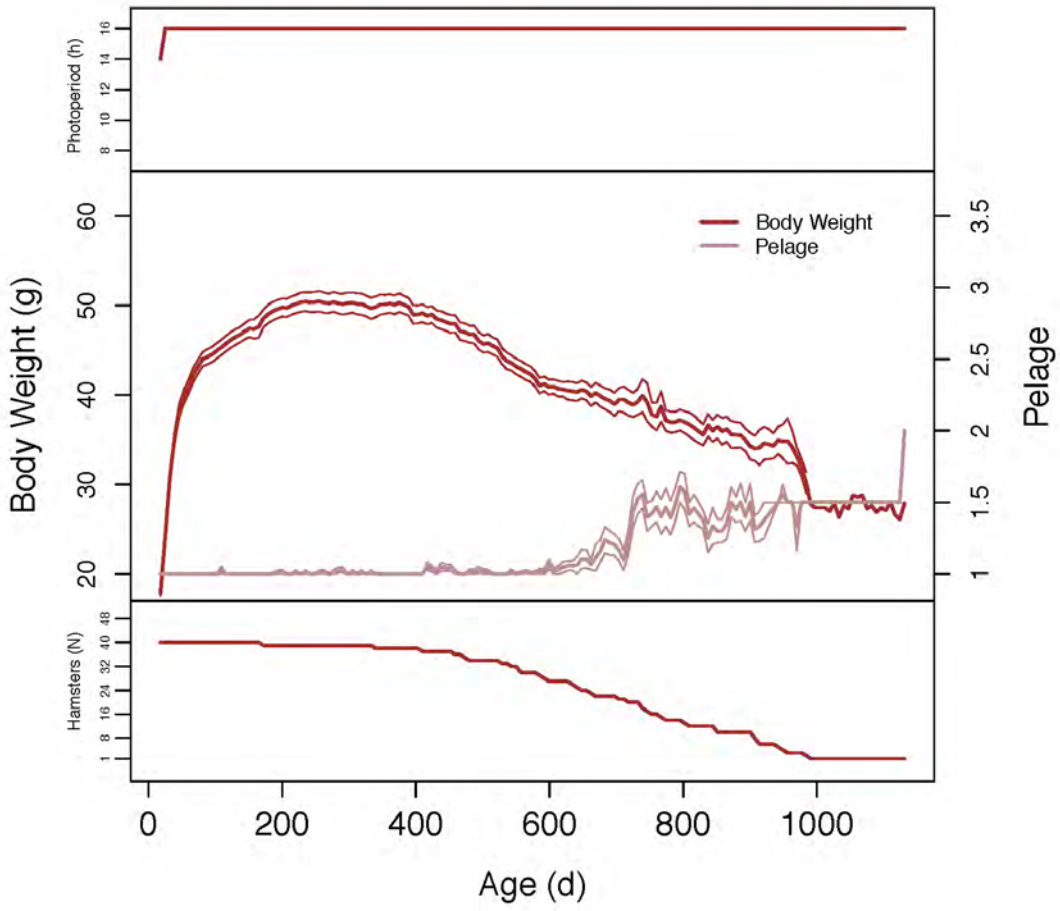

Figure 2.6. Continued.

D. SD Body Weight and Pelage History

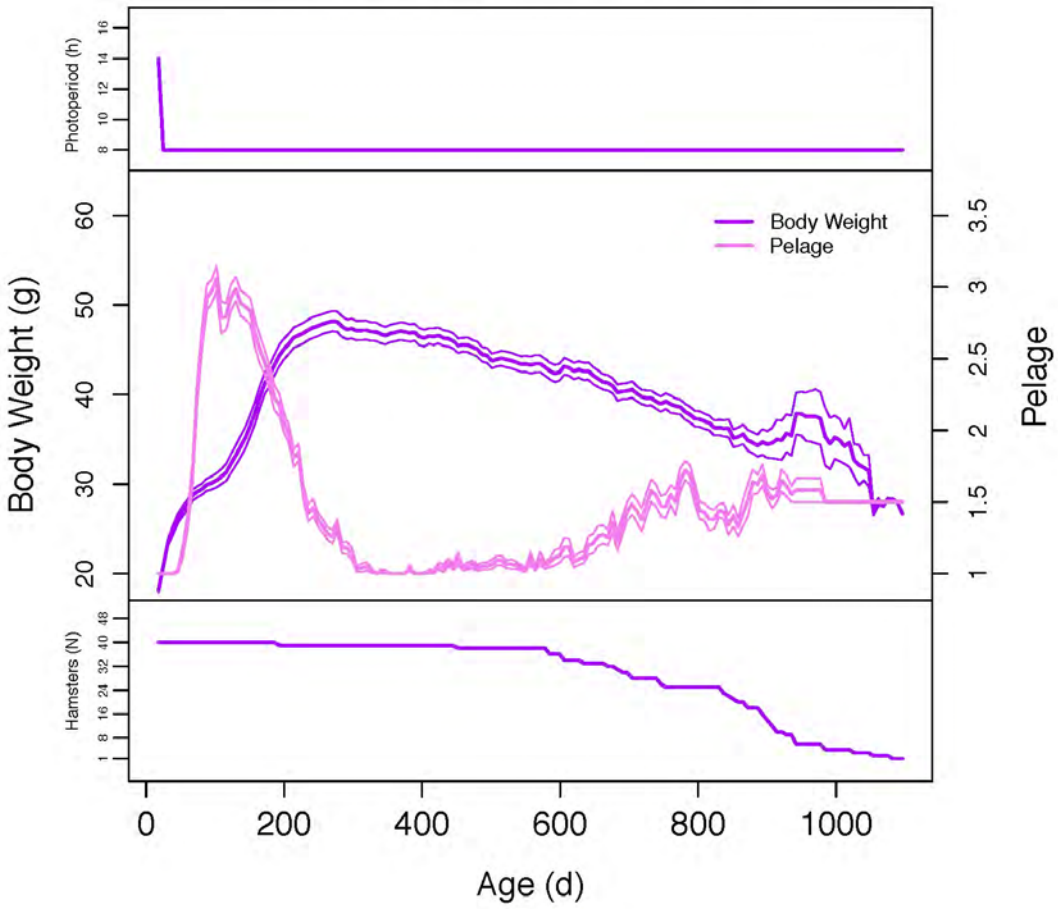

Figure 2.6. Continued.

E. LD Body Weight and Pelage History

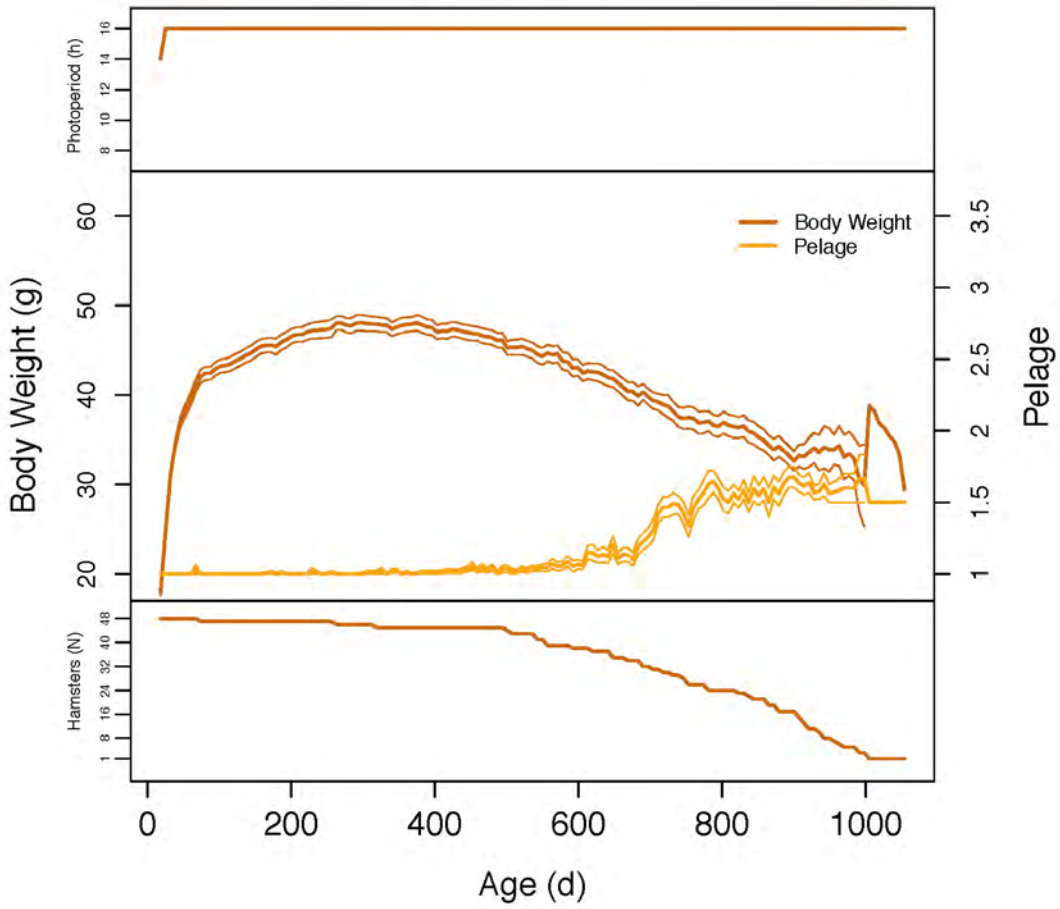

Figure 2.6. Continued.

F. DS Body Weight and Pelage

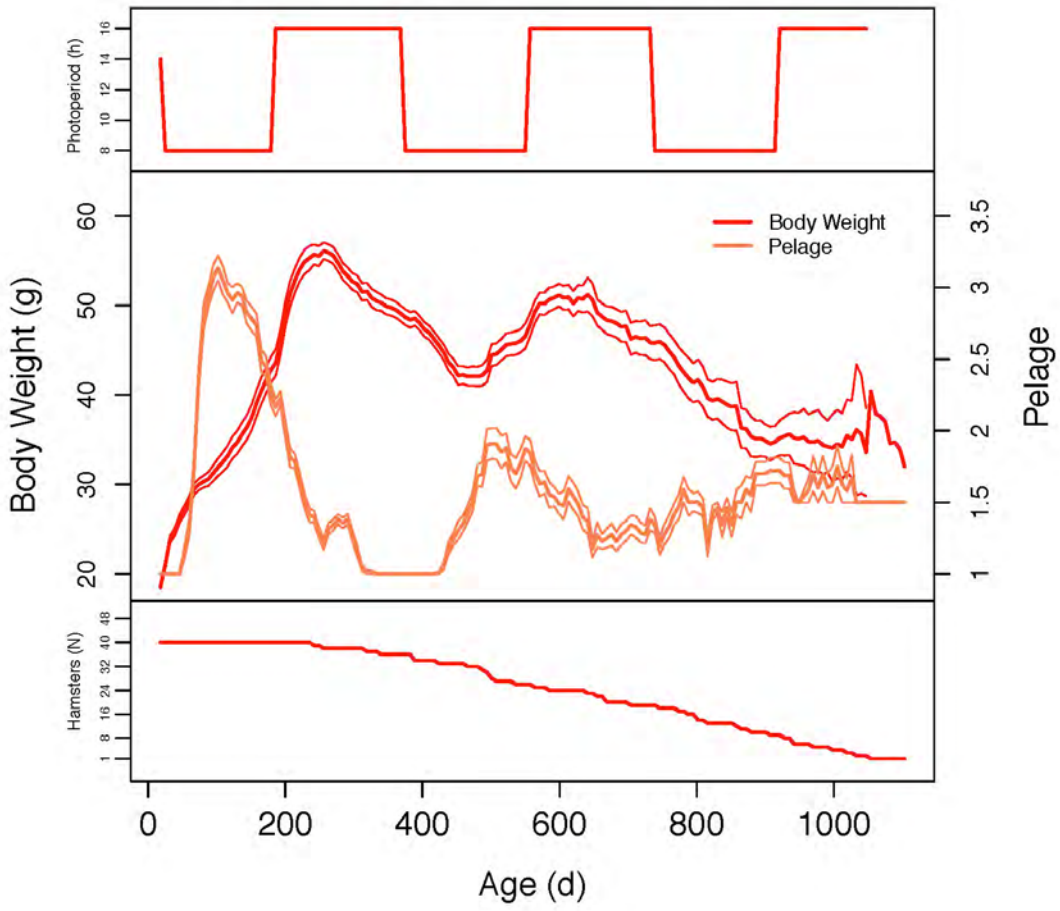

Figure 2.6. Continued.

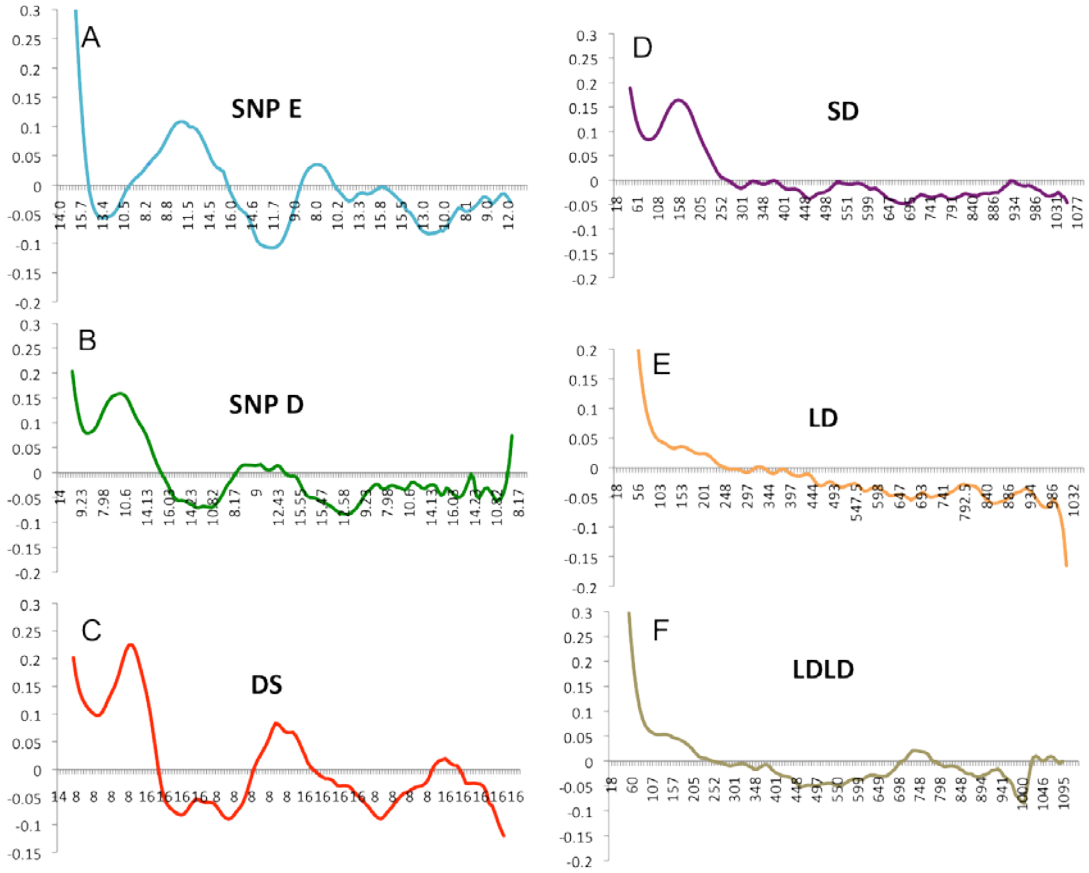

Figure 2.7. Mean 1st order derivatives of BW by photoperiod group. For seasonal groups (A) = SNP E, (B) = SNP D, (C) = DS x-axis represents current photophase duration (h); for fixed photoperiod groups (D) = SD, (E) = LD, (F) = LDLD x axis reflects chronological age (days). Y-axis = mean 1st order derivative of Body Weight. Data derived from 11 week moving cubic regression of real BW values.

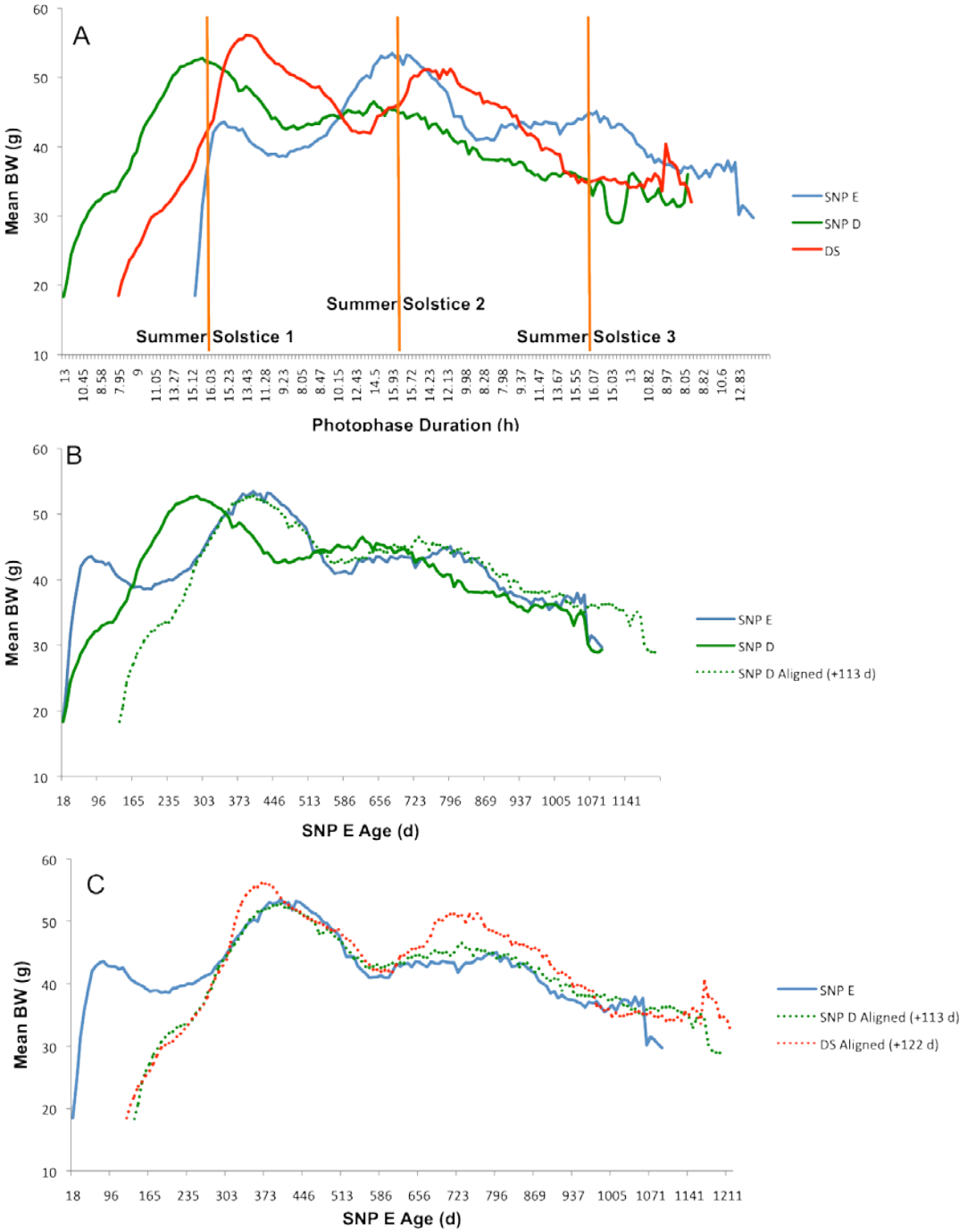

Figure 2.8. Alignment of mean BW in seasonal photoperiod groups. (A) SNP E, SNP D, and DS mean BW aligned by first summer solstice. X-axis = photophase duration (h), Y-axis = mean BW (g). (B) Optimal alignment between SNP E and SNP D occurs when SNP D is advanced 113 d. X-axis = age (d) of unshifted SNP E, y-axis = mean BW. Dashed line corresponds to offsetting SNP D BW by 113 d to yield optimal BW correlation between SNP groups. (C) Optimal alignment among all seasonal photoperiod groups, relative to SNP E. Conventions similar to (B).

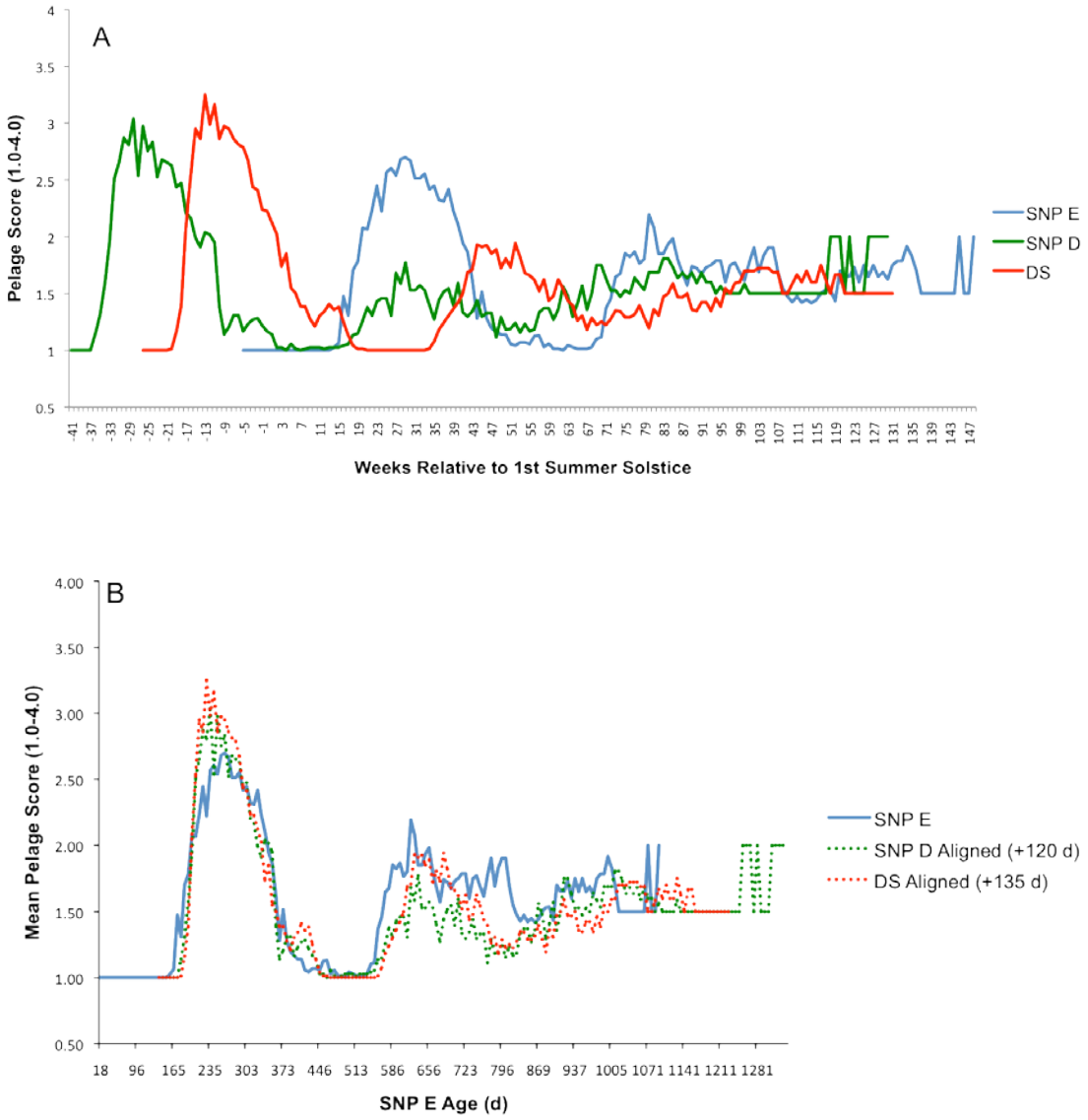

Figure 2.9. Seasonal pelage patterns. Mean pelage scores of hamsters in SNP E, SNP D, and DS relative to (A) timing of first summer solstice and (B) optimal pelage alignment relative to SNP E, corresponding to initial Short-Day exposure (first winter) among groups. X-axis represents weeks relative to summer solstice (A), and SNP E age (B).

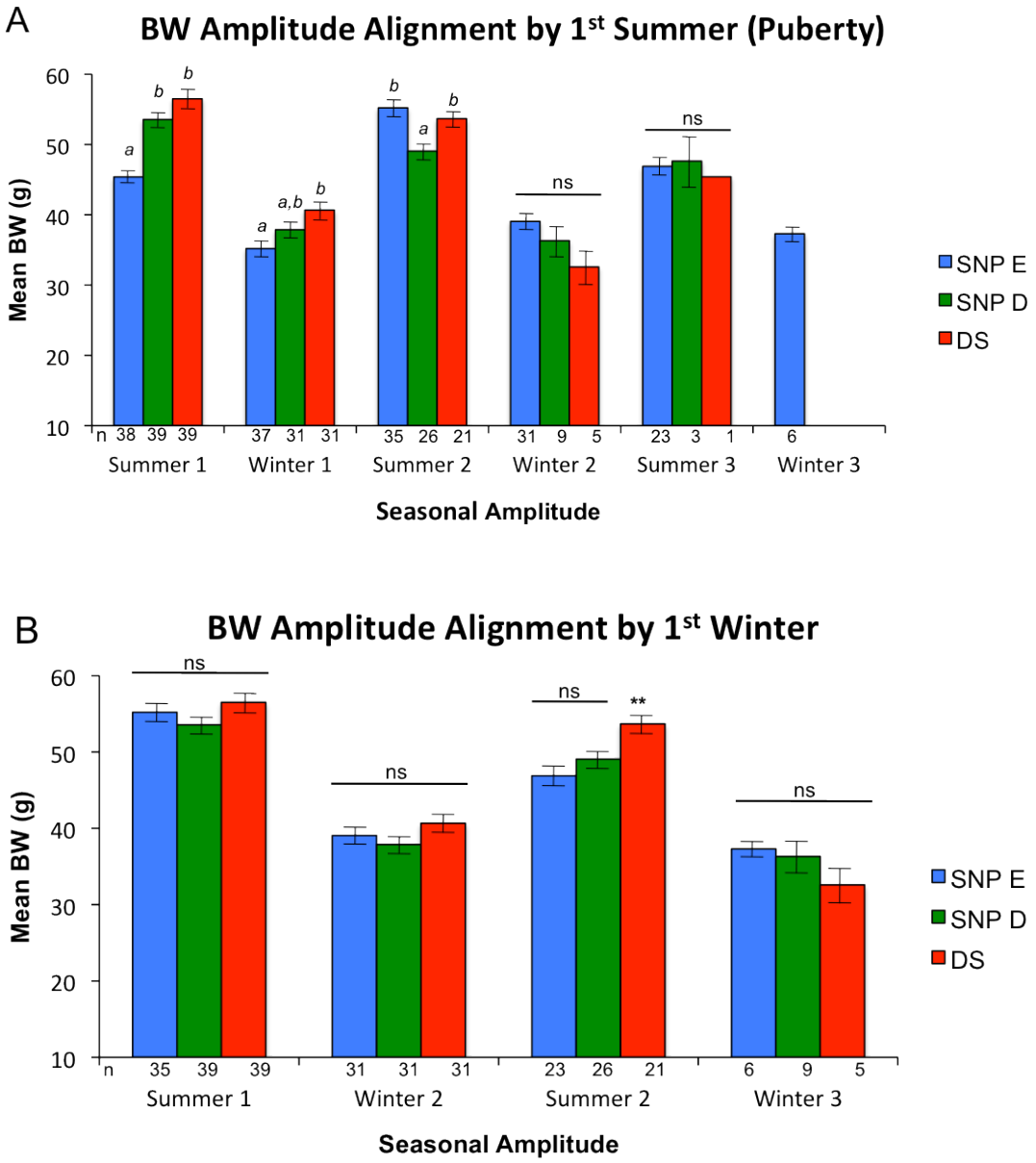

Figure 2.10. Photoperiodic response as measured by annual BW fluctuation of hamsters in seasonal photoperiods. Mean maximum summer BW and mean minimum BW in winter of SNP E, SNP D, and DS hamsters, organized relative to first summer (A) or first winter (B). X-axis = consecutive seasons, Y-axis = mean BW ± SE. Sample sizes are displayed beneath X-axis. Alignment of BW with respect to 1st winter, not first summer, accounts for differences between groups.

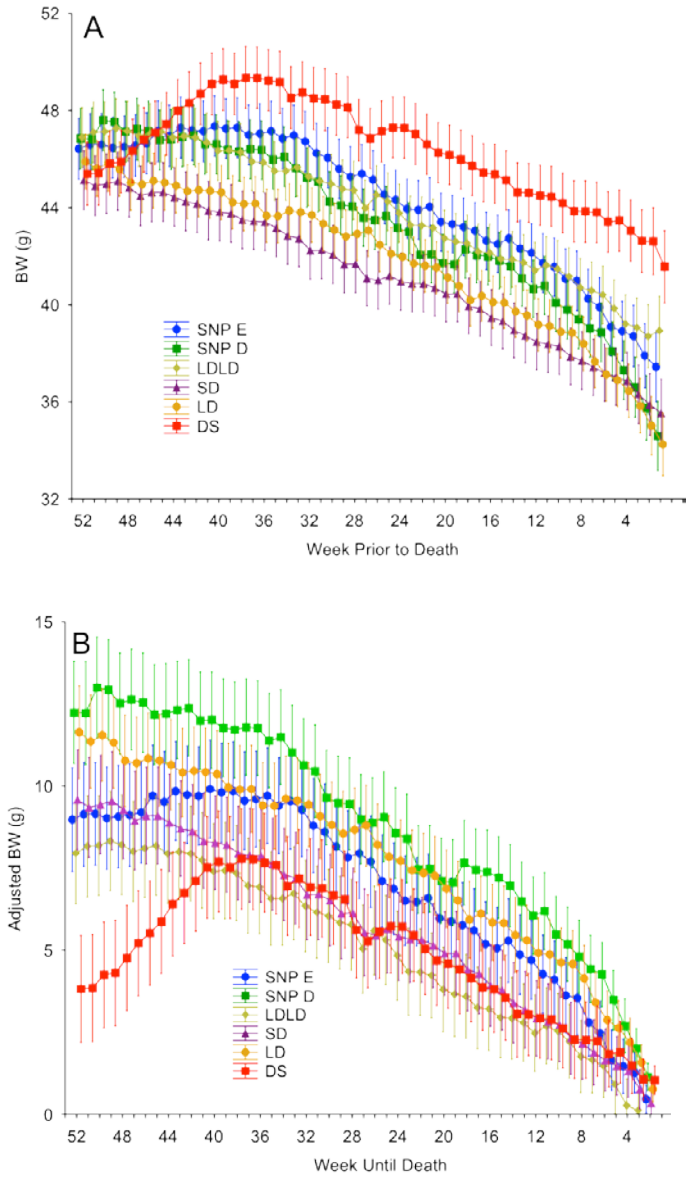

Figure 2.11. BW and Pelage in the final year of life. (A) The last 52 weekly BWs from individual males in the six photoperiods living at least one year (n = 229). Plots represent mean ± SE. (B) Adjusted weekly BW (mean ± SE) of hamsters in final year of life. Adjusted BW = current BW - final BW. Data points represent mean ± SE. (C) Mean ± SE pelage scores from final 52 weeks of life between groups.

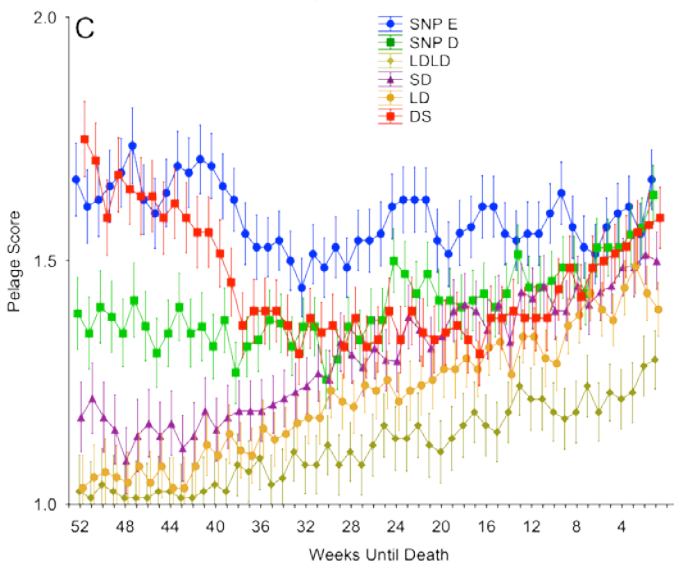

Figure 2.11. Continued.

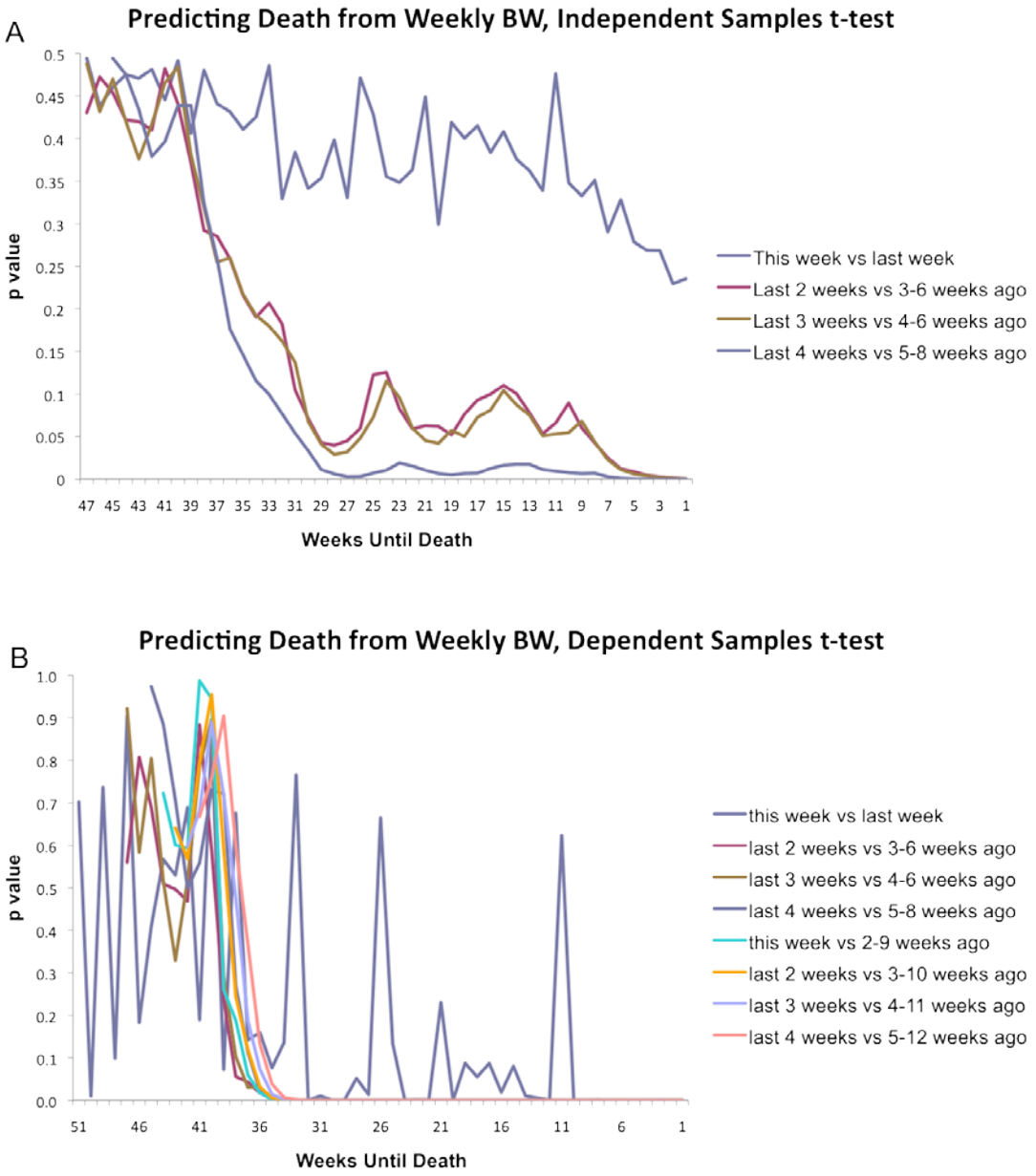

Figure 2.12. Predicting death from weekly BW loss during final year of life. Moving p-values (y-axis) calculated from independent samples t tests across each week during final year of life. For each of the remaining 47 weeks of life (x-axis), an independent samples t-test was conducted, as described in the legend, using group mean data from all males living longer than 1 year among all conditions (A) and by group (B). P-values (y-axis) calculated from dependent (within-subjects) samples t-tests across each week for final year of life. For each of the remaining 47 weeks of life (x-axis), a dependent samples t-test was conducted, as described in the legend, from all males living longer than 1 year among all conditions (C) and by group (D).

Table 2.1. Weekly Group Body Weights, 18-46 Days old

	Week 1 (18 d)		Week 2 (25 d)		Week 3 (32 d)		Week 4 (39 d)		Week 5 (46 d)	
PHOTOPERIOD	Mean	SD	Mean	SD	Mean	SD	Mean	SD	Mean	SD
Early Puberty										
SNP E (*n* = 39)	18.47 ± 1.55	*a*	24.29 ± 2.59	*b*	31.45 ± 3.53	*b*	35.82 ± 4.18	*b*	38.99 ± 4.45	*b*
LDLD (*n* = 40)	17.86 ± 1.87	*a*	24.08 ± 2.71	*b*	30.75 ± 3.41	*b*	35.13 ± 4.22	*b*	38.52 ± 4.84	*b*
LD (*n* = 48)	17.83 ± 1.97	*a*	24.68 ± 3.00	*b*	31.23 ± 3.25	*b*	34.70 ± 3.90	*b*	37.57 ± 4.19	*b*
Delayed Puberty										
SNP D (*n* = 39)	18.36 ± 1.43	*a*	20.85 ± 1.96	*a*	24.32 ± 2.30	*a*	26.04 ± 2.79	*a*	27.24 ± 3.42	*a*
SD (*n* = 40)	18.15 ± 1.68	*a*	20.84 ± 2.47	*a*	23.58 ± 2.59	*a*	24.85 ± 3.17	*a*	26.31 ± 3.40	*a*
DS (*n* = 40)	18.58 ± 1.47	*a*	21.01 ± 2.03	*a*	23.88 ± 2.37	*a*	24.72 ± 2.80	*a*	26.36 ± 2.98	*a*

Table 2.2. Parameters of delayed puberty timing

	SNP D (n =39)	SD (n = 40)	DS (n = 40)		
	Mean ± SD	Mean ± SD	Mean ± SD	$F_{(2,116)}$	p
Age (d)	166.74 ± 38.71 [b]	145.80 ± 28.16 [a]	157.93 ± 40.84	3.318	0.040
SNP Date	Feb 3 ± 39	-	-	-	-
Light (h)	9.61 ± 1.67	-	-	-	-
BW (g)	39.43 ± 6.08	36.47 ± 4.55 [c]	40.08 ± 6.67 [b]	4.357	0.015
Grams/Day	0.362 ± 0.091 [c]	0.343 ± 0.112 [c]	0.421 ± 0.124 [ab]	5.560	0.005
Pelage	2.51 ± 0.47	2.73 ± 0.64	2.46 ± 0.61	2.310	0.104

a = post-hoc comparison $p < .05$ vs. SNP D
b = post-hoc comparison $p < .05$ vs. SD
c = post-hoc comparison $p < .05$ vs. DS

Table 2.3. BW alignment schematic

Life Stage Timeline "Puberty Alignment"						
SNP E		Summer 1 (p)	Winter 1	Summer 2	Winter 2	Summer 3
SNP D	*Winter 1**	Summer 1 (p)	Winter 2	Summer 2	Winter 3	Summer 3
DS	*Winter 1**	Summer 1 (p)	Winter 2	Summer 2	Winter 3	Summer 3
Biological Timeline "1st Winter Alignment"						
SNP E	*Summer 1 (p)*	*Winter 1*	Summer 2	Winter 2	Summer 3	Winter 3
SNP D		*Winter 1**	Summer 1 (p)	Winter 2	Summer 2	Winter 3
DS		*Winter 1**	Summer 1 (p)	Winter 2	Summer 2	Winter 3

*BW data not analyzed
italics depicts times omitted from table
"(p)" indicates summer of puberty

Table 2.4. Life stage BW history

	SNP E	SNP D	DS
	Summer 1 (p) (n=38)	Summer 1 (p) (n=39)	Summer 1 (p) (n=39)
BW	45.38 ± 5.01 a	53.56 ± 6.61 b	56.49 ± 8.09 b
Age (d)	97 ± 34 a	266 ± 51 b	235 ± 31 b
SNP Date	30-Jul ± 34 b	13-May ± 51 a	11-Aug ± 31 b
	Winter 1 (n=37)	Winter 2 (n=31)	Winter 2 (n=31)
BW	35.20 ± 6.91 a	37.87 ± 6.38 a	40.66 ± 6.73 b
Age (d)	205 ± 48 a	433 ± 88 b	429 ± 85 b
SNP Date	15-Nov ± 48 a	26-Oct ± 88 a	22-Feb ± 85 b
	Summer 2 (n=35)	Summer 2 (n=26)	Summer 2 (n=21)
BW	55.21 ± 7.09 b	49.06 ± 5.69 a	53.68 ± 5.35 b
Age (d)	405 ± 53 a	607 ± 92 b	572 ± 100 b
SNP Date	3-Jun ± 53 b	19-Apr ± 92 a	14-Jul ± 100 c
	Winter 2 (n=31)	Winter 3 (n=9)	Winter 3 (n=5)
BW	39.06 ± 6.26 b	36.31 ± 6.36 b	32.58 ± 5.16 a
Age (d)	558 ± 64 a	794 ± 108 b	861 ± 40 b
SNP Date	3-Nov ± 64 a	24-Oct ± 108 a	30-Apr ± 40 b
	Summer 3 (n=23)	Summer 3 (n=3)	Summer 3 (n=1)
BW	46.90 ± 6.07 a	47.63 ± 4.99 a	45.4 ± 0
Age (d)	690 ± 109 a	821 ± 186 a	957 ± 0
SNP Date	15-Mar ± 109 a	21-Nov ± 186 a	4-Aug ± 0

a, b, c indicates statistically distinct subsets
"(p)" indicates summer of puberty

Table 2.5. Biological BW life history

	SNP E	SNP D	DS
	Summer 2 (n=35)	Summer 1 (p) (n=39)	Summer 1 (p) (n=39)
BW	55.21 ± 7.09	53.56 ± 6.61	56.49 ± 8.09
Age (d)	405 ± 53 [c]	266 ± 51 [b]	235 ± 31 [a]
SNP Date	3-Jun ± 53 [a]	13-May ± 51 [a]	11-Aug ± 31 [b]
	Winter 2 (n=31)	Winter 2 (n=31)	Winter 2 (n=31)
BW	39.06 ± 6.26	37.87 ± 6.38	40.66 ± 6.73
Age (d)	558 ± 64 [b]	433 ± 88 [a]	429 ± 85 [a]
SNP Date	3-Nov ± 64 [a]	26-Oct ± 88 [a]	22-Feb ± 85 [b]
	Summer 3 (n=23)	Summer 2 (n=26)	Summer 2 (n=21)
BW	46.90 ± 6.07 [a]	49.06 ± 5.69 [a]	53.68 ± 5.35 [b]
Age (d)	690 ± 109 [b]	607 ± 92 [a]	572 ± 100 [a]
SNP Date	15-Mar ± 109 [a]	19-Apr ± 92 [a]	14-Jul ± 100 [b]
	Winter 3 (n=6)	Winter 3 (n=9)	Winter 3 (n=5)
BW	37.30 ± 2.56	36.31 ± 6.36	32.58 ± 5.16
Age (d)	828 ± 152	794 ± 108	861 ± 40
SNP Date	31-Jul ± 152 [a]	24-Oct ± 108 [a]	30-Apr ± 40 [b]

[a,b,c] indicates statistically distinct subsets
"(p)" indicates summer of puberty

CHAPTER 3. LONGITUDINAL ASSESSMENT OF AGING THROUGH NOVEL 24 H BODY TEMPERATURE AND WHEEL RUNNING PROTOCOLS

GENERAL INTRODUCTION

The primary organization of this thesis was built upon assessing photoperiod history effects on longevity, and secondary goals consisted of collecting a battery of non-invasive measurements reported to reflect age-related changes in circadian controlled output, because photoperiod effects reflect a response of the circadian system function/organization. Our aim was to pair longevity data with rates of aging to determine whether accelerated measures of aging and/or life history events correlate with shorter lifespan. Locomotor activity and body temperature (BT) rhythms have been described as marker rhythms of aging in the circadian system (Mailloux, et al., 1999). The detection of augmented activity and BT has been used to index biological aging (Sacher & Duffy 1978; Duffy & Feuers, 1991), reporting a deterioration of temporal organization and decreased circadian amplitude in aged rodents. Furthermore, BT and activity onsets in LD12:12 and under LL or DD are reported to occur in temporal alignment. It has been proposed that circadian control of these two measures is governed by the same oscillators or at least two separate but tightly coupled oscillators under SCN control (Benstaali et al., 2001).

In this chapter two novel protocols are described, designed to non-invasively assess BT and wheel running activity rhythms at very discrete intervals over the lifetime. After validation, age related changes observed in each experiment are

analyzed. Parameters changing with age, thought to reflect either a functionally weakened circadian system or a deteriorating ability to encode circadian output in downstream systems regulating activity and BT, are discussed. Last, the influence of life-history events such as timing of puberty and age of reaching maximum BW upon rates of aging are addressed.

EFFECTS OF AGE AND LIFE HISTORY UPON WHEEL RUNNING PARAMETERS- INTRODUCTION

This experiment serves to investigate relationships between photoperiod history and aging, with a direct interest in characterizing age related changes to measures under circadian control. In rodents, locomotor activity is the behavioral "gold standard" surrogate of underlying circadian output. In addition, age-related differences in rodent locomotor profiles are well documented, associated with less intense and more sporadic activity in aged subjects (Peng & Kang, 1984). Activity onset begins earlier in subjective night in older rats (Dawson & Crowne 1980) and Syrian hamsters (Scarbrough et al., 1997), in addition to decreases in nightly total, and a shortening of the nightly active duration (alpha) in old mice (Valentinuzzi et al., 1997). Older animals also exhibit lower amplitude rhythms and become less selective about running during the photophase, compared to young hamsters with high amplitude night-to-day ratio reflecting higher intensity night activity and near absent activity during the photophase. This trend in decreasing amplitude in aged animals has

been putatively described to reflect a functional aging of the circadian system. A previous study has even developed an algorithm incorporating multiple wheel running parameters that categorically differentiates wheel running behavior between young and old hamsters with 95% accuracy (Penev et al., 1997).

This novel wheel running protocol will characterize rates of aging through a battery of discrete (i.e., non continuous) and non-invasive measurements across the lifespan of the Siberian hamster, including parameters of wheel running. The design of this novel wheel running protocol is first described, and following validation of the measure, utilized in order to analyze age-related changes and whether these parameters vary as a function of photoperiod history. Over the lifetime age related decreases in night-to-day wheel running i.e., "amplitude," and total nightly output i.e., "vigor", would be expected, with older hamsters running less at night and more during the photophase. It is surmised the stronger circadian systems of young hamsters will exhibit the largest amplitude, and aged circadian systems result in less discrimination between day and night activity. Analyzing age-related changes in vigor, separate from amplitude, will assess physical fitness of the hamster. These wheel running parameters will be further interpreted in chapter 6 with respect to predicting survival.

EFFECTS OF AGE AND LIFE HISTORY UPON WHEEL RUNNING PARAMETERS- METHODS

This protocol was designed around limitations of the overall longevity study: Group housing is not an ideal environment for collecting wheel running data, and Siberian hamsters are prone to fighting with lifelong cage mates if separated for as little as 24 h. Therefore, a protocol was generated in order to acutely measure individual wheel running data but allowed hamsters to return to their respective home cage prior to becoming hostile with cage-mates. The wheel running experiment of this study is referred to as the hamster "gym." There were eight total rounds in the hamster gym protocol beginning at 1 year of age and occurring every 3 months for 2 years. Each round consisted of one 30 min day bout and one 30 min night bout. For each bout, experimental male hamsters (n = 231) were transferred out of their home cage and placed into a running wheel (circumference = 11 cm), which could not be escaped. Running wheel activity was recorded for 30 min, and hamsters were returned to the home cage. Day bouts were conducted within 2 hours of the photophase onset (relative to each photoperiod condition); night workouts were conducted within 2 hours of the scotophase onset. To ensure returns to baseline, a 10 day recovery period between day and night runs was established. Order of day and night runs within rounds was randomized. Lighting conditions in the chamber during assessments were on during day runs and off with the assistance of dim green LED in an effort to maximally resemble home cage photoperiods because introducing novel wheel running in darkness during mid-photophase has been shown to induce bifurcation of activity rhythms. Running wheel activity counts were recorded with a sensor triggered by small magnets attached to opposite ends of the outside of the wheel. Each full wheel

revolution would produce two activity counts and thus data are most precisely described as "1/2 RPMs" and will be referred to simply as counts. Data were archived with DataQuest software, prepared for data analysis in Microsoft Excel, and analyzed in SPSS. 1 minute bins were used for precision. Wheels were washed and allowed to dry between successive uses.

Analysis: Main effects and interactions. The validity of this novel wheel running protocol is assessed by determining whether it was sensitive to time of day effects: If wheel novelty is too strong of a confounding factor to identify differences among day and night bouts, this protocol cannot reliably assess circadian controlled differences as a function of age and photoperiod. Main effects of Time of day (Day, Night), Minute (1-30) Round (1-8), and Photoperiod Condition (SNP E, SNP D, LDLD, SD, LD, and DS) were analyzed with the General Linear Model; Between-subjects factors were Photoperiod and Round. Within-subjects factors included Time of Day (Day, Night) and Minute (1-30) of each bout. The morning scotophase in LDLD was arbitrarily assigned the "night" bout for this analysis because of its temporal proximity to cage changes, a stimulus that has been identified as a potent entraining stimulus. Post-hoc comparisons were protected from Type I error inflation with Bonferroni corrections.

Sum and Maximum parameters explored. In an effort to optimally explore these data, the following measures were also analyzed to further investigate Photoperiod and Age effects on wheel running parameters. Individual summary data were obtained from each round: a) Day Maximum b) Night Maximum, c) Day

Maximum + Night Maximum (as a measure of overall vigor), and d) Maximum amplitude (Night Maximum - Day Maximum). Maximums were defined as the single highest intensity minute of each 30 min bout. These four Maximum parameters were assessed in a separate GLM looking for effects of Photoperiod and Round. In the same fashion, Sum parameters were also analyzed by totalling each hamsters activity within each individual round: a) Day Sum, b) Night Sum, c) Sum Total (Day Sum + Night Sum), and d) Sum Amplitude = (Night Sum - Day Sum).

Covariates. It is of interest to determine whether diminished vigor and amplitude are more appropriately accounted for by chronological age or life history events which have been identified in Chapter 2 (post pubertal age and age at maximum BW). Using data from Sum and Max parameters, the following covariates were tested with respect to changes in time of day, round, and photoperiod- a) Current BW, b) Chronological age, c) post pubertal age, and d) age since achieving maximum BW. Last, the number of days each hamster had left to live following the conclusion of each round was determined e.g., "Days until Death", a measure that will be incorporated in Chapter 6 into the Cox-regression model assessing factors predicting survival. Covariate analysis was not asessed in the overall main effects GLM: Sum parameters capture all components of the GLM except collapsed acrosss the "Minute" variable, which is not of primary interest in assessing trends in vigor or amplitude.

EFFECTS OF AGE AND LIFE HISTORY UPON WHEEL RUNNING PARAMETERS- RESULTS

Main Effects: Overall GLM. Table 3.1 provides overall source data. The General linear model incorporating Photoperiod x Round x Minute x Time of Day revealed significant main effects of all dependent measures: Hamsters ran more in the scotophase than during the photophase, resulting in an overall main effect of Time of Day ($F_{(1,1154)}$ = 52.2, p < .001; Figure 3.1A). These data are consistent with nearly all previous literature reporting higher activity during the active phase, thus validating the sensitivity of our protocol in detecting a circadian component upon wheel running tendency. Upon entering the wheel hamsters gradually increased running wheel intensity, contributing to a significant effect of Minute ($F_{(29,33466)}$ = 31.0, p < .001, Figure 3.1B). Wheel running differed significantly among Photoperiods ($F_{(5,1154)}$ = 5.7, p < .001; Figure 3.2). Importantly, a main effect of Round was found, as mean wheel running intensity decreased as hamsters aged ($F_{(7,1154)}$ = 5.9, p < .001).

Interactions. Patterns among day and night wheel running are paneled by photoperiod in Figure 3.3. Minute x Photoperiod and Minute x Round interactions were found ($F_{(145,33466)}$ = 1.8, p < .001; $F_{(203,33466)}$ = 2.0, p < .001, respectively), with no Minute x Photoperiod x Round interaction ($F_{(1015,33466)}$ = 1.0, p < .389). Time of Day run patterns differed among photoperiods, (Time of Day x Photoperiod interaction, $F_{(5,1154)}$ = 2.3, p < .040); Time of Day also interacted with Round ($F_{(7,1154)}$ = 5.8, p < .001), with no Time of Day x Photoperiod x Round interaction ($F_{(35,1154)}$ = 1.2, p < .212). There was only a marginally significant Photoperiod x Round interaction, ($F_{(35,1154)}$ = 1.3, p < .091).

Post-Hoc comparisons: Photoperiod. LDLD demonstrated the highest mean wheel running counts each bout (mean counts per minute = 76.6, 95% CI = 68.0-85.3), which was significantly more than SNP E ($p < .001$) and DS ($p < .024$). SNP E hamsters ran the least among photoperiodic conditions (mean counts per minute = 49.6, 95% CI = 42.9-56.0), significantly outran by all groups but DS (mean counts per minute = 54.9, 95% CI = 48.8-61.1). SNP D, SD, and LD groups ran equivalent overall, averaging 60.1, 62.8, and 63.6 counts per minute, respectively.

Post-Hoc comparisons: Round. Individual round characteristics are illustrated in Figure 3.4. An interesting U-shaped trend emerged across consecutive rounds as hamsters both grew older and died out (most apparent in Figure 3.1A). Bout totals were highest in earlier rounds, where rounds 1, 2, and 3 were statistically equivalent, although a decreasing trend in running wheel intensity was observed, reaching a nadir at round 4, a significantly lower bout total than the previous 3 rounds. Round 5 and 6 began increasing average intensity but were still significantly less than round 1. Finally, no differences were observed in rounds 7 and 8 compared to the previous 6 rounds. Further investigation of this trend shows that while all six photoperiods display this general pattern, SNP E hamsters appear to most markedly exhibit a drop in night wheel running intensity compared to the other groups. At this time the SNP E date was 15 January, with photophase duration increasing from 8.47 h.

Maximum Parameters. See Figures 3.5-3.8 for main effects of Round, Photoperiod, and Round x Photoperiod interactions among Sum and Max parameters. Time of Day (Day, Night) repeated measures of Max were compared across between

subject factors of Photoperiod and Round (Table 3.2A for source data). Overall, there was not a significant difference between Day and Night Maximum values ($F_{(1, 1143)}$ = 1.6, p < .198) but there were significant main effects of Round ($F_{(7, 1143)}$ = 2.4, p < .020), and Photoperiod ($F_{(5, 1143)}$ = 3.8, p < .001). There was also a significant Time of Day interaction with Round ($F_{(7, 1143)}$ = 2.2, p < .032), and a marginal Time of Day interaction with Photoperiod ($F_{(5, 1143)}$ = 2.1, p < .058). A marginal Round x Photoperiod interaction was also observed ($F_{(35, 1143)}$ = 1.3, p < .095). BW and Days until death both proved significant covariates to maximum minute values, (BW: $F_{(1, 1143)}$ = 39.5, p < .001; Days until death: $F_{(1, 1143)}$ = 50.4, p < .001). Time of Day (Max amplitude) was not affected by Days until Death ($F_{(1, 1143)}$ = 0.5, p < .480). Interestingly, Post puberty age was a significant covariate to maximum minute value ($F_{(1, 1143)}$ = 8.6, p < .003), whereas post Maximum BW age was not ($F_{(1, 1143)}$ = 1.7, p < .695), and neither was actual Chronological Age ($F_{(1, 1143)}$ = 1.2, p < .283). While overall running intensity, independent of time of day differences, was projected to assess individual rates of aging, it was also predicted that circadian fitness might be indexed by examining these covariates with respect to time of day interactions. Time of Day significantly interacted with post Maximum BW age ($F_{(1, 1143)}$ = 8.8, p < .003) but not with respect to post-puberty age ($F_{(1, 1143)}$ = 2.4, p < .125) or even Chronological Age ($F_{(1, 1143)}$ = 2.9, p < .088).

Sum Parameters. Time of Day (Day, Night) Repeated Measures of total (summed) wheel running of each bout was compared across between-subject factors of Photoperiod and Round and data are displayed in Table 3.2B. Overall, Time of Day

total counts were significantly different between night and day bouts ($F_{(1, 1143)} = 3.9$, $p < .048$), unlike bout maximum minute parameters above. Main effects of Round ($F_{(7, 1143)} = 2.4$, $p < .018$) and Photoperiod ($F_{(5, 1143)} = 3.944$, $p < .001$) were found, without a significant Round x Photoperiod interaction. Time of Day differences among bout totals significantly interacted with Round ($F_{(7, 1143)} = 2.8$, $p < .007$) and also Photoperiod ($F_{(5, 1143)} = 3.9$, $p < .002$). As these data are essentially equivalent to the "Main Effects Overall GLM" ran above in the primary analysis with the exception of dropping the Minute factor and assessing the contribution of possible covariates, the same pattern of main effects and interactions were found. With respect to covariates, BW and Days until Death were significant predictors of bout intensity (BW: $F_{(1, 1143)} = 90.7$, $p < .001$; Days until Death ($F_{(1, 1143)} = 33.1$, $p < .001$) where higher BW was consistent with more counts, and shorter latency to death was associated with less counts. Chronological Age significantly covaried with Time of Day differences ($F_{(1, 1143)} = 5.5$, $p < .020$), as older hamsters demonstrate less amplitude. Post Maximum BW age was an even stronger covariate to night-day amplitude ($F_{(1, 1143)} = 10.3$, $p < .001$), while post puberty age was not ($F_{(1, 1143)} = 2.1$, $p < .150$).

Covariates. A multivariate covariate analysis was run on Max and Sum parameters, incorporating Max day and night minute values of each hamster at each round, and Sum day and night wheel running counts of each hamster, at each round (Table 3.3A). These data were used to assess a) Max Total (Day Max + Night Max), b) Max Amplitude (Night Max - Day Max), c) Sum Total (Day Sum + Night Sum), and d) Sum Amplitude (Night Sum - Day Sum) across all 8 rounds and how they

would covary with respect to the following measures: current BW, Chronological age, Post puberty age, Post Maximum BW age, and Days until death.

All of the measures we assessed significantly covaried ($p < .05$) across multivariate parameters (A-D) described above. Current BW had the strongest covariate to bout characteristics ($F_{(4, 1140)} = 23.0$, $p < .001$), with heavier hamsters exhibiting the most vigor. Days until Death ($F_{(4, 1140)} = 13.5$, $p < .001$) positively covaried with Sum Amplitude, with largest amplitude in hamsters with the longest life ahead of them. Interestingly, Post-puberty age was the strongest covariate of any age measurement, ($F_{(4, 1140)} = 4.1$, $p < .003$), followed by Chronological age ($F_{(5, 1143)} = 3.3$, $p < .011$) and then post maximum BW age ($F_{(4, 1140)} = 2.9$, $p < .021$), all corresponding to higher running wheel counts in younger animals.

When assessing these covariates separately on measures A-D, a curious trend emerges (See Table 3.3B for source data). Current BW only covaries with Sum and Max totals (Day + Night) and not with Sum and Max (Night - Day) amplitudes. This is also the case for Days until Death, only predictive of Sum and Max totals but not Sum and Max amplitudes. Puberty Age is only predictive of Max total whereas conversely, age of maximum BW strongly covaries with Sum and Max amplitudes, but not with Sum and Max totals. Finally, chronological age is a significant predictor of Sum amplitude, with younger hamsters exhibiting larger night-to-day differences, and only marginally predictive of Max amplitude.

EFFECTS OF AGE AND LIFE HISTORY UPON WHEEL RUNNING PARAMETERS- DISCUSSION

Round. While "Round" factor was the best way to discretely categorize "age" over time in order to incorporate it into the analysis as a main effect rather than only a covariate, we observed a trend of decreasing running wheel activity and intensity over time. However we did not observe a simple linear decrease in activity upon successive rounds but an almost U-shaped pattern (in both day and night bouts) reaching minimum levels at round 4 where a pronounced drop in night running occurs. Following this marked pattern departure from all other bouts, running wheel intensity increases again but likely due to much smaller sample sizes at this time in conjunction with advanced aging. When all hamsters exceed two years of age, the final two rounds were so variable that they were not significantly different from any of the previous rounds. What is evident in the main effects of Round are decreasing trends in all parameters through the first 4 rounds after which parameters stabilize in mean value but variability of each successive round becomes greater.

Photoperiod. LDLD running profiles contributed towards a main effect of photoperiod, regardless of Time of Day (Sum), but influencing Time of Day dependent (Amplitude) measures. As observed in Figure (3.2A), increased running during day bouts both increased sum totals as well as reduced amplitude. This might be accounted for in one of two ways: either that LDLD hamsters were behaviorally bifurcated and readily ran in the wheel during both scotophases, or that they might

have run more in the day bout because the lights were off in this phase as well. A repeated measures t-test confirmed that LDLD groups had significantly higher cBT minutes before enclosure in the day wheel vs. night wheel during rounds 1-4, but in later rounds (5-8), day vs night cBTs were not statistically different. LDLD BT waveform will be assessed in detail in the following section of this chapter.

Chronological age and life-history events. Aside from detecting main effects of aging and photoperiod on wheel running parameters (e.g., vigor and amplitude), we explored which factors of aging might be most closely associated with our wheel running results. By analyzing covariate strength and correlations between wheel running parameters (Sum and Max) and aging factors (chronological age, post-puberty age, post maximum BW age, and days until death) it was determined that the strongest relationship to diminishing vigor was days until death, followed by post-puberty age, then post maximum BW age, and finally, the weakest covariate to wheel running vigor was actual Chronological age (days old). Chronological age was only predictive of Sum (Night-Day) amplitude, whereas vigor was predicted to diminish with chronological age.

Post-puberty age was only a significant covariate of Max total (Day + Night) values, which appears to be a differentiation among night value contributions towards sum vs. max measures: In maximum parameters, post-puberty age bears the strongest negative correlation to night values ($r_{(219)}$ = -.388 compared to day maximum $r_{(219)}$ = -.167, and Day + Night max total $r_{(219)}$ = -.288, all $p < .05$), whereas in sum parameters, post-puberty age is not as strongly influenced with respect to night ($r_{(219)}$ = -.180, $p <$

.01) or total ($r_{(219)}$ = -.142, p < .05) and not significantly correlated towards Day Sum ($r_{(219)}$ = .056, p > .05). These non-complementary Sum vs Max (Day + Night) totals, differing on correlational strength to post-puberty age, are possibly due to either a more sensitive relationship of night maximums, or the even weaker and non-significant relationship among Day Sum values and post-puberty age. It may be the case that young adult (post pubertal) hamsters have qualitatively different wheel running patterns where more intense "burst" running might result in higher maximum values but ultimately do not affect Sum totals.

Post Maximum BW age significantly covaried with both Sum and Max amplitude measures but did not covary with either Sum or Max bout totals, which perfectly contradict current BW results which appear to only covary with Sum and Max bout totals. While these results may appear contradictory, it is notable that post max BW age negatively covaries with all Sum and Max (vigor and amplitude) parameters, as would be predicted from diminished activity with any estimate of aging. However, current BW is (non-significantly) positively correlated to Sum and Max amplitudes but negatively correlated to Sum and Max totals, a result that may be explained by increased day running in hamsters that weigh less, which are then presumably older. All other factors held constant, increased day running in lighter hamsters would decrease amplitude (the non-significant positive correlation) and at the same time increase totals, accounting for the negative totals correlation. Indeed, the strongest correlation to BW among Max and Sum vigor and amplitude parameters is a negative correlation with day sum values ($r_{(219)}$ = -.220, p < .01). Finally, although

post maximum BW age is indeed a result of weighing a hamster continuously over time, it is more of an event based, timing measure, where current BW directly relates to the somatic state of the hamster while undergoing each wheel running bout. These two assessments of BW are of unique value; however, post maximum BW is only really matched with regard to aging and other dependent measures assessing aging, data expressed in "days since" (i.e., birth, puberty, max BW, or any other desired observable parameter), not quantitative ongoing assessments of physical performance.

Finally, Days until Death correlates with wheel running vigor, but not amplitude, similar to current BW. As discussed in Chapter 2, there is a characteristic trend in the pattern of decreasing BW in the final year of life, so the relationship between timing of death and losing BW ought to be expected. Whereas this trend in BW primarily covaried with increased Day Sum values, Days until Death was most closely (and positively) correlated with night max values ($r_{(219)} = .346$, $p < .01$), a unique differentiation warranting further investigation.

EFFECTS OF AGE AND LIFE HISTORY UPON WHEEL RUNNING PARAMETERS- CONCLUSION

This experiment employed a novel protocol to assess locomotor activity of individual hamsters, acutely over the lifetime in order to investigate how age-related changes and photoperiod history affect parameters of wheel running. The main difficulty centered on prior observations that when separated from group housed

conditions for less than a day, Siberian hamsters become hostile to lifelong cage mates, yet placing a wheel into a group housed environment does not allow for individual data collection. This wheel running protocol consisted of placing hamsters into an inescapable wheel for 30 min during photophase onset and scotophase onset in order to detect similar patterns of age-related changes previously observed in rodents and locomotor activity. It has been reported that overall counts of activity decrease with age, in addition to less scotophase running and increased photophase running. The design was sensitive enough to detect overall higher wheel running activity during the scotophase, which validated our protocol. Over the lifetime, total wheel running counts and amplitude decrease linearly from Round 1 through Round 4 (mean ages 342 d and 618 d, respectively). LDLD hamsters exhibited the highest mean counts per bout, and SNP E hamsters displayed the lowest overall running wheel activity. Whether LDLD counts were highest overall because of two scotophase bouts per round does not largely impact the conclusions of the study, since excluding this condition still reveals aging hamsters display less discrimination of day time, photophase running, corroborating previous literature (Scarbrough et al., 1997). Age-related changes are further evident by observing total wheel running counts also diminish systematically, consistent with other rodent studies (Valentinuzzi et al., 1997). Also, heavier hamsters produced higher total counts per round but this did not affect night-to-day amplitude, suggesting BW more directly shares a relationship with the physical fitness of individual hamsters rather than the circadian fitness of the animal assumed to primarily govern day versus night discrimination of wheel running

behavior. Finally, while hamsters grew older, total amplitude diminished, yet round totals (Day + Night bout totals) were positively correlated to the number of days left to live, independent of chronological age. Therefore, these results appear consistent with previous accounts of age-related changes to wheel running behavior but also distinguish between measures that might predict how old an animal is (circadian amplitude) versus how long it may have to live (total output e.g., vigor). The predictive values of these measures are tested in Chapter 6.

EFFECTS OF AGING AND LIFE HISTORY TIMING ON 24 H BODY TEMPERATURE REGULATION- INTRODUCTION

The homeostatic timing of mammalian thermoregulation is controlled by the circadian system: Near 24 h Body Temperature (BT) rhythms persist in constant conditions and are ablated in SCN-lesioned rodents (Ralph et al., 1990). Changes in BT waveform parameters have also been documented to change with age, where older animals display decreases in minimum, maximum, mesor, and amplitude (Refinetti et al., 1990). BT parameters have been reported to fluctuate systematically with season under naturalistic lighting conditions in the Siberian hamster, with higher minimums and maximums occurring with longer daylengths, and lowest values occurring December through February (Jefimow et al., 2011). Additionally, deficits to circadian waveform such as hypothermia and circadian periodicity have been used to predict mortality in aged mice weeks prior to death, as well as complete arrythmicity and

severe hypothermia upon imminent death (Tankersley et al., 2002; Weinert et al., 2002; Weinert & Weinert, 1998). This sensitivity of 24 h BT parameters to both photoperiod and age-related decline serve as an ideal measure to incorporate into the current study of longevity across various photoperiod-governed life history differences; however, traditional BT collection methods were not possible here. Conventional BT data collection consists of animals receiving telemeter implantation into the intraperitoneal cavity, and then individually stationed upon receivers capturing BT recordings at regular 6 minute intervals over consecutive days. In contrast, reliable individual recordings of BT waveform have been captured rectally with as little as 8 data points per 24 h in the rhesus monkey (Simpson & Galbraith, 1906), a more feasible schedule under the limitations of our study. Here a novel BT collection protocol is designed, taking 24 h BT assessments at discrete 90 day intervals across the lifespan in order to study age related changes in BT waveform and whether these changes interact with photoperiod history. As described in Chapter 1, rates of aging are affected by photoperiod history. It is surmised that if differential rates of aging accompany these changes in lifespan, then differential rates of aging in BT parameters might also be observed across the different photoperiod conditions in this study.

First, data collection protocol is described. Mean 24 h BT waveform is assessed and characterized as a function of aging and photoperiod. In addition, BT rhythms are fitted to a cosine model and its parameters explored. This protocol is validated by assessing whether elevated BT duration reliably reflects scotophase duration, and whether acrophase timing accurately coincides with the scotophase.

General linear model assessment of fit parameters measure photoperiod and aging effects on mesor, minimum, maximum, amplitude, and phase angle between acrophase and lights off (ZT12 in nocturnal animals). The goodness of fit of the cosine model from each hamster's final 24 h data collection is tested to see if rhythms dampen in the final days of life. Also, in a separate GLM, covariates that may influence BT parameters, such as current BW, age of puberty onset, age of reaching maximum BW, chronological age, and days until death, are tested for significant effects. Finally, results are discussed with respect to other literature identifying changes to temperature waveform in aging mammals.

EFFECTS OF AGING AND LIFE HISTORY TIMING ON 24 H BODY TEMPERATURE REGULATION- METHODS

Procedure. Beginning at 6 months of age, temperature profiles were obtained from the experimental males (n = 231) every 3 months, scanning each hamster every two hours to provide a circadian resolution of 12 BT values/24 h. The data collection protocol was executed as follows: All lights in the vivarium room housing the experimental photoperiod chambers were turned off, and a dim red lens head-mounted flashlight was worn by the experimenter. All LED buttons on the BMDS portable scanning receiver and scanning wand were covered up to eliminate all extraneous light. A single chamber was opened and only one cage at a time was removed and placed on a work cart beside the chamber. Hamsters were scanned without being

touched or picked up if possible. The LCD display screen was triple taped with a darkly tinted film and elevated above the work cart so hamsters were not exposed but the experimenter could still confirm the scanned ID of the hamster. If the lights were on in the current chamber, the experimenter would work by that light. The current chamber would be completely finished, all hamsters returned, and closed before proceeding to the next chamber to eliminate light scavenging and unintended light exposure during the scotophase. It happened randomly on rare occurrences that the light schedule would change in a chamber mid-way through the scanning process (lights turn on or lights turn off); this is the reason for only using ambient light from the open chamber, but the 2 h resolution was not designed for capturing minute details of before and after lights on or lights off, only enough data points estimate the 24 h waveform. All hamsters currently alive with working transponders would be scanned within each fixed 2 h time window (i.e., 4:00-6:00am PST, 6:00-8:00am PST, etc.). Scanning wand sensitivity recorded body temperatures to a tenth degree Celsius (e.g., 37.3 °C) This protocol was terminated after 9 rounds, when only sixteen hamsters remained among all six photoperiod conditions.

Analysis. With each round, the 12 data points were compiled relative to the median time point within each 2 hr interval (i.e., 4:00-6:00am = "5:00am" timepoint). 24 h clock times were transformed to cosine values, computed as follows:

$$cost = \cos(2(\pi)* ClockNum/24)$$

For all hamsters and days taken together, a nested mixed effects model was designed, with hamster and day specific cosines (days nested in hamsters). The model incorporated fixed effects of age in days, chamber, and interactions between cosine and age, and cosine and chamber. This model allows the estimation of individual (per hamster per day) circadian parameters and adjusts for the within-hamster dependence in the circadian parameters, accounting for trends and interactions common to all hamsters that affect BT. From this nested cosine model, fitted or "Fit" values were derived for acrophase, minimum, maximum, mesor, amplitude (doubling the distance from mesor to acrophase BT), and estimated 12 Fit timepoints corresponding to times of actual data collection (each hamster, each round) with which goodness of fit values were calculated (Goodness of Fit = 1 - (SSerror)/(SStotal)). To assess acrophase timing, phase angles were calculated with respect to lights off (phase angle OFF = 2.5 corresponds to acrophase 2.5 h *after* lights out). A General Linear Model (GLM) analyzed main effects of round and chamber, both incorporated as between subjects factors to avoid complications of unequal sample sizes between rounds, at the expense of losing statistical power of detecting real effects. Post-hoc tests were carried out for Photoperiod and Round factors. Bonferroni corrected comparisons yielding $p < .05$ are reported significant.

To assess the validity of this protocol estimating 24 h BT rhythms, it was tested whether group mean BT obtained at 2 h intervals were sensitive enough to measure the relationship between elevated BT duration (estimating alpha) and scotophase duration. Elevated BT duration was calculated two ways and compared to

each photoperiod's current scotophase duration (excluding LDLD) at the time of each 24 h BT collection. All elevated BT duration calculations used group means specific to each photoperiod condition, at each round (data depicted in Figure 3.9 as group means ± SE for each time point for each photoperiod, at each round). For the first elevated BT duration measure, the number of group mean BT data points (out of 12) above that photoperiod x round mean, were summed and multiplied by 2 h. The second elevated BT duration measure was calculated by counting the number of consecutive basal (non-elevated) BT timepoints from the middle of the photophase (1300 PST for all non-LDLD photoperiods) that were not elevated at least 1 standard error above the mesor, subtracted this from 12, and multiplied by 2. For example, if 4 timepoints e.g., 11:00am, 1:00pm, 3:00pm, and 5:00pm, were not elevated, then (12-4) x 2 = 16 h of elevated BT duration was calculated.

It was also of interest to determine which additional variables might influence parameters of circadian BT, so covariates of current BW (g), survival (d), chronological age, measured by days old (d), days old since achieving maximum BW "Post Max BW Age", days old since puberty onset "Post Puberty Age", and days remaining until death, "Days until Death." Phase angle between acrophase and lights off "Phase Angle OFF" were analyzed with GLM including Round and Photoperiod as factors, incorporating photophase duration (h) as a covariate.

EFFECTS OF AGING AND LIFE HISTORY TIMING ON 24 H BODY TEMPERATURE REGULATION- RESULTS

Validation- Real 24 h data. Figures 3.9A-B illustrate [Photoperiod x Round] array of real and fit mean 24 h profiles in relation to the current photoperiod. Representative individual hamster data collection and fitted cosines over successive rounds are shown in Figure 3.9C. The real mean 24 h waveforms demonstrate flat and basal BT values during the photophase, increasing sharply and peaking during the scotophase and return to baseline around the time of lights on. Scotophase duration and corresponding elevated BT duration are illustrated in Figure 3.10. Both of the elevated BT duration indexes we chose were highly proportional to duration of the current scotophase ($r_{(42)}$ = .689, p < .001; $r_{(42)}$ = .657, p <.001, for measure 1 and 2, respectively), validating the sensitivity of this novel 24 BT protocol to detect photoperiod-driven changes in circadian waveform.

Validation- Fitted cosine curves. Acrophase distribution trends are illustrated in Figure 3.11. Contrary to the majority of work in our laboratory, LDLD hamsters did not exhibit the expected bifurcation pattern in BT, a rather anomalous departure from typical findings. Corroborating with our wheel running data, LDLD hamsters adopted the 5:00-9:00am PST scotophase as the entrained active phase, displayed by their offset distribution in contrast to other photoperiod groups (the LDLD day scotophase occurring 0500-0900 PST was assigned as "Night" to coincide with the other 5 photoperiods exhibiting elevated Night activity). LD, with the shortest (non LDLD) scotophase, generated the least variable acrophase distribution, visibly distinct from the more widely distributed acrophase of SD group exposed to a lifetime of 16 h

scotophase. It is also apparent that when categorized by the appropriate (current) photoperiod, DS distributions either appear narrow or wide, corresponding to 8 h or 16 h scotophases equivalent to SD or LD at relative times. Overall, our cosine fitted BT curves estimate acrophase timing near the middle of the scotophase, demonstrating our data collection protocol is sensitive enough to properly align the phase of the generated curve fit to the appropriate time of day.

BT Minimum. Source data for all dependent variables (minimum, maximum, amplitude, and mesor) are presented in Table 3.5. Mean BT minimums began to decrease consistently at Round 4, a trend which continued through Round 9, creating a main effect of Round (Figure 3.12A). Minimum values also differed by photoperiod, and a Round x Photoperiod interaction was found (Figure 3.12B).

Post-hoc analyses of Photoperiod reveal the highest mean minimum BT in LDLD (35.80 °C) compared to all other groups. Interestingly, the only other group differences in minimum BT were between SD (the second highest mean min = 35.70 °C) and LD (lowest mean min = 35.56 °C). It is worth noting that the two photoperiods which define the low and high range of mean BT minimum values, LD (low) and LDLD (high), were the only two groups exposed to a fixed total of 16 h light each day.

Covariate source data for all BT measures are presented in Table 3.6. As hamsters grew older, BT minimum values decreased, while timing of life history events (puberty onset and age of maximum BW) had no relationship to BT minimum. BT minimum was also the only dependent variable that did not covary with current

BW. When accounting for these additional covariates to BT minimum into the GLM, Round and Photoperiod are both still significant main effects, but the significant Photoperiod x Round interaction is lost.

BT Maximum. Similar to BT minimums, mean BT maximum values decreased with age, confirmed with a significant effect of Round (Figure 3.12C). Photoperiodic conditions also produced a main effect on BT maximum values, though no Photoperiod x Round interaction was present.

Post hoc analysis of Round reveals reductions in the second half of the study on mean BT maximums, where overall mean maximum values held steady through Round 4 (range 36.70-36.78 °C), then decreasing gradually upon each additional round. Post-hoc analysis of Photoperiod revealed LD displayed the highest mean BT maximum value (36.78 °C) and LDLD demonstrated the lowest maximum average (36.35 °C), in stark contrast to BT minimum values. Photoperiod x Chamber interactions are presented in Figure 3.12D.

Covariate analysis reveals current BW and chronological age as covariates to maximum BT: Heavier and younger hamsters were associated to higher max BT. Results of main effects and interactions did not change upon incorporation of these covariate factors into the GLM analysis of BT maximum.

BT Amplitude. We report significant main effects of Photoperiod and Round on BT amplitude, as well as Photoperiod x Round interactions. However, in contrast to minimum and maximum BT trends, overall amplitude did not decrease gradually as hamsters aged (i.e., across rounds, Figure 3.12E). While BT amplitude was lowest at

Round 1 (0.78 °C), mean BT amplitude values only ranged four hundredths of a degree between Rounds 2-9 (0.88 - 0.96 °C). Therefore, surprisingly, BT minimum and maximum values must have decreased in parallel across rounds 2-9, and ultimately, BT amplitude is not attenuated in aged hamsters. While this is the overall BT amplitude trend, there were distinct differences among photoperiodic conditions (Figure 3.12F). Consistent with min and max data reported above, LD generated the highest amplitude BT waveform (1.20 °C), and LDLD the lowest (0.56 °C). The remaining four photoperiods overall amplitude ranged between 0.80 - 0.98 °C. The only two photoperiods with fixed 16 h daily light exposure, LD and LDLD, intriguingly compose the two most extreme ends of range of values for BT minimum, maximum, and amplitude measures.

Significant covariates of BT amplitude include survival and Days until death. Hamsters living longer apparently display higher amplitude BT rhythms early on, despite the fact that rhythms do not dampen at a later age. Current BW covaried with BT amplitude, and since heavier hamsters covary with higher maximum BT, but no relationship to minimum BT, that heavier hamsters therefore display larger amplitude BT rhythms. Photoperiod and Round main effects and interactions were maintained after incorporating covariates into the GLM.

BT Mesor. Overall, BT mesor values significantly decreased as hamsters aged, yielding a main effect of Round. (Figure 3.12G) This was the only BT parameter that did not vary differently among Photoperiod groups. Photoperiod by Round trends are illustrated in Figure 3.12H. There was no Photoperiod x Chamber interaction. Post-

hoc analysis reveals mesor BT was no lower than 36.26 °C through Rounds 1-4, all above the grand mean (36.20 °C), and then mesor values decrease in the final 5 Rounds, ranging 35.61-36.17 °C. Mesor BT covaried with current BW and Chronological age, where higher mesor was accompanied in higher BW hamsters at younger ages.

Goodness of Fit of Cosine Fitted Curves. Goodness of Fit means are illustrated in Figure 3.13. Main effects of Round, Photoperiod, and Round x Photoperiod interactions were found on Goodness of Fit values ($F_{(8,1343)} = 12.4$, $p < .001$; $F_{(5,1343)} = 6.0$, $p < .001$; $F_{(40,1343)} = 2.7$, $p < .001$, respectively). BT rhythms became less sine-like and gradually declined after Round 3 (mean hamster age = 374 d), and stabilized at approximately 0.19 through Rounds 5-8. LDLD had the lowest Goodness of Fit (0.14) and LD hamsters displayed the highest Goodness of Fit (0.35); the remaining photoperiod groups were all intermediate of these two extremes, narrowly ranging 0.20-0.25. Sample sizes naturally decreased each round as hamsters aged and died (n = 231, 224, 212, 203, 179, 148, 111, 72, 16, for Rounds 1-9, respectively). Unlike Phase Angle OFF, hours of daily light did not remotely covary with Goodness of Fit values. While there was no correlation overall between the Goodness of Fit for a given hamster and chronological age, or days until death ($r_{(219)} = .013$, *ns*), the Goodness of Fit of our cosine model became significantly weaker in the each hamsters 24 h final BT data collection, ($r_{(219)} = .262$, $p < .001$; Figure 3.9D). Because the cosine fitted data points were generated with a nested model, the Goodness of Fit values had the potential of exceeding the conventional range of 0.0-1.0 because SSerror was not

restricted to a value less than SStotal. Goodness of Fit values < 0 are interpreted to mean the real BT data is actually better estimated with a straight line (equal to the BT mean) over a cosine fit, therefore hamsters lose all rhythmic properties of sinusoidal BT waveform when Goodness of Fit < 0.00. Using the intercept of the regression line for goodness of fit values predicting days until death, hamsters exhibiting Goodness of Fit of the calculated cosine BT rhythm = .000 yield mean life expectancy of 57 days, indicating when a straight line better models the BT waveform compared to a sinusoidal rhythm, life expectancy is 57 days from this point. To separately assess Goodness of Fit using traditional cosine model conventions, BT data were fit to individual cosine curves (non nested, e.g., using only the 12 data points of each round for each hamster to derive the cosine fit) and found these respective Goodness of Fit results consistent, albeit with a weaker but still significant correlation ($r_{(219)}$ = .127, p < .0297) to days until death. This is important because employing this protocol to predict death *a priori* would not include the advantage of employing a nested model but rather only have available the 12 data points of each completed round without knowledge of whether or not it becomes the final round for the hamster in question.

Phase Angle OFF. Controlling for photophase duration, Phase angle OFF decreased as hamsters aged, yielding a main effect of Round ($F_{(8,213)}$ = 16.3, p <.001; refer back to Figures 3.11B-C). Overall, Phase Angle OFF was different among Photoperiods ($F_{(5,215)}$ = 35.064, p <.001), and an interaction between factors was found ($F_{(40,181)}$ = 2.445, p <.001). Closer inspection of Round revealed the mean Phase Angle OFF latency decreased linearly by 1.69 h (1 h 41m) between Rounds 1-9, from 6.20 h

to 4.50 h. Regarding Photoperiod, LDLD had a substantially smaller phase angle (3.96 h) than the other groups, followed by SD (5.07 h); the remaining group means were not statistically different from one another (5.74-5.97 h). This decreasing trend was rather equivalent among groups; the interaction likely arose from the abrupt differentiation in Round 9, where sample sizes diminish. Days until death was positively correlated to Phase Angle OFF ($r_{(219)} = .141$, $p < .036$), but survival was not ($r_{(219)} = .012$, *ns*). Phase Angle OFF was negatively correlated to chronological age ($r_{(219)} = -.136$, $p < .05$), yet post puberty age revealed a much stronger negative correlation ($r_{(219)} = -.262$, $p < .01$), a two-fold larger correlation coefficient compared to chronological age.

EFFECTS OF AGING AND LIFE HISTORY TIMING ON 24 H BODY TEMPERATURE REGULATION- DISCUSSION

BT Parameters. Overall the real values collected from subcutaneous transponder implants appeared slightly lower than BT data collected from telemeter implants into the abdominal cavity, where the majority of obtained data ranged 36-38°C in comparison to previously reported values collected from Siberian hamsters (Refinetti & Menaker, 1992a; 1992b). This is not surprising since core body temperature ought to maintain higher temperatures compared to peripherally located tissues, where heat loss is greater. Despite these minute parameter differences this experiment validates a novel BT collection protocol useful for non-invasive lifespan

studies. This protocol is also desirable for animal housing conditions that cannot accommodate a large number of telemeter receivers or where space constraints are not practical for individual housing. While there were distinct differences in fit BT cosine parameters among photoperiod groups, strong overall trends were also apparent: Mean BT minimum and maximum started out stable, and then values decreased upon reaching rounds 4-5, at roughly ~479-576 days old (median age of hamsters during Rounds 4-5). These lowered values resulted in lower mean mesor values but remarkably did not influence mean amplitude values. Significant covariates of BT amplitude include survival, and days until death, remarkable findings for two reasons. First, these two age based covariates were not significant with any other BT parameter (minimum, maximum, mesor). Second, the survival covariate was the fixed age at which the individual hamster died; therefore, a given hamster assessed with respect to a fixed covariate across rounds 1-9 maintained rather rigid amplitude. These results are consistent with finding chronological age as a covariate to BT amplitude, corroborating the hypothesis that higher amplitude hamsters will live longer. However, days until death should not be a significant covariate because round was not a significant main effect on amplitude. It is likely that while there is a generic increase in the probability of death as hamsters age, it is not sensitive enough to account for health/age-related decline at the individual level, where days until death is relative to each hamster. The second possibility is this significant covariate result of days until death and fit amplitude may be an artifact of initial low amplitudes described in Round 1, and not decreasing amplitudes during later rounds as hamsters approach individual

demise, but removing round 1 from the analysis did not substantially affect the results.

Acrophase timing. Also intriguing is the influence of the photoperiod duration on Phase Angle OFF, as illustrated in Figure 3.11B. Essentially, the magnitude of Phase Angle OFF wholly reflects the photoperiod condition each group is exposed to: LDLD, SD, and LD phase angles remain relatively rigid throughout all nine rounds, whereas SNP E, SNP D, and DS groups fluctuate almost exclusively using phase angle boundaries of SD and LD, analogous to the design of the minimum and maximum SNP light hours range between SD lower (8 h light) and LD upper (16 h) photophase limits. One slight exception to this correspondence is found where the phase angle OFF in SNP E, SNP D and DS exceeds the magnitude of SD (SD acrophase peaks at ~8 h after lights off). These differences in phase angles between photoperiods are accounted for when incorporating photophase duration as a covariate to these data, washing out these effects (see Figure 3.11C, although the inverse, scotophase duration, more concisely accounts for this as well). Therefore the cosine model fitting these data overall identifies the middle of the scotophase as the acrophase onset, but this timing systematically advances as hamsters age. It was found aged hamsters in later rounds reach acrophase values earlier in the night compared to younger hamsters. This advancing of Phase Angle OFF might either directly reflect an underlying shortening of the free running period commonly cited in aged free running rodents (Dawson & Crowne, 1980; Turek et al., 1995; Refinetti & Menaker, 1992a), but also because the acrophase timing is a product of cosine fitted curves, determined by the "center" of the elevated BT duration: If shortened duration of elevated BT

occurs through returning to basal values earlier in the night, it would also be expected the calculated acrophase would advance with this adjusted center of the elevated BT duration. Although these estimates of elevated BT duration are calculated at the group level rather than by individual data, an overall shortening of the elevated BT rhythm was found to occur at a rate of 44 minutes each round, suggesting the acrophase timing is influenced at least partially through this process. A somewhat less likely explanation might be a change in the circadian system's response to light exposure, i.e., reduced phase shifting effect from light at dusk (less potent phase delays), or perhaps an increase in sensitivity to light at dawn (more potent phase advances). Regardless of the reason, what is observed in the timing of this advancing acrophase is that while chronological age and post max BW age are weak but significant negative correlates to the timing of phase angle OFF ($-.136 < r < -.123$), but post puberty age bears a modest negative correlation to phase angle OFF ($r = -.262$). This suggests acrophase timing is influenced in older hamsters, where "older" is best defined with respect to days after achieving sexual maturity rather than chronological age.

It was determined that current BW significantly covaried with BT maximum, amplitude, and mesor parameters, but not with minimum values. This finding initially appears paradoxical given that minimum and maximum fit values maintain a rigid relationship and bear a strong correlation ($r = .791$); however, if current BW specifically influenced maximum BT, it would only influence amplitude and mesor, consistent with these results.

It is possible the thermoregulatory mechanisms underlying body temperature

rhythms might be more precisely maintained at lower, basal limits, a.k.a "OFF," whereas elevated values during the active phase may likely involve a less precisely controlled "ON" mechanism. In addition, elevated BT occurs during the active phase and is sensitive to locomotion in addition to BW (i.e., physical mass). This would fit with the observation that maximum BT values decline with age, concurrently with the decline in BW and locomotor (wheel running) vigor and intensity characterized in older hamsters. While this may appear not to account for the rigid relationship maintained at older age with regard to minimum and maximum values, BW did significantly covary with amplitude and mesor; this demonstrates that if BW may have had an effect specifically on maximum values, it would account for changes in mesor and amplitude without necessarily influencing baseline minimum values, for which the mechanism responsible is likely a separate independent variable aging at a comparable rate, or at least producing diminished output at a comparable rate.

With respect to aging on BT minimum, maximum, amplitude, and mesor, chronological age was a significant covariate to each of these parameters, whereas Post Puberty age, and Post Max BW age, had no significant influence. In contrast, Post Puberty age most directly accounted for age related trends in shorter phase angle latencies between peak BT and lights off. If the biological age of the circadian system, measured by changes in timing or magnitude of rhythmic output, functionally declines at an independent rate than that the biological system governing thermoregulation, as gauged by BT output parameters, one would expect to see age related differences in timing of BT waveform, rather than directly influence absolute (actual) BT

parameters, where overall 24 h waveform quality would reflect the sum interaction of these two aging systems. What was observed was precise timing of the decreasing minimum, maximum, and mesor did not emerge until Round 5, whereas the reduction in phase angle of acrophase to lights off is a linear trend that begins at Round 1 and apparently, is influenced at the individual level differentially most closely explained by post puberty age. This may reflect the interactions of two independently aging systems and their aggregate functional output, observed in 24 h BT profiles. With respect to mesor values these data coincide with other literature reporting lowered BT in older animals, although it was also recently reported that BT of Siberian hamsters can be influenced by the number of littermates (Jefimow et al., 2011), a parameter which certainly varied systematically in our experiment as animals died off.

EFFECTS OF AGING AND LIFE HISTORY TIMING ON 24 H BODY TEMPERATURE REGULATION- CONCLUSION

A novel 24 h BT waveform protocol is validated by confirming real alpha values are proportional to scotophase duration, and also that the acrophase timing calculated from the cosine fitted model is appropriately biased towards the middle of the scotophase. Minimum, maximum, and mesor values began to decline in middle age without affecting amplitude. Acrophase timing was advanced in older hamsters, at least in part by an earlier decline in the elevated BT duration. With respect to age, the

phase angle OFF advance was most closely correlated to when hamsters underwent puberty compared to chronological age or age of achieving maximum BW. Additionally, the predictive strength of the model's goodness of fit decreased as hamsters aged. A significant correlation was found between the amount of days of life left at the time of last 24 h data collection and Goodness of Fit value, suggesting the 24 h waveform in hamsters with less than 140 days to live becomes arrhythmic.

CONCLUSION

Overall age-related changes to BT and wheel running parameters were apparent, albeit at distinctly different ages. In this novel wheel running protocol, a decreasing linear trend in vigor and amplitude was observed through Rounds 1-4, staying at baseline lows for the remainder of the rounds. However, in BT, we find 24 h rhythms to be mostly stable until minimum, maximum, and mesor parameters decrease sharply upon round 5. Interestingly, although completely different patterns, the largest age-related changes in both of these variables emerge at the same time: during Round 4 in wheel running activity, with mean age 618 days old (previous Round 3 = mean age 505 days old), estimating this change occurred between 505-618 days of age. Similarly, 24 h parameters begin to decrease upon Round 5, mean age 563 days old (previous Round 4 = mean age 465 days old), and thus while the trends between the two measures are not equivalent, the timing of the largest quantitative age-related effect occurs within less than a 60 day range of 505-563 days old.

Another interesting finding was that parameters of amplitude between BT and wheel running revealed the same trend among photoperiods: LD exhibited the highest amplitude BT rhythm with the highest maximum and lowest minimum, and also the highest amplitude wheel running, where it appears only hamsters in this lone photoperiod never ran more during the day than at night each round for the entirety of the experiment. In addition, LDLD hamsters were found to have the lowest amplitude BT rhythm, generating the lowest maximums and highest minimums, but also exhibited the lowest amplitude wheel running activity, running equally in both 4 h scotophases. While one might surmise the hamsters entrained to LD maintained the most consolidated and therefore most robust active phase, accounting for the low amplitude BT and wheel running rhythms in LDLD appear less straightforward and could possibly result from independent factors. First, BT rhythms may not have been homogenous among individual hamsters, which may explain the relative proximity to the mesor of the overall group: There are multiple strategies that may have been adopted by hamsters in this exotic LDLD photoperiod condition; however, one limitation of this BT protocol is the poor resolution of individual waveforms. Second, LDLD wheel running activity was low amplitude because of elevated counts during both 4 h scotophases (arbitrarily assigned day and night), rather than low activity at both timepoints. In fact, (although not statistically significant), LDLD hamsters had the highest Sum and Max totals among overall round counts.

What might explain this effect is the lack of wheel running in during lights-on, as the other photoperiod conditions were exposed to. To reiterate, novel wheel running

in darkness has been reported to induce immediate phase shifts with one exposure, a confounding variable we sought to avoid in our longevity study. Thus, the novelty of being placed in the wheel might best be accounted for in the future by measuring the difference in wheel running between two sets of hamsters housed in equivalent photoperiods at equivalent ages and placing the control group in the wheels during subjective day with lights on and the experimental group in the wheels during the same time of day with the lights off. Regardless, even if these data are partially influenced by lights-on during the Day bout, age-related changes in wheel running parameters were still observed, therefore demonstrating the robustness of the protocol.

Finally, the degree to which life history events, such as puberty timing and age of achieving maximum BW might better predict age-related changes found in BT and wheel running compared to chronological age were investigated. Overall, there was not compelling evidence that life history events are a better predictor of aging compared to chronological age. This is interesting provided that puberty timing unambiguously delayed in three of the six conditions of this study. The following chapter will test differences in survival to determine if timing of life history events influences longevity without compromises to age-related measures or if timing of life history events have no impact on either aging or lifespan.

A

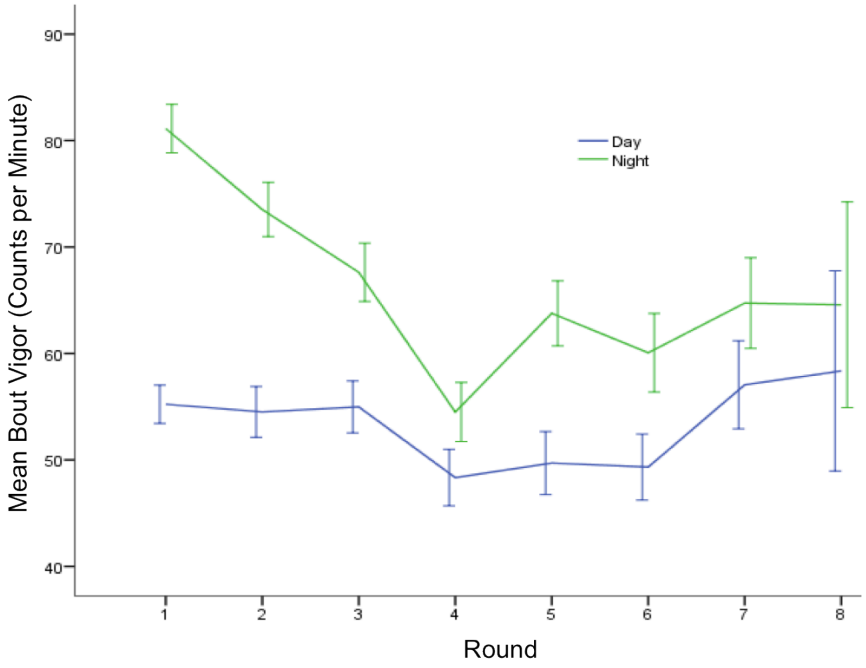

B

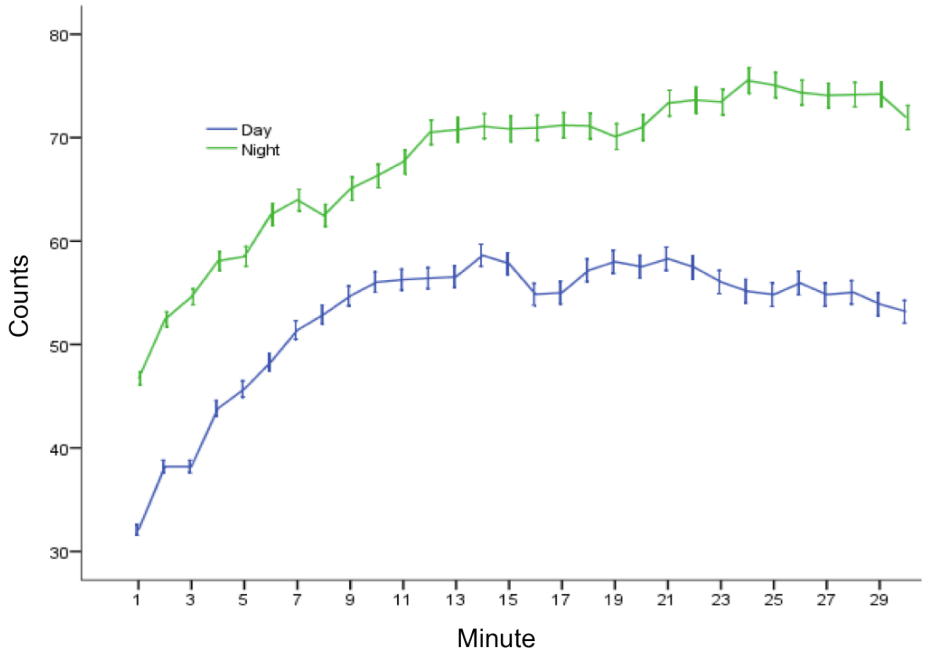

Figure 3.1. Mean ± SE Day and Night bout wheel running (counts per minute) displayed (A) across rounds and (B) overall 30 min profile.

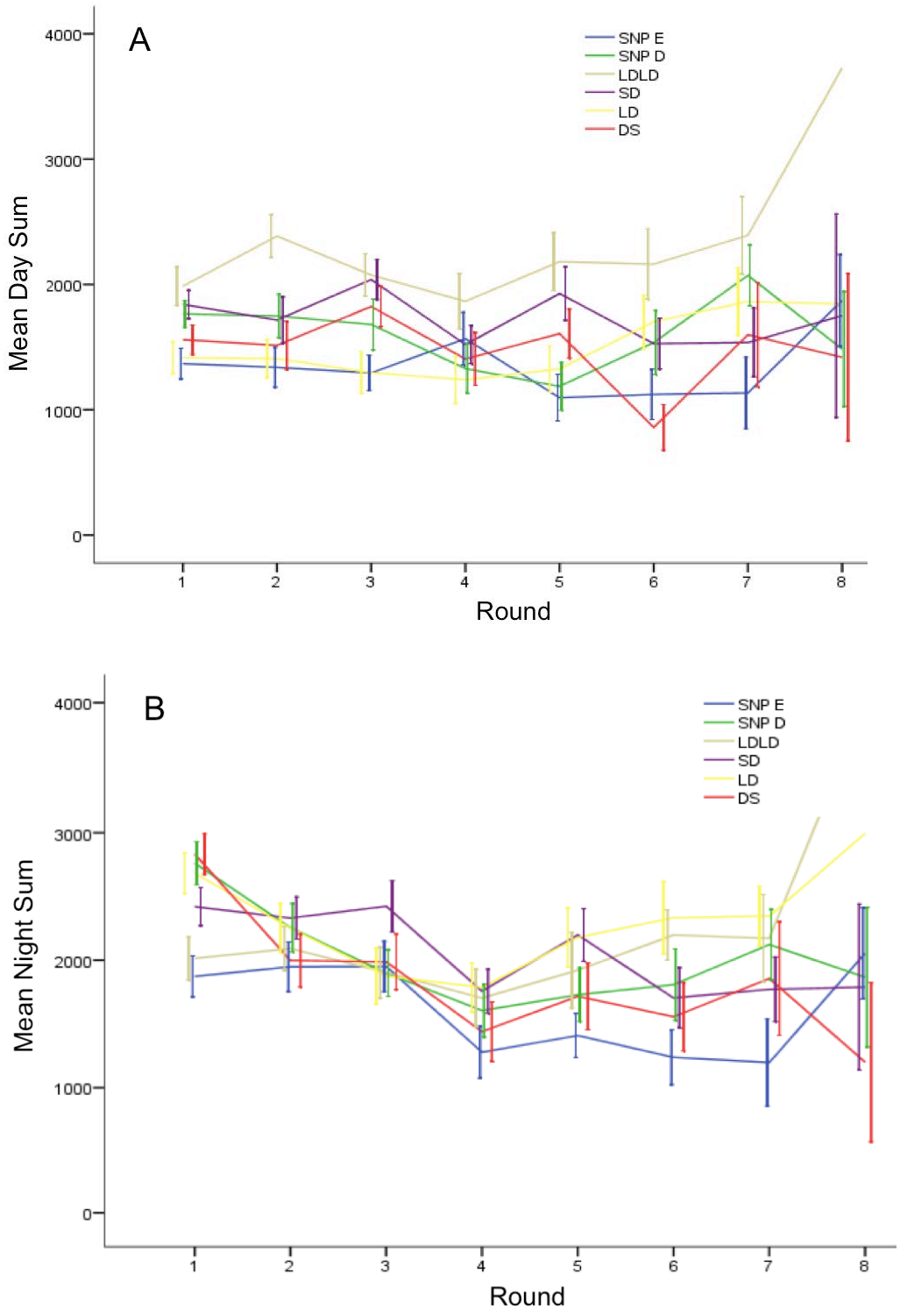

Figure 3.2. (A) Day and (B) Night wheel running total counts per bout among photoperiod conditions each round. Data are displayed as mean ± SE.

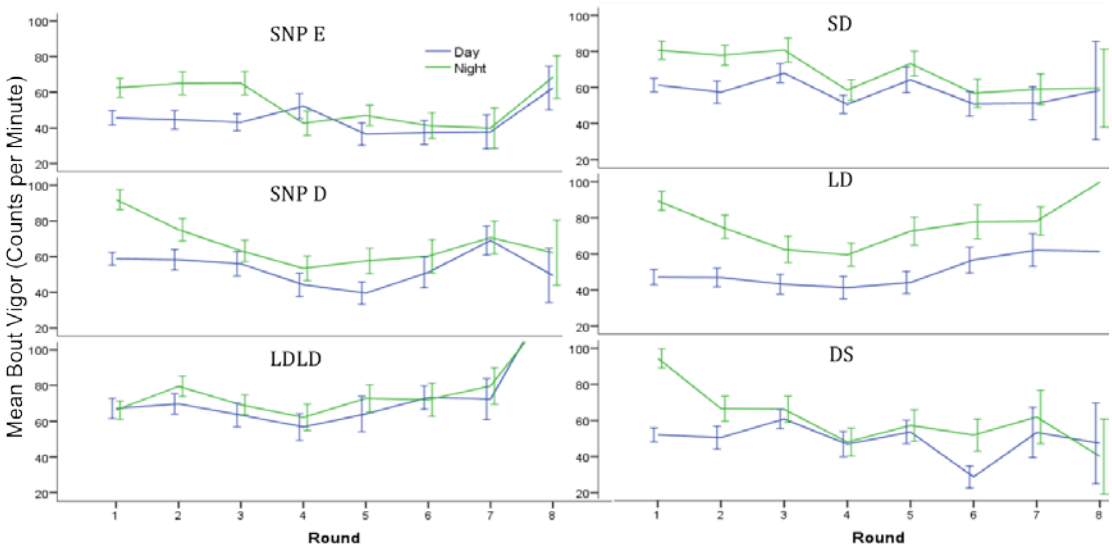

Figure 3.3. Mean ± SE Day and Night wheel running activity (counts per minute) across rounds, paneled by photoperiod group.

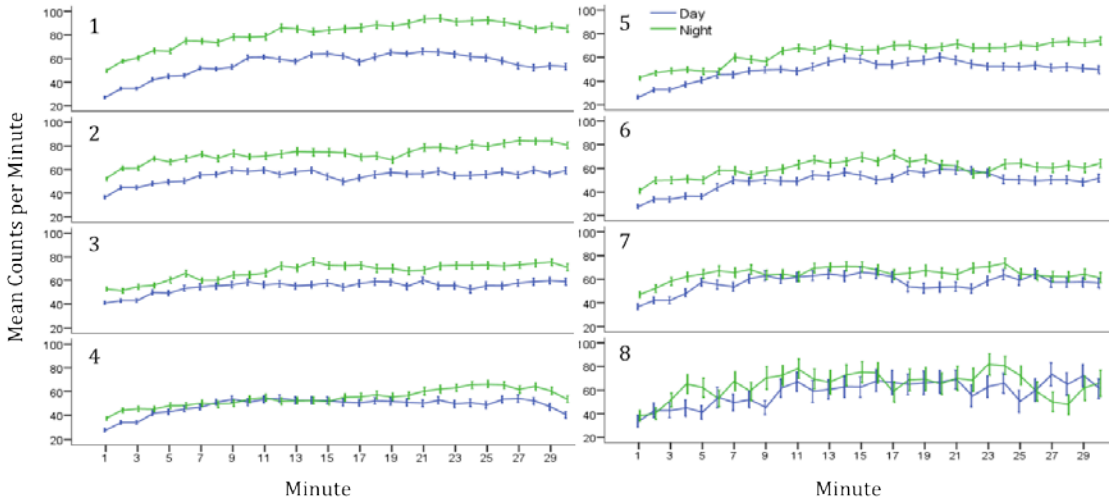

Figure 3.4. Mean ± SE Day and Night 30 minute wheel running activity profile for each Round (1-8). Data are displayed as mean counts per minute.

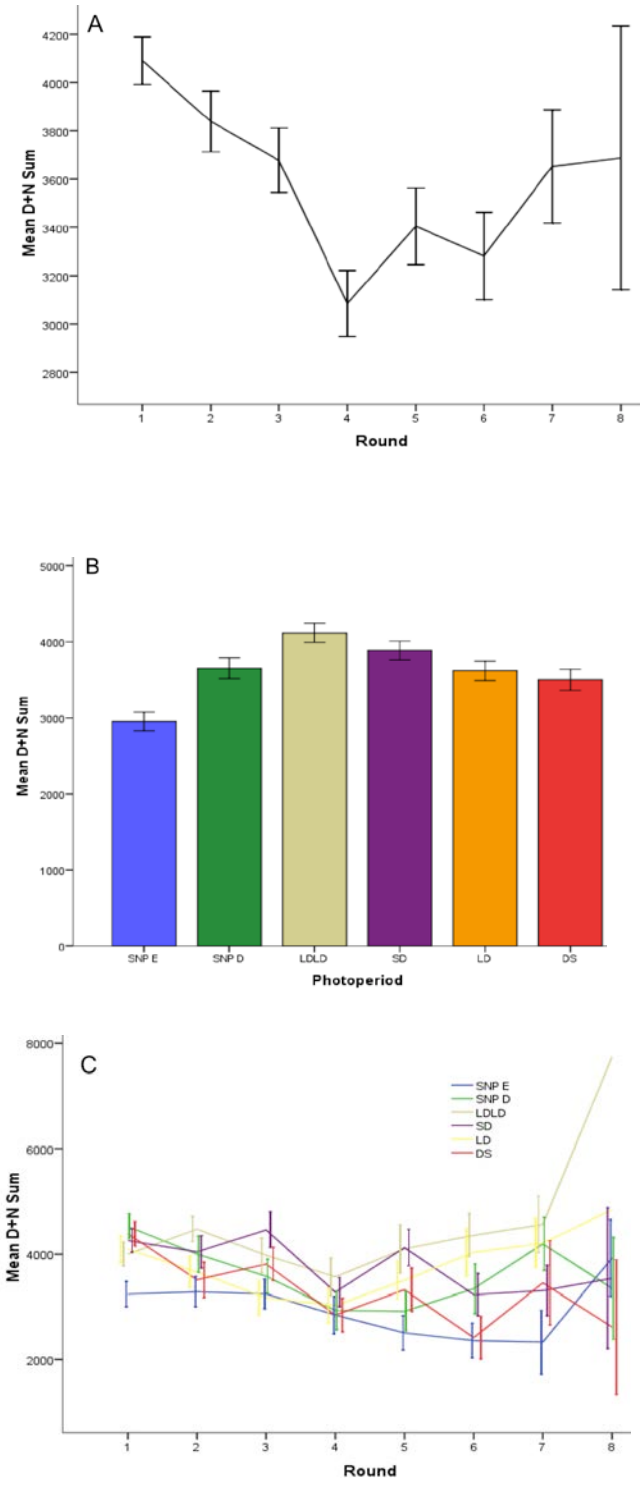

Figure 3.5. Sum Total wheel running parameters. Data represent mean ± SE of individual hamsters. Figures illustrate main effects of (A) overall Round (solid line; mean ± SE), (B) Photoperiod (bar chart mean ± SE), and (C) interactions (mean ± SE).

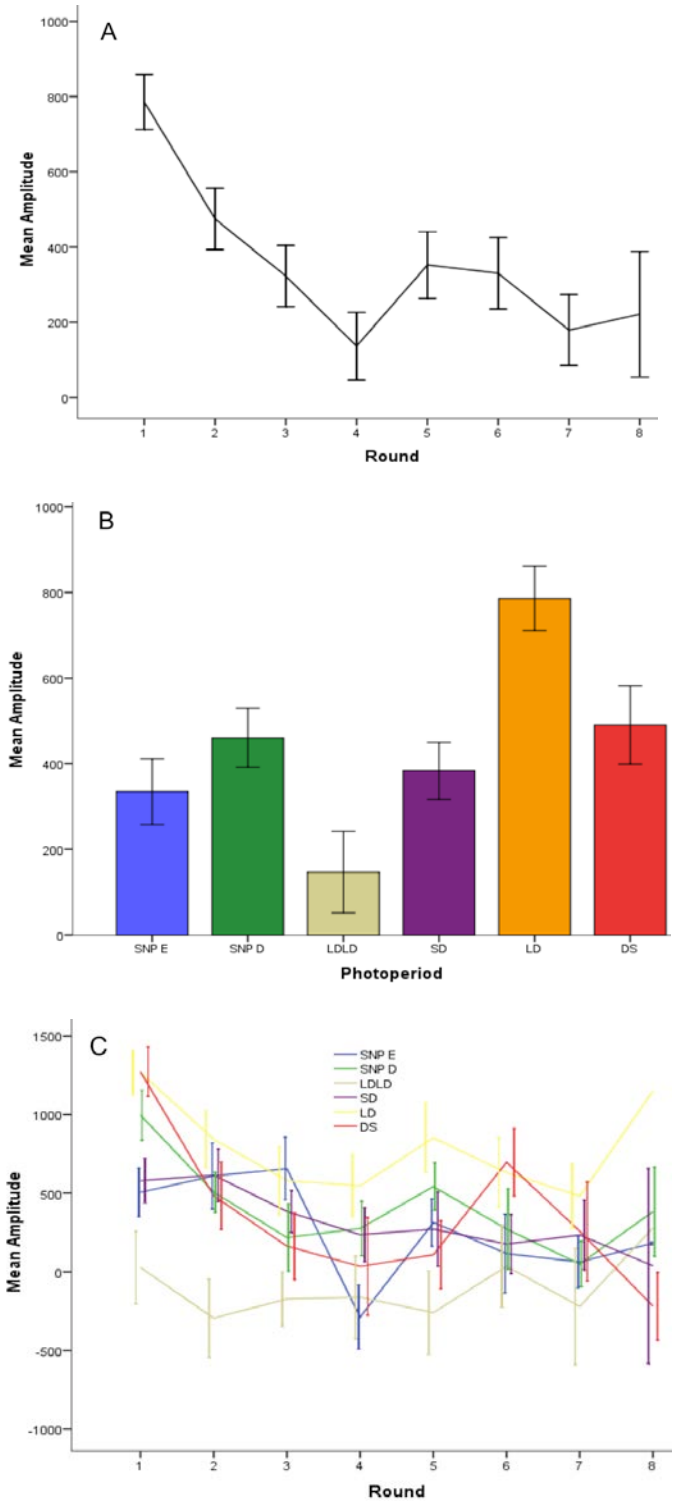

Figure 3.6. Mean Sum Amplitude wheel running parameters. Sum amplitude was determined by subtracting day sum from night sum. Conventions as in Figure 3.5.

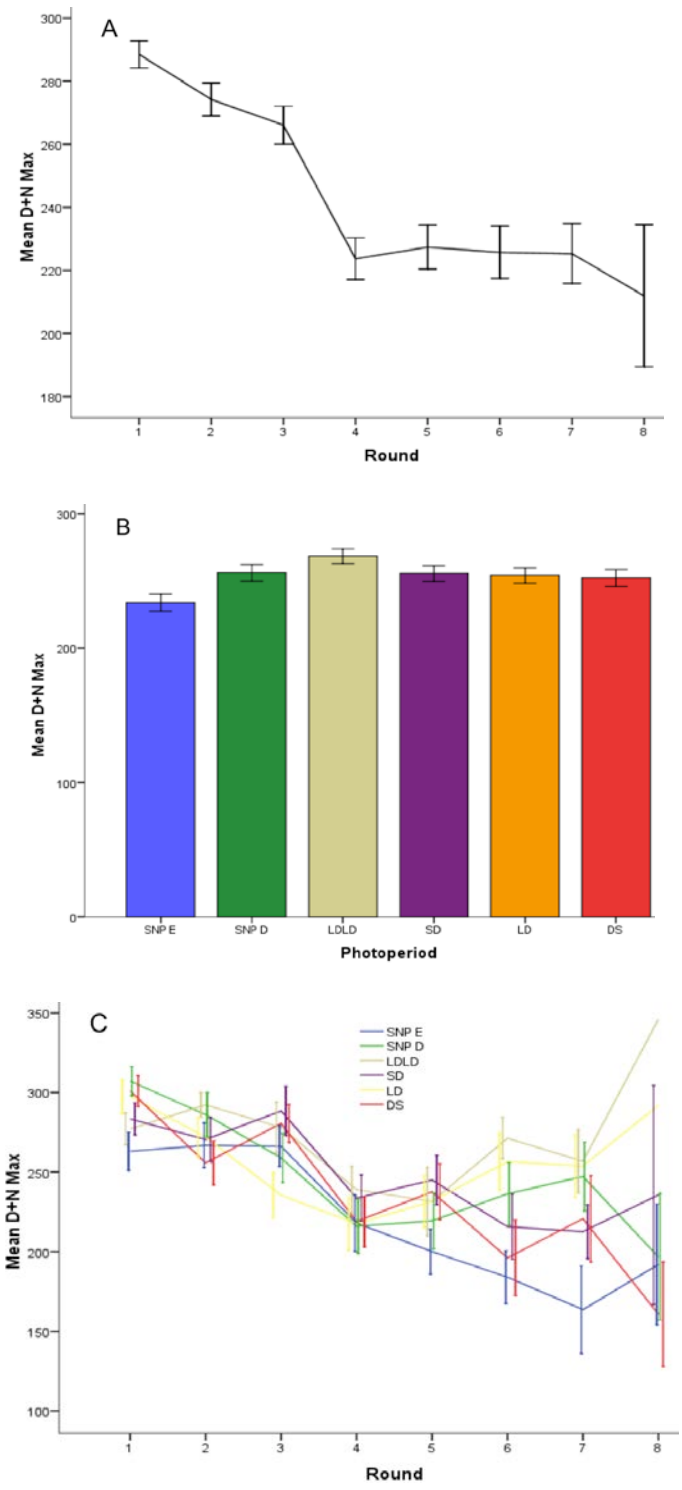

Figure 3.7. Max Minute wheel running parameters. Values depict the single highest intensity minute from each bout. Conventions as in Figure 3.5.

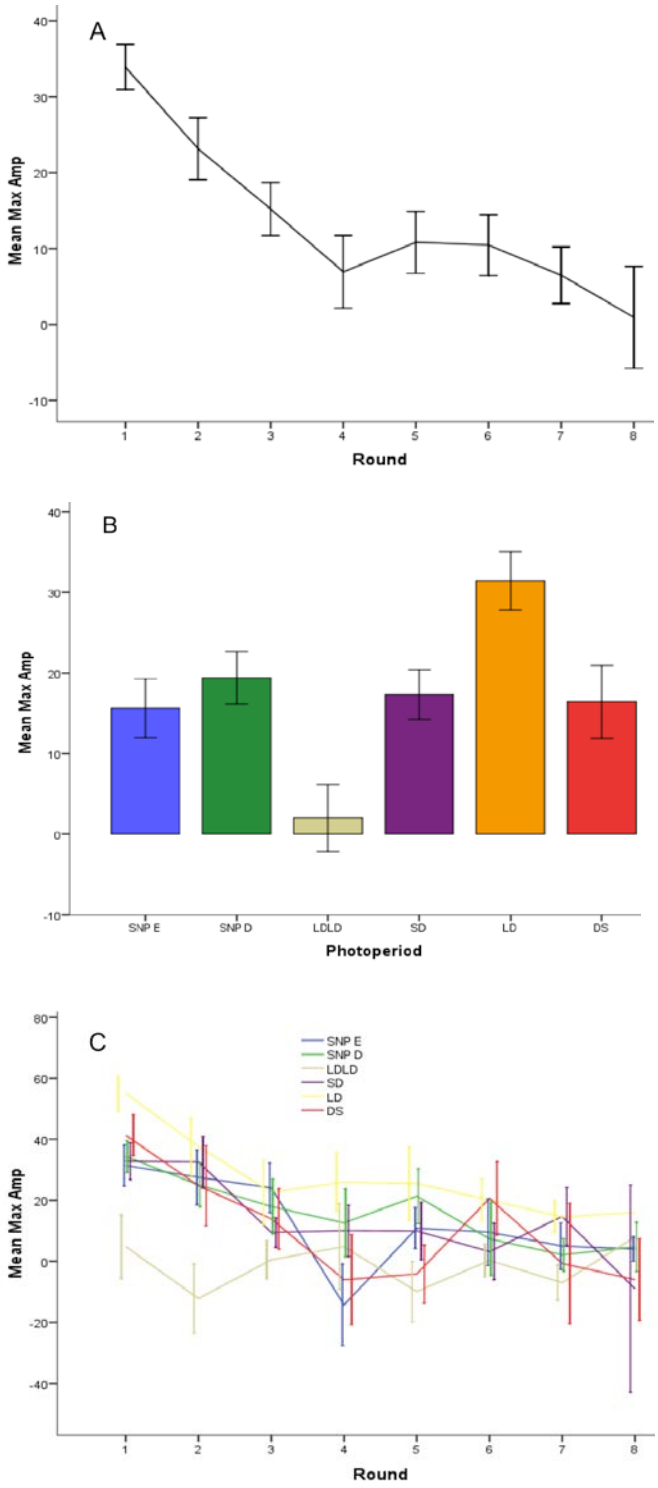

Figure 3.8. Max Amplitude wheel running parameters. Max Amplitude was determined as the Night Max-Day Max difference. Conventions as in Figure 3.5.

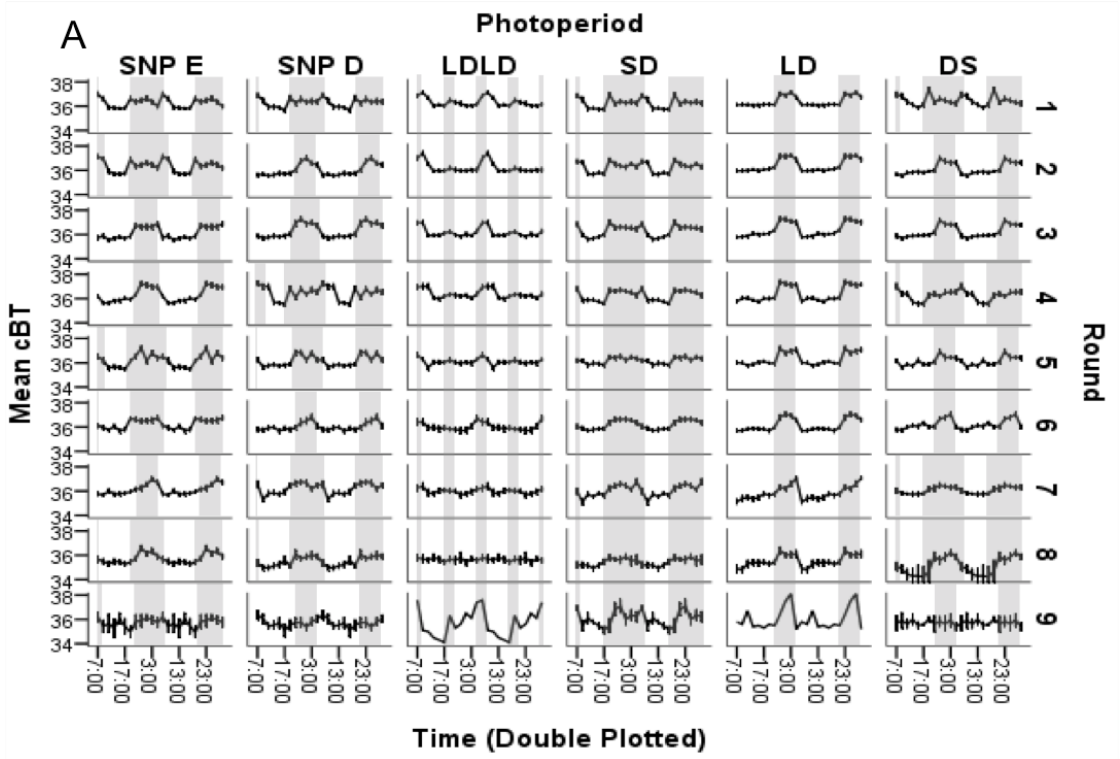

Figure 3.9. (A) Panel of Round x Photoperiod actual 24 h body temperature waveforms (double-plotted, mean ± SE). Shading depicts current lighting conditions during day of data collection. (B) Mean ± SE fitted 24 h cosine body temperature profiles (double-plotted), paneled by Photoperiod condition (columns) and Round (rows). (C) Representative 24 h cosine fitted model of BT across successive rounds of Hamster #8 (LD photoperiod). Values above each panel depict age during data collection.

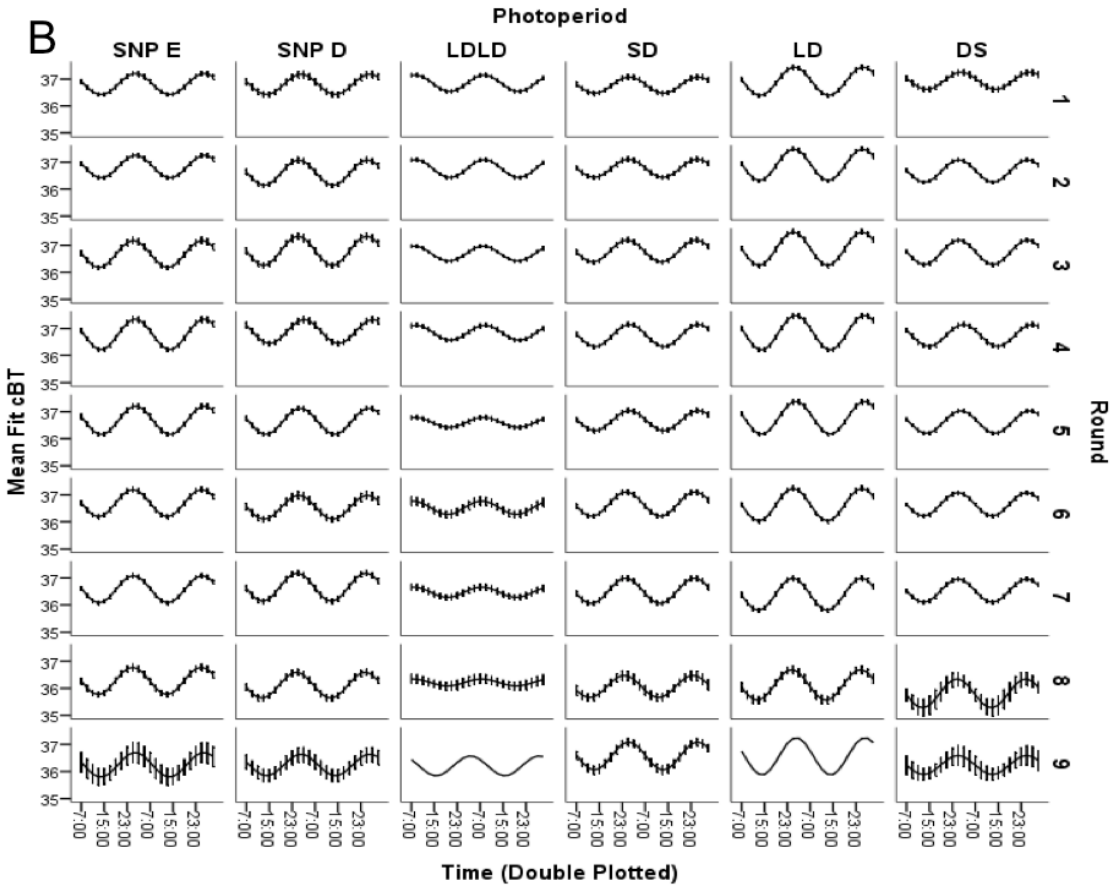

Figure 3.9. Continued.

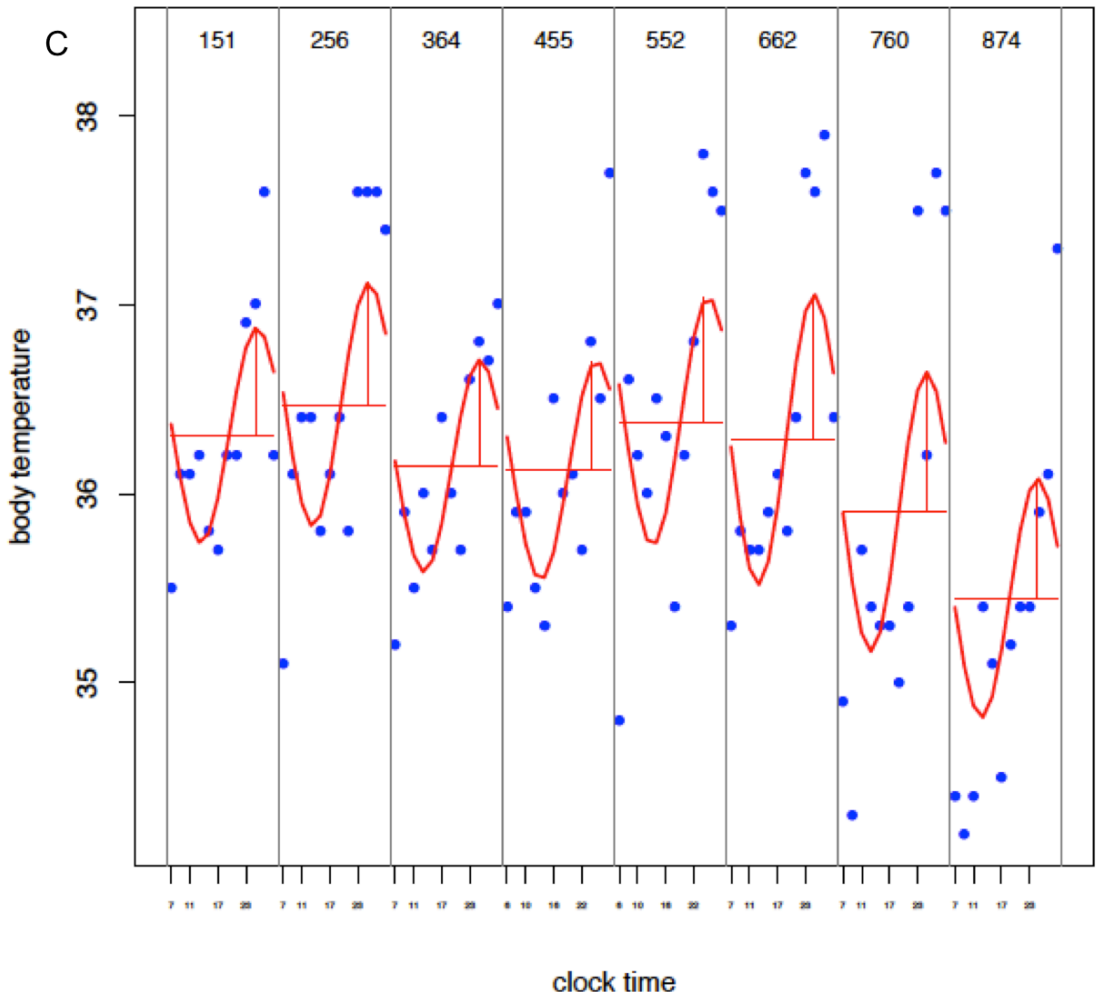

Figure 3.9. Continued.

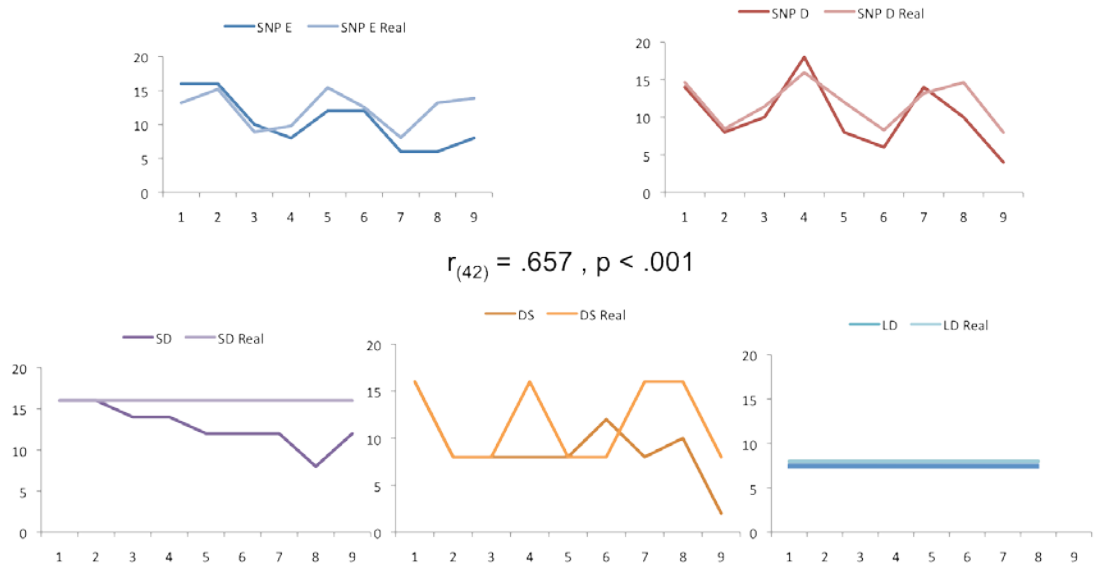

Figure 3.10. Elevated BT accurately corresponds to scotophase duration. Each graph illustrates a particular photoperiod group (SNP E, top left; SNP D, top right; SD, bottom left; DS, bottom middle; LD, bottom right) across successive BT collection rounds (x axis) comparing the real scotophase duration (lighter values in each graph) to the calculated estimate of elevated BT duration. Data used to estimate elevated BT duration comes from real group mean data and not cosine fitted values.

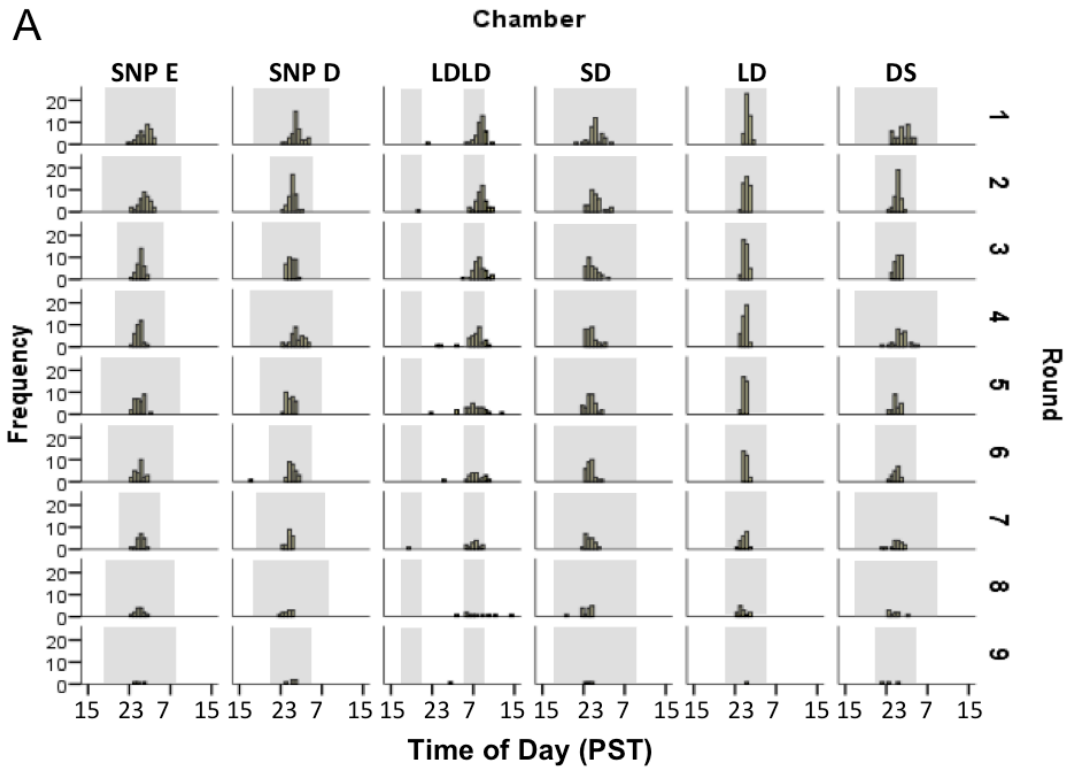

Figure 3.11. Acrophase timing of cosine fitted BT. (A) Group x Round array, acrophase timing of 24 h fitted values. Shading depicts timing of scotophase. (B) Mean ± SE trend of phase angle between fitted BT acrophase and lights off, depicted by condition across rounds. (C) Differences in body temperature acrophase and lights off phase angle between groups are accounted for by photophase duration. Covariates in the model are evaluated at light duration = 12.58 h. Plots are displayed as mean values. Accounting for photophase duration as a covariate, phase angles decrease linearly over time.

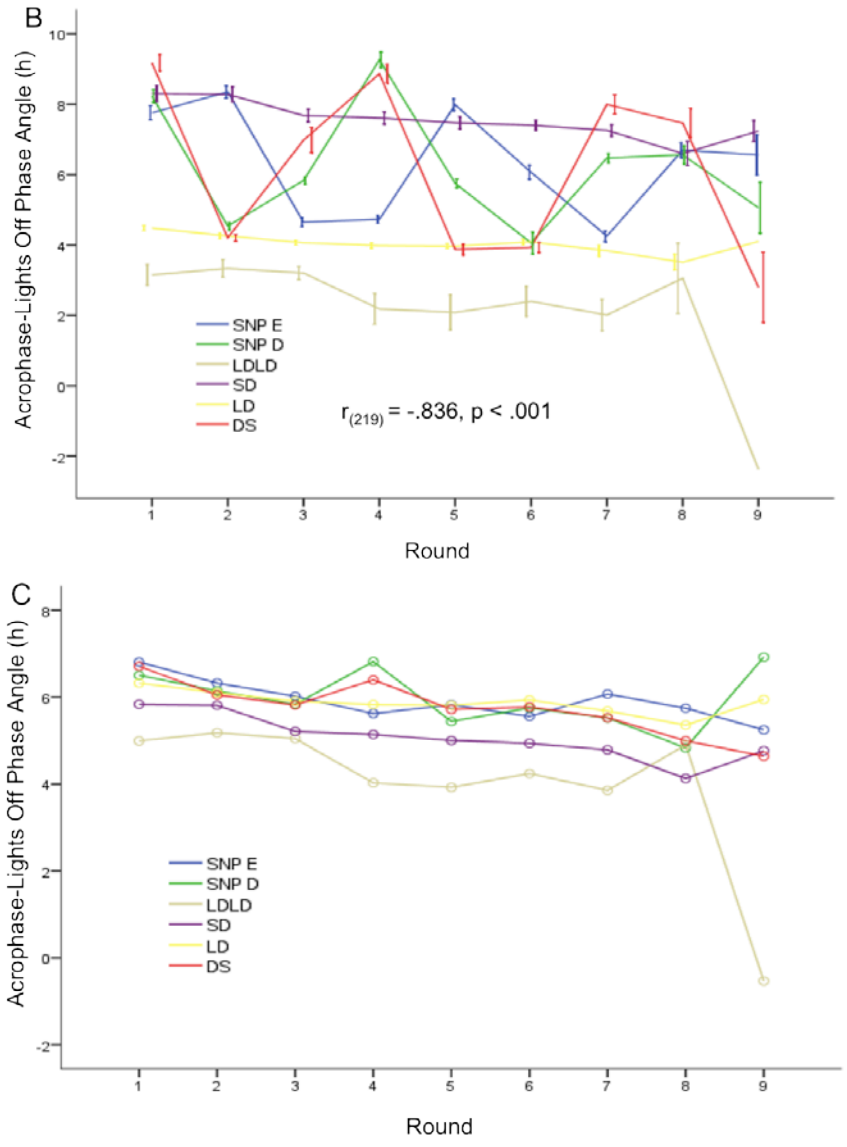

Figure 3.11. Continued.

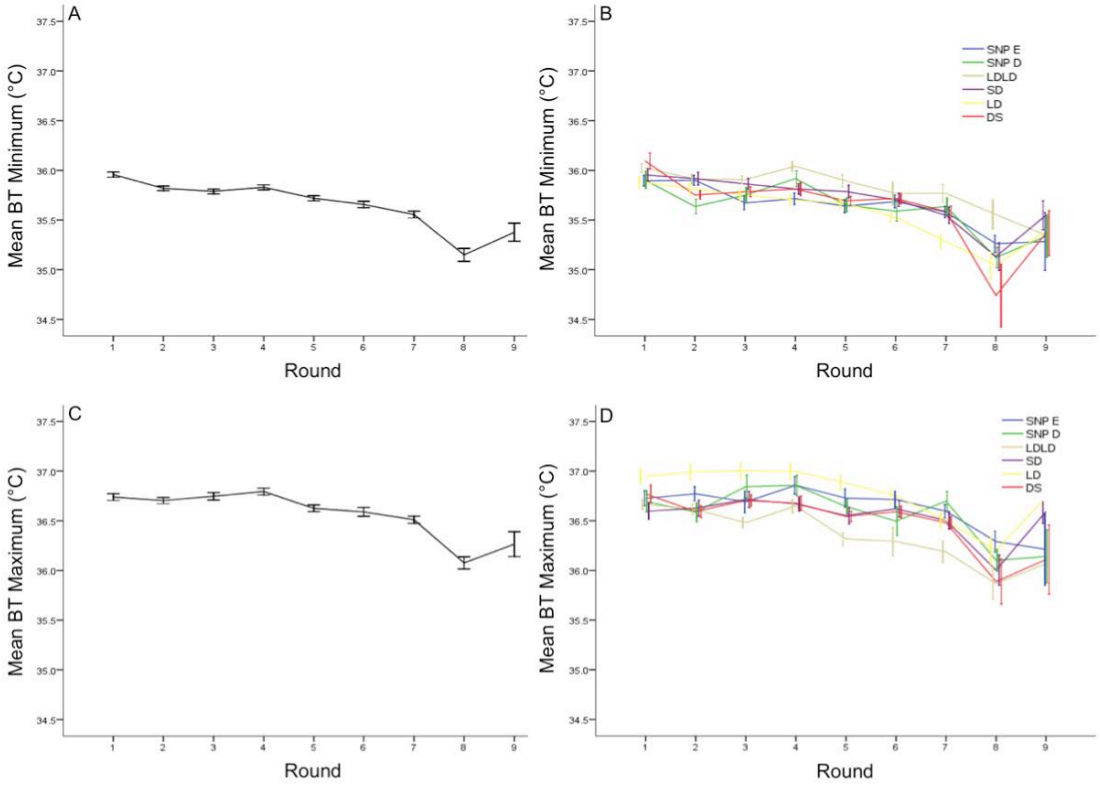

Figure 3.12. Cosine fit BT parameters. All data points represent mean ± SE derived from fitted cosine values. (A) Overall minimum BT decreases as hamsters age. (B) Minimum BT between photoperiod groups across rounds. (C) Overall maximum body temperature decreases as hamsters age. (D) Maximum BT between photoperiod groups across rounds. (E) Overall BT amplitude does not change as hamsters age. (F) BT amplitude between photoperiod groups across rounds. (G) Overall mesor BT decreases as hamsters age. (H) Mesor 24 h BT between photoperiod groups across rounds.

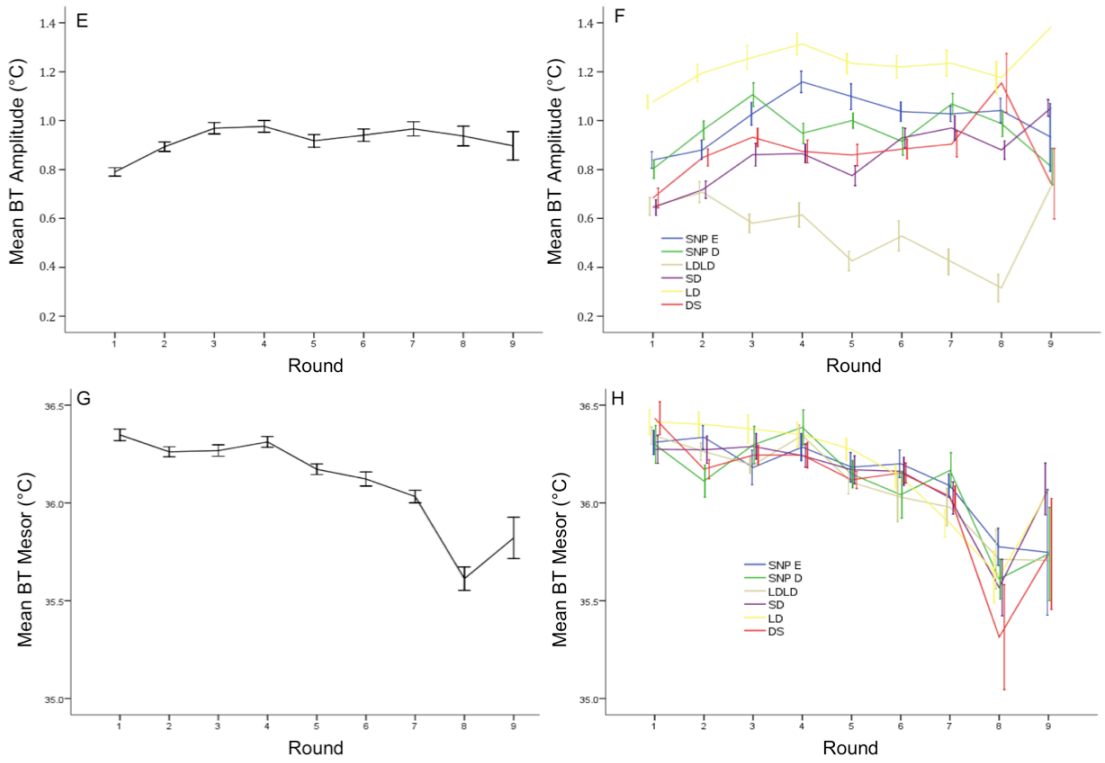

Figure 3.12. Continued.

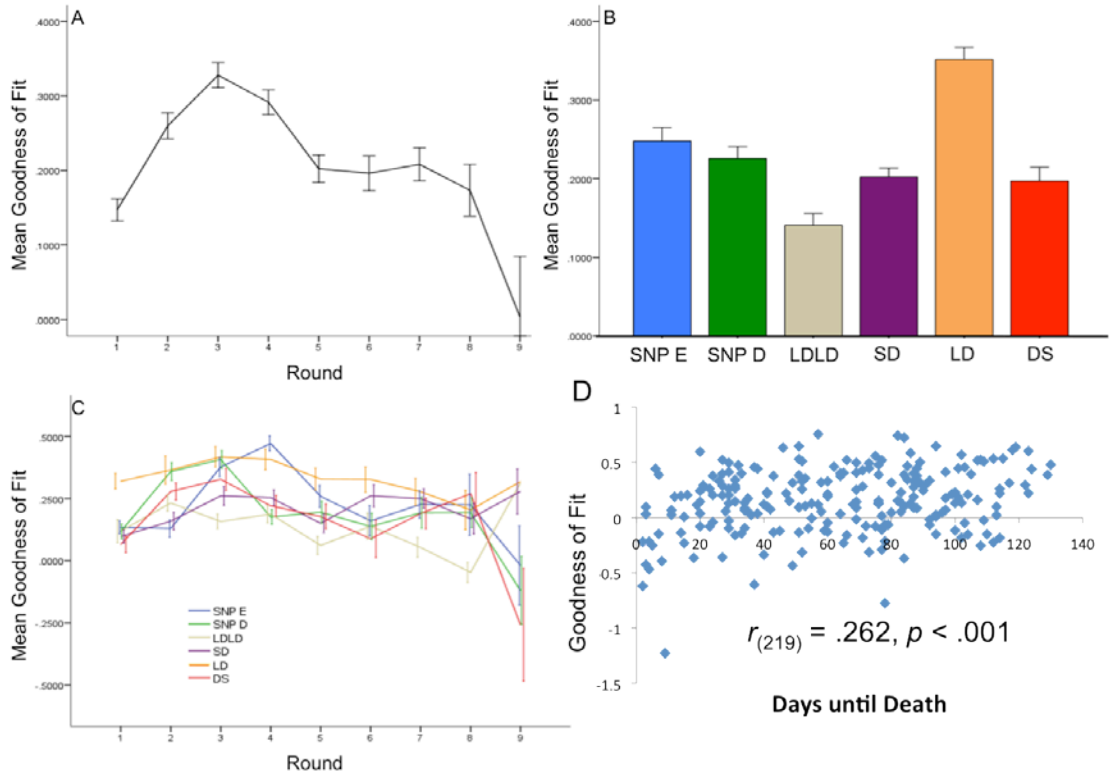

Figure 3.13. Goodness of Fit analysis overall, and in the final round prior to death. (A) Mean ± SE Goodness of Fit among all living hamsters at each Round of BT data collection. (B) Mean ± SE of overall Goodness of Fit for each Photoperiod condition. LD photoperiod demonstrated the best overall Goodness of Fit; LDLD overall show the worst Fit of cosine data to real 24 h waveform. (C) Goodness of Fit Round by Photoperiod interaction. Datapoints depict mean ± SE of each photoperiod group across successive Rounds. (D) Scatterplot between Goodness of Fit during each hamster's final 24 h BT collection and the number of days lived following the date of BT data collection. Derived cosine fit datapoints incorporated a nested model, extending the possible Goodness of Fit values into a negative range, where a straight line better approximates the underlying waveform over to a sinusoidal pattern.

Table 3.1. Overall wheel running GLM source data

Source	Sum of Squares	df	Mean Square	*F*	*p*
Between-Subjects Factors					
Photoperiod	1564288.456	5	312857.691	5.730	.000
Round	2257316.361	7	322473.766	5.906	.000
Photoperiod * Round	2558393.935	35	73096.970	1.339	.091
Error	63008943.553	1154	54600.471		
Within-Subjects Factors					
Time of Day (ToD)	1037382.907	1	1037382.907	52.194	.000
ToD * Photoperiod	231780.303	5	46356.061	2.332	.040
ToD * Round	807268.899	7	115324.128	5.802	.000
ToD * Photoperiod * Round	825777.903	35	23593.654	1.187	.212
Error(ToD)	22936556.919	1154	19875.699		
Minute	1410157.990	29	48626.138	31.011	.000
Minute * Photoperiod	417646.609	145	2880.321	1.837	.000
Minute * Round	627854.406	203	3092.879	1.972	.000
Minute * Photoperiod * Round	1610813.659	1015	1587.009	1.012	.389
Error(Minute)	52475061.449	33466	1568.011		
ToD * Minute	42408.346	29	1462.357	1.055	.384
ToD * Minute * Photoperiod	167177.264	145	1152.947	.832	.930
ToD * Minute * Round	261631.537	203	1288.825	.930	.754
ToD * Minute* Photoperiod* Round	1409050.785	1015	1388.227	1.002	.478
Error(ToD*Minute)	46374723.009	33466	1385.726		

Table 3.2.A. Bout maximum wheel running parameters

Source	Sum of Squares	df	Mean Square	*F*	*p*
Between-Subjects Factors					
Intercept	2796.232	1	2796.232	.933	.334
Chronological Age	3455.594	1	3455.594	1.153	.283
Biological Age (P)	25924.614	1	25924.614	8.648	.003
Biological Age (BW)	461.574	1	461.574	.154	.695
Days until Death	151111.877	1	151111.877	50.410	.000
Current BW	118350.171	1	118350.171	39.481	.000
Round	50014.311	7	7144.902	2.383	.020
Photoperiod	56476.285	5	11295.257	3.768	.002
Round * Photoperiod	139811.606	35	3994.617	1.333	.095
Error	3426320.577	1143	2997.656		
Within-Subjects Factors					
ToD	2195.552	1	2195.552	1.660	.198
ToD * Chron Age	3848.774	1	3848.774	2.910	.088
ToD * Bio Age (P)	3114.771	1	3114.771	2.355	.125
ToD * Bio Age (BW)	11640.761	1	11640.761	8.801	.003
ToD * Days until Death	661.397	1	661.397	.500	.480
ToD * BW	2005.003	1	2005.003	1.516	.218
ToD * Round	20424.173	7	2917.739	2.206	.032
ToD * Photoperiod	14171.670	5	2834.334	2.143	.058
ToD * Round * Photoperiod	35870.486	35	1024.871	.775	.824
Error(ToD)	1511807.668	1143	1322.666		

Table 3.2.B. Bout sum wheel running parameters

Source	Sum of Squares	df	Mean Square	*F*	*p*
Between-Subjects Factors					
Intercept	5.715E+06	1	5.715E+06	3.873	.049
Chronological Age	146237.542	1	146237.542	.099	.753
Biological Age (P)	3.056E+06	1	3.056E+06	2.071	.150
Biological Age (BW)	84850.364	1	84850.364	.058	.811
Days until Death	4.886E+07	1	4.886E+07	33.111	.000
Current BW	1.190E+08	1	1.190E+08	80.659	.000
Round	2.513E+07	7	3.589E+06	2.432	.018
Photoperiod	2.910E+07	5	5.820E+06	3.944	.001
Round * Photoperiod	6.650E+07	35	1.900E+06	1.288	.123
Error	1.687E+09	1143	1.476E+06		
Within-Subjects Factors					
ToD	2.326E+06	1	2.326E+06	3.904	.048
ToD * Chron Age	3.258E+06	1	3.258E+06	5.466	.020
ToD * Bio Age (P)	766994.213	1	766994.213	1.287	.257
ToD * Bio Age (BW)	6.122E+06	1	6.122E+06	10.273	.001
ToD * Days until Death	122930.150	1	122930.150	.206	.650
ToD * BW	344569.995	1	344569.995	.578	.447
ToD * Round	1.155E+07	7	1.650E+06	2.769	.007
ToD * Photoperiod	1.165E+07	5	2.329E+06	3.908	.002
ToD * Round * Photoperiod	2.472E+07	35	706183.879	1.185	.214
Error(ToD)	6.811E+08	1143	595915.993		

Table 3.3.A. Multivariate overall covariate source data

Source	Value	F	df_b	df_w	*p*
Chronological Age	.011	3.304	4	1140	.011
Biological Age-Puberty	0.014	4.070	4	1140	.003
Biological Age-Max BW	.010	2.909	4	1140	.021
Days until Death	.045	13.452	4	1140	.000
BW	.075	23.020	4	1140	.000
Photoperiod	.047	2.738	20	4572	.000
Round	.053	2.182	28	4572	.000
Photoperiod * Round	.122	1.031	140	4572	.386

Table 3.3.B. Covariate by dependent variable source data

Source	Dependent Variable	Sum of Squares	df	Mean Square	*F*	*p*
Chronological Age	D+N Sum	292475.084	1	292475.084	0.099	0.753
	Amplitude	6515030.949	1	6515030.949	5.466	0.020
	D+N Max	6911.188	1	6911.188	1.153	0.283
	Max Amp	7697.549	1	7697.549	2.910	0.088
Biological Age-Puberty	D+N Sum	6111163.987	1	6111163.987	2.071	0.150
	Amplitude	1533988.426	1	1533988.426	1.287	0.257
	D+N Max	51849.228	1	51849.228	8.648	0.003
	Max Amp	6229.542	1	6229.542	2.355	0.125
Biological Age-Max BW	D+N Sum	169700.728	1	169700.728	0.058	0.811
	Amplitude	12243386.989	1	12243386.989	10.273	0.001
	D+N Max	923.148	1	923.148	0.154	0.695
	Max Amp	23281.522	1	23281.522	8.801	0.003
Days until Death	D+N Sum	97715366.211	1	97715366.211	33.111	0.000
	Amplitude	245860.300	1	245860.300	0.206	0.650
	D+N Max	302223.754	1	302223.754	50.410	0.000
	Max Amp	1322.794	1	1322.794	0.500	0.480
BW	D+N Sum	238041010.132	1	238041010.132	80.659	0.000
	Amplitude	689139.989	1	689139.989	0.578	0.447
	D+N Max	236700.343	1	236700.343	39.481	0.000
	Max Amp	4010.006	1	4010.006	1.516	0.218
Photoperiod	D+N Sum	58197487.620	5	11639497.524	3.944	0.001
	Amplitude	23291089.436	5	4658217.887	3.908	0.002
	D+N Max	112952.569	5	22590.514	3.768	0.002
	Max Amp	28343.340	5	5668.668	2.143	0.058
Round	D+N Sum	50250576.504	7	7178653.786	2.432	0.018
	Amplitude	23103617.376	7	3300516.768	2.769	0.007
	D+N Max	100028.621	7	14289.803	2.383	0.020
	Max Amp	40848.346	7	5835.478	2.206	0.032
Photoperiod * Round	D+N Sum	132997008.694	35	3799914.534	1.288	0.123
	Amplitude	49432871.505	35	1412367.757	1.185	0.214
	D+N Max	279623.213	35	7989.235	1.333	0.095
	Max Amp	71740.971	35	2049.742	0.775	0.824
Error	D+N Sum	3373208152.441	1143	2951188.235		
	Amplitude	1362263959.214	1143	1191831.985		
	D+N Max	6852641.154	1143	5995.312		
	Max Amp	3023615.336	1143	2645.333		

Table 3.4. Wheel running parameters and correlates

n = 219	Chronological Age	Biological Age (P)	Biological Age (BW)	Days until Death	Survival (d)	Photophase Duration (h)	BW	Round
Chronological Age	1	0.932 **	0.904 **	-0.629 **	0.402 **	-0.085	-0.521 **	0.996 **
Biological Age (P)	0.932 **	1	0.796 **	-0.604 **	0.355 **	0.126	-0.474 **	0.930 **
Biological Age (BW)	0.904 **	0.796 **	1	-0.599 **	0.328 **	-0.074	-0.500 **	0.906 **
Days until Death	-0.629 **	-0.604 **	-0.599 **	1	0.458 **	-0.012	0.289 **	-0.632 **
Survival	0.402 **	0.355 **	0.328 **	0.458 **	1	-0.111	-0.256 **	0.395 **
Photophase Duration (h)	-0.085 **	0.126	-0.074 *	-0.012	-0.111	1	0.141 *	-0.097
BW	-0.521 **	-0.474 **	-0.500 **	0.289 **	-0.256 **	0.141 *	1	-0.528 **
Round	0.996 **	0.930 **	0.906 **	-0.632 **	0.395 **	-0.097	-0.528 **	1
Day Sum	-0.041	-0.056	-0.002	0.130	0.107	-0.039	-0.220 **	-0.035
Night Sum	-0.173 **	-0.180 **	-0.142 *	0.221 **	0.063	0.044	-0.115	-0.170 **
Day + Night Sum	-0.129 *	-0.142 *	-0.089	0.208 **	0.097	0.006	-0.192 **	-0.124
Sum Amplitude	-0.140 *	-0.133 *	-0.144 *	0.108	-0.033	0.080	0.082	-0.142 *
Day Max	-0.163 *	-0.167 *	-0.115	0.213 **	0.064	0.004	-0.084	-0.159 *
Night Max	-0.325 **	-0.323 **	-0.288 **	0.346 **	0.036	0.039	0.018	-0.321 **
Day + Night Max	-0.287 **	-0.288 **	-0.238 **	0.328 **	0.058	0.026	-0.038	-0.283 **
Max Amplitude	-0.159 *	-0.155 *	-0.168 *	0.133 *	-0.026	0.034	0.096	-0.160 *
Day S.D	-0.123	-0.128	-0.085	0.177 **	0.068	0.026	-0.030	-0.122
Night S.D.	-0.302 **	-0.299 **	-0.273 **	0.308 **	0.018	0.034	0.105	-0.302 **

* = $p < .05$ when $|r| > .129$

** = $p < .01$ when $|r| > .170$

Table 3.4. Continued

n = 219	Day Sum	Night Sum	Day + Night Sum	Sum Amplitude	Day Max	Night Max	Day + Night Max	Max Amplitude	Day S.D.	Night S.D.
Chronological Age	-0.041	-0.173 **	-0.129 **	-0.140 *	-0.163 *	-0.325 **	-0.287 **	-0.159 *	-0.123	-0.302 **
Biological Age (P)	-0.056	-0.180 **	-0.142 **	-0.133 *	-0.167 *	-0.323 **	-0.288 **	-0.155 *	-0.128	-0.299 **
Biological Age (BW)	-0.002	-0.142 *	-0.089 **	-0.144 *	-0.115	-0.288 **	-0.238 **	-0.168 *	-0.085	-0.273 **
Days until Death	0.130 *	0.221 **	0.208 **	0.108	0.213 **	0.346 **	0.328 **	0.133 *	0.177 **	0.308 **
Survival	0.107	0.063	0.097 **	-0.033	0.064	0.036	0.058	-0.026	0.068	0.018
Photophase Duration (h)	-0.039	0.044	0.006	0.080	0.004	0.039	0.026	0.034	0.026	0.034
BW	-0.220 **	-0.115	-0.192 **	0.082	-0.084	0.018	-0.038	0.096	-0.030	0.105
Round	-0.035	-0.170 **	-0.124 **	-0.142 *	-0.159 *	-0.321 **	-0.283 **	-0.160 *	-0.122	-0.302 **
Day Sum	1	0.472 **	0.839 **	-0.426 **	0.843 **	0.384 **	0.717 **	-0.426 **	0.661 **	0.221 **
Night Sum	0.472 **	1	0.876 **	0.597 **	0.435 **	0.853 **	0.759 **	0.413 **	0.328 **	0.568 **
Day + Night Sum	0.839 **	0.876 **	1	0.136 *	0.730 **	0.737 **	0.861 **	0.022	0.565 **	0.472 **
Sum Amplitude	-0.426 **	0.597 **	0.136 **	1	-0.320 **	0.527 **	0.127	0.811 **	-0.264 **	0.382 **
Day Max	0.843 **	0.435 **	0.730 **	-0.320 **	1	0.452 **	0.848 **	-0.509 **	0.909 **	0.343 **
Night Max	0.384 **	0.853 **	0.737 **	0.527 **	0.452 **	1	0.855 **	0.539 **	0.386 **	0.848 **
Day + Night Max	0.717 **	0.759 **	0.861 **	0.127	0.848 **	0.855 **	1	0.024	0.757 **	0.702 **
Max Amplitude	-0.426 **	0.413 **	0.022	0.811 **	-0.509 **	0.539 **	0.024	1	-0.486 **	0.494 **
Day S.D	0.661 **	0.328 **	0.565 **	-0.264 **	0.909 **	0.386 **	0.757 **	-0.486 **	1	0.342 **
Night S.D.	0.221 **	0.568 **	0.472 **	0.382 **	0.343 **	0.848 **	0.702 **	0.494 **	0.342 **	1

* = $p < .05$ when $|r| > .129$

** = $p < .01$ when $|r| > .170$

Table 3.5. Source data for cosine fit 24 h body temperature parameters

Source	Dependent Variable	Sum of Squares	df	Mean Square	F	*p*
Intercept	Mesor	734704.357	1	734704.357	4380917.590	.000
	Min	716261.552	1	716261.552	5256847.617	.000
	Max	753006.315	1	753006.315	3323121.928	.000
	Amp	117.376	1	117.376	8455.485	.000
Chamber	Mesor	.749	5	.150	.894	.484
	Min	2.498	5	.500	3.667	.003
	Max	6.798	5	1.360	6.000	.000
	Amp	3.997	5	.799	57.580	.000
Round	Mesor	39.559	8	4.945	29.486	.000
	Min	44.901	8	5.613	41.193	.000
	Max	36.663	8	4.583	20.225	.000
	Amp	1.260	8	.158	11.350	.000
Chamber* Round	Mesor	6.668	40	.167	.994	.482
	Min	8.710	40	.218	1.598	.011
	Max	8.817	40	.220	.973	.520
	Amp	2.167	40	.054	3.902	.000
Error	Mesor	225.229	1343	.168		
	Min	182.852	1342	.136		
	Max	304.092	1342	.227		
	Amp	18.643	1343	.014		

Table 3.6. Multivariate GLM with covariates

Source	Dependent Variable	Sum of Squares	df	Mean Square	F	*p*
Current BW (g)	Min	.184	1	.184	1.424	.233
	Max	1.616	1	1.616	7.500	.006
	Amp	.178	1	.178	13.659	.000
	Mesor	.722	1	.722	4.536	.033
Phase Angle ON	Min	.641	1	.641	4.967	.026
	Max	.071	1	.071	.328	.567
	Amp	.071	1	.071	5.498	.019
	Mesor	.284	1	.284	1.785	.182
Phase Angle OFF	Min	.411	1	.411	3.186	.075
	Max	.544	1	.544	2.526	.112
	Amp	.002	1	.002	.180	.672
	Mesor	.475	1	.475	2.985	.084
Survival	Min	.057	1	.057	.417	.518
	Max	.166	1	.166	.732	.392
	Amp	.104	1	.104	7.705	.006
	Mesor	.007	1	.007	.042	.837
Days until Death	Min	.042	1	.042	.305	.581
	Max	.234	1	.234	1.033	.310
	Amp	.118	1	.118	8.747	.003
	Mesor	.020	1	.020	.116	.733
Chronological Age	Min	.645	1	.645	4.748	.030
	Max	3.494	1	3.494	15.587	.000
	Amp	.284	1	.284	21.204	.000
	Mesor	1.785	1	1.785	10.716	.001
Bio Age (P)	Min	.097	1	.097	.753	.386
	Max	.024	1	.024	.111	.739
	Amp	.006	1	.006	.474	.491
	Mesor	.054	1	.054	.342	.559

Table 3.6. Continued

Source	Dependent Variable	Sum of Squares	df	Mean Square	F	*p*
Bio Age (BW)	Min	.130	1	.130	1.005	.316
	Max	.380	1	.380	1.764	.184
	Amp	.016	1	.016	1.265	.261
	Mesor	.238	1	.238	1.497	.221
Chamber	Min	2.547	5	.509	3.948	.001
	Max	6.596	5	1.319	6.121	.000
	Amp	3.735	5	.747	57.456	.000
	Mesor	.837	5	.167	1.051	.386
Round	Min	10.573	8	1.322	10.243	.000
	Max	21.056	8	2.632	12.212	.000
	Amp	1.376	8	.172	13.225	.000
	Mesor	14.439	8	1.805	11.332	.000
Chamber * Round	Min	7.010	40	.175	1.358	.069
	Max	8.824	40	.221	1.024	.431
	Amp	2.085	40	.052	4.009	.000
	Mesor	5.832	40	.146	.915	.622
Error	Min	168.888	1309	.129		
	Max	282.116	1309	.216		
	Amp	17.018	1309	.013		
	Mesor	208.483	1309	.159		

Table 3.7. Correlation coefficients of 24 h BT parameters, age, and photoperiod

n = 219	Round	Current BW (g)	Survival	Days until Death	Chronological Age	Biological Age (P)	Biological Age (BW)	Light (h)
Round	1	-0.282 **	0.358 **	-0.691 **	0.999 **	0.953 **	0.935 **	0.008
Current BW (g)	-0.282 **	1	-0.178 **	0.133 *	-0.279 **	-0.258 **	-0.258 **	0.255 **
Survival	0.358 **	-0.178 **	1	0.426 **	0.361 **	0.307 **	0.266 **	-0.072
Days until Death	-0.691 **	0.133 *	0.426 **	1	-0.690 **	-0.702 **	-0.711 **	-0.062
Chronological Age (d)	0.999 **	-0.279 **	0.361 **	-0.690 **	1	0.954 **	0.933 **	0.006
Bio Age (P)	0.953 **	-0.258 **	0.307 **	-0.702 **	0.954 **	1	0.851 **	0.158 *
Bio Age (BW)	0.935 **	-0.258 **	0.266 **	-0.711 **	0.933 **	0.851 **	1	0.010
Light (h)	0.008	0.255 **	-0.072	-0.062	0.006	0.158 *	0.010	1
Phase Angle ON	-0.143 *	0.209 **	-0.158 *	0.018	-0.145 *	0.010	-0.121	0.804 **
Phase Angle OFF	-0.140 *	-0.188 **	0.012	0.141 *	-0.136 *	-0.262 **	-0.123	-0.836 **
Acro Fit	0.098	-0.063	0.075	-0.034	0.094	0.089	0.093	-0.105
Min Fit	-0.384 **	0.064	-0.177 **	0.240 **	-0.389 **	-0.369 **	-0.362 **	-0.033
Min Real	-0.246 **	0.153 *	-0.134 *	0.139 *	-0.251 **	-0.217 **	-0.231 **	0.121
Max Fit	-0.238 **	0.025	-0.075	0.177 **	-0.242 **	-0.211 **	-0.244 **	0.033
Max Real	-0.241 **	-0.014	-0.052	0.197 **	-0.245 **	-0.230 **	-0.255 **	-0.078
Amp Fit	0.120	-0.044	0.113	-0.029	0.120	0.142 *	0.079	0.099
Amp Real	-0.021	-0.150 *	0.068	0.072	-0.020	-0.035	-0.047	-0.185 **
Mesor Fit	-0.320 **	0.045	-0.127	0.217 **	-0.326 **	-0.298 **	-0.314 **	0.004

* = p <.05, |r| > 0.129
** = p < .01, |r| > 0.170

Table 3.7. Continued

n = 219	Phase Angle ON	Phase Angle OFF	Acrophase (Fit)	Min cBT (Fit)	Min cBT (Real)	Max cBT (Fit)	Max cBT (Real)	Amplitude (Fit)	Amplitude (Real)	Mesor (Fit)
Round	-0.143 *	-0.140 *	0.098	-0.384 **	-0.246 **	-0.238 **	-0.241 **	0.120	-0.021	-0.320 **
Current BW (g)	0.209 **	-0.188 **	-0.063	0.064	0.153 *	0.025	-0.014	-0.044	-0.150 *	0.045
Survival	-0.158 *	0.012	0.075	-0.177 **	-0.134 *	-0.075	-0.052	0.113	0.068	-0.127
Days until Death	0.018	0.141 *	-0.034	0.240 **	0.139 *	0.177 **	0.197 **	-0.029	0.072	0.217 **
Chronological Age (d)	-0.145 *	-0.136 *	0.094	-0.389 **	-0.251 **	-0.242 **	-0.245 **	0.120	-0.020	-0.326 **
Bio Age (P)	0.010	-0.262 **	0.089	-0.369 **	-0.217 **	-0.211 **	-0.230 **	0.142 *	-0.035	-0.298 **
Bio Age (BW)	-0.121	-0.123	0.093	-0.362 **	-0.231 **	-0.244 **	-0.255 **	0.079	-0.047	-0.314 **
Light (h)	0.804 **	-0.836 **	-0.105	-0.033	0.121	0.033	-0.078	0.099	-0.185 **	0.004
Phase Angle ON	1	-0.524 **	-0.130 *	0.149 *	0.180 **	0.029	-0.035	-0.150 *	-0.195 **	0.087
Phase Angle OFF	-0.524 **	1	-0.151 *	0.107	-0.023	0.080	0.114	-0.011	0.134 *	0.097
Acro Fit	-0.130 *	-0.151 *	1	-0.158 *	-0.199 **	-0.238 **	-0.088	-0.180 **	0.090	-0.214 **
Min Fit	0.149 *	0.107	-0.158 *	1	0.813 **	0.791 **	0.614 **	-0.034	-0.112	0.934 **
Min Real	0.180 **	-0.023	-0.199 **	0.813 **	1	0.697 **	0.441 **	0.060	-0.451 **	0.791 **
Max Fit	0.029	0.080	-0.238 **	0.791 **	0.697 **	1	0.781 **	0.584 **	0.157 *	0.957 **
Max Real	-0.035	0.114	-0.088	0.614 **	0.441 **	0.781 **	1	0.461 **	0.602 **	0.746 **
Amp Fit	-0.150 *	-0.011	-0.180 **	-0.034	0.060	0.584 **	0.461 **	1	0.405 **	0.324 **
Amp Real	-0.195 **	0.134 *	0.090	-0.112	-0.451 **	0.157 *	0.602 **	0.405 **	1	0.038
Mesor Fit	0.087	0.097	-0.214 **	0.934 **	0.791 **	0.957 **	0.746 **	0.324 **	0.038	1

* = p <.05, |r| > 0.129
** = p < .01, |r| > 0.170

CHAPTER 4. SURVIVAL ANALYSES FOLLOWING PHOTOPERIOD DRIVEN VARIATION OF LIFE HISTORY

INTRODUCTION

The primary objective of this study was to determine whether life-stage progressing events, such as timing of sexual maturation, increased or decreased lifespan, through the simple, non-invasive manipulation of photoperiod history. A number of vastly different biological measures were recorded over the lifetime of Siberian hamsters in order to concurrently investigate patterns of aging among six different photoperiod regimens, with the goal of identifying (or at least eliminate) potential mechanisms governing differences in lifespan. The experiment also serves to investigate effects of naturalistic versus artificial (either fixed, or discrete) photoperiod exposure on lifespan, as well as assess potential hazardous consequences of LDLD, an entrainment protocol currently under refinement seeking to reduce human disease (risk) factors associated with human shift work. In this chapter survival rates will be assessed between early and late puberty conditions, fixed and seasonal photoperiods, and with respect to cumulative effect of winter phenotype. It will also be determined whether there are increased deaths associated with a certain time of year in seasonal photoperiod groups, and also whether any observed survival differences between photoperiod groups might be accounted for by differences in puberty timing or age of attaining maximum BW.

METHODS

Procedure. Deceased hamsters were recovered each morning during daily health checks. Weekly health checks by a veterinarian were also scheduled. The attempt to relieve moribund hamsters when severe injury or imminent death threatened quality of life was part of the survival protocol: As described by Cavigelli & McClintock (2003), there are a number of observable symptoms which triple in frequency of occurrence upon imminent death, including: shallowness or constriction of breath, inability to ambulate, inability to consume food or water, diarrhea, and half-closed eyes. When two or more of these symptoms were observed, the animal was euthanized. Overall, six hamsters were euthanized upon determining imminent death, but the vast majority of hamsters (97.5%) in the study succumbed to natural causes. Two hamsters were removed from the study- one was a misidentified female, the other the other was a male who was not moribund but had an unacceptably large tumor burden. The endpoints of the remaining 246 males were used in the survival analysis. While female hamsters were also included in the study, they had much smaller sample sizes, (n = 12-16, per photoperiod). In addition, there were not enough transponders to implant in all of the females and therefore the process of obtaining all of the additional measures (weekly BW and pelage, wheel running, 24 h cBT) was not practical. Because we wish to interpret individual survival through individual differences of biological aging as accounted in Chapters 2-3, females are only included in order to

compare to males as well as investigate potential gender differences in survival among early and delayed puberty photoperiods.

Data Analysis. Survival rates were analyzed among the following categorical variables: Photoperiod (all conditions), Puberty Timing, (early vs delayed), Photoperiod Waveform (fixed vs. seasonal), and Winter Phenotype history (number of winter state transitions). Data were analyzed using chronological age (days old) and compared to life stage markers: conventions as determined by Puberty Date, and Date of max BW. To optimize power of the statistical test, proportional hazards assumption was assessed prior to analysis with the Q-test described in Martinez and Naranjo (2010). Because survival correlates, covariates, and regression analysis treat survival as a ratio scale measurement and assume normal distribution of data and homogeneity of variance, a 1-way ANOVA (survival across the six photoperiod groups) and Levene's test of variance was used to assess survival data for comparison (but not to draw conclusions), as any time related or "event" based correlations with data from previous chapters are more appropriately interpreted with respect to these results rather than conventional survival statistics. Cox regression analysis with survival covariates is incorporated into a comprehensive lifespan prediction model presented in Chapter 6. To determine the influence of seasonal timing on survival (i.e., summer or winter solstice, or equinox), Rayleigh's test of circular statistics was employed to analyze trends in SNP E, SNP D, and DS (seasonal) photoperiod groups.

RESULTS

None of the 246 male hamsters in the study were censored. The Gehan-Breslow (generalized Wilcoxon) statistical test was selected over Log Rank (Mantel-Cox) because it is a more appropriate test when survival curves differentiate early, rather than late, a violation of the proportional hazards assumption implied in Log Rank (Mantel-Cox) survival analysis. Mean, median, and quartile data are arranged in Tables 4.1-4.2. Kaplan-Meier survival curves among all six photoperiods are presented in Figure 4.1. Female survival and data are only referred to in the Chronological Age- Females section; all other data refers to the 246 experimental males only, unless otherwise specified.

Chronological Age- Males. Unless described otherwise, all measures of central tendency are reported as median survival. Overall, there was a significant difference in hamster survival rates between photoperiod groups, $X^2_{(5)} = 12.386$, $p < .030$, with overall survival = 777 d (Figure 4.1). Hamsters in SD, SNP E, and SNP D lived the longest (856 d, 832 d, and 811 d, respectively), and LDLD and DS hamsters died earliest (716 d and 665 d, respectively; LD = 800 d). Stratification of hamsters into early (SNP E, LD, LDLD) and delayed (SNP D, SD, DS) puberty photoperiods did not account for differences in overall survival ($X^2_{(1)} = .285$, $p < .593$), where on the contrary, survival curves appear nearly identical (Figure 4.2A). In addition, segregating into seasonal (SNP E, SNP D, DS) and fixed (SD, LD, LDLD) groups did not account for overall group differences ($X^2_{(1)} = .047$, $p < .828$, Figure 4.2B). The

number of short day seasons (e.g., Winters) also did not influence survival rates ($X^2_{(3)}$ = 4.414, p < .220, Figure 4.2C). We attribute the largest factor in determining significant overall survival differences among the six photoperiod groups to the accelerated demise of DS and LDLD hamsters: DS hamster survival rates were considerably lower compared to hamsters in SNP D and SD ($X^2_{(1)}$ = 4.441, p < .035 and $X^2_{(1)}$ = 6.843, p < .009, respectively), and LDLD hamster survival rates were significantly lower than those of SD, SNP D, and SNP E ($X^2_{(1)}$ = 5.842, p < .016; $X^2_{(1)}$ = 4.547, p < .032; $X^2_{(1)}$ = 4.032, p < .045, respectively). A 1-way ANOVA of lifespan across conditions was consistent with our findings ($F_{(5,241)}$ = 2.3, p < .044), and lifespan distributions between photoperiod conditions did not violate assumptions of homogeneity of variance (Levene's Statistic$_{(5,241)}$ = 1.251, p < .286). The power to detect photoperiod differences among males = .775. Finally, analysis of decile male survival revealed differences in median lifespan among the oldest (n = 4) living hamsters of each group ($X^2_{(5)}$ = 11.550, p < .042; median survival of 1056 d). This overall main effect of decile was driven by SNP D (1104 d) and SNP E (1067 d) hamsters outliving LDLD (975 d) and LD (996 d; also SD = 1056, DS = 1030 d).

Chronological Age- Females. Overall, female survival rates were not found to be different among photoperiod conditions ($X^2_{(5)}$ = 7.376, p < .194, Figure 4.1), power = .567. Female survival was not influenced by early or delayed puberty timing ($X^2_{(1)}$ = 1.308, p < .253, Figure 4.2D). Male and Female survival rates did not statistically differ ($X^2_{(1)}$ = 0.312, p < .576, Figure 4.2E), although power analysis revealed the ability to detect real gender differences was quite low (gender = .075; overall

Photoperiod = .621; Gender x Photoperiod = .749). Gender data were not combined in order to remain consistent with regard to the integration and discussion of other reported measures, which only pertain to males in the study.

Biological Age- Puberty Onset. To determine whether the duration of time hamsters lived after puberty onset was equal across groups (e.g., "post-puberty survival"), survival rates were assessed across groups in similar fashion as above, except the dependent variable was the number of days each hamster lived after puberty onset. Overall, post-puberty survival varied substantially among groups ($X^2_{(5)}$ = 29.464, $p < .001$, Figure 4.3A), consistent with our finding above that inducing early vs. late puberty does not affect survival measured by chronological age. Median post-puberty survival was greatest in SNP E and LD photoperiods, (807 d and 752 d respectively, grand median = 708); DS and SNP D experienced the shortest post-puberty survival (544 d and 646 d, respectively). As expected then, when comparing post-puberty survival between early (SNP E, LD, LDLD) and delayed (SNP D, SD, DS) puberty photoperiods, early puberty groups spend more (median) days as adults compared to delayed groups (early = 740 d, delayed = 642 d; $X^2_{(1)}$ = 16.189, $p < .001$, Figure 4.3B). There was no effect of seasonal vs. fixed photoperiod conditions on post-puberty survival, $X^2_{(1)}$ = .347, $p < .556$ (Figure 4.3C). Finally, although the number of short day seasons (e.g., "winters") did not affect chronological age based survival rates, post-puberty survival significantly differed on this factor, $X^2_{(3)}$ = 21.423, $p < .001$ (Figure 4.3D), but without respect to a linear trend in either direction: Hamsters never exposed to a short day (8 h light) condition (LD and LDLD, median =

748 d) exhibit comparable post-puberty survival to hamsters exposed to 3 or more winters (SNP D, DS, median = 766 d), where hamsters exposed to one (SD) or two (SNP E) winters exhibit median post-puberty survival of 866 d and 865, respectively. We attribute this significant result to be an artifact of the way SNP E was separately categorized from the other two seasonal photoperiod conditions: When combining SNP E into the same winter category of SNP D and DS, this effect is lost.

Post Maximum BW age as a life stage progression. The second measure of life history progression and survival we wish to investigate is how long individual hamsters live after reaching a maximum body weight (post Max BW survival), a measure previously determined in Chapter 2. Overall, post Max BW survival significantly differed between photoperiod groups, $X^2_{(5)} = 13.996$, $p < .016$, (Figure 4.3E, median survival = 493 d. Hamsters in SNP E, LDLD, and DS photoperiods demonstrate the shortest survival after achieving maximum body weight (416 d, 422 d, and 425 d, respectively) and LD, SD, and SNP D lived longest (533 d, 571 d, and 575 d, respectively). Stratifying these groups into early and delayed puberty reveals hamsters in early puberty photoperiods have shorter survival (median = 452 d) after post Max BW compared to hamsters in delayed puberty photoperiods (median = 535 d; $X^2_{(1)} = 5.224$, $p < .022$, Figure 4.3F). In contrast, there was not a significant effect of seasonal or fixed photoperiod conditions on post Max BW survival, $X^2_{(1)} = 2.240$, $p < .134$, (Figure 4.3G). Similar to the main effect of number of short day "winter" photoperiod exposure, there is a main effect of post Max BW survival ($X^2_{(3)} = 7.981$, $p < .046$, Figure 4.3H).

Influence of seasonal timing on incidence of death. Trends in death month were assessed with Rayleigh's test of significance upon vector strength. Circular death plots and distributions are presented in Figure 4.4. Seasonal light timing did not influence the frequency of deaths in any single seasonal group (SNP E, $Vr_{(39)} = .223$, $p < .15$; SNP D, $Vr_{(39)} = .091$, $p < .2$; DS, $Vr_{(40)} = .048$, $p < .4$). This did not change when SNP E and SNP D were combined into one group and aligned with respect to the SNP year ($Vr_{(78)} = .067$, $p < .4$). Last, all seasonal groups were combined by month of the SNP year; for DS, the SD-LD transition was considered Summer Solstice, and LD-SD transition considered Winter Solstice. There was not a significant effect of photoperiod season when assessing vector radius of all seasonal groups together ($Vr_{(118)} = .031$, $p < .4$).

Planned comparisons. Groups matched in certain light schedule parameters (i.e., 16 h total daily light, delayed and seasonal photoperiod, SNP schedule etc.,) were assessed independently to gain more direct assessment of specific light history components of survival (Chronological Age, Post-Puberty survival, and post Max BW survival) and light parameters.

SNP E versus SNP D. SNP E and SNP D experienced the only naturalistic photoperiod regimen in the study, and only differ in the phase of the SNP to which they were born. Any difference in lifespan implies some factor related to the difference in offset seasonal timing between them. Survival curves of chronological age appear identical, crossing or overlapping over 12 different times across the lifespan, $X^2_{(1)} = 0.022$, $p < .881$. Consequently, the early puberty onset of hamsters in

SNP E yield longer post-puberty survival than SNP counterparts ($X^2_{(1)}$ = 7.005, p < .008). However, recalling SNP E hamsters adopted a BW rhythm matching that of SNP D during SNP E's second summer, relative to SNP D's first summer (during which puberty was achieved); the result is that SNP D hamsters lived longer after Max BW, $X^2_{(1)}$ = 8.693, p < .003.

LD versus SD. We sought to compare SD and LD survival to other reported literature using long and short day lifespan studies using other rodent species with less salient photoperiodic responses compared to the Siberian hamster. Other studies have looked at LD versus SD survival but only after controlling for potential effects of puberty timing (i.e., sharing pre-puberty photoperiod history). LD and SD hamsters did not exhibit different survival rates ($X^2_{(1)}$ = 0.856, p < .355), despite the fact LD hamsters reached puberty onset by 25 d, driving a main effect of post-puberty survival ($X^2_{(1)}$ = 3.903, p < .048) between conditions. LD and SD hamsters shared equivalent post Max BW survival, (533 d and 571 d, respectively; $X^2_{(1)}$ = 0.507, p < .476), strengthening the hypothesis that age of maximum BW is under the control of a separate timing mechanism, or at least not controlled by the same interval timer regulating somatic changes associated with hormone driven BW gain associated with puberty onset.

LD versus LDLD. LD and LDLD groups both receive 16 hours of daily light, live under fixed photic conditions, and began puberty onset by 25 days of age. Any difference in lifespan between these groups would be attributable to the difference in how the 16 h photophase was distributed within each 24 h light cycle (e.g., 8 h light, 4

h dark, 8 h light in LDLD). Survival was equivalent between LD and LDLD with respect to all three measures of age (Chronological Age, $X^2_{(1)} = 2.273$, $p < .132$; post-puberty survival, $X^2_{(1)} = 2.273$, $p < .132$; post Max BW survival, $X^2_{(1)} = 2.498$, $p < .114$). Also unique to these groups was they were the only two photoperiod conditions that had median decile survival under 1000 days of age.

LD versus DS. LD and DS hamsters occupied the same photoperiod and therefore equivalent conditions for 50% of the study. Whereas survival did not differ between groups ($X^2_{(1)} = 2.502$, $p < .114$), there was a significant difference in post-puberty survival times, $X^2_{(1)} = 16.157$, $p < .001$, as LD was early and DS delayed puberty conditions. However, post Max BW survival appears equivalent, $X^2_{(1)} = 0.786$, $p < .375$.

SD versus DS. SD and DS hamsters began the study in the same LD8:16 photoperiod chamber, thus any significant differences between groups is a result of light history differences occurring after 6 months of age. As reported above, SD hamsters outlived DS hamsters ($X^2_{(1)} = 6.843$, $p < .009$). Hamsters in SD also exhibit longer post-puberty survival $X^2_{(1)} = 7.949$, $p < .005$, however, post Max BW survival was equivalent between groups, $X^2_{(1)} = 2.297$, $p < .130$.

SNP D versus DS. Both SNP D and DS groups were exposed to delayed puberty under seasonal photoperiods. As described above, SNP D survived longer than DS, $X^2_{(1)} = 4.441$, $p < .035$. SNP D also outlived DS long enough to result in differences in post puberty survival $X^2_{(1)} = 3.930$, $p < .047$, so while SNP D was the last delayed puberty group to achieve puberty onset, the survival margin between these

groups far outweighed this difference. There was no difference in post Max BW survival $X^2_{(1)} = 2.680$, $p < .102$.

DISCUSSION

Overall our lifespan study of the Siberian hamster demonstrates survival rates are influenced by specific parameters of photoperiodic conditions. Namely, we demonstrate photoperiods that do not allow for either stable or naturalistic entrainment to the light-dark cycle shorten the lifespan of hamsters. In this study, the two photoperiods we found to accelerate mortality were LDLD and DS. Discretely changing, or "square wave" seasonal photoentrainment has been previously shown to reduce lifespan in the lesser mouse lemur compared to naturally occurring seasonal changes to the light dark cycle (Perret, 1997), although in the former experiment the square wave season was complicated with an 8 month annual period alternating between 5 months of long days and 3 months of short days instead of matching period parameters of the naturalistic light cycle it was designed to control for. In our experiment, the average DS hamster endogenously initiated puberty onset at 158 days of age, 25 days prior to their first long day transition occurring at 6 months of age. Prior to this shift the survival rates among SD and DS groups were identical, where no deaths had occurred before 6 months of age; however after 6 months, when DS was transferred to LD16:8, they began to differentiate on two measures. First, this transfer to LD16:8 in DS hamsters during their puberty growth spurt accelerated growth rates,

not just compared to SD hamsters compared to all other photoperiod groups in the study, likely the reason DS hamsters reached the highest mean BW, and at the youngest age (56.5 g at 235 days of age). Second, DS survival plummets during the second SD exposure of LD8:16, occurring between 12-18 months of age. During this 6 month short day interval, survival in DS drops 22.5%, from 90% to 67.5%, when survival among all other photoperiod groups aside from LDLD (80%) remains above 90% at 18 months of age. This reduction of nearly a quarter of all DS hamsters implies some type of causal response to the discrete photoperiod transition from long to short days, or a latent response from the initial LD 16:8 transition. Though we did not find a relationship between seasonal timing and increased mortality in this group overall, it might be because the deaths were rather variable within this 6 month window. Alternatively, if there were in fact a bimodal distribution with respect to increased deaths about the long and short day transitions, the effects would cancel each other out at the annual level. Closer inspection of the overall occurrence of DS hamster deaths actually suggest a possible bimodal distribution, with peaks at 500 and 100 days of age, where the central tails of each respective distributions overlap between 700-800 days to create a third smaller peak in the center. Finally, the last discovery pertaining to the distribution deaths in DS appears to be that the least likely occurrence of death seems to occur during the last month of either short or long days: a grand total of 3 hamsters died during this interval of the photoperiod schedule, 1 in the final month of LD and 2 in the final month of SD. This implies DS hamsters were somewhat acutely

affected by the abrupt photoperiod transition, and survival probability of individual hamsters increased the longer ago the previous transition occurred.

Regarding LDLD entrainment we propose one of two accounts of the shortened survival times: Hamsters either did or did not possess a circadian system endowed with the flexibility to maintain bifurcated entrainment to this LDLD exotic photoperiod for their entire lives. If they did, we would interpret these results to mean output of this particular state of circadian organization is non optimal in at least one organ or biological system necessary for sustaining life. However, we propose the more probable account that LDLD hamsters were more than likely not stably entrained to this unnatural photoperiod for the duration of their lives, if at all. Previous literature most prevalently reports stable bifurcated entrainment maintenance through access to wheel running in each of the two daily scotophases, though stable LDLD entrainment has been successfully maintained without wheel access (Rosenthal et al., 2005). Running wheels were not provided in this study for reasons of confounding factors with respect to the other photoperiod conditions. Therefore, given waveform data from 24 h BT, we assert LDLD did not maintain bifurcated entrainment from 18 days of age until death, and one of three scenarios was likely to be the alternative entrainment categorization of LDLD hamsters. First, hamsters in LDLD may have adopted stable entrainment to the equivalent of a quasi-skeleton LD20:4 photoperiod, essentially ignoring the nightly 4 h scotophase. Second, LDLD hamsters might not have ever become stably entrained to this photoperiod, continually phase shifting each day, a previously reported cause of increased mortality in rodents, compared to hamsters

under similar light schedules that instead go arrhythmic or free run independently of the LD cycle. Third, hamsters in LDLD may have started out with stable bifurcated entrainment and adopted one or both of the two strategies named above. Of course, it is likely that not all hamsters in LDLD fit into exactly one of these three proposed entrainment alternatives to pure LDLD entrainment, but rather hamsters were distributed across these proposed alternative entrainment types based on differences among individual chronotypes. The combination of supplementary data collected in these hamsters appear to suggest the majority of these hamsters adopted to an LD20:4 photoperiod: BT analysis of LDLD hamsters were consistently elevated at the same acrophase (e.g., during the 4 h day scotophase), suggesting indeed hamsters in LDLD were not bifurcated, at least with respect to body temperature on a continual, lifetime basis. Moreover, the observed stability of this acrophase across consecutive rounds demonstrates hamsters were not free running independently of the light:dark cycle. What was not consistent with LD20:4 entrainment, however, was that LDLD wheel running was high during both day and night bouts, suggesting these hamsters might have indeed had a second active phase that was masked in the absence of wheel availability. A methodological disparity might account for this observation: lights were off during both day and night wheel running assessments, where all other groups experienced day wheel running during the photophase. It has been previously reported that hamsters readily bifurcate wheel running entrainment that begins with the very first exposure to a wheel during subjective day when the lights are turned off (Gorman

& Lee, 2001); this might explain robust wheel running during the non-entrained night scotophases.

Certainly the BW growth rates among early puberty groups demonstrate LDLD hamsters achieve the highest mean BW at 200 days of age, data supporting the notion of adopting entrainment to LD20:4, a trend consistent with previous studies reporting BW growth rates during puberty correlates positively with respect to the length of the (non-SNP) photophase (Gorman 1995). This reason alone, early BW acceleration, might directly insult survival, as hamsters in the photoperiod condition resulting in the shortest median lifespan, DS, exhibited the highest growth rates upon puberty onset and achieving the highest maximum BW among all groups. Repercussions to organ health or function in young hamsters with increased growth acceleration resulting from a photoperiodic response to unnatural light exposure may be one causal agent of accelerated demise observed in LDLD and DS hamsters. SD hamsters, in contrast, demonstrated both the smallest BW gains in the study in addition to longest median survival, however this group also experienced the only photoperiod that allowed complete interval timer control, independent of light timing, to promote puberty onset. The longer scotophase of SD might allow for the closest 24 h alignment of phase angles that would have been maintained endogenously under constant darkness, a photoperiodic schedule which permits full control of the circadian system to generate individual free running rhythm without having to perpetually align with an external light timing. Constant lighting conditions (Tapp & Natelson, 1986) and SD photoperiods (Natelson et al., 1993) have previously been reported to yield the

highest survival in rodents compared to LD12:12 and non 24 h photoperiods, which we also find with our SD hamsters substantially outliving LDLD hamsters. It is also worth noting both SD and DS groups mean projected puberty onset occurred before 6 months of age, when DS hamsters were first transferred to LD16:8. Therefore, the interval timer in DS hamsters had also been permitted complete internal control, yet lifespan differences were greatest between SD and DS, suggesting complete interval timer control of puberty onset alone is not a sufficient mechanism to prolong lifespan.

Timing of life-stage progression on lifespan. The schematics of life stage progressions observed here are illustrated in Figure 4.5. These results strongly demonstrate lifespan is unaffected by age of puberty onset. Manipulating the percent of life spent as an adolescent from 3.2% in early puberty groups to 20.2% in delayed puberty groups had no effect on survival rates. In addition to overall early vs delayed puberty survival rates (previously illustrated in Figure 4.2A), more appropriately matched comparisons of SNP E to SNP D, and of LD to SD, both independently assert that puberty timing does not affect lifespan. Therefore in conclusion, observational studies estimating the relationship of puberty timing and lifespan *between* species (Prothero 1993; Wootton 1987) present strictly correlational data, as the present study demonstrates that manipulating puberty timing *within* species does not causally affect longevity.

Overall differences in survival were determined after the age of achieving maximum BW. Also, early puberty groups demonstrated a longer young adult life stage, with longer latency between puberty onset and maximum BW compared to

delayed groups, reaching maximum BW soon after puberty onset. However a significant difference was still observed in post Max BW survival among early and delayed puberty groups, where post Max BW survival was longer in delayed puberty groups. Two conclusions result from these findings: First, age at maximum BW is not proportionally delayed with respect to puberty onset, but, excluding SNP E, occurs within a surprisingly narrow range of 235-297 d of age. Second, there is not a rigid relationship between the onset of max BW and remaining survival, suggesting this parameter does not strongly identify the initial decline and deterioration to health observed in aging organisms entering senescence. Perhaps additional BW parameters such as lifetime mean, maximum growth rate, or the actual BW maximum value might be useful in predicting lifespan, which will be incorporated into the lifespan regression model we propose in Chapter 5.

Laboratory versus Naturalistic Photoperiods and Lifespan. The study served to test two separate hypotheses on about survival differences among hamsters living in fixed vs. seasonal photoperiod conditions. The first hypothesis was that seasonal transitions between winter and summer phenotype somatic states might induce hazardous consequences to health that could accumulate over time, analogous to health hazards associated with human "yo-yo" dieting. Evidence of this hypothesis would be supported if the fixed photoperiod groups outlived the seasonal photoperiod groups. Controlling for puberty differences, this is tested by comparing SNP E to LD and SNP D to SD. The second hypothesis states biological ramifications of the winter phenotype include protective effects to health and or aging, for this phenotype must be

accompanied with an incredibly strong benefit if evolution is dependent upon successful reproduction and the winter phenotype completely retards this capability. Explicitly, reduced (male) testosterone, lower BW, and BT waveforms are all greatly differentiated between summer and winter phenotypes. In the Siberian hamster, short day lengths have been shown to augment stress induced leukocyte trafficking, and skin immune function (Bilbo et al., 2002), macrophage responsiveness (Navara et al., 2007), and altered responses to delayed-type hypersensitivity challenges (Workman et al., 2010). If this strategy of ultimately using less resources to overwinter has beneficial health consequences in addition to simply increasing the probability of living long enough to complete another breeding season, one would surmise hamsters spending more time in the winter state would outlive hamsters that either completely forego the winter phenotype or even at a proportionate rate to hamsters with smaller fractions of life spent in the winter state. Stratification for this assessment would be LDLD and LD (0 days spent in winter phenotype) vs. SD (a single winter phenotype) compared to hamsters under naturalistic conditions transitioning to the winter state annually. Results indicate there is no difference in lifespan among hamsters living in fixed and seasonal photoperiods. These findings are complemented by the analysis of death frequencies relative to timing of season. If specific components of winter or summer phenotype transitions were insulting health one would expect to observe clusters of increased mortality around these relative times of year. This was not observed among SNP groups, and therefore two explanations might account for this: First, summer versus winter phenotypes do not differentially impact health risk

factors; the winter state is preserved through natural selection for the sole benefit of conserving environmental resources during winter. Second, no gender differences in lifespan in the Siberian hamster were found: In a species with a strong photoperiodic response and also reliable gender differences in lifespan, the associated chronic attenuation of testosterone during winter might reduce or potentiate gender differences.

The observation of equivalent survival rates between LD and SD hamsters disprove two critical hypotheses. First, advancing or delaying puberty does not result in a proportionate influence on lifespan (as previously discussed). The second hypothesis that can be rejected asserts that the longer nights associated with SD photoperiods provide a functionally increased health benefit, namely from a longer nightly secretion of the hormone melatonin. This widely held notion that melatonin acts as a vitally important oncostatic agent has been widely cited, yet lacks causal evidence (Reiter et al., 2009; Blask 2009; Korkmaz et al., 2009; Kakizaki et al, 2008), although a recent large cohort study did not find a correlation among melatonin and breast cancer (Wu et al, 2013). Perhaps there is indeed additional benefit to more nightly melatonin secretion, but there may not necessarily be unequal total melatonin output among short and long nights in humans. Previous studies investigating melatonin secretion reveal there is not a simplistic on and off mechanism governing melatonin duration, but is more accurately modeled by a dual-oscillator system both controlling independent bouts of melatonin secretion, where the phase angle timing between them depends on dawn and dusk entrainment. Thus, the *duration* of nightly

melatonin secretion between long and short nights certainly differs, and in the Siberian hamster, this indeed does result in increased nightly *total* pineal output of melatonin, but whether this is enough to drive a functional benefit in humans remains unknown.

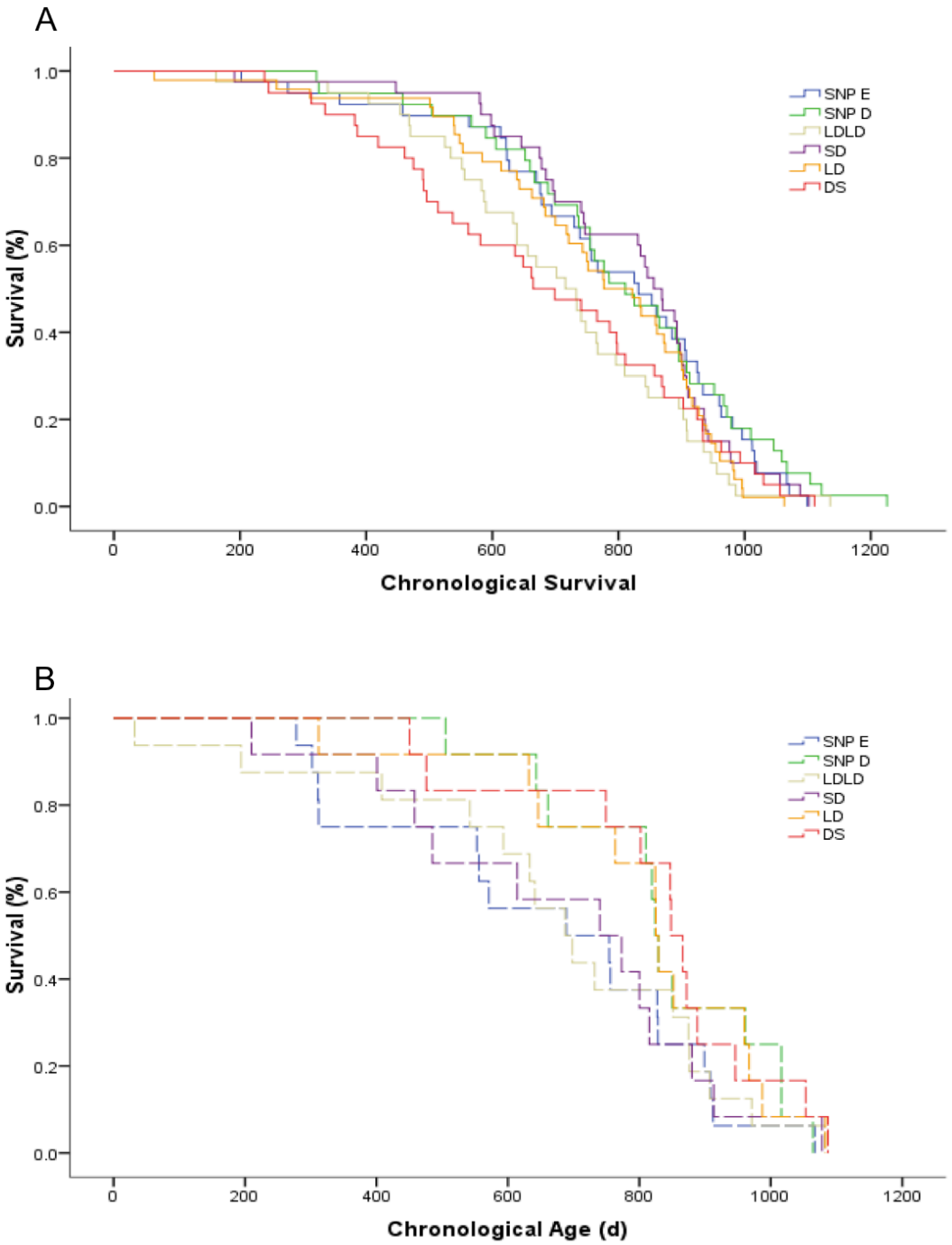

Figure 4.1. Kaplan Meier survival curves for male (A) and female (B) hamsters. Males began with n = 39-48 for each photoperiod, (N = 246); Females, n = 12-16 per photoperiod, (N = 80). X-axis = age in days, Y-axis = % surviving.

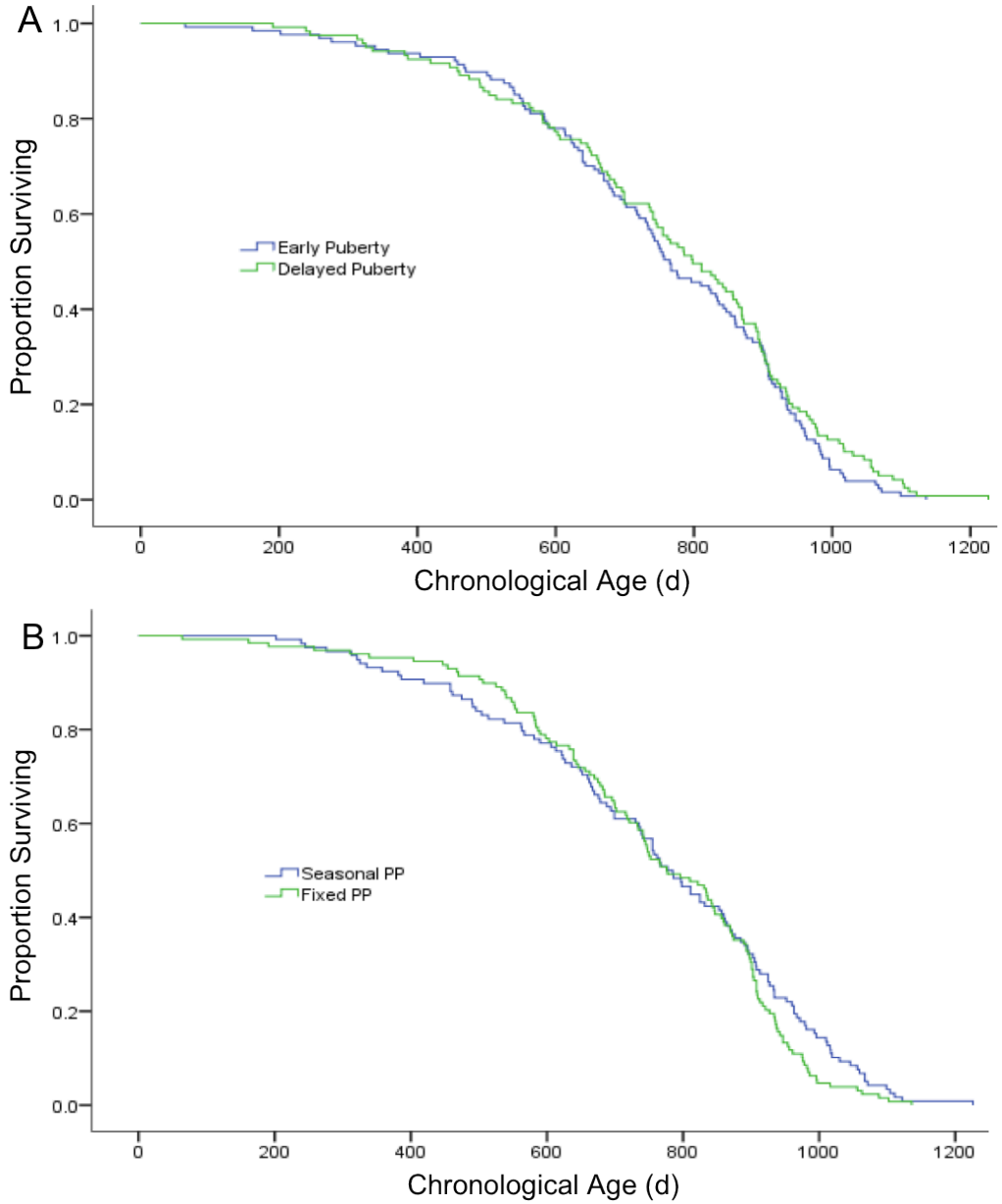

Figure 4.2. Kaplan Meier survival curves of male hamsters (N =246) comparing chronological survival of (A) early (SNP E, LD, LDLD, n = 127) versus delayed (SNP D, SD, DS, n = 119) puberty photoperiods, and (B) fixed (SD, LD, LDLD n = 128) versus seasonal (SNP E, SNP D, DS, n = 118) photoperiods. (C) Kaplan Meier survival curves of male hamsters (N =246) comparing chronological survival of number of winter transitions (0 = LD, LDLD, n = 88; 1 = SD, n = 40; 2 = SNP E, n = 39; 3 = SNP D, DS, n = 79). (D) Female Kaplan Meier survival curves comparing early (blue hatched, n = 44) and delayed (green hatched, n = 36) puberty photoperiods. (E) Kaplan Meier survival curves comparing overall chronological survival between male (n = 246, blue) and female (n = 80, green hatched) hamsters.

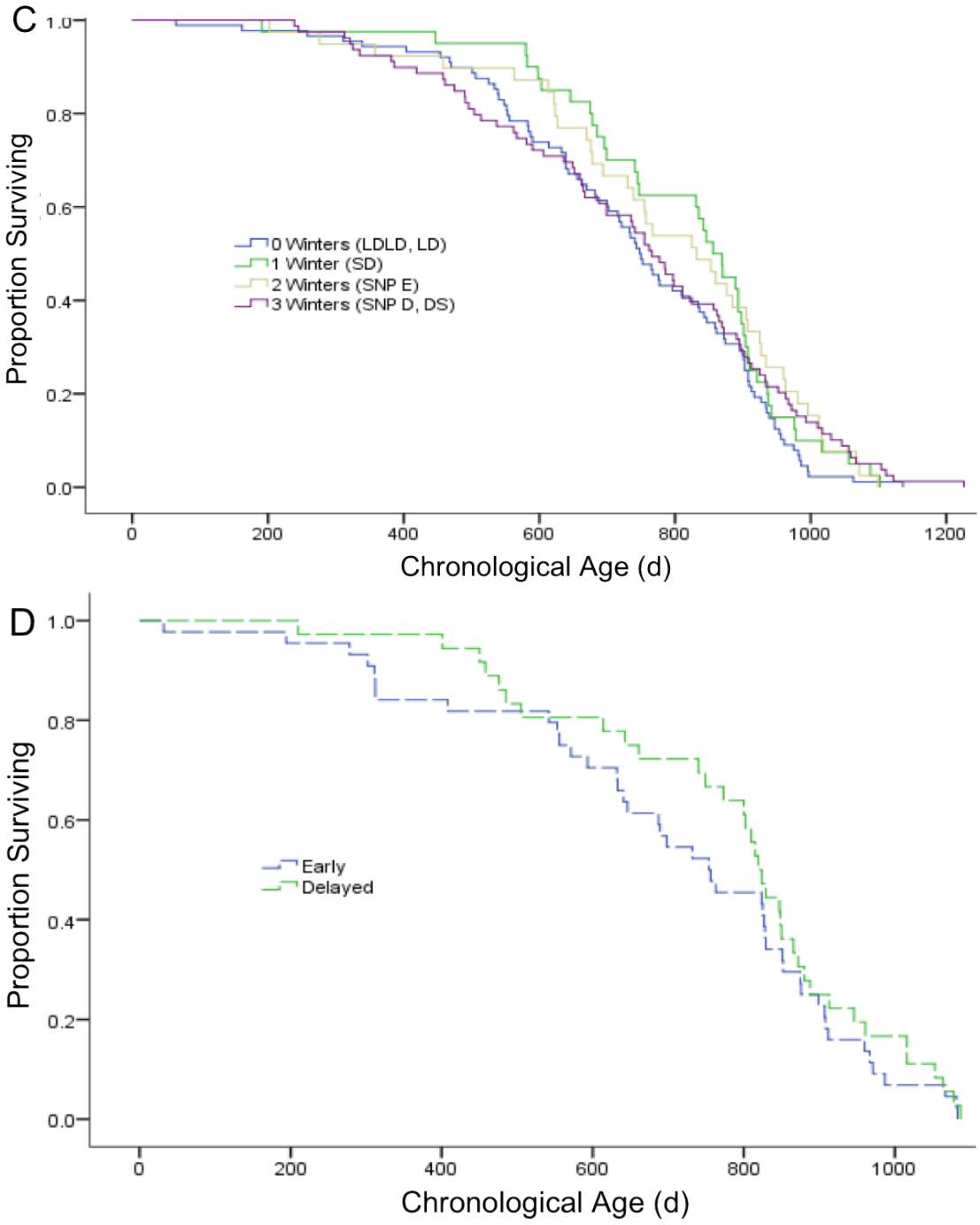

Figure 4.2. Continued

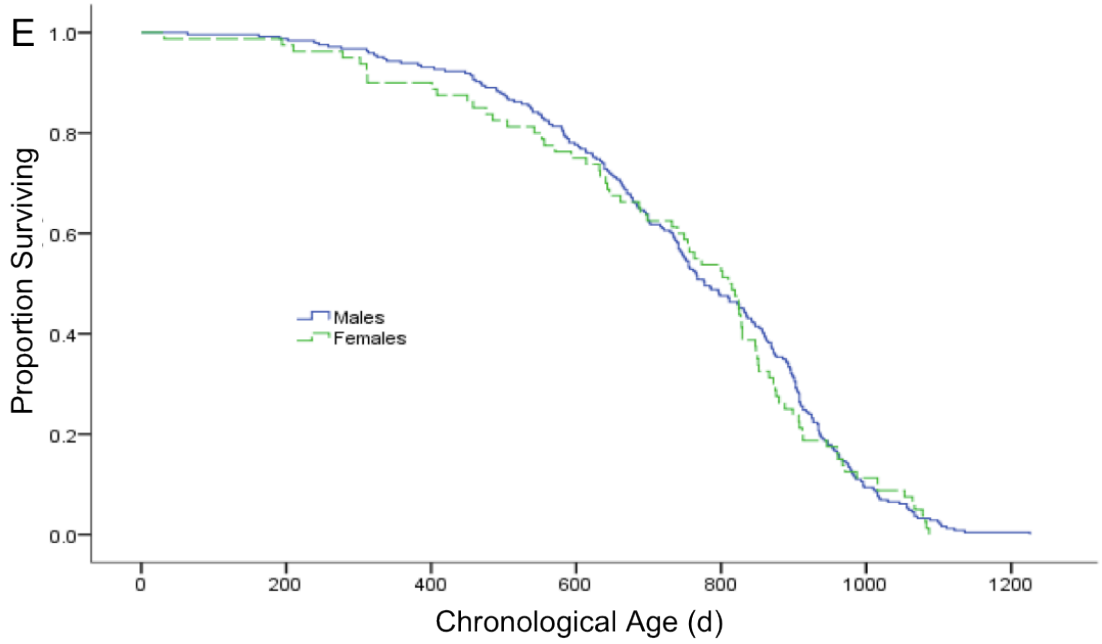

Figure 4.2. Continued

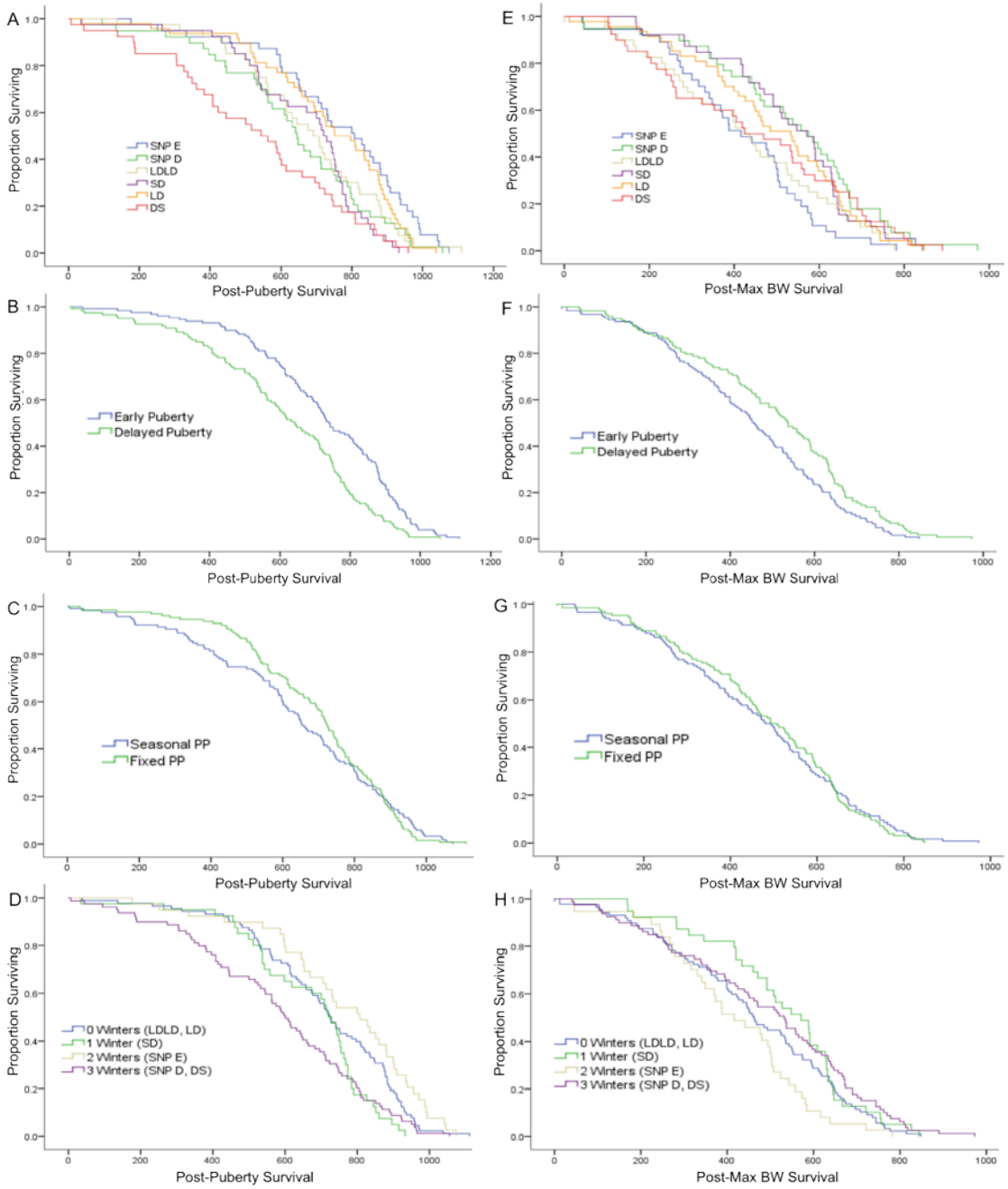

Figure 4.3. Kaplan Meier survival curves depicting post-puberty survival of male hamsters (n = 246) across (A) photoperiod conditions, (B) early versus delayed puberty photoperiods, (C) fixed versus seasonal photoperiods, and (D) number of winter transitions. X-axis = number of days lived after puberty onset. Y-axis = proportion surviving. Kaplan Meier survival curves indicating post-Max BW survival of male hamsters (n = 246) across (E) photoperiod conditions, (F) early versus delayed puberty photoperiods, (G) fixed versus seasonal photoperiods, (H) number of winter transitions. X-axis = post-Max BW survival, y axis= proportion surviving.

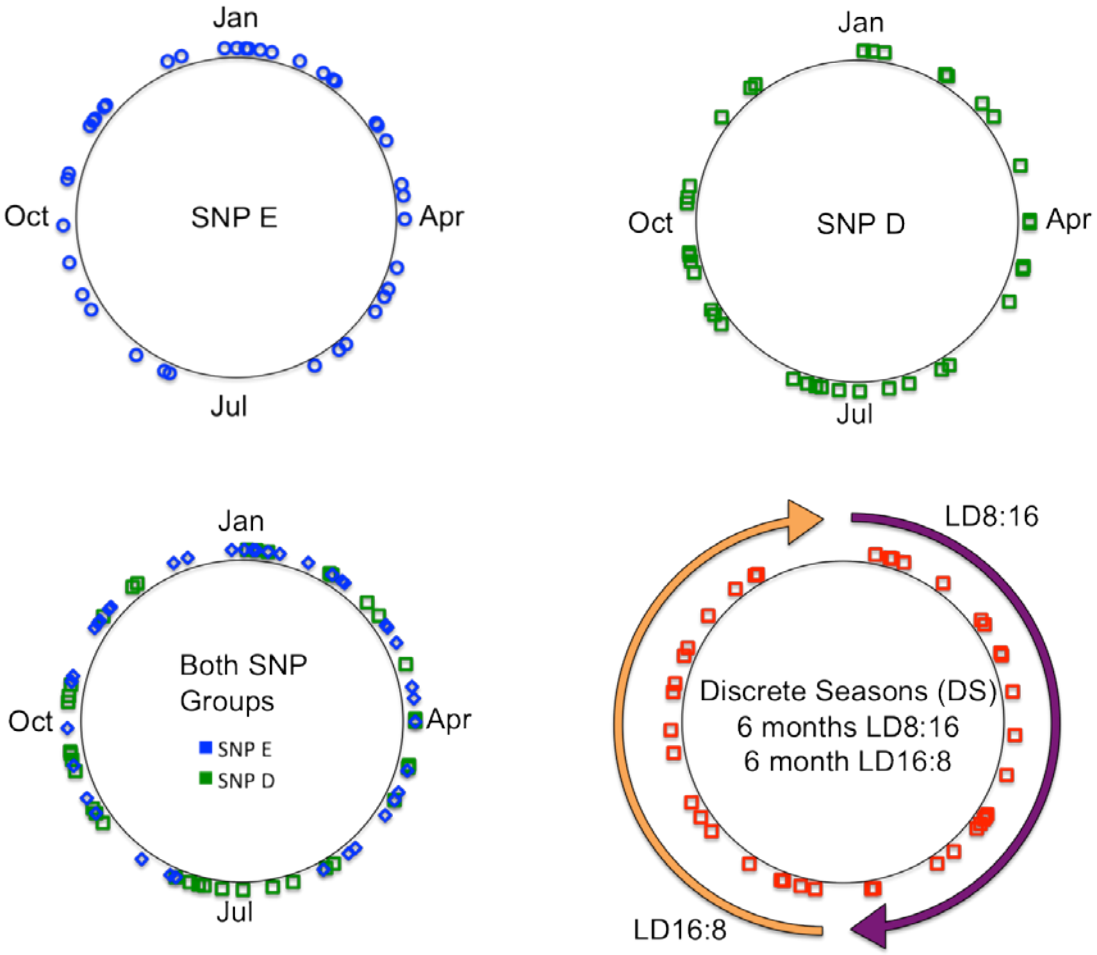

Figure 4.4. Frequency of death relative to seasonal light timing in SNP E, SNP D, and DS male hamsters. Circular plots of SNP E (top left), SNP D (top right), and DS (bottom right) hamster death rates with respect to seasonal light timing. SNP timing is identified quarterly by month (January, April, July, October); arrows on DS group identify the transition timing between LD8:16 and LD16:8 photoperiods every 6 months. Both SNP groups are also graphed together in the same plot (bottom left) to emphasize the absence of synchronizing effects of the naturalistic photoperiod schedule had with regard to the occurrence of natural death.

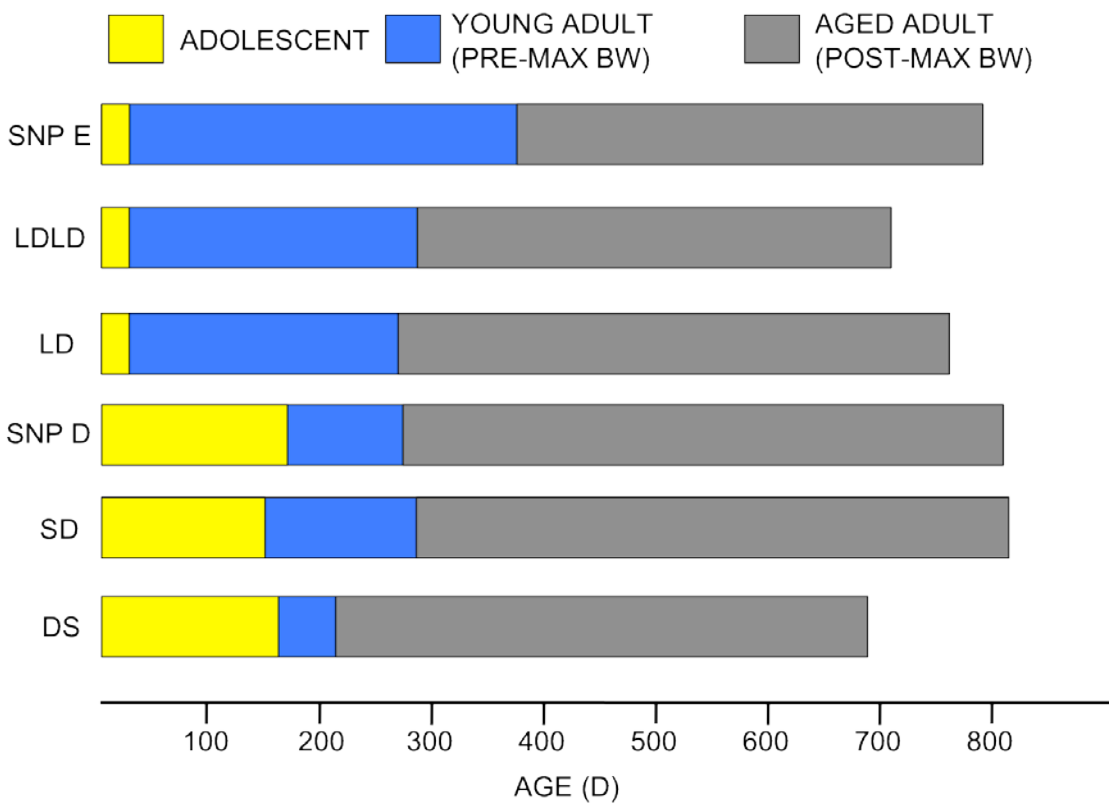

Figure 4.5. Lifespan schematic with life events by photoperiod condition- illustrating proportions of life history with regard to juvenile stage (yellow), young adult (blue) and aged adult (post max BW; gray).

Table 4.1. Means and medians for survival time

MALES

	Mean				Median			
			95% Confidence Interval				95% Confidence Interval	
Photoperiod	Age (d)	SE	Lower Bound	Upper Bound	Age (d)	SE	Lower Bound	Upper Bound
SNP E	788	34.70	720	856	832	64.30	706	958
SNP D	805	33.71	739	872	811	62.43	689	933
LDLD	705	32.05	643	768	716	50.60	617	815
SD	810	28.69	754	866	856	22.14	813	899
LD	757	30.22	698	817	777	49.65	680	874
DS	685	38.41	610	760	665	72.73	522	808
Overall	758	13.68	731	785	767	25.03	718	816

FEMALES

	Mean				Median			
			95% Confidence Interval				95% Confidence Interval	
Photoperiod	Age (d)	SE	Lower Bound	Upper Bound	Age (d)	SE	Lower Bound	Upper Bound
SNP E	658	63.57	533	782	689	183.00	330	1048
SNP D	833	48.55	738	928	824	8.66	807	841
LDLD	670	69.68	534	807	687	57.00	575	799
SD	681	72.19	539	822	740	137.70	470	1010
LD	807	59.30	690	923	825	4.33	817	833
DS	824	55.93	714	933	848	16.45	816	880
Overall	737	26.63	685	789	810	34.10	743	877

Table 4.2. Percent surviving by quartile

	75%		50%		25%	
Photoperiod	Age (d)	Std. Error	Age (d)	Std. Error	Age (d)	Std. Error
SNP E	670	30.54	832	64.30	960	29.47
SNP D	667	50.72	811	62.43	967	37.36
LDLD	556	36.29	716	50.60	847	63.67
SD	685	16.43	856	22.14	910	21.91
LD	639	64.50	777	49.65	913	16.50
DS	490	23.96	665	72.73	872	46.56
Overall	627	21.79	777	25.03	913	9.12

CHAPTER 5. ORGAN WEIGHT ANALYSIS

INTRODUCTION

Age-related pathology has been documented in the hamster, where disease is often accompanied by organ hypertrophy, generally manifesting in older animals (Schmidt et al., 1983). While longevity studies provide a valuable approach towards understanding effects of photic manipulation on the ultimate measure of health- the ability to sustain life- the disadvantage is that underlying pathology and cause of death typically go unstudied. Many mammalian organ systems deteriorate in advanced age, typically associated with diminished function accompanied by qualitative changes in gross physiological makeup. However, this aging process can be hastened through photoperiod manipulation. For example, increased heart size has been found to accompany pathological evidence of cardiac disease (e.g., widespread myocyte hypertrophy, myocardial fibrosis, gross cardiac hypertrophy), specifically, gross cardiac hypertrophy, in the tau mutant hamster (Martino et al., 2008) when photic conditions facilitate chronic circadian disruption. Renal pathology in these hamsters reveals severe kidney disease evidenced by tubular dilation, widespread collagen deposits, and glomerular ischemia with a lack of immune type deposits, excluding infection or autoimmune activity as an underlying cause.

The aims of the following organ weight analyses are three fold. The first aim is

to describe the pattern of age related changes to various organ systems in the Siberian hamster. The second is to explore whether the photoperiod history effects employed in this study influence individual health estimated from organ weight, since lifespan alone provides no information about possible repercussions on specific organ systems. Third, it is of interest whether hamsters succumbing to a natural death display proportionately aged organs compared to healthy, age-matched euthanized controls.

In this chapter, data collection among LD14:10 controls and experimental groups are first described. Overall effects of Gender, Age, and BW will be assessed among LD14:10 controls. For each organ system in the experimental males, a general linear model will test for photoperiod history effects, the relationship to covariate strength to BW and age at death, and also compare to age matched LD14:10 controls. Finally, organ-organ correlations are explored to determine whether specific relationships can be uncovered among various organ systems.

METHODS

Healthy Aging in LD14:10 Controls. Organs of old (567-716 d; except one old male = 947 d) and young (63-152 d) Siberian hamsters (38 M, 36 F) maintained in LD14:10 since birth were collected. Organs were either immediately preserved in formalin for 18 months, and then weighed, or double bagged and frozen at -80° C for 13 months, then thawed and placed in formalin for 6 months and then weighed. Brain, liver, spleen, heart, kidneys, adrenal glands, and gonads weights were included in this

analysis to test for main effects of gender, age, and assess covariate strength to BW to determine which organs grow as a function of BW. Final BWs were obtained at time of death, and again after being thawed out to assess the influence of freezing on body weight. Uncovering potential influences of freezing prior to bring placed in formalin was primarily to compare these data with future necropsies in subsequent experiments. This also ensures any effects on specific organs of frozen control hamsters (n=43) are appropriately adjusted in this study as well.

Experimental Males- Natural Death. A subset of naturally deceased male (*n* = 86) hamsters in the six experimental photoperiods recovered by UCSD animal care technicians were identified during routine daily health checks, (between 05:00-07:00 PST) sealed in a container, and refrigerated until necropsy, which typically occurred within 1-3 hours upon discovery. The remaining experimental hamsters were frozen in the same fashion as LD14:10 controls above but were not included in this Chapter. Final BWs were also obtained. Organs were then extracted, preserved in formalin for 12 months, trimmed, and weighed on a scale with precision to one thousandth of a gram.

Age-matched, Photoperiod-matched Euthanized Controls- Supplemental Analyses. Rather than have controls strictly obtained from the LD14:10 colony room bearing no dim scotophase illumination nor replication of experimental photoperiods, 18 d male "experimental control" hamsters were transferred from the LD14:10 colony into SNP-E (*n* = 6), SNP-D (*n* = 4), and LDLD (*n* = 4) photoperiods exactly 1 year after the experiment began, matching SNP control hamsters to the same photoperiod

protocol as the main experimental groups. These males were killed at 808 ± 18 d old (where Chapter 4 males hamsters bear 47.2% survival) in order to assess differences between organ weights of euthanized hamsters and hamsters dying naturally. These hamsters will be assessed separately from the main analysis due to small sample size, euthanization, and do not represent all six experimental photoperiods.

Analysis- LD14:10 Controls. A 2 x 2 (Gender x Age) ANOVA tested initial differences in BW among LD14:10 controls. In addition, a repeated measures t-test was run to determine possible effects of freezing on BW. For each organ type, a Levene's test of variance ensured assumptions of homogeneity of variance were met. When met, a Gender (Male/Female) x Age (Young/Old) General Linear Model incorporating BW as a covariate was used to test for main effects. In the event of unequal variability among groups ($p < .05$) organ weight factors were assessed independently with Mann-Whitney U non-parametric tests. Because non-parametric tests do not permit the inclusion of covariates (e.g., total body weight in this study) organ weight percentage of total body weight was determined as described below:

Organ Weight:Body Weight percent = 100 x [Organ Weight / Body Weight],

where

BR:BW = Brain Weight:Body Weight

LW:BW = Liver Weight:Body Weight

SW:BW = Spleen Weight:Body Weight

HW:BW = Heart Weight:Body Weight

KW:BW = Paired Kidney Weight:Body Weight

AW:BW = Paired Adrenal Weight:Body Weight

GW:BW = Paired Gonad Weight:Body Weight

Male and female data were combined when no main effect of Gender was found for comparison to experimental groups; otherwise only male hamster organs were used.

Analysis- Experimental Hamsters. For each organ, a General Linear Model assessed photoperiod effects of Puberty timing (Early/Late) x Season Type (Fixed/Annual), including age at death and BW as covariates. When assumptions of homogeneity were violated, factors were assessed independently with Mann-Whitney U using conventions of organ weight as %BW. Last, Pearson's product-moment correlation coefficients (r) were calculated between organ system weights and ages of life history events (n = 86).

RESULTS

LD14:10 Controls. Males outweighed females by approximately 4 g ($F_{(1,70)}$ = 4.8, $p < .032$) but BW did not differ between young and old hamsters ($F_{(1,70)}$ = .1, $p < .750$). It is interesting to note the similarity in BW among young and old male LD14:10 controls relative to the most closely matched experimental group photoperiod, LD: Referring back to Figure 2.6E, LD males exhibit equivalent BW at

130 d and 698 d but also to LD14:10 controls at this age (male BW mean ± SD = 44.56 ± 6.58g among young and old, control and LD). There was not a significant interaction between Age and Gender. ($F_{(1,70)}$ = 2.2, p < .146). Freezing had no effect body weight, $t_{(42)}$ = .55, p < .59, but elevated heart and liver weights, which were adjusted in order to be included into the dataset consisting primarily of non-frozen organs. There were no violations of homogeneity of variance among any organ systems.

For each organ studied, mean values of non-moribund young and old hamsters in LD14:10 are tabulated alongside experimental group data (e.g., brain, Table 5.1 and Figure 5.1; liver, Table 5.2 and Figure 5.2, etc.), establishing a baseline for functional organ weights (e.g., non-pathological), at ages reflecting 97.6% and 75.0% survival among LD males (99.7% and 72.4% survival among all six experimental groups at 126 d and 639 d, respectively). In LD14:10 hamsters, female livers were heavier ($F_{(1,69)}$ = 7.0, p < .010) although when adjusting for BW this effect disappeared (see below). Brain, liver, heart, and kidneys weighed more in older hamsters ($F_{(1,58)}$ = 8.3, p < .006; $F_{(1,69)}$ = 25.9, p < .001; $F_{(1,68)}$ = 45.5, p < .001; $F_{(1,69)}$ = 8.0, p < .006, respectively). Interestingly, gonads weighed the same in young and old males (Young = .698 ± .239g; Old = .556 ± .182g, *ns*). BW covaried positively with liver and heart ($F_{(1,69)}$ = 55.3, p < .001; $F_{(1,68)}$ = 61.7, p < .001, respectively), accounting for the gender difference in liver weight. BW also covaried with gonads ($F_{(1,35)}$ = 11.4, p < .002), displaying a sizeable positive correlation ($r_{(36)}$ = .519, p <

.001). In addition, BW did not account for any Age effects. There were no Age x Gender interactions.

Experimental Males- Natural Deaths. Each Table summarizes mean post-mortem organ weight of naturally deceased hamsters as a function of puberty timing and seasonal photoperiod, in addition to source table data of this analysis, and also pairwise comparisons to young and old LD14:10 controls (same Tables and Figures as mentioned above; 5.1-5.7). Individual photoperiod conditions were not assessed in order to focus the analysis on the main factors suspected to underlie any potential photoperiod group differences. Overall, Puberty timing and Seasonal photoperiod regimen had no effect on any organ weight, though kidney weight was marginally influenced by puberty photoperiod: Mean kidney weights in early puberty photoperiods were 50% heavier than in delayed puberty conditions. Hamsters under fixed seasons had heart weights that were marginally lower than those in seasonal photoperiods. There were no Puberty x Season photoperiod interactions. The only organ to (positively) covary with BW was liver. Survival was a significant covariate to kidney and gonads, where older hamsters exhibited bigger kidneys and smaller gonads.

Pairwise comparisons of organs in experimental males (mean age 830 d) to old (639 d) and young (126 d) LD14:10 controls are presented in Tables 5.1-5.7. To summarize, experimental males were equivalent to old LD14:10 controls and both outweighed young LD14:10 controls in brain, liver, spleen, and adrenal gland. Organs

where all three groups significantly differed from lightest to heaviest in order of young LD14:10 controls < LD14:10 controls < experimental males were found in heart and kidney. There were 5-fold and 6-fold reductions to gonad weight in experimental males compared to young and old controls, respectively. There was no comparison where old controls either outweighed or under weighed both experimental males and young controls.

Photoperiod Matched Controls. Organ weights of euthanized, photoperiod matched controls were compared to experimental males, creating age-matched controls for organ weight among healthy hamsters vs. hamsters with a fatal health complication (mean age of death in experimental hamsters = 830 d; euthanized photoperiod matched controls = 808 d). Gonad weight was significantly lower in experimental males, $t_{(97)} = 3.099$, $p < .003$. In addition, adrenal glands were significantly heavier in experimental males, (Mann-Whitney $U = 355.5$, $Z = -2.067$, $p < .039$).

Organ-Organ Correlations. Correlations between organ systems, and timing of life history events of experimental males were explored and results presented in Table 5.8. Referring to the Table, "Puberty Age (d)" is the age of puberty onset and "Max BW Age (d)" represents age at Maximum BW, whereas "Post-Puberty Survival (d)" represents the number of days lived after puberty onset, and "Post-Max BW Survival (d)" is the number of days lived after reaching maximum BW. Lifespan (d) is the age at death, and would also equal Puberty Age + Post-Puberty Survival, and also Age at Max BW + Post-Max BW survival of individual hamsters.

DISCUSSION

Gonads. Gonads were 5-6 times heavier in young and old 14:10 controls in comparison to the experimental males, which display attenuated values and variability upon natural death in advanced age. There were two main differences between groups that might account for these findings. First, it is plausible gonad weight is roughly stable in non-aged hamsters, and proportional to BW until a much later age (i.e., > 639 d), as our experimental group was older on average by 191 days. Second, gonads atrophy as death approaches, since 14:10 control hamsters were healthy and the experimental males had by definition, died of some health complication at time of organ collection. Critically, our age-matched, photoperiod matched, euthanized controls also possessed larger gonads than experimental males, suggesting the latter account as more probable. Taken together, gonad weight appears sensitive to advanced chronological age but also relative to when death approaches. This trend is easily visible in Figure 5.7 where the variability of gonad weight shrinks substantially between 700-1000 days of age, and importantly, the few outliers to this pattern are actually from euthanized control groups.

Given that survival was a significant covariate to gonads in the primary GLM analysis, it is not surprising to also find gonad weight negatively correlated to lifespan (r = -.380). However, it was unexpected to find the variable with the strongest correlation to gonad weight was Post-Max BW survival (r = -.405), over Post-Puberty survival. Therefore, based on gonad size, life after puberty onset is not as predictive of

lifespan as survival after attaining maximal BW, where ironically, puberty age is the permissive signal for initial testosterone, and the max BW might be more of an indication of peak testosterone (functional) output signaling peak reproductive fitness (or age), after which is followed by a systematic, age-related functional decline. Previous literature identifies delayed reproductive aging in female Siberian hamsters as a function of the frequency of induced winter states (Place et al., 2004). In this study, Post-Puberty survival and Chronological age were both equal strength correlates to gonad size, yet both of these were less correlated to gonad size compared to Post-Max BW survival. In addition, no main effect or interaction was observed on gonad size relative to photic manipulation of puberty timing or to frequency of winter state. However, the experimental males in this study demonstrate no such effect of maintaining gonad size in advanced age, either due to gender differences (e.g., male gonad size is not the reproductive aging equivalent to female follicular count or fecundity) or because any beneficial repercussions from delayed reproductive aging have been exhausted by the advanced age wherein natural death occurs. Furthermore, a separate study investigated differential delays in female reproductive aging; however, what also occurred was a differential age upon achieving maximum BW (Place & Cruickshank, 2010), the more highly correlated factor to gonad size in this study. In fact, manipulation of BW history has already been documented to delay female reproductive aging in mice through moderate calorie restriction (Selesniemi et al., 2008). Finally, it is worth considering that the widely acknowledged relationship between gonad size and BW among healthy adult hamsters demonstrate a correlation

of $r_{(36)} = .519$, $p < .001$, where $R^2 = 26.9\%$ of variance accounted for during any given day, whereas the relationship between how long ago a hamster achieved maximum BW and the final weight of the gonads upon natural death ($r_{(84)} = -.405$, $p < .001$, $R^2 = 16.4\%$) also account for a striking percent of variance. This is a remarkable degree of correlation given that the latter relationship compares a passage of time to a biological variable rather than two biological measurements from the same day.

Kidneys. Kidneys in our experimental males succumbing to natural death were twice as heavy as old LD14:10 controls, and three times heavier than young LD14:10 controls. Likewise, variability of kidney weights among experimental males was four times higher than old 14:10 controls, and 17 times higher than young LD14:10 controls. These data result in a funnel-shaped scatterplot, (see Figure 5.5) ranging between 500- 1000 days of age. Interestingly, all remaining hamsters living longer than 1050 d bear non-elevated kidney weights in departure to the established trend, barely elevated above values prior to 500 days of age. However, compared to age-matched, photoperiod matched euthanized controls, kidney weights were no different, suggesting the probability that renal hypertrophy progresses in a linear fashion with chronological age, but also that kidney weight alone may not reliably diagnose the onset of life threatening renal complications. This might be due to contingent interactions with other failing organ systems as a necessary requisite for renal disease to become fatal. Therefore, renal hypertrophy may well be used to index chronological aging but not necessarily informative to the rate of aging occurring at the individual level. This is not to say kidney *pathology* is not a sensitive measure towards rates of

aging, because previous documentation of the tau mutant hamster cite effects of photoperiod history on the frequency and severity of a myriad of renal diseases and known precursors, but at the same time detect no differences in KW:BW among groups (Martino et al., 2008). Furthermore, histological and pathological assessment of male Siberian hamster anatomy suggests a chronic disposition towards progressive glomerulonephropathy, observed in 83.3% of animals between 540-600 d old (McKeon et al., 2011); Renal adenoma was also found in 5.6% of hamsters at this age. It is probable that paired kidney weights alone may not warrant a powerful enough measure to detect renal disease vs. non diseased hamsters, and a more sophisticated approach such as those previously described may prove necessary. More likely however, is the prospect that a sizeable proportion of the euthanized age-matched, photoperiod matched control hamsters were also in the latter stages of renal disease, as less than half of the hamsters from the survival study cohort (n = 246) lived longer than 808 days.

Follow up analyses reveal 86.0% of naturally dying hamsters bear elevated kidney weights two standard errors above young LD14:10 controls mean values and 47.7% above old LD14:10 control mean kidney values. Similarly, 100% of age-matched photoperiod matched euthanized controls bear kidneys weighing more than two standard errors above mean kidney weights of young LD14:10 controls and 57.1% above old LD14:10 controls; the larger proportion of heavier kidneys is attributed to the reduced variability in age among euthanized controls.

As kidney weights were found to increase with age it is not surprising to also find kidney weights both correlate positively to lifespan and negatively with gonad weight, the only other organ weight to covary with survival, albeit in the opposite direction. However, three interesting and related findings are revealed in the kidney weight correlation analysis. First, kidney weights are just as closely correlated to gonad size as to lifespan. Second, post-puberty survival is the strongest correlational variable to kidney weight, and third, the only negative correlation between kidney weights and life history events is the age of puberty onset, though only marginally significant. Taken together these results suggest the age at which testosterone becomes present is more influential with respect to the onset of kidney weight increase than is chronological age. This also complements the marginal main effect of puberty group on kidney weight in the GLM, whereas no other organ weight approached marginal significance in either puberty or season factors. Puberty photoperiod may have in fact yielded a significant main effect in the GLM if the high variability in kidney weights was not such an influence; overall, kidneys of early puberty photoperiods were 50% heavier with twice the standard deviation compared to delayed puberty photoperiod kidney weights (1.426 ±1.901g and 0.980 ±0.740g, respectively).

Spleen. Spleens showed pronounced increases to mean and standard deviation with age (Figure 5.3). Experimental males dying naturally demonstrated a six fold increase in mean spleen weight vs. young LD14:10 controls and nearly double (1.81x) the mean weight of old 14:10 controls. The standard deviation of spleen weights in experimental males dying naturally was .800 g, a 48 fold increase compared to young

LD14:10 controls and triple that of old LD14:10 controls. The heaviest spleen among male LD14:10 controls was from the oldest male hamster (.256 g), 231 days older than the second oldest of all LD14:10 controls. Also curious about the distribution of spleen weight among experimental males dying naturally is that 13 of the 15 elevated values prior to 850 days are from hamsters living under fixed photoperiods (LDLD, SD, and LD). Another trend is revealed in the oldest living experimental males dying naturally, exhibiting non-elevated spleen weight. There was no correlation among spleen weight to any other organ, or to timing of any life history event. Overall it appears spleen weight increases with age but that this trend begins at an earlier age with respect to age related increases observed in other organ systems.

Heart. Increased HW:BW has been found to accompany pathological evidence of cardiac disease (e.g., widespread myocyte hypertrophy, myocardial fibrosis, gross cardiac hypertrophy), specifically, gross cardiac hypertrophy, in the tau mutant hamster (Martino et al., 2008). In the current study heart weights of the experimental males were heavier than old LD14:10, which in turn outweighed young LD14:10 controls. This trend is evident is Figure 5.4, where average heart weight and dispersion increase with age. However, hearts of experimental males were equivalent to age-matched, photoperiod matched euthanized controls, suggesting heart size simply increases with age and not necessarily predictive of imminent mortality. Another interpretation, in line with kidney weights, would be that hamsters around this age (~800 d) begin to develop cardiac hypertrophy but by definition the euthanized hamsters had not yet succumbed to the disease despite, bearing equivalent risk factors

as experimental males dying naturally, seeing as in the scatterplot the euthanized age-matched controls are a representative sample within the broader age-range distribution of the natural death experimental males.

Adrenal gland. Adrenal glands of experimental males dying naturally significantly outweighed young LD14:10 controls by 390% and were twice as heavy as old LD14:10 controls; however the extreme variability likely prevented a significant difference among the latter comparison. Importantly, adrenal gland weights of experimental males outweighed age-matched euthanized controls. Referring to Figure 5.6, the scatterplot of adrenal gland weights depict an abrupt increase in value, and dispersion near 600 days of age. Uniquely, adrenal gland weights bear no significant correlations to any other organ system or life history event. For perhaps this reason, in conjunction with being elevated in experimental males compared to all other groups, adrenal gland weight appears to be sensitive to approaching mortality, but uniquely, without respect to chronological age.

Liver. Liver weight in every condition exhibited a reliable relationship to BW, consistently near 5.75% of total BW (Figure 5.2). Despite equivalent body weights, old LD14:10 controls had larger livers than young LD14:10 controls, but this difference might be attributed to the juvenile somatic state rather than the fully developed adult. Combined with the lack of any discernable trend in liver weight scatterplots (Figure 5.2), the non-significance of any main effect or survival covariate, it is likely that liver disease leading to death is hardly a frequent occurrence in the Siberian hamster.

Brain. While young LD14:10 control hamsters had lighter brains than old LD14:10 controls and experimental males, brain size did not covary with age in experimental males. Whereas body weight was comparable among young and old LD14:10 controls, it is possible reduced brain weights in young LD14:10 controls reflect an under-developed central nervous system where at this age, organs have not reached adult size or function. This would be consistent with other organs systems in LD14:10 controls (liver, spleen, heart, kidney, and adrenal weights) weighing significantly less than older LD14:10 controls despite equivalent body weight. Brain weight (g) alone did not correlate to any other measure; however, BR:BW was strongly correlated to liver weight (-.658) and HW:BW (.644), but not LW:BW or heart weight, though the underlying cause remains unclear. Finally, there was no difference between experimental males and euthanized photoperiod matched controls, it can be concluded that brain weight is not a reliable indicator of age-related decline in older hamsters but might be sensitive to rates of development in juveniles prior to attaining maximum BW.

CONCLUSION

Pronounced aging effects were revealed by increased brain, liver, heart, and kidney weight in old LD14:10 controls compared to young LD14:10 controls. However, these changes alone cannot account for differences in lifespan, as these hamsters were euthanized and contain no information about how specific organ system

weights might depart from basic age related changes upon natural death. Atrophied gonads and hypertrophied adrenal glands were present in naturally dying hamsters compared to euthanized hamsters of the same age from the same photoperiod conditions, indicating the state of these organs become fundamentally different depending upon whether death is approaching. However, this exploratory analysis only implies non-causal relationships; gonadal and adrenal responses might simply be a response to the onset of a separate life threatening complication. In this context, renal failure becomes a candidate mechanism whereby these other organ systems undergo the changes observed in hamsters dying naturally compared to euthanized hamsters: Chronic glomerulonephropathy has been identified in male Siberian hamsters (McKeon et al., 2011), and renal hypertrophy is most closely linked to the timing of puberty onset. This gender specific disposition, in conjunction with puberty onset timing, implicates testosterone as a risk factor towards developing this disease. Specifically, the initial emergence of elevated testosterone may possibly play a critical role, given that the degree of renal hypertrophy is correlated to both earlier age at puberty onset as well as longer post puberty survival (even more so than with chronological age), as this study reveals.

Photoperiodic manipulation of life history events did not appear to play a significant role in the augmentation of age-related changes to organ weight, although the degree of kidney hypertrophy was at least marginally attenuated in delayed puberty groups. The only evidence seasonal photoperiods differentially affect any organ systems compared to fixed photoperiods lie in a marginally significant ($p <$

.055) reduction of heart weights in hamsters living in annual photoperiods, and the informal observation that 86.7% of elevated spleen weights < 850 d came from hamsters living under fixed photoperiod schedules. Unfortunately neither of these organ weights covary with survival nor were they different in euthanized hamsters versus age-matched hamsters succumbing to natural death.

Finally, previous literature identifies delayed *reproductive* female aging as a function of short day induction into the winter state (Place et al., 2004; Place & Cruickshank, 2010), but in this exploratory organ weight analysis no such added benefit is apparent either in the (male) reproductive system or from any therapeutic benefits of the winter state to any particular organ system. However, Post Max BW survival most closely correlated to the rate of gonad atrophy, a parameter also reported to vary in the aforementioned delayed female reproductive aging studies. Coupled with the same effect of calorie restriction on age of max BW and delayed reproductive aging, it is possible that factors responsible for delaying reproductive aging might more squarely rest on manipulations which ultimately influence the age of attaining maximum BW.

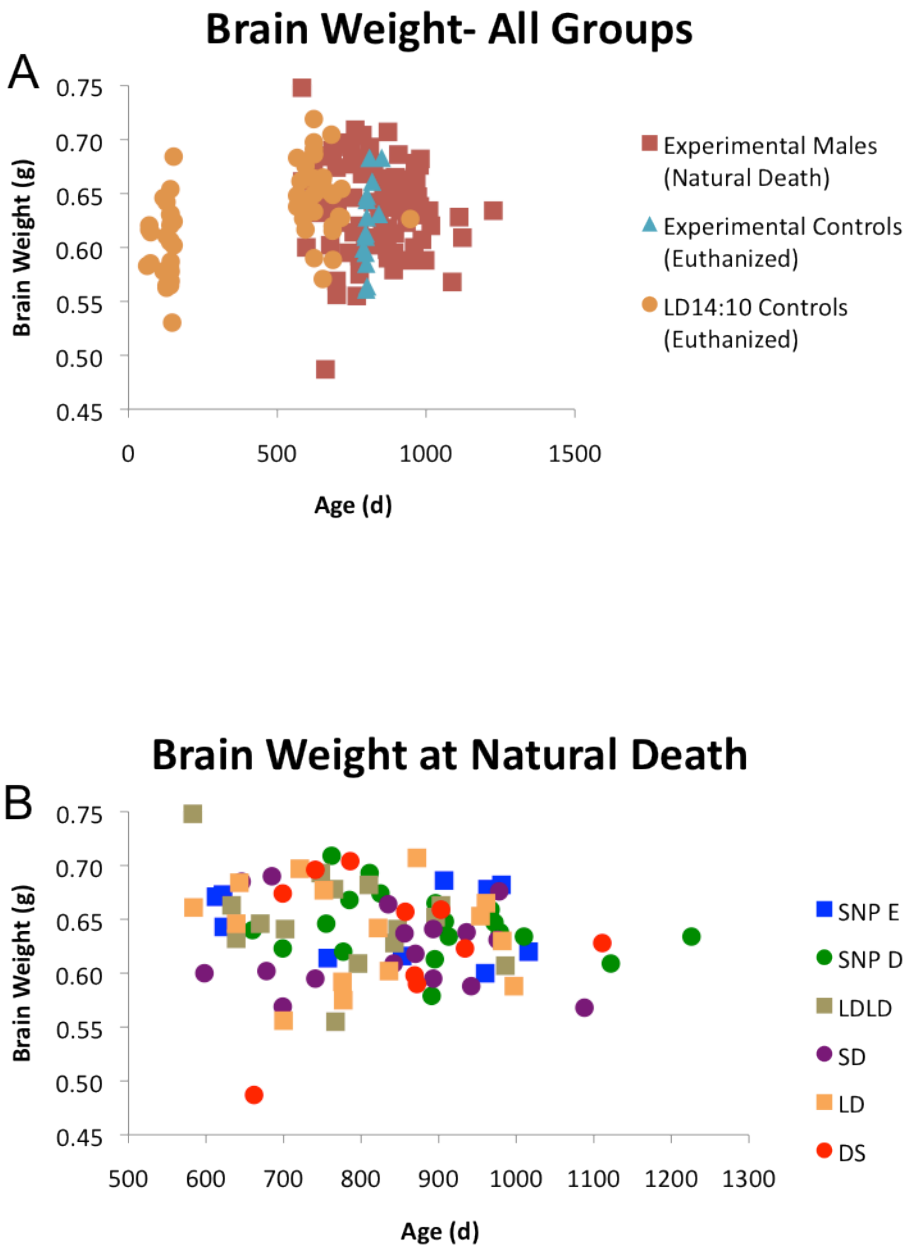

Figure 5.1. Brain weight scatterplots. (A) Scatterplots depicting the relationship between chronological age in days (x axis) and brain weights among experimental males dying naturally (red square) or euthanized (blue triangle)in comparison to euthanized LD14:10 male and female controls (orange circle). (B) Scatterplots of brain weight and age of natural death among experimental groups segregated by photoperiod condition. Squares denote early puberty, circles denote delayed puberty.

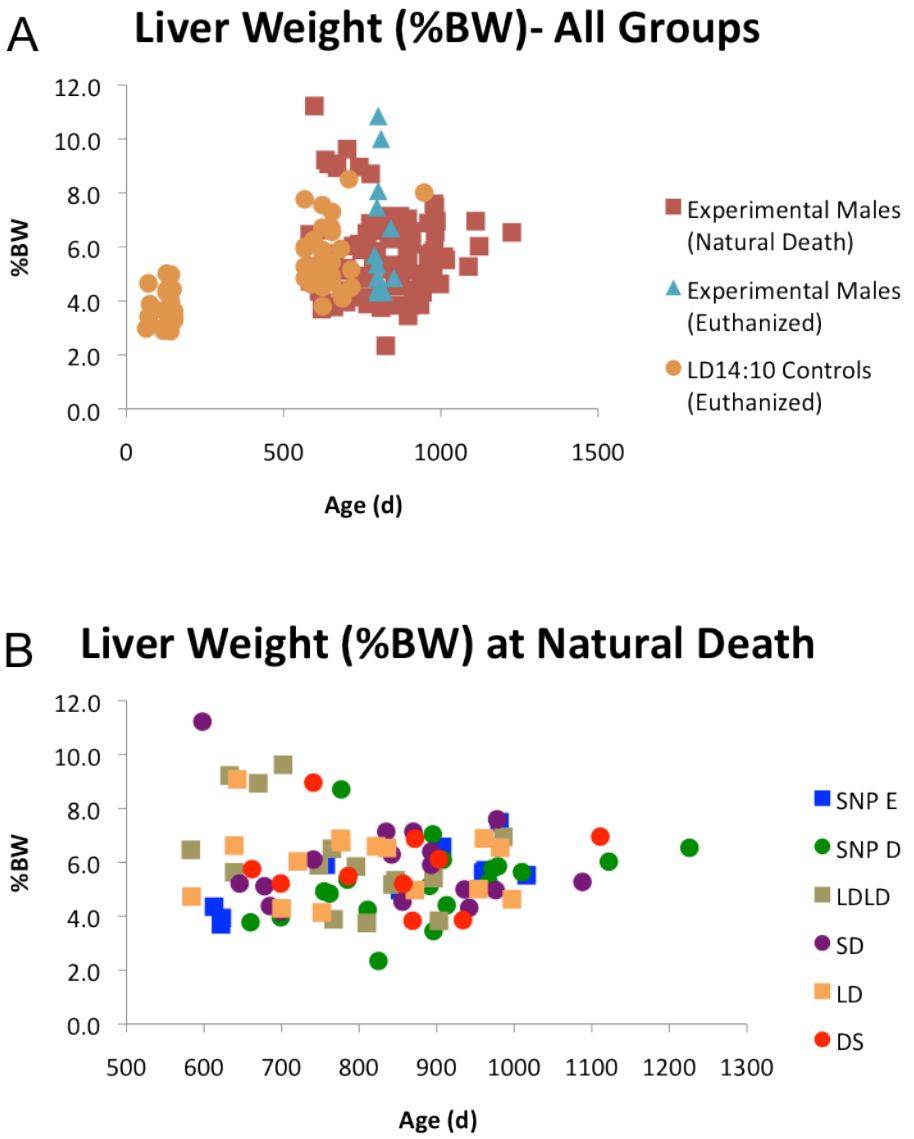

Figure 5.2. Liver weight scatterplots. Scatterplots depicting liver as %BW to chronological age of death. Conventions as in Figure 5.1.

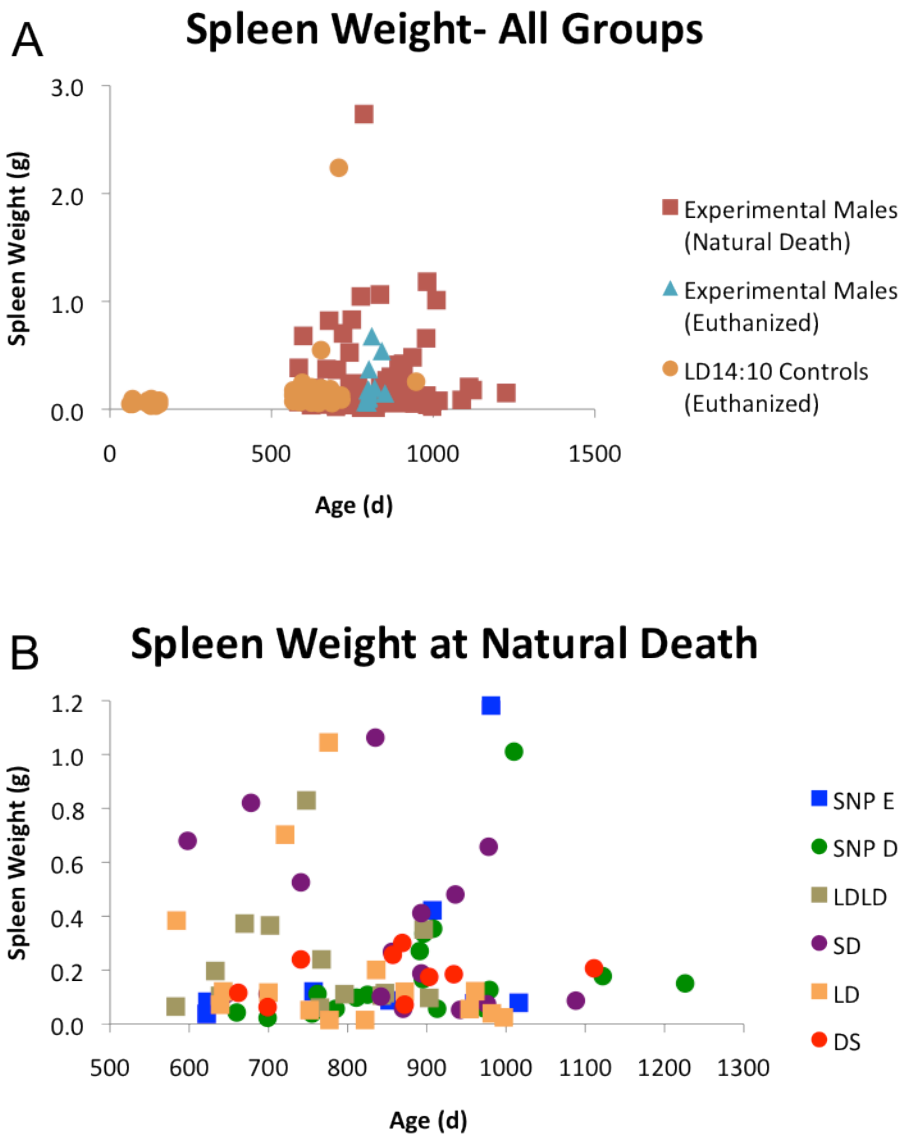

Figure 5.3. Spleen weight scatterplots. Conventions as in Figure 5.1.

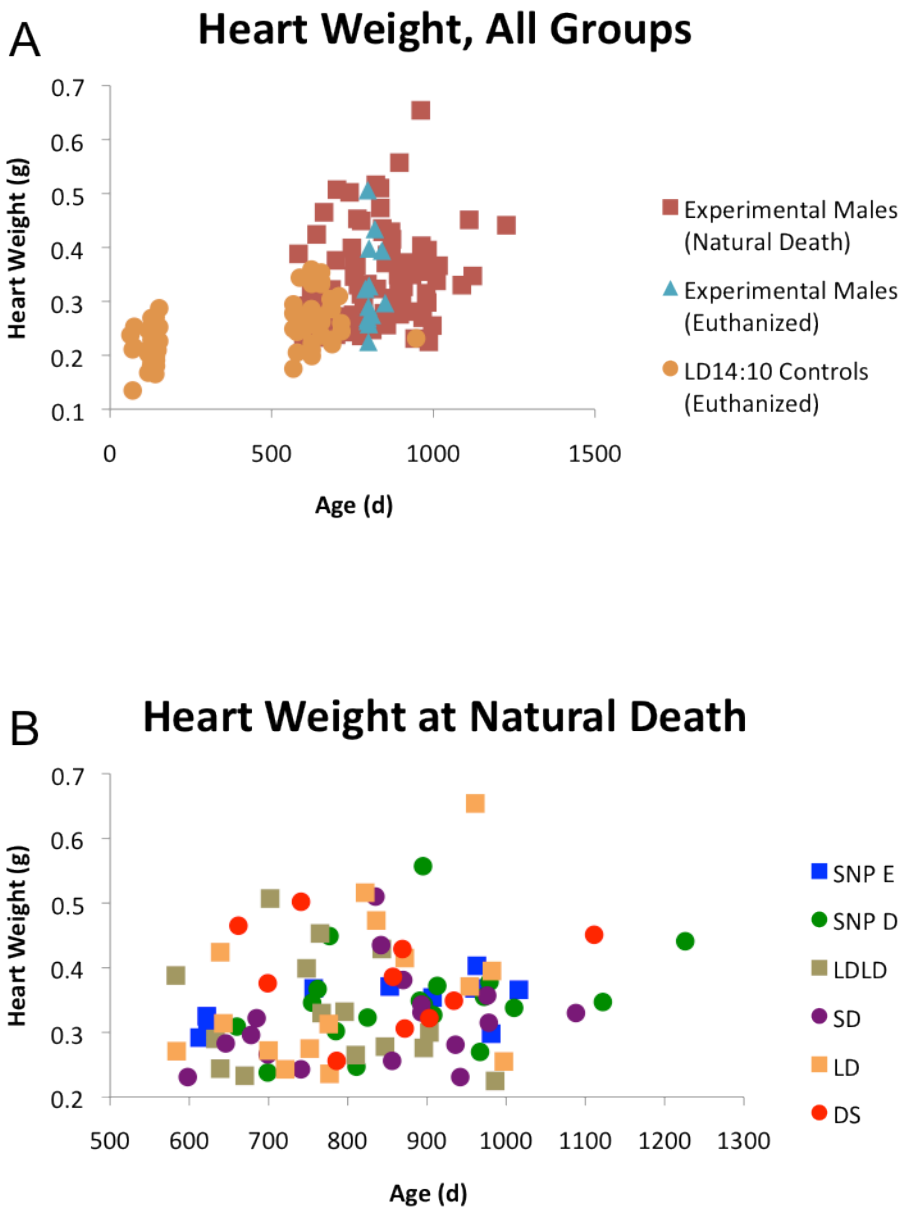

Figure 5.4. Heart weight scatterplots. Conventions as in Figure 5.1.

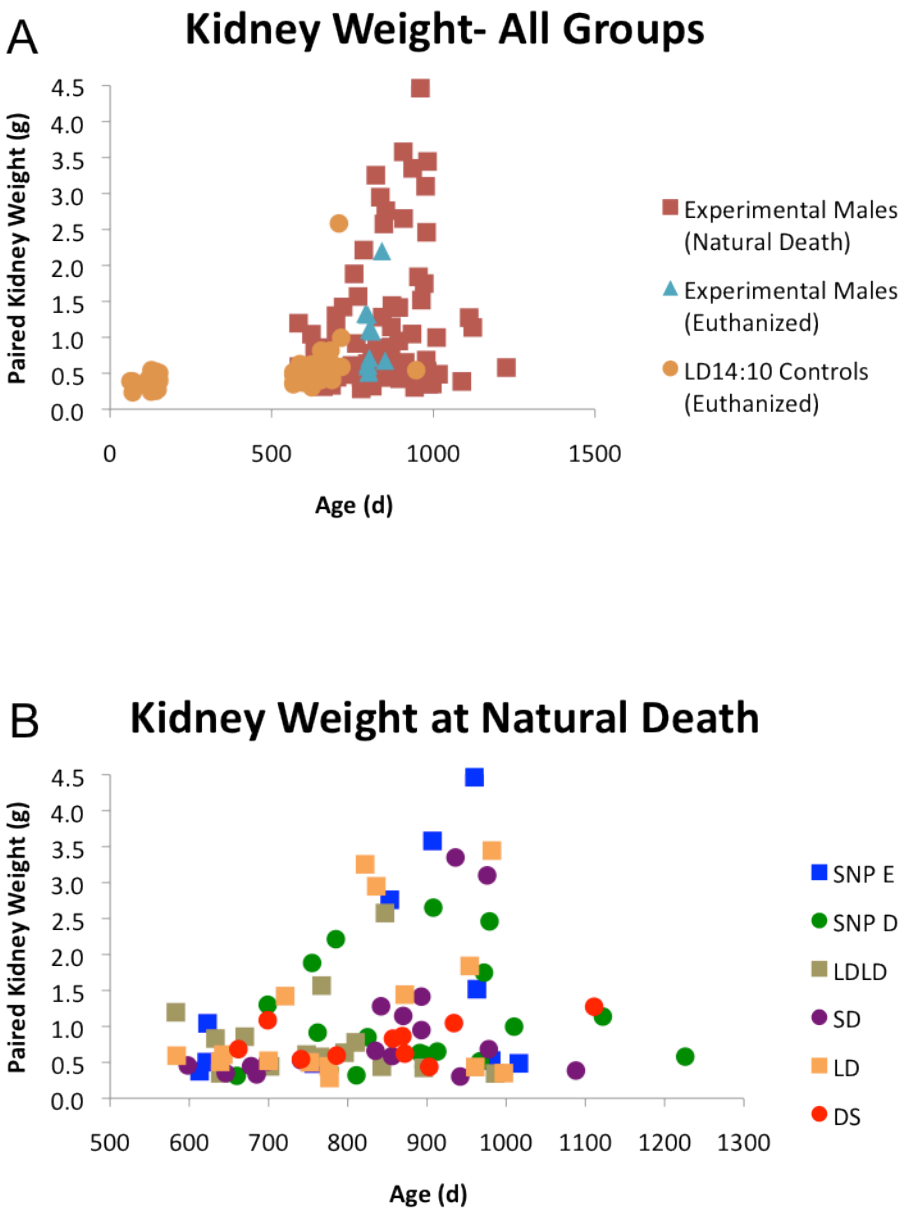

Figure 5.5. Kidney weight scatterplots. Conventions as in Figure 5.1.

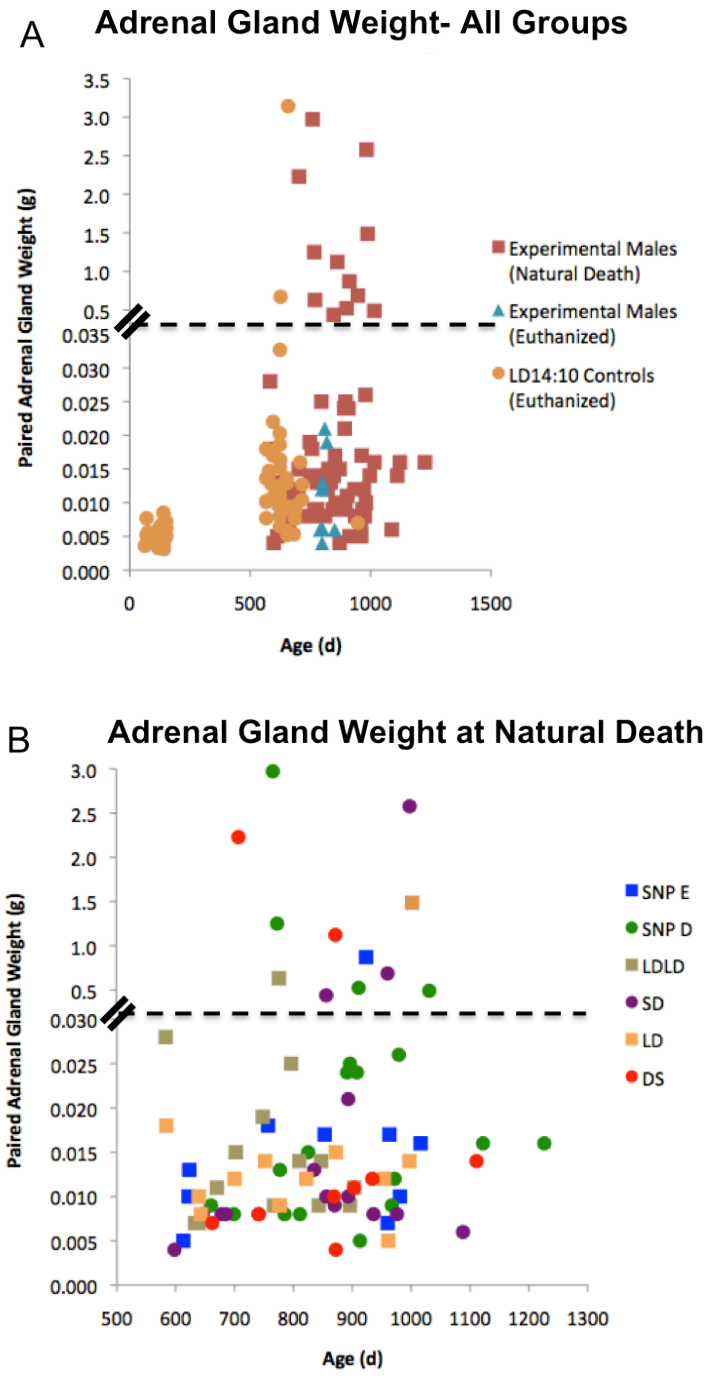

Figure 5.6. Adrenal gland weight scatterplots. Conventions as in Figure 5.1.

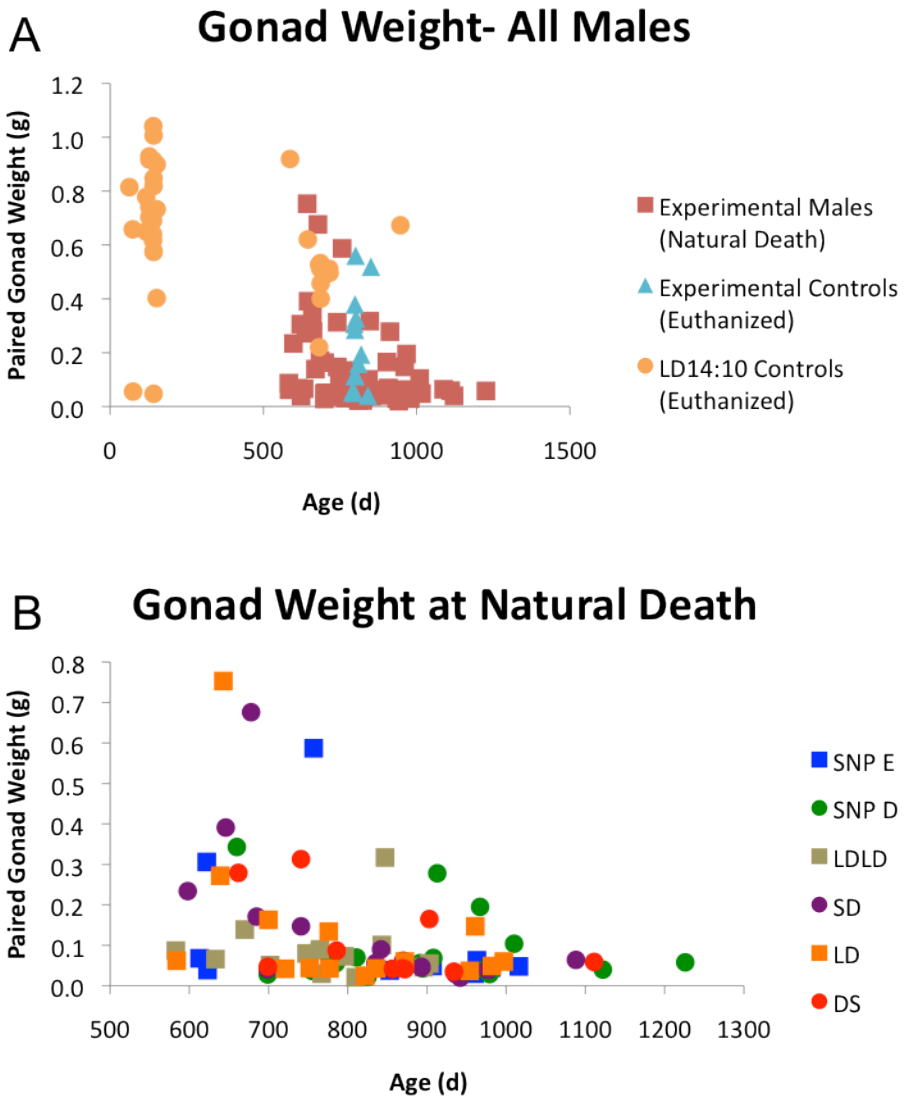

Figure 5.7. Gonad weight scatterplots. Conventions as in Figure 5.1.

Table 5.1. Brain weight summary

PUBERTY	SEASON	Mean	SD	n	
Early	Fixed	0.644	0.045	30	
	Annual	0.648	0.033	10	
	Total	0.645	0.042	40	
Delayed	Fixed	0.624	0.038	17	
	Annual	0.640	0.044	29	
	Total	0.634	0.042	46	
Total	Fixed	0.637	0.043	47	
	Annual	0.642	0.041	39	
	Total (830 d)	0.639	0.042	86	
LD14:10	Young (126 d)	0.593	0.071	29	**
(M+F)	Old (639 d)	0.649	0.034	33	**

SOURCE	SS	df	MS	F	p
BW	.001	1	.001	.525	.471
Survival	.002	1	.002	1.246	.268
Puberty	.002	1	.002	1.342	.250
Season	.002	1	.002	1.107	.296
Puberty x Season	.001	1	.001	.303	.584
Error	.142	80	.002		
Total	35.26	86			

Table 5.2. Liver weight summary

PUBERTY	SEASON	Mean	SD	n	
Early	Fixed	2.099	0.839	30	
	Annual	2.016	0.801	10	
	Total	2.078	0.821	40	
Delayed	Fixed	1.971	0.872	17	
	Annual	1.886	0.583	29	
	Total	1.917	0.695	46	
Total	Fixed	2.053	0.844	47	
	Annual	1.919	0.637	39	
	Total (830 d)	1.992	0.756	86	
LD14:10	Young (126 d)	1.645	0.370	30	*
(M+F)	Old (639 d)	2.228	0.557	44	**

SOURCE	SS	df	MS	F	p	
BW	19.300	1	19.3	56.446	.000	**
Survival	.008	1	.008	.024	.877	
Puberty	.003	1	.003	.010	.922	
Season	.817	1	.817	2.390	.126	
Puberty x Season	.000	1	.000	.001	.971	
Error	27.354	80	.342			
Total	389.8	86				

Table 5.3. Spleen weight summary

PUBERTY	SEASON	Mean	SD	n	
Early	Fixed	0.218	0.255	28	
	Annual	0.242	0.370	9	
	Total	0.224	0.282	37	
Delayed	Fixed	0.356	0.318	16	
	Annual	0.490	1.286	29	
	Total	0.442	1.045	45	
Total	Fixed	0.268	0.284	44	
	Annual	0.432	1.137	38	
	Total (830 d)	0.344	0.800	82	
LD14:10	Young (126 d)	0.057	0.017	30	*
(M+F)	Old (639 d)	0.190	0.326	44	*

SOURCE	SS	df	MS	F	p
BW	1.255	1	1.25	1.935	.168
Survival	.435	1	.435	.670	.415
Puberty	.667	1	.667	1.028	.314
Season	.001	1	.001	.001	.977
Puberty x Season	.103	1	.103	.159	.691
Error	49.288	76	.649		
Total	61.534	82			

Table 5.4. Heart weight summary

PUBERTY	SEASON	Mean	SD	n
Early	Fixed	0.346	0.104	30
	Annual	0.346	0.037	10
	Total	0.346	0.091	40
Delayed	Fixed	0.318	0.074	17
	Annual	0.362	0.076	29
	Total	0.346	0.077	46
Total	Fixed	0.336	0.094	47
	Annual	0.358	0.068	39
	Total (830 d)	0.346	0.083	86
LD14:10 (M+F)	Young (126 d)	0.217	0.034	30
	Old (639 d)	0.268	0.044	43

EXPERIMENTAL MALES NPT FACTOR ANALYSIS

Measure	Factor	n	Mann-Whitney U	SE	Z	p
Heart (g)	Puberty	86	951.5	115.493	0.273	0.785
	Season	86	1137.5	115.274	1.917	0.055
HW:BW	Puberty	86	924	115.499	0.035	0.972
	Season	86	941	45.279	0.213	0.832

EXPERIMENTAL VS. LD14:10 (YOUNG AND OLD)

Measure	n	Kruskal-Wallis K	df	p
Heart	159	72.513	2	0.002
HW:BW	159	95.043	2	0.001

PAIRWISE COMPARISONS- EXPERIMENTAL VS. LD14:10 (YOUNG AND OLD)

Measure	Pair	Kruskal-Wallis K	SE	Z	p
Heart (g)	Young-Old	37.951	10.953	3.465	0.001
	Young-Experimental	79.532	9.763	8.128	0.001
	Old-Experimental	41.401	8.600	4.814	0.001
HW:BW	Young-Old	38.864	10.953	3.532	0.001
	Young-Experimental	89.370	9.763	9.154	0.001
	Old-Experimental	50.686	8.600	5.894	0.001

Table 5.5. Kidney weight summary

PUBERTY	SEASON	Mean	SD	n	
Early	Fixed	1.376	2.039	30	
	Annual	1.574	1.495	10	
	Total	1.426	1.901	40	
Delayed	Fixed	0.970	0.913	17	
	Annual	0.986	0.635	29	
	Total	0.980	0.740	46	
Total	Fixed	1.229	1.717	47	
	Annual	1.137	0.945	39	
	Total (830 d)	1.187	1.413	86	
LD14:10 (M+F)	Young (126 d)	0.382	0.079	30	** ** **
	Old (639 d)	0.561	0.339	44	

SOURCE	SS	df	MS	F	p	
BW	1.24	1	1.24	.645	.424	
Survival	11.88	1	11.88	6.202	.015	*
Puberty	6.10	1	6.10	3.185	.078	
Season	0.04	1	0.04	.019	.890	
Puberty x Season	0.13	1	0.13	.069	.793	
Error	153.29	80	1.92			
Total	291.09	86				

Table 5.6. Adrenal weight summary

PUBERTY	SEASON	Mean	SD	n
Early	Fixed	0.094	0.293	29
	Annual	0.098	0.271	10
	Total	0.095	0.284	39
Delayed	Fixed	0.229	0.634	17
	Annual	0.308	0.717	29
	Total	0.279	0.681	46
Total	Fixed	0.144	0.448	46
	Annual	0.254	0.636	39
	Total (830 d)	0.195	0.542	85
LD14:10	Young (126 d)	0.005	0.002	30
(M+F)	Old (639 d)	0.103	0.479	44

EXPERIMENTAL MALES NPT FACTOR ANALYSIS

Measure	Factor	n	Mann-Whitney U	SE	Z	p
Adrenal (g)	Puberty	85	881	113.959	-0.141	0.888
	Season	85	1008	113.159	0.981	0.327
AW:BW	Puberty	85	936	113.388	0.344	0.731
	Season	85	959	113.388	0.547	0.585

EXPERIMENTAL VS. LD14:10 (YOUNG AND OLD)

Measure	n	Kruskal-Wallis K	df	p
Adrenal	159	58.923	2	0.001
AW:BW	159	68.438	2	0.001

PAIRWISE COMPARISONS- EXPERIMENTAL VS. LD14:10 (YOUNG AND OLD)

Measure	Pair	Kruskal-Wallis K	SE	Z	p
Adrenal (g)	Young-Old	70.169	10.897	6.439	0.001
	Young-Experimental	72.296	9.774	7.397	0.001
	Old-Experimental	2.127	8.547	0.249	1.00
AW:BW	Young-Old	65.45	10.902	6.008	0.001
	Young-Experimental	80.576	9.778	8.241	0.001
	Old-Experimental	15.081	8.551	1.764	0.233

Table 5.7. Gonad weight summary

PUBERTY	SEASON	Mean	SD	n	
Early	Fixed	0.110	0.144	28	
	Annual	0.127	0.181	10	
	Total	0.115	0.152	38	
Delayed	Fixed	0.129	0.170	17	
	Annual	0.096	0.093	29	
	Total	0.108	0.126	46	
Total	Fixed	0.117	0.153	45	
	Annual	0.104	0.120	39	
	Total (830 d)	0.111	0.138	84	**
LD14:10 (M)	Young (130 d)	0.698	0.239	26	**
	Old (698 d)	0.556	0.183	12	

SOURCE	SS	df	MS	F	p	
BW	.000	1	.000	.000	.996	
Survival	.218	1	.218	12.789	.001	**
Puberty	.002	1	.002	.138	.711	
Season	.001	1	.001	.075	.785	
Puberty x Season	.012	1	.012	.697	.406	
Error	1.330	78	.017			
Total	2.614	84				

Table 5.8. Organ-Organ correlations- natural death

N = 86	Post Puberty Survival (d)	Post Max BW Survival (d)	Max BW Age (d)	Puberty Age (d)	Lifespan (d)	Brain (g)	LW:BW	Spleen (g)	Heart (g)	Kidneys (g)	Adrenals (g)	Gonads (g)
Post Puberty Survival (d)	1	.670**	.115	-.300**	.880**	-.101	.002	.004	.204	.299**	-.048	-.365**
Post Max BW Survival	.670**	1	-.565**	.345**	.861**	-.182	-.103	.084	.190	.106	.121	-.405**
Max BW Age (d)	.115	-.565**	1	-.370**	-.066	.114	.114	-.023	-.046	.137	-.162	.155
Puberty Age (d)	-.300**	.345**	-.370**	1	.189	-.092	-.113	.165	-.016	-.192	.191	-.009
Lifespan (d)	.880**	.861**	-.066	.189	1	-.150	-.054	.087	.202	.213*	.046	-.380**
Brain (g)	-.101	-.182	.114	-.092	-.150	1	.013	.140	.035	.057	.148	.006
LW:BW	.002	-.103	.114	-.113	-.054	.013	1	.051	.261*	-.121	.026	.171
Spleen (g)	.004	.084	-.023	.165	.087	.140	.051	1	-.167	-.106	-.046	.067
Heart (g)	.204	.190	-.046	-.016	.202	.035	.261*	-.167	1	.055	.067	-.043
Kidneys (g)	.299**	.106	.137	-.192	.213*	.057	-.121	-.106	.055	1	.062	-.202
Adrenals (g)	-.048	.121	-.162	.191	.046	.148	.026	-.046	.067	.062	1	-.153
Gonads (g)	-.365**	-.405**	.155	-.009	-.380**	.006	.171	.067	-.043	-.202	-.153	1

* Indicates statistically significant at $p < .05$
**Indicates statistically significant at $p < .01$

CHAPTER 6. ASSESSING VALUE OF MULTIVARIATE COX REGRESSION ANALYSIS TOWARDS PREDICTING LIFESPAN

INTRODUCTION

As an analytical construct, aging can be defined as a manifestation of time-related biological processes that result in the decreased viability and increased vulnerability of the organism and thus enhance the probability of death (Comfort 1964). It has been previously demonstrated that measures of aging can be more valuable in predicting individual lifespan than chronological age (Ingram 1983; Ingram et al, 1982). Simply put, a subject determined to score "younger" on some age-related measure should be predicted to live longer than another subject of equal age scoring "older" on the same test. There is no value in explaining variation among individual lifespan as nothing more than random error about a population mean, whereas interpreting lifespan of an individual as a function of aging can be of predictive utility. The idea is that chronological age is a rough index of an underlying process of biological aging, i.e., functional aging. This has been demonstrated in behavioral tests sensitive to aging, where variation of performance in two year old mice accounted for 44% of variability in lifespan and up to 54% when including biological measures of body weight and body temperature (Ingram et al., 1982; Ingram & Reynolds, 1986). In humans, hand-grip strength has been identified as a predictor of lifespan (Bohannon 2008). Combining social, biological, and behavioral

measures into a multiple regression model as a means of predicting survival has been established for decades (Bartko et al., 1971; Baer & Gaitz, 1971).

With respect to body mass in particular, wealth of literature reports no direct relationship between body mass and lifespan (Anisimov et al., 2008; Gaillard et al., 2000; Conover et al., 2010, Nussey et al., 2011); however, there are persistent reports presenting evidence of increased longevity in (same-species) animals with lower body mass (Quarrie & Riabowol, 2004; Miller et al., 2002; Miller et al., 2000). Calorie-restriction, on the other hand, is one of the few body weight modulating manipulations shown to reliably affect organisms across many taxa (Mair & Dillin, 2008; Fontana et al., 2010; Nakagawa et al., 2012; Simons et al., 2013). Calorie restriction been shown to delay rates of aging (Weindruch 2008), and is also of high relevance to this study as it accompanies the winter state in the Siberian hamster.

Differences in individual longevity among the 246 male Siberian hamsters were explored by assessing parameters described in the previous chapters. As the single independent variable in the study was photoperiod history, the dependent measures were centered around variables with an expected sensitivity to circadian age. First, categorical differences in life history events are tested for predictive value of lifespan, assessing fixed vs. seasonal photoperiod, puberty timing, and strength of photoperiodic response. Second, age-related changes in BW, wheel running activity, and BT parameters will be individually analyzed in a univariate cox regression model in order to evaluate potential variables affecting lifespan. Last, a multivariate cox regression model predicting lifespan will be ran and results described. The

multivariate model incorporates potentially significant predictors of lifespan from BW, wheel running activity, and BT parameters found to significantly impact lifespan.

METHODS

There were three tiers of analysis in this chapter: an exploratory assessment of BW parameters, univariate cox regression among all parameters, and finally, multivariate cox regression model of selected variables believed to predict lifespan. First, 46 potential BW parameters are explored with respect to correlational strength with lifespan. After determining which BW parameters significantly correlate to survival, predictive value to lifespan is individually tested in a univariate cox regression model. Predictive strengths of individual wheel running counts and BT parameters are also assessed with respect to lifespan in univariate cox regression. Finally, parameters with significant predictive value to lifespan are identified, and after assessing independent variables for multicolinearity, a multivariate cox regression model is composed to assess overall predictive value of all data collected throughout the study. Data used for survival regression analyses here are derived from previously described data found in the prior chapters of this dissertation. Of interest are two distinct types of data regarding lifespan predicting power. First was categorical data and second was repeated measurement data. Categorical data did not change as hamsters aged, and were not composed of an average, or slope of multiple data points, but rather marked a single index of a life history event, including early vs.

delayed puberty onset, fixed or seasonal photoperiod history, BW at weaning, and finally, maximum BW and the age maximum BW was reached.

Repeated measurement data were parameters that changed with age and were sampled at discrete intervals across the lifetime. Data of this type included in the regression model are parameters of Body Weight, wheel running, and Body Temperature.

PART ONE: EXPLORATORY BW CORRELATIONS

Methods

For BW parameters, 46 preliminary measures were assessed on correlation strength to lifespan. The overall mean BW across the lifetime of all hamsters showed a clear trend which would influence results, illustrated in Figure 6.1: The longer the hamster lived was confounded with heavier lifetime mean BWs, as BW of juvenile hamsters in the first months of life are significantly less than at any time in life. Similarly, 1st and 2nd order BW derivatives generated from the moving 11 week cubic regression model from Chapter 2 are influenced by BW trends during roughly the first 200 days of age. To account for this, overall mean BW trends were partitioned into 5 age categories: a) overall mean BW, b) mean BW before 100 d old "< 100 d", c) mean BW after 100 d old " > 100 d", d) mean BW before 225 d old "< 225 d", and e) mean BW after 225 d old "> 225 d." These age intervals were determined in an attempt to isolate periods of initial growth (< 100 d), growth leading to maximum BW (< 225 d), and the qualitatively distinct BW trend after reaching max BW, when BW

gradually declines (> 225 d) until death. Within each of these age categories, lifespan correlations to mean BW, Max BW, and 1st and 2nd order derivatives of BW, as well as measures of BW variability (i.e., mean standard deviation of BW, and mean standard deviation of 1st and 2nd order derivatives of BW) were tested. Standard deviation measures were to investigate the influence of tightly versus weakly controlled BW regulation on lifespan. Also, with respect to standard deviation of 1st and 2nd order derivatives of BW, it was of interest to explore what possible influences the variability from a lifetime of growth rates might have on lifespan. In the end, 46 different BW parameters and their relationship to lifespan were explored to select the best measures to include into the next phase: Parameters with significant correlation to lifespan would be assessed in a univariate cox regression model.

Results

BW-lifespan correlation data are presented in Table 6.1. With respect to BW, mean BW after 225 d was negatively correlated to lifespan; therefore lighter hamsters (mean BW from 225 d old until death) lived longer (Figure 6.1). Variability of individual BW also correlated to lifespan, both overall SD and SD after 225 days old; however, overall SD was positively correlated to lifespan whereas SD > 225 d negatively correlated to lifespan.

Overall 1st derivative of BW trends and variability are illustrated in Figure 6.2. Regarding 1st order derivatives of BW, overall mean value was strongly and negatively correlated to lifespan, as well as mean rate of change >100 d. In contrast,

the 1st order derivative of BW > 225 d was positively correlated to lifespan. Variability of BW 1st order derivative was also found to correlate negatively with lifespan, demonstrating overall SD, SD > 100 d, and SD > 225 d to all have moderate and significant correlation coefficients.

For 2nd order derivatives of BW (see Figure 6.3 for lifetime trends), overall mean, mean >100 d, and mean > 225 d were found to positively correlate with lifespan. Finally, looking at mean standard deviation of BWs 2nd order derivatives, all measures except standard deviation of the 2nd order derivative of BW < 100 d are significantly and negatively correlated to lifespan. Characteristic low and high values of standard deviation among 2nd order derivative of BW during the first 225 days of life are illustrated in Figure 6.4. The standard deviation of the 2nd order derivative of BW < 225 d is the only measure of early life history to significantly (and negatively) correlate to lifespan. Representative examples of hamsters exhibiting low and high lifetime variability of 2nd order derivative of BW > 225 d are illustrated in Figure 6.5.

Discussion

Across the lifespan, weekly mean and standard deviation of BW history both display characteristic patterns, illustrated in Figure 6.1. Overall, mean BW does not correlate to lifespan, but less overall BW variability predicts longer lifespan. One issue with taking mean lifetime BW as a variable to correlate with lifespan is that mean lifetime BW is essentially a measure of mean "cumulative" BW. The overall study of 246 hamsters and their BW history produces a characteristic mean weekly curve,

described by a rapid growth within the first few hundred days, reaching a maximum BW between 200-300 days, and gradually and systematically declining for the rest of the study. This pattern in BW history creates a cumulative BW average that is affected by a) early low BWs and b) hamsters living longest lose weight. Intriguingly, when each weekly BW of the study was correlated to lifespan (Figure 6.1A) across all hamsters, a very different trend is apparent: A steady and near zero correlation of current BW is observed through the first 200 days of life, when this correlation suddenly drops to the most negative values recorded, during 200-300 days of age. Finally, a systematic *increase* in the correlation of individual weekly BW to lifespan emerges and persists throughout the remainder of the experiment. This suggests current BW prior to ~200 days of age as inconsequential, but then two opposite factors emerge. First, hamsters with lower maximum BW have the potential to live longer (n = 231), but in much older hamsters (the weekly *r* value crosses from negative to positive through 600-800 days old) heavier hamsters begin to possess the advantage in longer lifespan potential, reaching significance at 900 days of age (n = 69). These different cumulative vs. weekly BW to lifespan correlations might reflect time-sensitive ages where higher vs. lower BWs have opposite impact on lifespan, a finding cumulative mean BW alone cannot detect. Although it may seem arbitrary to partition up (cumulative) mean BWs at 100 d and 225 days, it was an effort to both avoid confounding of early low BW paired with rapid growth, and also to test whether this might yield a sensitivity to the relationship underlying BW in older hamsters and

lifespan. The remainder of this discussion pertains to findings separately addressing early and later life trends in mean (cumulative) BW history and lifespan.

Overall, early BW history does not significantly influence lifespan, as wean BW (Table 6.2), and mean BW measures restricted to the first 100 or 225 days of age were not correlated to lifespan. The only BW parameter found to correlate to lifespan in early life was the mean standard deviation of the 2nd order derivative of BW > 225 d: less variability in BW acceleration was correlated to longer lifespan ($r_{(242)}$ = -.174, p < .001). Differences among representative hamsters demonstrating high and low variability in 2nd order derivatives of BW are illustrated in Figure 6.4 In contrast, this same measure during only the first 100 d was not significant. Therefore overall, while early BW history does not impact lifespan, there is evidence that high variability of growth acceleration, possibly analogous to human yo-yo dieting, may manifest permanent somatic complications.

While most early life BW parameters did not correlate with lifespan, the analysis did reveal several measures during adult life (> 225 d) that did. Overall, lower mean BWs of adult hamsters, as well as greater variability, were associated with longer lifespan. Unfortunately this finding might be confounded with the observation that the overall mean of hamster BW across the lifetime reflects hamsters living the longest would have the highest probability of a natural death (i.e., avoiding acute onset of tumor formation, cardiovascular disease and renal failure at later stages of life) characterized by a progressively decreasing and less stable BW. This account may be further supported by mean and mean standard deviations of 1st and 2nd order

derivatives of BW > 225 d also significantly correlating to lifespan; however, the direction of the relationship is reversed, where 1st and 2nd order derivatives are positive for mean BW and negative for mean SD. While these results initially appear paradoxical, this might be a result of cumulative mean data collection. Overall, mean BW > 225 d = 45.35, and is negatively correlated to lifespan. In light of the age sensitive trends to weekly BW and lifespan correlations, these data might be explained if lighter hamsters after 225 days of age either gained a small amount of weight, due to later max BW ages, and heavier hamsters did not. This hypothesis is tested in the following section by assessing whether the absolute value of maximum BW, and the age upon reaching maximum BW, might predict lifespan.

PART TWO: UNIVARIATE COX REGRESSION MODEL

Methods

Life History Event (non-averaged) Measures. A total of 52 parameters were independently assessed using a univariate cox regression model to assess predictive strength of each parameter on lifespan. Categorical (non-averaged) data tested were: Photoperiod (fixed/seasonal), Puberty timing (early/delayed photoperiod), Photoperiodic response (BW loss between summer of Max BW and following winter, in SNP E, SNP D, and DS), Age at Puberty onset (d old), age at reaching max BW, value/mass of max BW, and BW at weaning.

Body Weight Parameters. Based on correlational analyses from Part I (above), mean BW data was narrowed down to seven parameters that would be assessed in a univariate cox regression model: BW and SD > 225 d, 1st order BW and SD > 225 d, 2nd order BW and SD > 225 d, and 2nd order BW SD < 225 d.

Wheel Running Parameters. 10 wheel running parameters were assessed, with data collected from each hamster up to 8 rounds. Wheel running parameters calculated from each Round include: Day Sum, Night Sum, Round Sum Total (Day + Night Sum), Sum Amplitude (Night Sum - Day Sum), Day Max, Night Max, Round Max Total (Day + Night Max), Max Amplitude (Night Max - Day Max), Day standard deviation ("Day SD"), and Night standard deviation ("Night SD"). With each of these parameters, a mixed effects linear regression model was applied for each individual hamster. A mixed effects model was employed to account for trends which may have arose from unequal round counts (i.e., hamsters dying young went through fewer rounds than longer living hamsters). What results for each of the parameters listed above is a slope and intercept, where the slope represents each hamster's rate of change for that variable over the hamster's lifetime, and the intercept represents each hamster's adjusted overall lifetime average of that measure. For example, each hamster has a slope value for Day Sum, which represents the rate of change in Day Sum counts across the lifetime. A negative slope indicates this hamster's particular Day Sum decreased across rounds and ultimately decreased with age. The intercept for Day Sum represents whether or not this hamster was a strong or weak Day Sum runner *overall*, where the intercept value alone has no intrinsic value or meaning, but when compared

across all hamsters, will reveal if a trend emerges with respect to predicting lifespan (i.e., do hamsters with higher mean Day Sum values live longer?). This resulted in 20 separate univariate cox regression models being tested.

Body Temperature Parameters. The following 9 BT parameters were run through individual univariate cox regression analysis: Phase Angle OFF (Fitted Acrophase timing relative to lights off), Minimum Fit, Minimum Real, Maximum Fit, Maximum Real, Amplitude Fit, Amplitude Real, Mesor Fit, and Goodness of Fit. A mixed effects linear regression model (see wheel running methods above) generated slope and intercept values for each hamster, yielding a total of 18 separate univariate cox regression models.

Results

For each parameter listed above, a univariate cox regression model was assessed on predicting lifespan. Coefficients, p-values, and R^2 values for each predictor were calculated. To control for multiple comparisons, only parameters yielding p-values < .005 are considered significant.

Life History Event (non-averaged) Measures. Univariate cox regression survival models of Life History Event measures are presented in Table 6.2. Max BW (g) and age at Max BW (d) were the only parameters to account for more than one percent of lifespan variability (0.017 and 0.024, respectively), but still not enough to be considered a statistically significant predictor of lifespan. Combined with survival

rates in Chapter 4, these results strongly argue that timing of early life history events are of no consequence to longevity.

Body Weight. Significant BW predictors of lifespan include mean BW > 225 d, BW and SD of 1st order derivatives, and BW and SD of 2nd order derivatives. With respect to these predictors, shorter survival (positive regression coefficients) was found to be associated with increased mean BW > 225 d, and SD of 1st and 2nd order BW derivatives. In contrast, BW predictors associated with longer survival (negative regression coefficients) were mean BW rate of change > 225 d, and mean BW growth acceleration > 225 d (1st and 2nd order BW derivatives, respectively).

Wheel running. Age-related changes (slope values) in a number of wheel running parameters were found to significantly predict lifespan (Table 6.3), all bearing the same relationship: Attenuated age-related decline in Day Sum, Night Sum, Round Sum Total, and Round Max Total, all predicted longer lifespan (i.e., the less negative the slope, the longer the life expectancy). Day Sum accounted for the smallest proportion of variance accounted for (0.034); Round Sum Total accounted for the largest (0.051; Night Sum and Round Max Total both = 0.045). There were no significant overall mean (intercept) predictors of any wheel running parameter.

Body Temperature. There were no age-related changes (slope values) in BT parameters found to significantly predict survival (see Table 6.4). With respect to overall means (i.e., intercept values), hamsters with the lowest (cosine-fitted) minimum BTs predict longer lifespan. In addition, marginally significant (intercept)

predictors of increased survival include lower (actual, not cosine-fitted) minimum BTs, and higher (actual, not cosine fitted) BT amplitude.

Discussion

Life History Parameters. Photoperiod type (season versus fixed), puberty timing (early or delayed photoperiods), puberty onset age (d), photoperiodic response, and wean BW, were all non-significant predictors of lifespan, each accounting for less than 0.01 proportion of variance (R^2) of lifespan. Max BW (g) and age at reaching Max BW (d) were significant ($p < .05$) predictors prior to applying control for multiple comparisons; however, independent of the *p*-value, the R^2 proportion of (lifespan) variance accounted for were still relatively weak (0.017 and 0.024, respectively). The earlier hypothesis proposing to explain age-related changes to BW-lifespan correlations is not strongly supported.

Body Weight Parameters. Seven BW parameters were tested on their capacity to predict lifespan in separate univariate cox regression models and found that of six significant predictor variables, five only considered BW data after 225 d of age. Of these five parameters pertaining to data > 225 d, increased survival was predicted by lower mean BW, increased 1st order derivative of BW, increased 2nd order derivative of BW, and lower variability among 1st and 2nd order derivatives of BW.

The simplest way to account for these results is to take each component into consideration separately: lower BW average, positive growth rates, and rigid BW variability. As previously discussed, a potential explanation of lower BW predicting

longer lifespan results from a robust trend in the final year of life (end of Chapter 2) showing hamsters losing weight gradually but with increasing rates, most notably between 26-32 weeks of life remaining (i.e., 1st and 2nd order derivatives become more negative). An account to these findings might appear complicated, but on the contrary, simply describes a long-lived hamster is predicted by being relatively smaller than average, maintaining the same BW for the longest, steadiest amount of time. Referring to Figure 6.2, while the cumulative 1st order derivative of BW is always just above zero, the overall weekly mean, after approximately 321 days of age, is nearly always negative. Thus, a positive 1st order (or 2nd order) derivative is not the underlying factor but rather the *least negative* growth rate is observed in the longest living hamsters. Combining these ideas, it may be impossible to separate completely the fact that smaller hamsters also have less BW to lose, and therefore might also have less negative cumulative 1st order derivatives of BW.

The final (sixth) significant BW predictor parameter was the 2nd order derivative of BW *prior* to 225 d. This parameter is especially unique being the single predictor variable pertaining only to early life BW history. Two explanations for this result are presented: First, smaller BW growth acceleration could result in hamsters reaching smaller overall BWs, a factor determined to predict lifespan. In contrast, hamsters with larger early BW growth accelerations might result in younger and heavier maximum BW; a pattern that would also account for the marginal predictive value of maximum BW (g) and maximum BW age (d). The second explanation would be that qualitative health insults to physiology may accompany rapid BW acceleration

at such early age; this possibility is strengthened when considering that the two photoperiod groups, LDLD and DS, had the two heaviest mean BW at 225 days old, and also produced the shortest median survival among all groups.

Wheel Running Parameters. While no significant overall mean (intercept) wheel running parameters were determined to predict lifespan, four age-related changes (slope) were identified to have predictive value: Smaller age-related declines in Day Sum, Night Sum, Round Sum Total, and Round Max Total measures all predicted longer lifespan. What is immediately obvious is the absence of any parameters measuring the circadian component of the wheel running protocol, Sum Amplitude and Max Amplitude. While it was established previously that amplitude did in fact diminish in aged hamsters it was unclear whether this reflected functional aging of the circadian system or a decline in overall physical ability. Given that age-related reduction in amplitude was not found to predict lifespan the latter appears a more probable account.

Furthermore, the strength of the respective parameters with regard to proportion of (lifespan) variability accounted for, in descending value, are Round Sum Total (0.051), Night Sum Total/Round Max Total (both = 0.045), and Day Sum (0.034). It is of interest that the Round Sum Total exactly reflects the addition of Day and Night Sums, individually bearing less predictive value than its aggregate measure. This finding suggests that while wheel running counts during the inactive phase is a significant lifespan determinant, and total active phase counts also bear slightly more predictive worth, that the more sensitive measure is an overall ability to be placed into

the wheel unexpectedly and generate high volume, i.e., vigorous output as the most predictive parameter of the wheel running protocol. Round Max Total is also a function of combined Day + Night activity, further supporting the notion that the lifespan predicting sensitivity of this wheel running protocol lies primarily in assessing overall physical output, in the absence of detecting an underlying circadian system functional decline.

Body Temperature Parameters. Despite the absence of age-related (slope) changes of BT parameters in accounting for variability of lifespan, a significant predictor variable in lifetime mean (intercept) fitted BT minimums was found. The lower the mean fitted BT minimum, the longer the predicted lifespan; however, this parameter produced only a modest proportion of variance accounting for lifespan variability (.034) among hamsters in the study. This observation might be partially explained by observing that, similar to mean BW results, trends in older hamsters record more lowered values than those who die sooner, and as a result, these lowered trends are determined (when assessing mean/intercept parameters as predictor variables) to predict longer living hamsters because they covary together. However, if this was the only factor, it would be expected to observe similar predictive power in the other BT parameters determined to also diminish with age, such as mesor and maximum fitted values.

PART THREE: MULTIVARIATE COX REGRESSION MODEL

Methods

Out of the 52 parameters selected for univariate regression analysis, 10 were selected for incorporation into the multivariate cox regression model. We reduced multicolinearity by identifying highly correlated measures, and of those, choosing parameters with the highest R^2 among them. As a result, the included parameters are 1) mean BW > 225 d, 2) mean 1st order derivative of BW > 225 d, 3) mean 2nd order derivative of BW > 225 d, 4) mean standard deviation of 1st order derivative of BW > 225 d, 5) mean standard deviation of 2nd order derivative of BW > 225 d, 6) Day Sum Slope (wheel running), 7) Night Sum Slope (wheel running), 8) Round Sum Total Slope (wheel running), Round Max Total Slope (wheel running), and 10) cosine fitted BT minimum (Intercept). Before generating a multivariate cox regression model of lifespan, parameter-parameter correlations are assessed to identify highly correlated variables in order to avoid issues of multicolinearity. Among BW predictors, only 1st and 2nd order derivatives of BW standard deviations > 225 d were highly correlated. Therefore, the measure with the weaker predictor strength (standard deviation of 1st order BW > 225 d) was removed. Regarding wheel running parameters, most were moderately correlated, thus only Round Sum Total, the parameter yielding the highest predictive capacity (out of wheel running measures), was included into the multivariate model. Finally, only one BT was found to predict lifespan, (intercept) minimum fitted BT values. The result is a multivariate cox regression survival model

incorporating six parameters- A) mean BW > 225 d, B) mean 1st order derivative of BW > 225 d, C) mean 2nd order derivative of BW > 225 d, D) mean 2nd order derivative of BW > 225 d, E) Age-related changes (slope) in Round Sum Total, and F) lifetime mean (intercept) of minimum fitted BT.

Results

Multivariate Source data are presented in Table 6.5. Overall, the model was a significant predictor of lifespan, (Likelihood-ratio test (df = 6) = 75.45, $p < .0001$; logrank test (df = 6) = 86.00, $p < .0001$) accounting for 29.3 % of individual differences in lifespan among the cohort of 246 male Siberian hamsters (mean = 763 d, standard deviation = 203 d). Concordance was found to be in a desirable (0.65-0.70) range = 0.691. Individual parameters were considered statistically significant predictors of lifespan at $p < .05$. In order of strength, parameters found to predict longer lifespan are: Lower mean BW after 225 d of age, reduced variability in BW acceleration rates (e.g., 2nd order derivative of BW) after 225 d old, decreased mean (intercept) minimum cosine fitted BT, increased mean BW growth rates (1st order derivative of BW) after 225 d old, and finally, Round Sum Total wheel running rates which do not rapidly decline with age. The only variable found not to significantly predict changes in lifespan was mean 2nd order derivative of BW after 225 d.

Discussion

Six variables were used in the multivariate cox regression model, selected from BW, wheel running, and BT parameters collected across the lifetime. From these six measures the regression model generated a remarkable proportion of variance accounted for among intracohort lifespan variability from an out-bred Siberian hamster colony.

Similar to the single measure analysis in univariate regression (Part II), mean BW after > 225 d was the strongest predictor of lifespan, with smaller animals living longest. Additional BW history characteristics predicting longer lifespan include larger 1st and 2nd order derivatives of BW, and reduced variability in 2nd order derivatives of BW. Summing the individual proportion of variance in lifespan accounted for = .437 among these four BW measures alone, and clearly the premier contributor in determining a significant multivariate model.

Of the non BW parameters, the fitted mean (intercept) BT minimum exhibited the highest predictor strength, $Z = 3.118$, $p < .002$, with lower minimum BT predicting extended lifespan. These results might also be viewed with caution, as with mean BW, this is an observed age-related change: In this study, older animals decrease in BW and minimum BT as a function of age. These older animals by mere logic live longer, and therefore have a higher frequency of lowered values contributing to their mean of a given parameter known to change with age.

Perhaps the only measure in the multivariate survival analysis protected from the shortcomings listed above where obtaining mean values across measures sensitive

to age related changes is data acquired from wheel running parameters. Because these data reflect the *rate* of change, it measures more precisely how severe the age-related decline of the measure is within individuals at assesses these differences with respect to the lifespan of each. The rate at which wheel running Round Sum Totals (Day Sum + Night Sum) decreased is a significant predictor of lifespan, where less decline in total running counts predict longer lifespan. Recalling the overall profiles from Chapter 3 (Figure 3.5A), the pattern of Round Sum Totals demonstrate the steepest decline during the first 4 Rounds, after which increase slightly but mostly do not recover. Animals dying younger would bear a mean slope much more negative, as the decrease sum totals flatten out after Round 5. The longer the hamster lives, the more non-negative slope values will be incorporated into the calculated slope mean. Therefore, despite being the only measure assessing the rate of change (e.g., slope) rather than the mean (e.g., intercept), the predictive value in estimating lifespan may be confounded with obtaining additional data at later ages, which unfortunately must only come from long lived hamsters.

CONCLUSION

The purpose of this chapter was to explore the predictive power of a multivariate cox regression survival model upon lifespan variability in this cohort of 246 male Siberian hamsters. Thus overall, while photoperiod condition was found to influence puberty timing, number of winter phenotypes, and lifetime BW history,

these responses are not accompanied with predictive relationship to lifespan, finding which corroborate with the survival analysis in Chapter 4. In addition, there was predictive value in the mean 2nd order derivative of BW during the first 225 days of life, which also complements the survival analysis: LDLD and DS groups both displayed the highest BW at 225 days of age, and these were also the two photoperiod groups to exhibit shortest median survival. Regarding BW history, there is a differentiation between the impact of life history event *timing* with the *magnitude* of BW growth. These three components taken together (univariate regression R^2 of age of maximum BW (d), maximum BW (g), and early life growth acceleration) account for 0.07 proportion of lifespan variance among all groups, a quite remarkable result if it was truly driven primarily by only two of six photoperiods.

In addition to categorical (i.e., non-cumulative data) variables, a lifetime of data collection was included: BW, wheel running activity from a novel wheel running protocol, and 24 h Body Temperature assessment in a novel BT collection protocol. The original variable list included 52 potential variables that were ultimately reduced to six. The proportion of variance in lifespan accounted for was 0.293 from this model. We find the lower mean BW of adult (> 225 d) hamsters exhibiting the least BW loss, and lowest BW variability, predicted longer survival. In addition, hamsters exhibiting lowest mean cosine fitted BT minimum were predicted to live longest. Finally, hamsters exhibiting the lowest rate of age-related decline in Total Round counts (Day Sum + Night Sum) were predicted to live longest.

While the multivariate cox regression model certainly accounts for a significant proportion of variability in lifespan, there are important caveats to the results. This model confounds age-related trends in older hamsters with predictive measures. For example, a number of variables (i.e., lower mean BW, lower min BT, decreased rate of wheel count decline) predict longer life; however, every one of these results merely reflects overall age-related trends observed in these measures. If any of these variables were predicting trends in the opposite direction of the age-related trends found, they might be truly indicative of an underlying causal variable of lifespan. Therefore, the multivariate cox regression model is not an ideal approach when attempting to reconcile intracohort variability if the underlying variables are cumulative means and not single point measures. For example, BW at weaning, and BW at 2 years old may certainly be useful independently, but not combining weekly measures over the course of the lifetime into a slope/intercept reduction. This is strikingly evident in Figure 6.1A, where weekly BW-lifespan correlations are independently calculated across the lifetime. This strongly shows age-related changes to the predictive value of BW, where essentially no predictive value is apparent within the first ~200 days, but afterwards, drops to r ~ -0.2 and then increases linearly throughout the lifetime. This single illustration is far more applicable with respect to truly estimating longevity: Hamsters who maintain lower than average BW around the time of achieving maximum BW live longer, but as hamsters age, this trend reverses and hamsters weighing more than average would be predicted to live longer. In the future, the integrity of a multivariate cox regression might be improved if sampling

single point values at discrete ages across the lifetime (i.e., nine independent multivariate cox regression analyses occurring every 100 days looking at only that narrow range of data) would alleviate the confounding issues that were encountered. Fortunately, a number of non-cumulative measures were incorporated this way (i.e., puberty timing, age at max BW (d), max BW (g), age upon puberty onset, photoperiod type) which, after adjusting for multiple comparison, were not significant predictors of lifespan in separate univariate cox regression model. Previous multivariate cox regression survival studies incorporating behavioral and somatic age-sensitive measurements account for 0.44 to 0.54 proportion of lifespan variability in mice (Ingram & Reynolds, 1986; Ingram et al., 1982). The current study departs from these prior analyses by reducing the total number of different measurement protocols (i.e., BW, wheel running, and BT) but record data longitudinally, whereas former studies expand the number of different protocols (8) and only collect data at a single timepoint at 24 months of age. Future regression analysis upon longitudinal data may benefit by partitioning each interval of data collection into separate analyses in order to avoid confounds between overall trends in animals living longer with functional decline associated with biological aging as a predictor to remaining survival. This might also reveal the best age at which to assess predictive value of individual measures, as they all likely do not occur optimally at exactly the same age; this would be consistent with the differential age of decline observed between wheel running (early age onset decline) and BT parameters (middle age onset of decline).

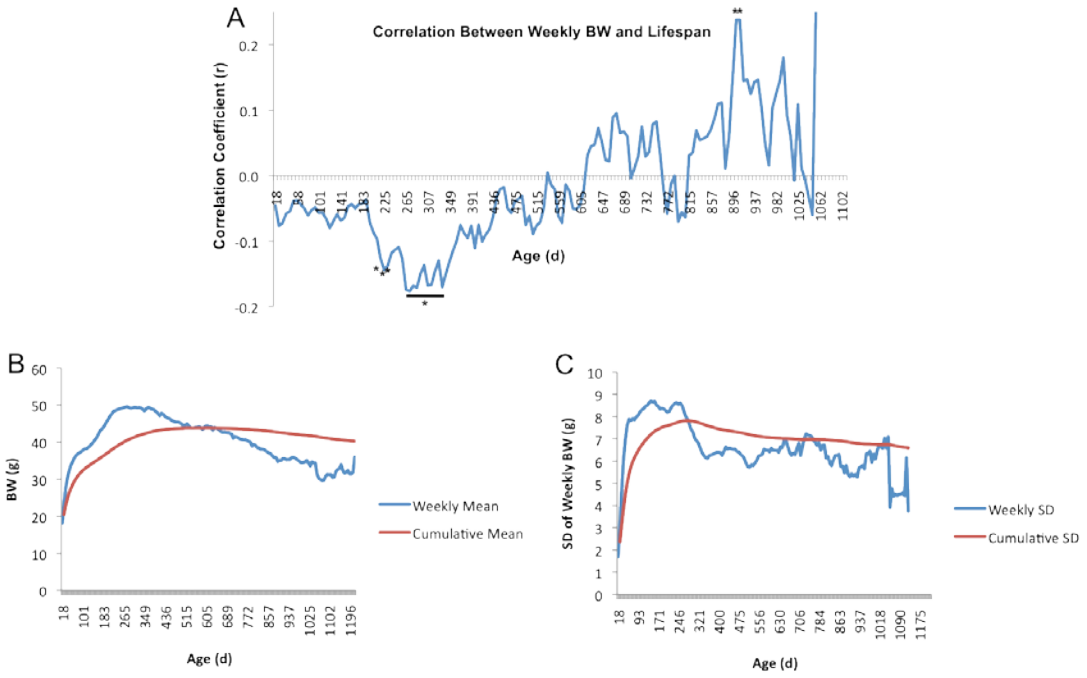

Figure 6.1. Weekly and cumulative trends in BW among experimental males dying naturally. (A) Weekly correlations between each weekly mean body weight among all living male experimental hamsters at that age and lifespan. (B) Mean weekly and cumulative BW trends as a function of chronological age across the lifespan. (C) Mean weekly and cumulative standard deviations of BW across the lifespan.

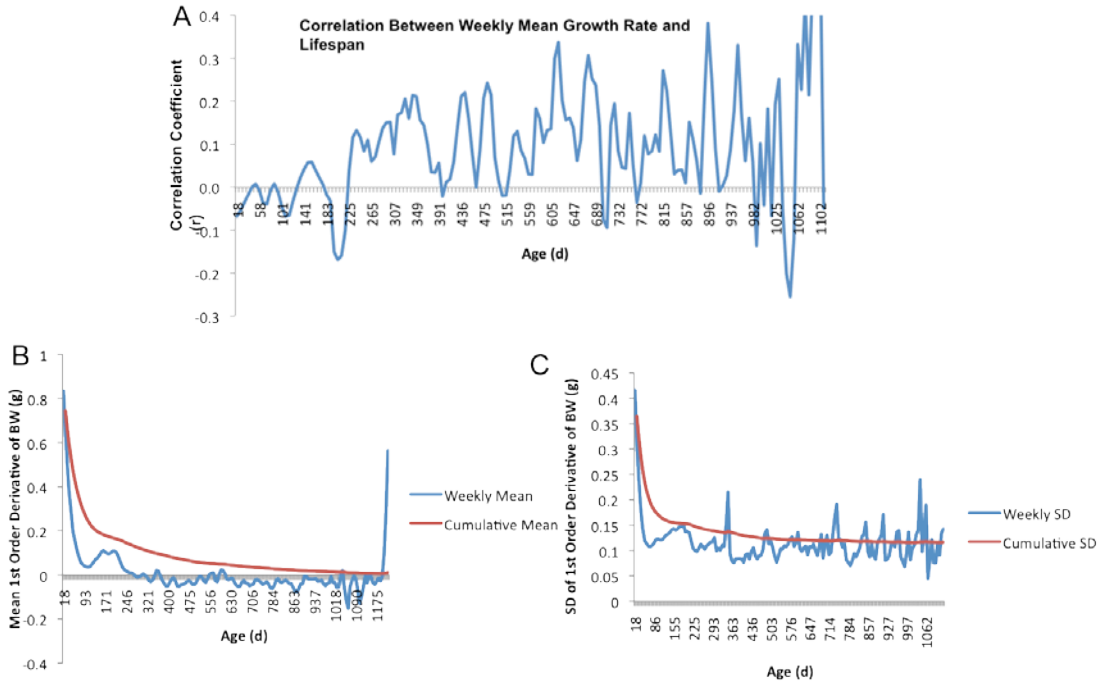

Figure 6.2. Weekly and cumulative trends in 1st order derivative of BW. For conventions see Figure 6.1.

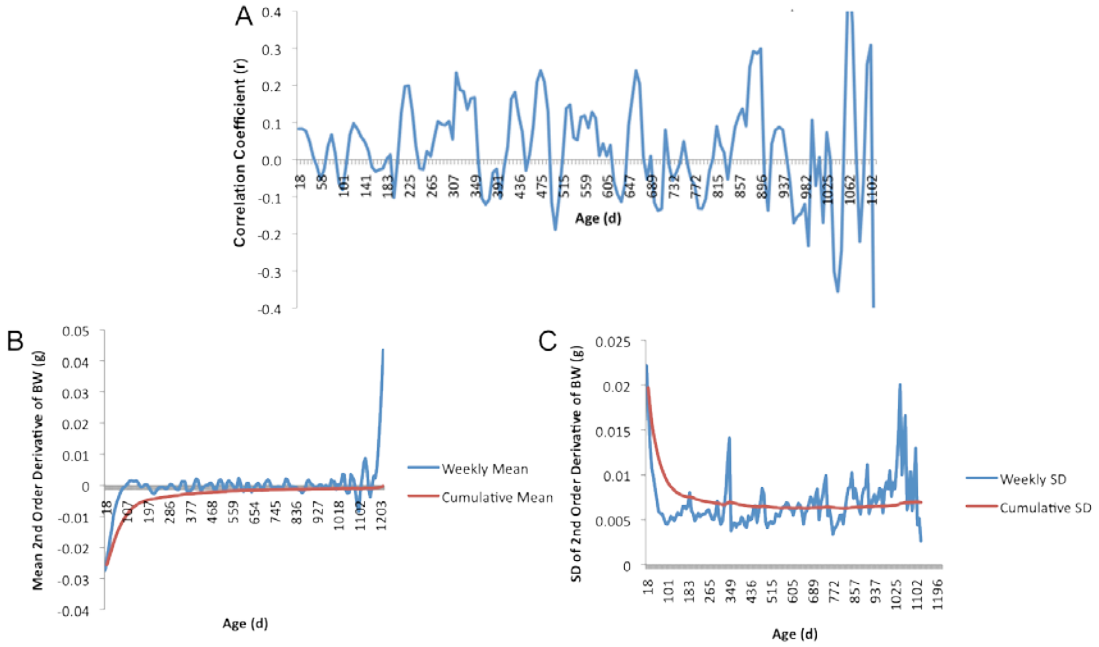

Figure 6.3. Weekly and cumulative trends in 2nd order derivative of BW. For conventions see Figure 6.1.

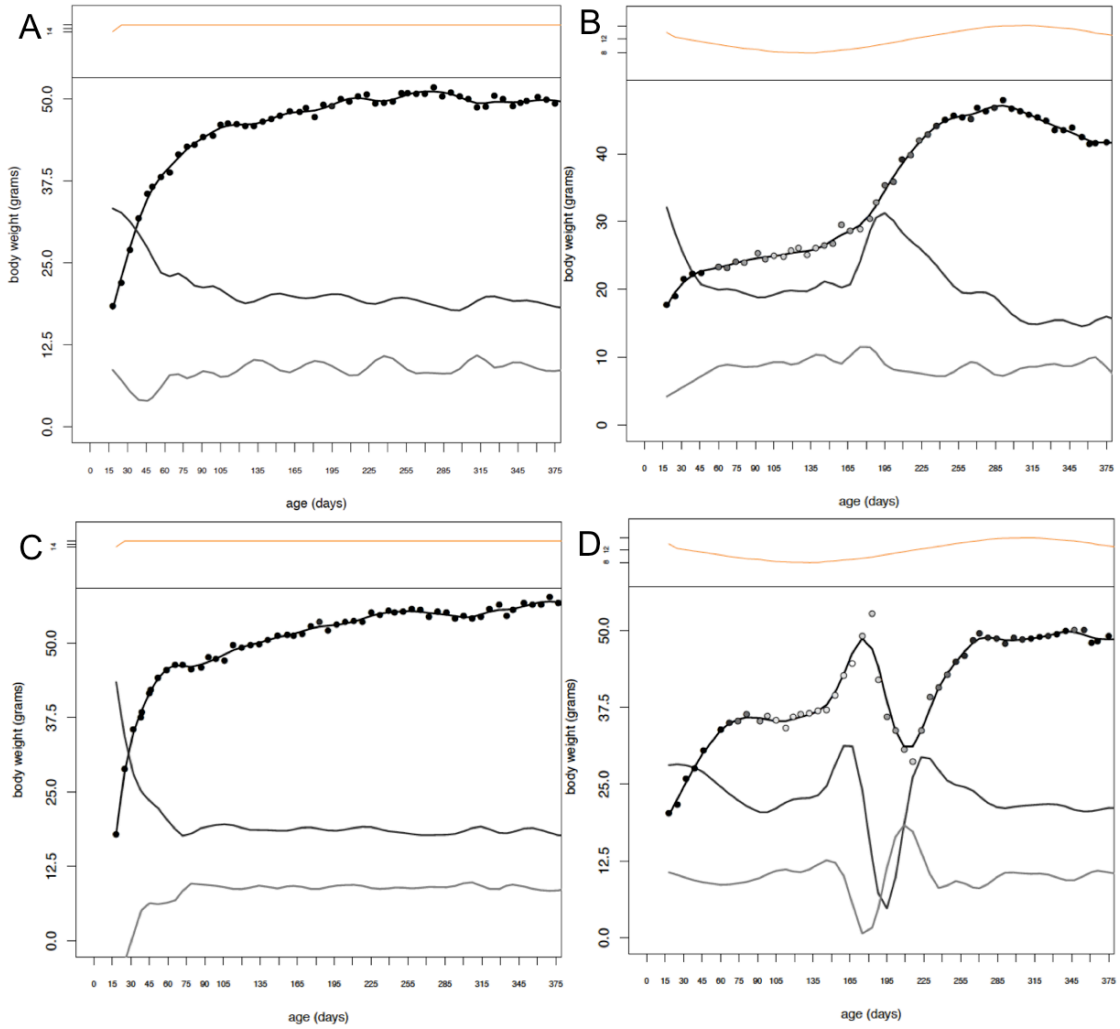

Figure 6.4. Representative of low and high 2nd order derivatives in BW < 225 d. Male hamsters determined to have the lowest (A-B) and highest (C-D) mean 2nd order derivative of BW (e.g., BW acceleration) during the first 225 d of life. Top line: actual body weight, middle (dark) line = 1st order derivative of BW, bottom (light) line = 2nd order derivative of BW. Increased mean BW acceleration as associated with reduced life expectancy.

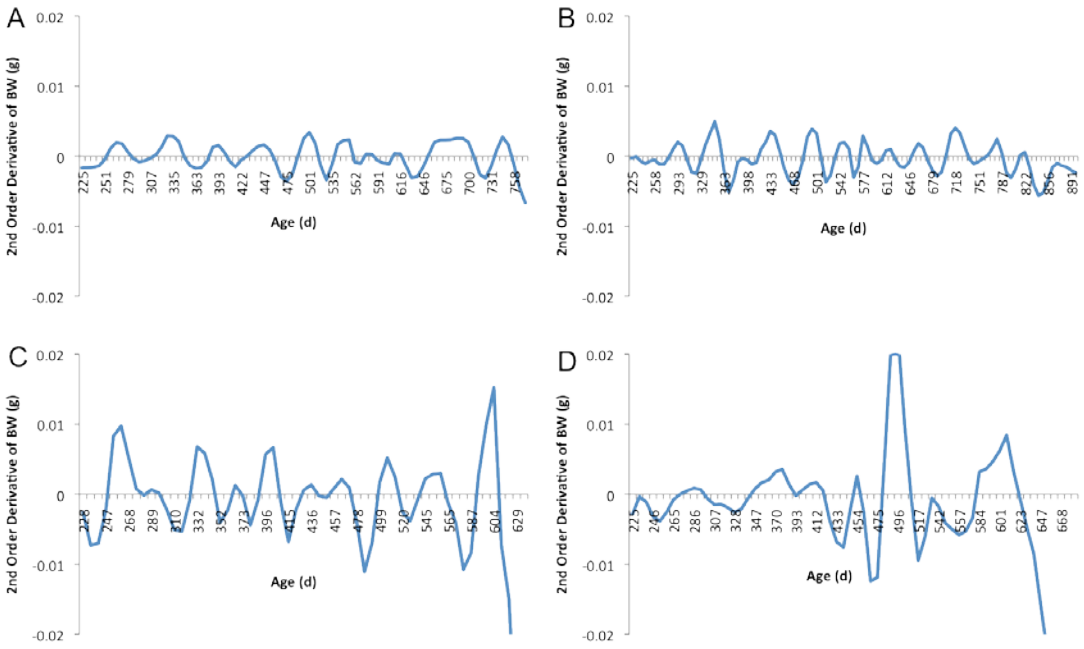

Figure 6.5. Representative low and high variability among 2nd order derivatives in BW > 225 d. Representative males hamsters demonstrating an example of hamsters with the lowest (A-B) and highest (C-D) standard deviation of 2nd order derivative of BW older than 225 days of age. Lower variability was associated with longer life expectancy.

Table 6.1. BW parameters: Correlation and univariate regression coefficients

BW	Mean	SD	N	r	*p*		Coefficient	*p*	R^2
Lifespan	763.44	207.16	246	-	-				
Max	53.37	7.11	244	-0.050	0.439				
Max (<100)	38.08	8.01	244	-0.057	0.375				
Max (>100)	53.35	7.13	244	-0.043	0.507				
Max (<225)	49.08	7.06	244	-0.102	0.111				
Max (>225)	53.44	7.06	241	-0.093	0.152				
Mean	42.88	5.38	244	-0.032	0.662				
Mean (<100)	31.88	6.19	244	-0.054	0.401				
Mean (>100)	44.44	5.75	244	-0.124	0.052				
Mean (<225)	37.93	6.38	244	-0.066	0.302				
Mean (>225)	45.35	5.83	241	-0.288	0.001	**	0.079	0.001	0.143
SD	7.48	2.16	244	-0.159	0.013	*			
SD (<100)	6.35	2.53	244	-0.039	0.540				
SD (>100)	5.82	2.14	244	0.053	0.410				
SD (<225)	7.86	2.30	244	-0.041	0.525				
SD (>225)	5.17	2.20	241	0.197	0.002	**	-0.083	0.009	0.028

BW f '(x)	Mean	SD	N	r	*p*		Coefficient	*p*	R^2
Lifespan	763.44	207.16	246	-	-				
Max	0.8713	0.3799	244	-0.068	0.291				
Max (<100)	0.8428	0.4035	244	-0.062	0.336				
Max (>100)	0.3269	0.1978	244	-0.025	0.700				
Max (<225)	0.8596	0.3839	244	-0.074	0.248				
Max (>225)	0.2364	0.2040	241	0.101	0.118				
Mean	0.0349	0.0233	244	-0.711	0.001	**			
Mean (<100)	0.2786	0.1141	244	-0.049	0.449				
Mean (>100)	0.0003	0.0263	244	-0.160	0.013	**			
Mean (<225)	0.1605	0.0413	244	-0.116	0.071				
Mean (>225)	-0.0246	0.0478	241	0.254	0.001	**	-11.867	0.001	0.101
SD	0.1822	0.0616	244	-0.537	0.001	**			
SD (<100)	0.2786	0.1384	244	-0.056	0.384				
SD (>100)	0.1213	0.0592	244	-0.422	0.001	**			
SD (<225)	0.2309	0.0918	244	-0.109	0.088				
SD (>225)	0.1062	0.0645	241	-0.302	0.001	**	5.665	0.001	0.083

BW f "(x)	Mean	SD	N	r	*p*		Coefficient	*p*	R^2
Lifespan	763.44	207.16	246	-	-				
Max	0.01815	0.01210	244	0.047	0.463				
Max (<100)	0.00284	0.00583	244	-0.023	0.722				
Max (>100)	0.01779	0.01215	244	0.041	0.521				
Max (<225)	0.00971	0.00571	244	-0.063	0.329				
Max (>225)	0.01657	0.01276	241	0.107	0.096				
Mean	-0.00171	0.00185	244	0.512	0.001	**			
Mean (<100)	-0.01121	0.00671	244	0.057	0.378				
Mean (>100)	-0.00037	0.00166	244	0.309	0.001	**			
Mean (<225)	-0.00441	0.00283	244	0.087	0.177				
Mean (>225)	-0.00065	0.00285	241	0.337	0.001	**	-158.822	0.001	0.104
SD	0.00823	0.00359	244	-0.478	0.001	**			
SD (<100)	0.01122	0.00623	244	-0.108	0.092				
SD (>100)	0.00616	0.00394	244	-0.398	0.001	**			
SD (<225)	0.01043	0.00419	244	-0.174	0.006	**	41.306	0.005	0.029
SD (>225)	0.00620	0.00462	241	-0.342	0.001	**	79.216	0.001	0.089

* = statistically significant at $p < .05$

** = statistically significant at $p < .01$

Table 6.2. Univariate cox regression, life events

Parameter	Coefficient	*p*	R^2
Photoperiod (Seasonal vs. Fixed) n = 246	0.162	0.209	0.006
Puberty (Advanced vs. Delayed) n = 246	-0.135	0.295	0.004
Photoperiodic Response n = 118	0.011	0.556	0.004
Wean BW (g) n = 246	0.042	0.343	0.004
Puberty Age n = 244	0.000	0.521	0.002
Max BW (g) n=244	0.021	0.043	0.017
Max BW (Age) n =244	-0.002	0.019	0.024

Table 6.3. Wheel running parameters: Correlation and univariate cox regression coefficients

Parameter	Lifespan (n = 231)	Chronological Age (n = 231)	Days until Death (n = 231)	Slope			Intercept		
				Coefficient	*p*	R^2	Coefficient	*p*	R^2
Day Sum	0.107	-0.041	0.130 *	-0.273	0.005	0.034	-0.001	0.021	0.023
Night Sum	0.063	-0.173 **	0.221 **	-0.207	0.001	0.045	-0.001	0.113	0.011
Day + Night Sum	0.097	-0.129 *	0.208 **	-0.104	0.001	0.051	-0.001	0.038	0.019
Sum Amplitude	-0.033	-0.140 *	0.108	-0.327	0.255	0.006	0.001	0.255	0.005
Day Max	0.064	-0.163 *	0.213 **	-5.021	0.011	0.027	-0.006	0.04	0.018
Night Max	0.036	-0.325 **	0.346 **	-3.711	0.032	0.019	-0.005	0.091	0.012
Day + Night Max	0.058	-0.287 **	0.328 **	-2.276	0.001	0.045	-0.003	0.056	0.015
Max Amplitude	-0.026	-0.159 *	0.133 *	-15.854	0.345	0.004	0.007	0.345	0.004
Day S.D	0.068	-0.123	0.177 **	-13.318	0.035	0.019	-0.022	0.035	0.019
Night S.D.	0.018	-0.302 **	0.308 **	-17.407	0.023	0.022	-0.013	0.218	0.007

Table 6.4. Body temperature parameters: Correlation and univariate cox regression coefficients

Parameter	Lifespan (n=231)	Chronological Age (n=231)	Days until Death (n = 231)	Slope			Intercept		
				Coefficient	*p*	R^2	Coefficient	*p*	R^2
Phase Angle OFF	0.012	-0.136 *	0.141 *	3.900	.986	.000	-.001	.986	.000
Min Fit	-0.177 **	-0.389 **	0.240 **	514.187	.012	.027	.605	.004	.034
Min Real	-0.134 *	-0.251 **	0.139 *	127.928	.204	.007	.569	.006	.032
Max Fit	-0.075	-0.242 **	0.177 **	330.735	.034	.019	.170	.312	.004
Max Real	-0.052	-0.245 **	0.197 **	493.672	.058	.016	.051	.815	.000
Amp Fit	0.113	0.120	-0.029	-308.330	.687	.001	-1.174	.045	.017
Amp Real	0.068	-0.020	0.072	-666.010	.223	.007	-1.878	.009	.029
Goodness of Fit	0.022	-0.040	0.013	993.660	.336	.004	-.484	.726	.000
Mesor Fit	-0.127	-0.326 **	0.217 **	395.040	.026	.021	.369	.056	.015

Table 6.5. Multivariate cox regression survival summary

Parameter	Variable	Coefficient	β	SE	Lower 95%	Upper 95%	Z	*p*
BW	Mean BW (>225 d)	0.0066	1.068	0.0153	1.037	1.101	4.327	.0000***
BW	Mean BW f '(x) (>225 d)	-11.1900	0.0001	4.1910	3.727×10^{-9}	5.074×10^{-2}	-2.671	.0075**
BW	Mean BW f "(x) (> 225 d)	-78.7600	0.0000	83.9000	2.391×10^{-106}	1.617×10^{37}	-0.939	.3478
BW	SD f "(x) (> 225 d)	113.600	2.118×10^{49}	30.1400	4.689×10^{23}	9.572×10^{74}	3.768	.0000***
Gym	Day + Night Sum (Slope)	-0.0739	0.9287	0.0346	0.8677	0.9940	-2.133	.0329*
BT	Fitted Min (Intercept)	0.7098	2.034	.2276	1.302	3.177	3.118	.0018**

Concordance = 0.691, SE = 0.023

R^2 = .293

Likelihood Ratio Test = 75.45 (df=6), $p < .3.109 \times 10^{-14}$

Wald Test = 82.01 (df=6), $p < 1.332 \times 10^{-15}$

Logrank Test = 86 (df=6), $p < 2.22 \times 10^{-16}$

CHAPTER 7: CONCLUSION

This is the first study to ask whether photoperiod manipulation of life history affects rates of aging and ultimately impacts longevity in a mammal. Overall, lifespan of the Siberian hamster was determined among a cohort of 246 males (mean = 758 d, median = 777 d, maximum = 1126 d) and 80 females (mean = 737 d, median 810 d, maximum = 1087 d) where it was firmly established that manipulation of life history does not affect lifespan. There were also no gender differences. For context, the lifespan of the Siberian hamster appears longer than Syrian hamster (*Mesocricetus auratus*), where males (mean = 656 d, median = 693 d, n = 38) outlive females (mean = 529 d, median = 553, n = 39; Oklejewicz and Daan, 2002).

To summarize the primary findings of this dissertation:

1) Photoperiod manipulations led to starkly different life histories as reflected in differential patterns of BW. Initial and rapid BW growth among early puberty groups was evident at 25 days of age, significantly outweighing delayed puberty group hamsters merely 7 days after weaning. Meanwhile, delayed puberty group hamsters transitioned into the winter phenotype characterized by the generation of white pelage, before undergoing puberty. Timing of puberty onset was delayed by 131 days in Siberian hamsters exposed to short or decreasing photoperiods. Mean percent of life as

a juvenile was 3.2% in early puberty photoperiods and 20.2% in delayed puberty photoperiods.

2) As verified by weekly BW and pelage data, hamsters responded as expected to their respective photoperiodic conditions, generating an array of photoperiod-mediated life history. Hamsters in seasonal photoperiods experienced annual short day and long day transitions, exhibiting photoperiodic responses in BW and pelage, which diminished in amplitude with age each successive season. Hamsters were exposed either to zero, one, or multiple short day photoperiods that induced the winter phenotype at different frequencies and at different ages among groups. Despite the age differences, changing patterns of daylength had strong synchronizing effects on cohorts of hamsters. In addition, there was no "time of year" influence with respect to the timing or frequency of deaths observed among hamsters in the seasonal photoperiods. Finally, BW trends in the final year prior to death display systematic and gradual weight loss, and this rate increases substantially between 31-37 weeks of life remaining, providing a useful single variable model with which to reliability estimate days until death.

3) Survival curves between early and delayed puberty photoperiod groups were identical, and overall (independent of photoperiod), age of puberty onset of individual hamsters did not correlate with or predict lifespan. In addition, the duration of lifetime spent in the presumed "slow aging" winter state did not affect survival. Whereas photoperiod governed alterations to life history had no impact on lifespan, there is

evidence from LDLD and DS photoperiod groups that acute *entrainment* driven effects of light (more appropriately categorized as chronodisruption than photoperiod history), can in fact manifest undesirable health consequences and ultimately shorten lifespan.

4) In a novel wheel running protocol, hamsters exhibit age-related decline in overall night running and as a result, night-day amplitude and day-night totals diminished over successive rounds. This linear decrease in night running counts was observed primarily throughout the first 500-600 days of life, and afterward maintain overall lower values; however, overall, night running vigor consistently exceeded day running vigor each round. Finally, the single highest intensity minute of each bout bears the largest predictive value estimating days until death (r = .346), akin to the idea that in humans, one's 40-yard dash time is a better assessment of remaining life compared to a two-mile run time (i.e., "burst" vs. "stamina" capacity).

5) A novel 24 h BT collection protocol was designed, and validated by demonstrating the length of the elevated BT duration is proportional to the scotophase duration, in separate groups and also in the same hamsters subject to varying scotophase length. The acrophase timing was reliably and appropriately determined to reflect the middle of the scotophase. An age-related decline in 24 h subcutaneous body temperature parameters began to emerge between 465-563 days of age, concurrent with the age at which wheel running parameters established rather basal values which were

maintained for the remainder of the study. Upon reaching this age, cosine fitted BT minimum, maximum, and mesor parameters decreased linearly throughout remainder of the experiment. Minimum and maximum values decreased at such a proportional rate that amplitude was not affected; however, mean amplitude was found to covary with lifespan, where hamsters endowed with robust amplitude BT rhythms appear to live longer. Finally, gradual deterioration of sine-like BT rhythms were observed across progressive rounds as hamsters aged, but also demonstrate a complete breakdown of a circadian BT waveform roughly 60 days prior to death.

6) Several age-related changes in organ weights were found, with healthy older hamsters containing heavier brain, liver, heart, and kidneys compared to young adult BW matched controls. Average weight and variability of spleen, heart, and adrenal glands begin to increase dramatically after 700 d. Atrophied gonads and hypertrophied adrenal glands were found in male hamsters succumbing to natural death compared to age-matched euthanized controls, indicating a fundamentally different biological state in hamsters where death is fast approaching. In experimental males, longer lifespan was accompanied with increased kidney weight and decreased gonad mass. Hamsters dying naturally exhibited proportionately increased kidney weight between 600-1000 days old, whereas younger hamsters, and hamsters killed prior to natural death exhibit weights in the typical range. Larger liver weights significantly covaried with larger hamsters. Gonad mass was negatively correlated to age, with older hamsters possessing severely atrophied and putatively non-functional gonads. This trend in

diminishing gonad mass becomes apparent around 600 days of age. Notably, in hamsters dying naturally, the degree of age-related weight change to some organs was most closely accounted for by the timing of different life history events rather than chronological age: The severity of kidney hypertrophy was positively correlated to Post-Puberty survival and negatively correlated to age of puberty onset. In addition, the degree of gonad atrophy was most closely tied to Post-Max BW survival and not chronological aging.

7) Factors influencing individual lifespan variation among 246 male Siberian hamsters were testing in a multivariate cox regression model. Combined individually, age at max BW, actual max BW, and mean 2nd order derivative of BW prior to 225 days of age account for .07 of lifespan variation in our population, a small but significant effect which suggests rapid weight gain at a young age (or possibly underlying hormonal or somatic factors contributing to this overt measure) can compromise longevity. Both timing of puberty, and early vs. delayed photoperiod condition had no predictive value to lifespan, concurrent with our survival analysis. BW at age of weaning (18 d) was not a significant predictor of lifespan. The cox regression model was found non-optimal when including data collected across the lifetime, after reduction into slope and intercept values which reflect the rate of change and overall mean of each hamster. The result of this component of the analyses was bias in that it merely reflected the trends observed in old hamsters rather than generating actual predictive value. For example, lifetime mean BW decreases in older hamsters prior to

death, whereas cox regression gives predictive value to lower weight hamsters, predicting increased longevity. This was the case for other longitudinal data collection in BT and wheel running as well.

At the onset of the study, there were several compelling reasons to expect a possible role of photoperiod history on lifespan. First, there was suggestive empirical evidence that organisms might live a set number of annual seasons: Primates exposed to 8 month seasonal cycles lived proportionately shorter than controls housed under 12 month seasonal cycles (Perret, 1997). Second, evolutionary theory of life history posits a relationship between sexual development and lifespan (Baer & Gaitz, 1971; Prothero 1993; Wootton 1987). Third, aging of specific organ systems, namely the reproductive system, has been slowed by delaying puberty, but also through short day induction into the winter state post puberty (Place et al., 2004; Place & Cruickshank, 2010). In fact, the winter phenotype has been highly revered as a biological state suspected to slow the aging process through putative mechanisms including altered immune function (Bilbo et al., 2002), self imposed caloric restriction, hibernation, and also possibly through augmentation of melatonin waveform, and reduction in circulating testosterone. Indeed, photoperiod manipulation aside, survival studies show hamsters undergoing hibernation live longer (Lyman et al., 1981; Turbill et al., 2011), putatively through the associated drop in BT. On this note, transgenic mice with overall decreased BT live longer (Conti et al., 2006). Caloric restriction has been reliably and repeatedly shown to slow the aging process and increase longevity in many species (Nakagawa et al., 2012; Mair & Dillin, 2008; Weindruch et al., 2008;

Weindruch 1996). There is also evidence that telomere length is protected in hamsters that overwinter (Turbill et al., 2012). Thus, all of these factors separately proposed to increase lifespan are included within the suite of physiological changes accompanying the winter phenotype.

Photoperiod-modulated control of puberty timing in the Siberian hamster did not influence longevity, despite good statistical power. Our findings contrast with previous experiments in *D. melanogaster* where specifically selecting late versus early age of sexual reproduction results in up to 50% increase in lifespan (Luckinbill & Clare, 1985). Granted, these are not the same phyla, but perhaps of equal importance, this trait in *D. melanogaster* was accomplished over 29 generations of selection, and not directly manipulated in randomly selected individuals as in this current design. The evolutionary theory of life history (Hill 1993; Charnov & Berrigan, 1990) asserts age of sexual maturity and lifespan are not merely positively correlated but assume a fixed proportion to one another, and in the mammalian taxa, reflect that sexual maturation occurs at roughly 1/3 of the expected lifespan. Thus, while natural selection is capable of altering the age of mammalian puberty, it might be accompanied by genetic polymorphisms which affect projected lifespan in the process; however, we do not find evidence that abiotic manipulation of puberty timing has any repercussion or consequence to lifespan among genetically equivalent (e.g., non-selected) cohorts.

It has been identified previously in the female Siberian hamster that accelerated reproductive aging occurs in LD (LD14:10) housed hamsters compared to

aged-matched controls delaying puberty under SD (LD10:14) photoperiods. When compared at 10 months of age, SD housed hamsters were found to have twice as many ovarian primordial follicles, as well as greater fecundity as judged by reproductive success as mean litter size. In contrast to this study, there was no difference in lifespan among early and delayed puberty conditions in male hamsters, but more directly, there were no group wise differences in lifespan among our female hamsters either, where presumably, the advanced aging effects found in Place et al., (2004) between early and delayed photoperiod groups were replicated. Therefore while timing of puberty and reproductive aging might hasten the loss of reproductive function, it does not causally influence lifespan. Other accounts posit caloric restriction may retard reproductive aging through similar mechanisms as the SD photoperiod (Nelson et al., 1985), namely delaying atresia and increased meiotic activity (Dorland et al., 1998; Theuring & Hansmann, 1986). These two mechanisms are reproductive system specific and would not be assumed to have consequences to the overall health, lifespan, or rate of aging of the organism.

Other theories of mechanisms thought to impact lifespan include caloric restriction, melatonin, and testosterone, all of which were consequently altered in our experimental design manipulating photoperiod history, independently from our control of puberty timing. Physiological ramifications of the winter phenotype include testicular regression, increased melatonin secretion duration, and self-imposed caloric restriction reflected in BW loss (Yellon & Goldman, 1984; Bartness et al, 1993; Butler et al., 2010). While each one of these parameters was shifted in the direction assumed

to enhance longevity (e.g., increased caloric restriction, increased melatonin, and decreased testosterone), we did not find that increasing the proportion of life spent in short days, or more directly, proportion of life in the winter state, resulted in any extension of lifespan.

Qualitatively distinct from photoperiod history is the notion of chronodisruption, or acute but cumulative effects of repeated phase shifting in an attempt of the circadian system to properly align its phase to that of the environmental light dark cycle. Chronic weekly phase advances result in increased mortality in aged mice (Davidson et al., 2006), and chronic circadian desynchronization has also been shown to have life-shortening consequences (Penev et al., 1998). Intriguingly, the degree of severity caused by chronodisruption to an animals' health is largely dependent upon the response of the circadian system. Hamsters exposed to non-entrainable photoperiod schedules either become completely arrythmic or are chronically subjected to large daily phase shifts in a perpetual attempt to reentrain. Chronic circadian disorganization resulted in profoundly increased incidences of renal and heart disease at 17 months old, whereas remarkably, hamsters receiving SCN ablations at 6 months were completely protected from these abnormal cardiac and renal phenotypes (Martino et al., 2008).

Interestingly, the only two photoperiod groups in our study exposed to non-naturalistic or fixed lighting conditions were the two groups exhibiting the shortest median survival, LDLD and DS. With respect to LDLD a rather straightforward explanation would be that the entrainment to this photoperiod was not optimal and,

consistent with reports of chronic circadian misalignment, were subject to cumulative health insults. In contrast to the abundance of studies in our lab demonstrating complete bifurcated entrainment to this light schedule we did not observe any indication that the hamsters in this experiment were ever bifurcated at any age. We surmise that the shortened median survival in this photoperiod group might be ameliorated in hamsters that demonstrate complete bifurcated entrainment, possibly in part through the employment of a wheel or by singly housing animals.

In this study, discrete long-to-short day and equally abrupt short-to-long day transitions were the critical manipulation responsible for reduced lifespan, in comparison to naturalistic seasonal transitions and even compared to fixed photoperiods. Therefore it is not photoperiod driven differences in life history that explain reduced lifespan in the DS group, but rather photoperiod transitions. The results of the only other mammalian study to date investigating the influence of photoperiod history on lifespan could also be reconciled by this effect (Perret, 1997). The reduced lifespan in mouse lemurs under accelerated seasons was probably not dependent upon the length of each photoperiod year as the author surmises. Rather, lifespan differences likely manifested from the hazardous consequences associated with the discrete seasonal transitions that only accompany the shorter 8 month year condition, since the 12 month year was also a natural photoperiod.

Unique to the survival curve of DS, we observed a reduction of nearly a quarter of the group population between 1-1.5 yrs old, following the first LD-SD transition. Perhaps more important was the effect of the initial SD-LD transition at 6

months old, when the plastic interval timer triggered a refractory response and initiated puberty onset in the majority of these hamsters *prior* to the SD-LD transition. This resulted in a quantitatively distinct growth rate pattern that "slingshot" mean BW to the overall highest BW average among all groups throughout the entire study. If circadian disorganization can occur abruptly in a response to acute misalignment of the circadian phase and the daily light schedule, there may too be consequences of misalignment among physiological mechanisms with respect to circannual timing, in this case the endogenously timed emergence of sexual maturation, and misalignment to the seasonal environment. Alternatively, where there is necessarily a mechanism whereby the endogenous interval timer triggers refractory to short day lengths and induces puberty, the SD-LD transition may have triggered a parallel signal in a distinct pathway or simply gain in the interval timer signal pathway to induce physiological changes accompanying sexual maturation and as a result of the combination of stimulatory signals generated much larger BW and growth in DS hamsters, the result of which could have been severe insult to organ composition and or overall health insult. This notion is consistent with respect to the univariate regression analysis, which revealed the only parameter prior to 225 d old with predictive value to lifespan was growth acceleration.

While the battery of longitudinal assessments distinctly tracked timing of age-related decline in BW, wheel running, and BT profiles, there was not strong evidence that any of the photoperiod groups aged at an overall distinct rate, although some differences were detected. SNP E BW history revealed that peak BW occurred during

the 2nd summer phenotype near 400 days of age and effectively aligned with the other two younger seasonal groups, SNP D and DS. Despite this BW alignment of nearly perfect correlation in spite of a chronological age difference of 113 days, there was not a proportionate increase in longevity for SNP E, suggesting the age-related decline in the circadian-mediated photoperiodic response is ultimately not a factor impacting longevity. Another notably distinct group-wise difference was amplitude in both wheel running and 24 h BT, where LDLD had lowest amplitude and LD exhibited the highest in both measures. However, despite various parameters indexing rates of aging, these differences do not explain or account for variations in survival. This suggests that overall, while age-related changes can be observed in variables also sensitive to the decline in circadian function, that ultimately, there is not sufficient evidence that an aging circadian pacemaker causally contributes to demise in aged hamsters. If it were, circadian based measures such as BW decline, 24 h BT parameters, and wheel running amplitude would account for much more variability in lifespan than what was found in our regression model. Instead, the more salient age-related changes in parameters we found were non-circadian indices of health reflecting the functionality of other systems, including lowered BT parameters as mesor, minimum, and maximum. In addition, the wheel running parameters with the largest predictive value of lifespan were summed across day and night bouts, (e.g., Round Sum and Max Sum), reflecting more directly the overall total output ability of the hamster, more directly assessing the physical fitness of the hamster rather than the circadian system function. Therefore, the more likely conclusion is that these age-

related dampening of rhythms in old age reflects weakened or deteriorating ability of other systems with respect to encoding and receiving circadian output. The lack of a strong photoperiod effect on organ weights is evidence that photoperiod history is not a tremendously influential factor.

Last, a consideration about the human implications from this comprehensive study. Since the routine use of artificial lighting conventions have evolved, from the mastery of fire, to light bulbs, to LEDs and LCDs- which are now an inescapable facet of our every day lives, human beings have essentially opted out of a purely naturalistic photoperiod regulated environment, casting aside a complex and dynamic relationship to the planet Earth's rotational schedule. The consequences of this shift from natural to artificial lighting with regard to human life history, health, and lifespan were not a consideration and remain to be addressed with a fully mechanistic account; however, here in this study using an animal that relies heavily on photoperiod for major life history regulation, there were no identifiable consequences. This does not mean humans are immune to health insult from photoperiod effects, but based on the findings within this dissertation there is at least a lack of evidence suggesting manipulation of life history presents any imminent or obvious repercussions to health. In contrast, what is known is that humans do have to contend with cumulative hazardous effects of frequent and abrupt phase realignment. The human application of dim scotophase illumination, in conjunction with LDLD bifurcation is currently under preliminary testing for its therapeutic use in reducing the carcinogenic effects of chronodisruption experienced in humans subject to nightshift work, in professions

requiring frequent time zone changes such as pilots and flight attendants, and also in jobs requiring the generation of completely artificial photoperiod conventions (i.e., submarine crews). I end by stating that the result of this work further elucidates the potential effects of chronodisruption, rather than the differentiation of life history events and resulting effects on physiology (i.e., winter phenotype), as the more life-threatening factor mediated through photoperiod history, as interpreted by the circadian system.

REFERENCES

Albrecht, U. (2002). Invited review: regulation of mammalian circadian clock genes. *J Appl Physiol*, *92*(3), 1348-1355.

Anisimov, V. N., Arbeev, K. G., Popovich, I. G., Zabezhinksi, M. A., Rosenfeld, S. V., Piskunova, T. S., Arbeeva, L. S., Semenchenko, A. V., & Yashin, A. I. (2004). Body weight is not always a good predictor of longevity in mice. *Exp Gerontol*, *39*(3), 305-319.

Arendt, J. (2000). Melatonin, circadian rhythms, and sleep. *N Engl J Med*, *343*(15), 1114-1116.

Baer, P. E., & Gaitz, C. M. (1971) In: *Prediction of Life Span* (E. Palmore & F. C. Jeffers, Eds.), 153-166. Heath Lexington Books, Lexington, MA.

Bartko, J. J., Patterson, R. D., & Butler, R.N. (1971). In: *Prediction of Life Span* (E. Palmore & F.C. Jeffers, Eds.), 123-138. Heath Lexington Books, Lexington, MA.

Bartness, T. J., Powers, J. B., Hastings, M. H., Bittman, E. L., & Goldman, B. D. (1993). The timed infusion paradigm for melatonin delivery: what has it taught us about the melatonin signal, its reception, and the photoperiodic control of seasonal responses? *J Pineal Res 15*, 161–190.

Beaulé, C., Robinson, B., Lamont, E. W., & Amir, S. (2003). Melanopsin in the circadian timing system. *J Mol Neurosci*, *21*(1), 73-89.

Benstaali, C., Mailloux, A., Bogdan, A., Auzéby, A., & Touitou, Y. (2001). Circadian rhythms of body temperature and motor activity in rodents their relationships with the light-dark cycle. *Life Sci*, *68*(24), 2645-2656.

Bilbo, S. D., Dhabhar, F. S., Viswanathan, K., Saul, A., Yellon, S. M., & Nelson, R. J. (2002). Short day lengths augment stress-induced leukocyte trafficking and stress-induced enhancement of skin immune function. *Proc Natl Acad Sci U S A*, *99*(6), 4067-4072.

Blask, D. E (2009). Melatonin, sleep disturbance and cancer risk. *Sleep Med Rev*, *13*, 257-264.

Bliwise, N. G. (1992). Factors related to sleep quality in healthy elderly women. *Psychol Aging*, *7*(1), 83-88.

Bohannon, R. W. (2008). Hand-grip dynamometry predicts future outcomes in aging adults. *J Geriatr Phys Ther*, *31*(1), 3-10.

Butler, M. P., Turner, K. W., Park, J. H., Schoomer, E. E., Zucker, I., & Gorman, M. R. (2010). Seasonal regulation of reproduction: altered role of melatonin under naturalistic conditions in hamsters. *Proc Biol Sci*, *277*(1695), 2867-2874.

Butler, M., Turner, K., Park, J., Butler, J., Trumbull, J., Dunn, S., Villa, P., & Zucker, I. (2007a). Simulated natural day lengths synchronize seasonal rhythms of asynchronously born Siberian hamsters. *Am J Physiol Regul Integr Comp Physiol*, *293*(1), R402-412.

Butler, M. P., Trumbull, J. J., Turner, K. W., & Zucker, I. (2007b). Timing of puberty and synchronization of seasonal rhythms by simulated natural photoperiods in female Siberian hamsters. *Am J Physiol Regul Integr Comp Physiol*, *293*, R413-420.

Cai, A., Scarbrough, K., Hinkle, D. A., & Wise, P. M. (1997). Fetal grafts containing suprachiasmatic nuclei restore the diurnal rhythm of CRH and POMC mRNA in aging rats. *Am J Physiol*, *273*(5 Pt 2), R1764-1770.

Charnov, E. L., & Berrigan, D. (1990). Dimension-less numbers and life history evolution: Age at maturity vs the adult lifespan. *Evol Ecol*, *5*, 63-68.

Comfort, A. (1964). *Ageing: The Biology of Senescence*. Routledge & Kegan Paul, London.

Conover, C. A., Bale, L. K., Grell, J. A., Mader, J. R., & Mason, M. A. (2010). Longevity is not influenced by prenatal programming of body size. *Aging Cell*, *9*(4), 647–649.

Conti, B., Sanchez-Alavez, M., Winsky-Sommerer, R., Morale, M. C., Lucero, J., Brownel, S., Fabre, V., Huitron-Resendiz, S., Henriksen, S., Zorrilla, E. P., de Lecea, L., & Bartfai, T. (2006). Transgenic mice with a reduced core body temperature have an increased life span. *Science*, *314*(5800), 825-828.

Czeisler, C. A., Dumont, M., Duffy, J. F., Steinberg, J. D., Richardson, G. S., Brown, E. N., Sánchez, R., Ríos, C. D., & Ronda, J. M. (1992). Association of sleep-wake habits in older people with changes in output of circadian pacemaker. *Lancet*, *340*(8825), 933-936.

Daan S., & Pittendrigh C. S. (1976). A functional analysis of circadian pacemakers in nocturnal rodents II: The variability of phasic response curves. *J Comp Physiol [A]*, *106*, 253-266.

Davidson, A. J., Sellix, M. T., Daniel, J., Yamazaki, S., Menaker, M., & Block, G. D. (2006). Chronic jet-lag increases mortality in aged mice. *Curr Biol, 16*(21), R914-916.
Dawson, D. P., & Crowne (1980). Longitudinal development of activity rhythms in Long-Evans rats. *J Gerontol, 35*, 339.

de la Iglesia, H. O., Meyer, J., & Schwartz, W. J. (2004). Using per gene expression to search for photoperiodic oscillators in the hamster suprachiasmatic nucleus. *Brain Res Mol Brain Res*, *127*(1-2), 121-127.

Dijk, D. J., Duffy, J. F., Riel, E., Shanahan, T. L., & Czeisler, C. A. (1999). Ageing and the circadian and homeostatic regulation of human sleep during forced desynchrony of rest, melatonin and temperature rhythms. *J Physiol, 516* (2), 611-627.

Dijk, D. J., Duffy, J. F., & Czeisler, C. A. (2000). Contribution of circadian physiology and sleep homeostasis to age-related changes in human sleep. *Chronobiol Int, 17*(3), 285-311.

Dorland, M., van Kooij, R. J., & te Velde, E. R. (1998). General ageing and ovarian ageing. *Maturitas, 30*, 113–118.

Duffy, P.H., & Feuers, R. J. (1991). Biomarkers of aging: changes in circadian rhythms related to the modulation of metabolic output. *Biomed Environ Sci*, *4*(1-2), 182-191.

Duffy, J. F., Dijk, D. J., Klerman, E. B., & Czeisler, C. A. (1998). Later endogenous circadian temperature nadir relative to an earlier wake time in older people.
Am J Physiol, *275*, R1478–1487.

Duncan, M. J., & Goldman, B. D. (1984a). Hormonal regulation of the annual pelage color cycle in the Djungarian hamster, *Phodopus sungorus*. I. Role of the gonads and pituitary. *J Exp Zool*, *230*(1), 89-95.

Duncan, M. J., & Goldman, B. D. (1984b). Hormonal regulation of the annual pelage color cycle in the Djungarian hamster, *Phodopus sungorus*. II. Role of prolactin. *J Exp Zool*, *230*(1), 97-103.

Elliott, J. A. (1976). Circadian rhythms and photoperiodic time measurement in mammals. *Fed Proc*, *35*(12), 2339-2346.

Elliott, J.A., & Tamarkin, L. (1994). Complex circadian regulation of pineal melatonin and wheel-running in Syrian hamsters. *J Comp Physiol* [*A*], *174*, 469–484.

Erren, T. C., Reiter, R. J., & Piekarski, C. (2003). Light, timing of biological rhythms, and chronodisruption in man (Review). *Naturwissenschaften*, *90*(11), 485-494.

Farajnia, S., Michel, S., Deboer, T., vanderLeest, H. T., Houben, T., Rohling, J. H., Ramkisoensing, A., Yasenkov, R., & Meijer, J. H. (2012). Evidence for neuronal desynchrony in the aged suprachiasmatic nucleus clock. *J Neurosci, 32*(17), 5891-5899.

Florez-Duquet, M., & McDonald, R. B. (1998). Cold-induced thermoregulation and biological aging. *Physiol Rev, 78*(2), 339-358.

Fontana, L., Partridge, L., & Longo, V. D. (2010). Extending healthy life span -from yeast to humans. *Science, 328*, 321–326.

Froy, O., & Miskin, R. (2010). Effect of feeding regimens on circadian rhythms: implications for aging and longevity (Review). *Aging, 2*(1), 7-27.

Froy, O., & Miskin, R. (2007). The interrelations among feeding, circadian rhythms and ageing. *Prog Neurobiol, 82*(3), 142-150.

Froy, O., Chapnik, N., & Miskin, R. (2006). Long-lived alphaMUPA transgenic mice exhibit pronounced circadian rhythms. *Am J Physiol Endocrinol Metab, 291*(5), E1017-1024.

Gaillard, J., Festa-Bianchet, M., Delorme, D., & Jorgenson, J. (2000). Body mass and individual fitness in female ungulates: bigger is not always better. *Proc R Soc Lond B, 267*, 471-477.

Goldman, B. D., & Darrow, J. M. (1983). The pineal gland and mammalian photoperiodism. *Neuroendocrinology, 37*(5), 386-396.

Goldman, B.D. (1991). Parameters of the circadian rhythm of pineal melatonin secretion affecting reproductive responses in Siberian hamsters. *Steroids, 56*, 218–225.

Gomez, D., Barbosa, A., Théry, M., Aujard, F., & Perret, M. (2012). Age affects photoentrainment in a nocturnal primate. *J Biol Rhythms, 27*(2), 164-171.

Gorman, M.R. (2001). A plastic interval timer synchronizes springtime pubertal development of summer and fall-born Siberian hamsters. *Am J Physiol Reg Int Comp Physiol, 281*(5), R1613-1623.

Gorman, M. R. (1995). Seasonal adaptations of Siberian hamsters. I. Accelerated gonadal and somatic development in increasing versus static long day lengths. *Biology of Reproduction, 53*, 110-115.

Gorman, M. R., & Zucker, I. (1995a). Seasonal adaptations of Siberian hamsters. II. Pattern of change in day length controls annual testicular and body weight rhythms. *Biology of Reproduction*, *53*, 116-125.

Gorman, M. R., & Zucker, I. (1995b). Testicular regression and recrudescence without subsequent photorefractoriness in Siberian hamsters. *Am J Physiol*, *269*(4 Pt 2), R800-806.

Gorman, M. R., & Lee, T. M. (2001). Daily novel wheel running reorganizes and splits hamster circadian activity rhythms. *J Biol Rhythms*, *16*(6), 541-551.

Gorman, M. R. (2001). Exotic photoperiods induce and entrain split circadian activity rhythms in hamsters. *J Comp Physiol A*, *187*, 793–800.

Gorman, M. R., Goldman, B. D., & Zucker, I. (2001a). Mammalian photoperiodism. In J. S. Takahashi, F. W. Turek and R. Y. Moore (Eds), *Circadian Clocks*, pp. 481-508. New York: Plenum Press.

Gorman, M. R., Yellon, S. M., & Lee, T. M. (2001b). Temporal reorganization of the suprachiasmatic nuclei in hamsters with split circadian rhythms. *J Biol Rhythms*, *16*(6), 552-563.

Gutman, R., Genzer, Y., Chapnik, N., Miskin, R., & Froy, O. (2011). Long-lived mice exhibit 24 h locomotor circadian rhythms at young and old age. *Exp Gerontol*, *46*(7), 606-609.

Ha, M., & Park, J. (2005). Shiftwork and metabolic risk factors of cardiovascular disease. *J Occup Health*, *47*,89–95.

Halberg, J., Halberg, E., Regal, P., & Halberg, F. (1981). Changes with age characterize circadian rhythm in telemetered core temperature of stroke-prone rats. *J Gerontol*, *36*(1), 28-30.

Hazlerigg, D. G. (2012). The evolutionary physiology of photoperiodism in vertebrates. *Prog Brain Res*, *199*, 413-422.

Hazlerigg, D. G., & Wagner, G. C. (2006). Seasonal photoperiodism in vertebrates: from coincidence to amplitude. *Trends Endocrinol Metab*, *17*(3), 83-91.

Herzog, E. D., Aton, S. J., Numano, R., Sakaki, Y., & Tei, H. (2004). Temporal precision in the mammalian circadian system: a reliable clock from less reliable neurons. *J Biol Rhythms*, *19*(1), 35-46.

Hill, K. (1993). Life history theory and evolutionary anthropology. *Evolutionary Anthropology: Issues, News, and Reviews, 2*(3), 78-88.

Hoffmann, K. (1982). The critical photoperiod in the Djungarian hamster *Phodopus sungorus*. In J. Aschoff, S. Daan, and G. Gross (Eds.), *Vertebrate Circadian Systems: Structure and Physiology*, 297–304. New York: Springer.

Illnerová, H. (1991). The suprachiasmatic nucleus and rhythmic pineal melatonin production. In D. C. Klein , R. Y. Moore, and S. M. Reppert (Eds), *Suprachiasmatic nucleus: the mind's clock*, 197-216. New York: Oxford University Press.

Illnerová, H., Sumová, A., Trávnícková, Z., Ják, M., & Jelínková, D. (2000). Hormones, subjective night and season of the year. *Physiol Res*, *49* Suppl 1, S1-10.

Illnerová, H., & Sumová, A. (1997). Photic entrainment of the mammalian rhythm in melatonin production. *J Biol Rhythm*, *12*(6), 547-555.

Ingram, D. K., Archer, J. R., Harrison, D. E., & Reynolds, M. A. (1982). Physiological and behavioral correlates of lifespan in aged C57BL/6J mice. *Exp Gerontol*, *17*(4), 295-303.

Ingram, D.K. (1983). Towards the behavioral assessment of biological aging in the laboratory: Concepts, terminology, and objectives. *Exp Aging Res*, *9*(4), 225-238.

Ingram, D.K., & Reynolds, M. A. (1986). Assessing the predictive validity of psychomotor tests as measures of biological age in mice. *Exp Aging Res*, *12*(3), 155-162.

Jefimow, M., Głabska, M., & Wojciechowski, M. S. (2011). Social thermoregulation and torpor in the Siberian hamster. *J Exp Biol*, *214*(7), 1100-1108.

Johnson, C. H. (1999). Forty years of PRCs--what have we learned? *Chronobiol Int*, *16*(6), 711-743.

Kakizaki, M., Kuriyama, T., Sone, K., Ohmori-Matsuda, K., Hozawa, A., Nakaya, N., Fukudo, S., & Tsuji, I. (2008). Sleep duration and the risk of breast cancer: the Ohsaki Cohort Study. *Br J Cancer*, *99*, 1502-1505.

Kelly G. S. (2006). Body temperature variability (Part 1): a review of the history of body temperature and its variability due to site selection, biological rhythms, fitness, and aging (Review). *Altern Med Rev*, *11*(4), 278-293.

Kelly, G. S. (2007). Body temperature variability (Part 2): masking influences of body temperature variability and a review of body temperature variability in disease (Review). *Altern Med Rev*, *12*(1), 49-62.

Kenney, W. L., & Munce, T. A. (2003). Invited review: aging and human temperature regulation. *J Appl Physiol*, *95*(6), 2598-2603.

Ko, C. H., & Takahashi, J. S. (2006). Molecular components of the mammalian circadian clock. *Hum Mol Genet*, *15*, Spec No 2:R271-277.

Korkmaz, A., Sanchez-Barcelo, E. J., Tan, D. X., & Reiter, R. J. (2009). Role of melatonin in the epigenetic regulation of breast cancer. *Breast Cancer Res Treat*, *115*, 13-27.

Liu, C., Weaver, D. R., Jin, X., Shearman, L. P., Pieschl, R. L., Gribkoff, V. K., & Reppert, S. M. (1997). Molecular dissection of two distinct actions of melatonin on the suprachiasmatic circadian clock. *Neuron*, *19*(1), 91-102.

Luckinbill, L. S., & Clare, M. J. (1985). Selection for life span in Drosophila melanogaster. *Heredity* (Edinb), *55*(1), 9-18.

Lyman, C. P., O'Brien, R. C., Greene, G. C., & Papafrangos, E. D. (1981). Hibernation and longevity in the Turkish hamster Mesocricetus brandti. *Science*, *212*(4495), 668-670.

Mahlberg, R., Tilmann, A., Salewski, L., & Kunz, D. (2006). Normative data on the daily profile of urinary 6-sulfatoxymelatonin in healthy subjects between the ages of 20 and 84. *Psychoneuroendocrinology*, *31*(5), 634-641.

Mailloux, A., Benstaali, C., Bogdan, A., Auzéby, A., & Touitou, Y. (1999). Body temperature and locomotor activity as marker rhythms of aging of the circadian system in rodents. *Exp Gerontol*, *34*(6), 733-740.

Mair, W., & Dillin, A. (2008). Aging and survival: the genetics of life span extension by dietary restriction. *Annu. Rev. Biochem.*, *77*, 727–754.

Martinez, M. C., & Naranjo, J. D. (2010). A pretest for choosing between logrank and Wilcoxon tests in the two-sample problem. *Metron: Int J Statistics*, *68*(2), 111-125.

Martino, T. A., Oudit, G. Y., Herzenberg, A. M., Tata, N., Koletar, M. M., Kabir, G. M., Belsham, D. D., Backx, P. H., Ralph, M. R., & Sole, M. J. (2008). Circadian rhythm disorganization produces profound cardiovascular and renal disease in hamsters. *Am J Physiol Regul Integr Comp Physiol*, *294*(5), R1675-1683.

McAuley, J. D., Miller, J. P., Beck, E., Nagy, Z.M., & Pang, K. C. (2002). Age-related disruptions in circadian timing: evidence for “split” activity rhythms in the SAMP8. *Neurobiol Aging*, *23*, 625–632.

McKeon, G. P, Nagamine, C. M., Ruby, N. F., & Luong, R. H. (2011). Hematologic, serologic, and histologic profile of aged Siberian hamsters (*Phodopus sungorus*). *J Am Assoc Lab Anim Sci*, *50*(3), 308-316.

Meijer, J. H., & Schwartz, W. J. (2003). In search of the pathways for light-induced pacemaker resetting in the suprachiasmatic nucleus. *J Biol Rhythms*, *18*(3), 235-249.

Messager, S., Hazlerigg, D. G., Mercer, J. G., & Morgan, P. J. (2000). Photoperiod differentially regulates the expression of Per1 and ICER in the pars tuberalis and the suprachiasmatic nucleus of the Siberian hamster. *Eur J Neurosci*, *12*(8), 2865-2870.

Miller, R. A., Harper, J. M., Galecki, A., & Burke, D. T. (2002). Big mice die young: early life body weight predicts longevity in genetically heterogeneous mice. *Aging Cell*, *1*(1), 22-29.

Miller, R. A., Chrisp, C., & Atchley, W. (2000). Differential longevity in mouse stocks selected for early life growth trajectory. *J Gerontol A Biol Sci Med Sci*, *55*(9), B455-B461.

Min, K. J., Lee, C. K., & Park, H. N. (2012). The lifespan of Korean eunuchs. *Curr Biol*, *22*(18), R792-793.

Mohawk, J. A., Green, C. B., & Takahashi, J. S. (2012). Central and peripheral circadian clocks in mammals. *Annu Rev Neurosci*, *35*, 445-462.

Monk, T. H. (1991). Sleep and circadian rhythms. *Exp Gerontol*, *26*(2-3), 233-243.

Moore, R., & Leak, R. (2001). Suprachiasmatic nucleus. In J. Takahashi, F. Turek and R. Moore (Eds), *Handbook of behavioral neurobiology: Circadian clocks*, Vol 12, pp. 141-179. New York: Kluwer Academic / Plenum Publishers.

Moore, R. Y. (1995). Organization of the mammalian circadian system. *Ciba Found Symp*, *183*, 88-106.

Morin, L. P. (1988). Age-related changes in hamsters circadian period, entrainment and rhythm splitting. *J Biol Rhythms*, *3*, 237–248.

Morin, L. P., Blanchard, J.H., & Provencio, I. (2003). Retinal ganglion cell projections to the hamster suprachiasmatic nucleus, intergeniculate leaflet, and visual

midbrain: bifurcation and melanopsin immunoreactivity. *J Comp Neurol*, *465*(3), 401-416.

Mrugala, M., Zlomanczuk, P., Jagota, A., & Schwartz, W. J. (2000). Rhythmic multiunit neural activity in slices of hamster suprachiasmatic nucleus reflect prior photoperiod. *Am J Physiol Regul Integr Comp Physiol*, *278*(4), R987-994.

Nakagawa, S., Lagisz, M., Hector, K. L., & Spencer, H. G. (2012). Comparative and meta-analytic insights into life extension via dietary restriction. *Aging Cell*, *11*, 401–409.

Nakamura, T. J., Nakamura, W., Yamazaki, S., Kudo, T., Cutler, T., Colwell, C. S., & Block, G. D. (2011). Age-related decline in circadian output. *J Neurosci*, *31*(28), 10201-10205.

Natelson, B. H., Tapp, W. N., Drastal, S., Gross, J., & Ottenweller, J. E. (1993). Constant light extends life in hamsters with heart disease. *Proc Soc Exp Biol Med*, *202*(1), 69-74.

Navara, K. J., Trainor, B. C., & Nelson, R. J. (2007). Photoperiod alters macrophage responsiveness, but not expression of Toll-like receptors in Siberian hamsters. *Comp Biochem Physiol A Mol Integr Physiol*, *148*(2), 354-359.

Nelson, J. F., Gosden, R. G., & Felicio, L. S. (1985). Effect of dietary restriction on estrous cyclicity and follicular reserves in aging C57BL/6J mice. *Biol Reprod*, *32*, 515–522.

Nelson, W., & Halberg, F. (1986a). Meal-timing, circadian rhythms and life span of mice. *J Nutr*, *116*(11), 2244-2253.

Nelson, W., & Halberg, F. (1986b). Schedule-shifts, circadian rhythms and lifespan of freely-feeding and meal-fed mice. *Physiol Behav*, *38*(6), 781-788.

Nelson, D. E., & Takahashi, J. S. (1991). Comparison of visual sensitivity for suppression of pineal melatonin and circadian phase-shifting in the golden hamster. *Brain Res*, *554*(1-2),272-277.

Nussey, D. H., Coulson, T., Delorme, D., Clutton-Brock, T. H., Pemberton, J. M., Festa-Bianchet, M., & Gaillard, J. M. (2011). Patterns of body mass senescence and selective disappearance differ among three species of free-living ungulates. *Ecology*, *92*(10), 1936-1947.

Oklejewicz, M., & Daan, S. (2002). Enhanced longevity in tau mutant Syrian hamsters, Mesocricetus auratus. *J Biol Rhythms*, *17*(3), 210-216.

Ong, K. K. (2006). Size at birth, postnatal growth and risk of obesity. *Horm Res*, *65*, (Suppl 3), 65-69.

Pandolf, K. B. (1997). Aging and human heat tolerance (Review). *Exp Aging Res*, *23*(1), 69-105.

Park, N., Cheon, S., Son, G., Cho, S., & Kim, K. (2012). Chronic circadian disturbance by a shortened light-dark cycle increases mortality. *Neurobiol Aging*, *33*(6), 1122.e11-1122.e22.

Penev, P. D., Zee, P. C., & Turek, F. W. (1997). Quantitative analysis of the age-related fragmentation of hamster 24-h activity rhythms. *Am J Physiol*, *273*(6 Pt 2), R2132-2137.

Peng, M. T., & Kang, M. (1984). Circadian rhythms and patterns of running-wheel activity, feeding and drinking behaviors of old male rats. *Physiol Behav*, *33*, 615–620.

Perret, M. (1997). Change in photoperiodic cycle affects life span in a prosimian primate (*Microcebus murinus*). *J Biol Rhythms*, *12*(2), 136-145.

Perret, M., & Aujard, F. (2006) Aging and biological rhythms in primates (Review). *Med Sci*, *22*(3), 279-283.

Pierpaoli, W., & Regelson, W. (1994). Pineal control of aging: effect of melatonin and pineal grafting on aging mice. *Proc Natl Acad Sci U S A*, *91*(2), 787-791.

Pittendrigh, C. S., &. Daan, S. (1974). Circadian oscillations in rodents: a systematic increase in their frequency with age. *Science 186*, 548–550.

Pittendrigh, C. S., & Daan, S. (1976). A functional analysis of circadian pacemakers in nocturnal rodents. *J Comp Physiol*, *106*, 253-355.

Place, N.J., Tuthill, C.R., Schoomer, E.E., Tramontin, A.D., & Zucker, I. (2004). Short day lengths delay reproductive aging. *Biol Reprod*, *71*(3), 987-992.

Place, N. J., & Cruickshank, J. (2010). Short photoperiod initiated during adulthood sustains reproductive function in older female siberian hamsters more effectively than short photoperiod initiated before puberty. *Biol Reprod*, *82*(4), 778-782.

Portier, C. J. (2000). Decisions About Environmental Health Risks: What are the Key Questions and How Does this Apply to Melatonin? In T. C. Erren, and C. Piekarski (Eds), *Low Frequency EMF, Visible Light, Melatonin, and Cancer, International Symposium*, Vol. 50, pp. 298-314. Arbeitsmed.

Prothero, J. (1993). Adult lifespan as a function of age at maturity. *Experimental Gerontology, 28*, 529-536.

Quarrie, J. K., & Riabowol, K. T. (2004). Murine models of life span extension. *Sci Aging Knowledge Environ, 2004*(31), re5.

Ralph, M. R., Foster, R. G., Davis, F.C., & Menaker, M. (1990). Transplanted suprachiasmatic nucleus determines circadian period. *Science, 247*(4945), 975-978.

Refinetti, R. (2006). *Circadian Physiology* (2nd Edition). Boca Raton, FL: CRC Press.

Refinetti, R., & Menaker, M. (1992a). The Circadian Rhythm of Body Temperature. Review, *Physiology & Behavior, 51*, 613-637.

Refinetti, R., & Menaker, M. (1992b). The circadian rhythm of body temperature of normal and tau-mutant golden hamsters. *J Thermal Biol, 17*(2), 129–133.

Refinetti, R., Ma, H., & Satinoff, E. (1990). Body temperature rhythms, cold tolerance, and fever in young and old rats of both genders. *Exp Gerontol, 25*(6), 533-543.

Reiter, R. J., Tan, D. X., Erren, T. C., Fuentes-Broto, L., & Paredes, S. D. (2009). Light-mediated perturbations of circadian timing and cancer risk: a mechanistic analysis (Review). *Integr Cancer Ther, 8*(4), 354-360.

Reppert, S. M., & Weaver, D. R. (2002). Coordination of circadian timing in mammals. *Nature, 418*(6901), 935-941.

Roenneberg, T., & Foster, R. G. (1997). Twilight times: light and the circadian system (Review). *Photochem Photobiol, 66*(5), 549-561.

Rosenberg, R. S., Zee, P. C., & Turek, F. W. (1991). Phase response curves to light in young and old hamsters. *Am J Physiol, 261*(2 Pt 2), R491-495.

Rosenthal, S. L., Vakili, M. M., Evans, J. A., Elliott, J. A., & Gorman, M. R. (2005). Influence of photoperiod and running wheel access on the entrainment of split circadian rhythms in hamsters. *BMC Neurosci, 6*(41).

Roth, G., Lane, M., Ingram, D., Mattison, J., Elahi, D., Tobin, J., Muller, D., & Metter, E. (2002). Biomarkers of Caloric Restriction may Predict Longevity in Humans. *Science, 297*, 811.

Sacher, G. A., & Duffy, P. H. (1978). Age changes in rhythms of energy metabolism, activity and body temperature in Mus musculus and Peromyscus. In: Aging and Biological Rhythms; Samis, H. V., & Capobianio, A. (Eds.), 105–124. Plenum Press: New York.

Satinoff, E. (1998). Patterns of circadian body temperature rhythms in aged rats. *Clin Exp Pharmacol Physiol, 25*(2), 135-140.

Scarbrough, K., Losee-Olson, S., Wallen, E. P., & Turek, F. W. (1997). Aging and photoperiod affect entrainment and quantitative aspects of locomotor behavior in Syrian hamsters. *Am J Physiol, 272*(4 Pt 2), R1219-R1225.

Schernhammer, E. S., Kroenke, C. H., Laden, F., & Hankinson, S. E. (2006). Night work and risk of breast cancer. *Epidemiology, 17*, 108–111.

Schmidt, R. E., Eason, R. L., Hubbard, G. B., Young, J. T., & Eisenbrandt, D. L. (1983). Pathology of aging Syrian hamsters. *CRC Press*, Boca Raton, Florida.

Selesniemi, K., Lee, H. J., & Tilly, J. L. (2008). Moderate caloric restriction initiated in rodents during adulthood sustains function of the female reproductive axis into advanced chronological age. *Aging Cell, 7*(5):622-629.

Shearman, L. P., Zylka, M. J., Weaver, D. R., Kolakowski, L. F., & Reppert, S. M. (1997). Two period genes: circadian expression and photic regulation in the suprachiasmatic nuclei. *Neuron, 19*, 1261–1269.

Simons, M. J., Koch, W., & Verhulst, S. (2013). Dietary restriction of rodents decreases aging rate without affecting initial mortality rate - a meta-analysis. *Aging Cell, 12*(3), 410-414.

Simpson, S., & Galbraith, J. J. (1906). Observations on the normal temperature of the monkey and its diurnal variation, and on the effect of changes in the daily routine on this variation. *Trans. Royal Soc. Edinburgh, 45*, 65-104.

Sollars, P. J., Smeraski, C. A., Kaufman, J. D., Ogilvie, M. D., Provencio, I., & Pickard, G. E. (2003). Melanopsin and non-melanopsin expressing retinal ganglion cells innervate the hypothalamic suprachiasmatic nucleus. *Vis Neurosci, 20*(6), 601-610.

Sumová, A., Kováciková, Z., & Illnerová, H. (2007). Dynamics of the adjustment of clock gene expression in the rat suprachiasmatic nucleus to an asymmetrical change from a long to a short photoperiod. *J Biol Rhythms, 22*(3), 259-267.

Sumová, A., Jác, M., Sládek, M., Sauman, I., & Illnerová, H. (2003). Clock gene daily profiles and their phase relationship in the rat suprachiasmatic nucleus are affected by photoperiod. *J Biol Rhythms*, *18*(2), 134-144.

Suwazono, Y., Dochi, M., Sakata, K., Okubo, Y., Oishi, M., Tanaka, K., Kobayashi, E., Kido, T., & Nogawa, K. (2008). A longitudinal study on the effect of shift work on weight gain in male Japanese workers. *Obesity* (Silver Spring), *16*, 1887–1893.

Tankersley, C. G., Irizarry, R., Flanders, S. E., Rabold, R., & Frank, R. (2003). Unstable heart rate and temperature regulation predict mortality in AKR/J mice. *Am J Physiol Regul Integr Comp Physiol*, *284*(3), R742-750.

Tapp, W. N., & Natelson, B. H. (1986). Life extension in heart disease: an animal model. *Lancet*, *1*(8475), 238-40.

Terrien, J., Zizzari, P., Epelbaum, J., Perret, M., & Aujard, F. (2009). Daily rhythms of core temperature and locomotor activity indicate different adaptive strategies to cold exposure in adult and aged mouse lemurs acclimated to a summer-like photoperiod. *Chronobiol Int*, *26*(5), 838-853.

Theuring, F., & Hansmann, I. (1986). Follicular development in immature Djungarian hamsters (Phodopus sungorus) and the influence of exogenous gonadotropins. *Biol Reprod*, *35*, 407–412.

Touitou, Y., Reinberg, A., Bogdan, A., Auzéby, A., Beck, H., & Touitou, C. (1986). Age-related changes in both circadian and seasonal rhythms of rectal temperature with special reference to senile dementia of Alzheimer type. *Gerontology*, *32*(2), 110-118.

Turbill, C., Smith, S., Deimel, C., & Ruf, T. (2012). Daily torpor is associated with telomere length change over winter in Djungarian hamsters. *Biol Lett*, *8*(2), 304-307.

Turbill, C., Bieber, C., & Ruf, T. (2011). Hibernation is associated with increased survival and the evolution of slow life histories among mammals. *Proc Biol Sci*, *278*(1723), 3355-3363.

Turek, F. W., Penev, P., Zhang, Y., Van Reeth, O., & Zee, P. C. (1995). Effects of age on the circadian system (Review). *Neurosci. Biobehav*, *19*, 53–58.

Valentinuzzi, V. S., Scarbrough, K., Takahashi, J. S., & Turek, F. W. (1997). Effects of aging on the circadian rhythm of wheel-running activity in C57BL/6 mice. *Am J Physiol*, *273*(6 Pt 2), R1957-1964.

Van Someren, E. J., Raymann, R. J., Scherder, E. J., Daanen, H. A., & Swaab, D. F. (2002). Circadian and age-related modulation of thermoreception and temperature

regulation: mechanisms and functional implications (Review). *Ageing Res Rev, 1*(4), 721-778.

Vitiello, M. V., Smallwood, R. G., Avery, D. H., Pascualy, R. A., Martin, D. C., & Prinz, P. N. Circadian temperature rhythms in young adult and aged men. *Neurobiol Aging, 7*(2), 97-100.

Weindruch, R., Colman, R. J., Perez, V, & Richardson, A. G. (2008). How does caloric restriction increase the longevity of mammals? In Molecular Biology of Aging (Guarente LPL, Wallace D, eds). New York: Cold Spring Harbor Laboratory Press, pp. 409–425.

Weindruch, R. (1996). The retardation of aging by caloric restriction: studies in rodents and primates (Review). *Toxicol Pathol, 24*(6), 742-745.

Weinert, H., & Weinert, D. (1998). Circadian activity rhythms of laboratory mice during the last weeks of their life. *Biol Rhythm Res, 29*, 159–178.

Weinert, H., Weinert, D., & Waterhouse, J. (2002). The circadian activity and body temperature rhythms of mice during their last days of life. *Biol Rhythm Res, 33*, 199–212.

Weitzman, E. D., Moline, M. L., Czeisler, C. A., & Zimmerman, J. C., 1982. Chronobiology of aging: temperature, sleep–wake rhythms and entrainment. *Neurobiol Aging 3*, 299–309.

Welsh, D. K., Logothetis, D. E., Meister, M., & Reppert, S.M. (1995). Individual neurons dissociated from rat suprachiasmatic nucleus express independently phased circadian firing rhythms. *Neuron, 14*(4), 697-706.

Witting, W., Mirmiran, M., Bos, N. P., & Swaab, D. F. (1994). The effect of old age on the free-running period of circadian rhythms in rat. *Chronobiol Int, 11*(2), 103-112.

Wootton, T. J. (1987). The effects of body mass, phylogeny, habitat, and trophic level on mammalian age at first reproduction. *Evolution, 41*, 732-749.

Workman, J. L., DeWitt, S. J., Fonken, L. K., & Nelson, R. J. (2010). Environmental enrichment enhances delayed-type hypersensitivity in both short- and long-day Siberian hamsters. *Physiol Behav, 99*(5), 638-643.

Wu, A. H., Stanczyk, F. Z., Wang, R., Koh, W. P., Yuan, J. M., & Yu, M. C. (2013). Sleep duration, spot urinary 6-sulfatoxymelatonin levels and risk of breast cancer among Chinese women in Singapore. *Int J Cancer, 132*(4), 891-896.

Yamazaki, S., Numano, R., Abe, M., Hida, A., Takahashi, R., Ueda, M., Block, G. D., Sakaki, Y., Menaker, M., & Tei, H. (2000). Resetting central and peripheral circadian oscillators in transgenic rats. *Science*, *288*(5466), 682-685.

Yellon, S.M., & Goldman, B.D. (1984). Photoperiod control of reproductive development in the male Djungarian hamster (*Phodopus sungorus*). *Endocrinology*, *114*(2), 664-670.

Yunis, E. J., Fernandes, G., Nelson, W., & Halberg, F. (1974). Circadian temperature rhythms and aging in rodents. In L. E. Scheving, F. Halberg, and J. E. Pauly (Eds.), *Chronobiology*, Georg Thieme Publishers, Stuttgart, pp. 358–371.

Zee, P. C., Rosenberg, R. S., & Turek, F. W. (1992). Effects of aging on entrainment and rate of resynchronization of circadian locomotor activity. *Am J Physiol*, *263*(5 Pt 2), R1099-1103.